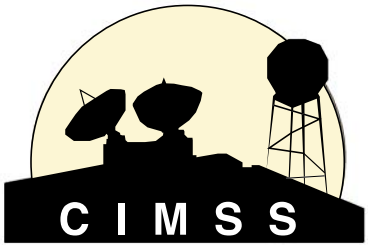

University of Wisconsin-Madison

Cooperative Institute for Meteorological Satellite Studies

(CIMSS)

Cooperative Agreement Annual Report

1 January 2006 to 31 December 2006

Grant Number NA06NES4400002

Submitted to:
National Oceanic and Atmospheric Administration (NOAA)

Cooperative Agreement Annual Report

1 January 2006 to 31 December 2006

Steve Ackerman
Director, CIMSS

Tom Achtor,
Executive Director, Editor

Contributing Authors

Steve Ackerman
Scott Bachmeier
Ralf Bennartz
Wayne Feltz
Mat Gunshor
Andy Heidinger
Allen Huang
Bormin Huang
Jim Jung
Jeff Key
Bob Knuteson
Jim Kossin
Jun Li
Sanjay Limaye
Zhengyu Liu
Paul Menzel
Margaret Mooney
Jim Nelson
Tim Olander
Ralph Petersen
Elaine Prins
Chris Schmidt
Tim Schmit
Tony Schreiner
Dave Tobin
Paul van Delst
Chris Velden
Tom Whittaker
Tom Zapotocny

NOAA Collaborators

Jeff Key
Bob Aune
Andy Heidinger
Mike Pavolonis
Tim Schmit
Gary Wade

The work conducted as part of the CIMSS Cooperative Agreement for 1 January 2006 to 31 December 2006 is detailed in this report. In the Table of Contents and in the report, the primary author, either the UW-Madison PI or PM, or the NOAA collaborator working on the particular effort is indicated for each section. While primary authors are noted, the research discussed in this report has been a result of numerous collaborations with other CIMSS and NOAA colleagues.

CIMSS Cooperative Agreement Annual Report
1 January 2006 to 31 December 2006

Table of Contents

1 GIMPAP (GOES Improved Measurements and Product Assurance Program)

1.1 GOES Retrieval System (GRS) – Jun Li

Proposed Work
We proposed to improve the GOES Sounder single field-of-view (SFOV) products (sounding and total column ozone) by:

- Improving the retrieval algorithm,
- handling surface emissivity and clouds better, and
- taking into account time continuity and synergy with other measurements.

The specific goals for 2006 were:

(1) To improve sounding using spatial/temporal noise filtering, time continuity (TC) and spatial continuity,

(2) To evaluate SFOV, 3x3 Field of View (FOV) and 5x5 FOV retrievals using Atmospheric Radiation Measurement (ARM) CART (Cloud and Radiation Testbed) Site microwave Total Precipitable Water (TPW) and best estimated profiles,

(3) To improve SFOV sounding with ancillary information,
(4) To improve ozone using Ozone Monitoring Instrument (OMI) and other ozone measurement data.

Summary of GRS 2006 Accomplishments and Findings

Sounding improvement using spatial/temporal noise filtering, time continuity and spatial continuity
We have implemented spatial continuity (SC) and time continuity (TC) in the sounding retrieval algorithm by assuming constant temperature and variable moisture in two adjacent time steps. Initial results are neutral (Li et al. 2006).

Evaluation of physical retrievals using ARM CART Site microwave Total Precipitable Water and best estimated profiles
A new GOES sounding physical retrieval algorithm has been developed to retrieve temperature and moisture profiles, surface skin temperature, surface emissivities and TPW. The forecast error covariance (derived from historical forecast/RAOB matchup data) is used in the maximum likelihood (ML) optimal estimation algorithm. We find that the forecast error covariance information plays an important role in the GOES sounding retrieval, which is consistent with in the results of a NWP data assimilation study.

The new algorithm has been verified using three years of microwave radiometer measured TPW over the ARM CART site. Compared to the CIMSS legacy and NOAA/NESDIS operational method (Ma et al. 1999), the new algorithm is less sensitive to noise. The updated algorithm improves the TPW over the legacy algorithm for both 3x3 FOV and SFOV retrievals (Li et al. 2006). Figure 1.1.1 shows the scatterplot between GOES Sounder TPW from 3x3 FOV radiances and microwave TPW. The improvement of the new algorithm over both the forecast and legacy products is significant.

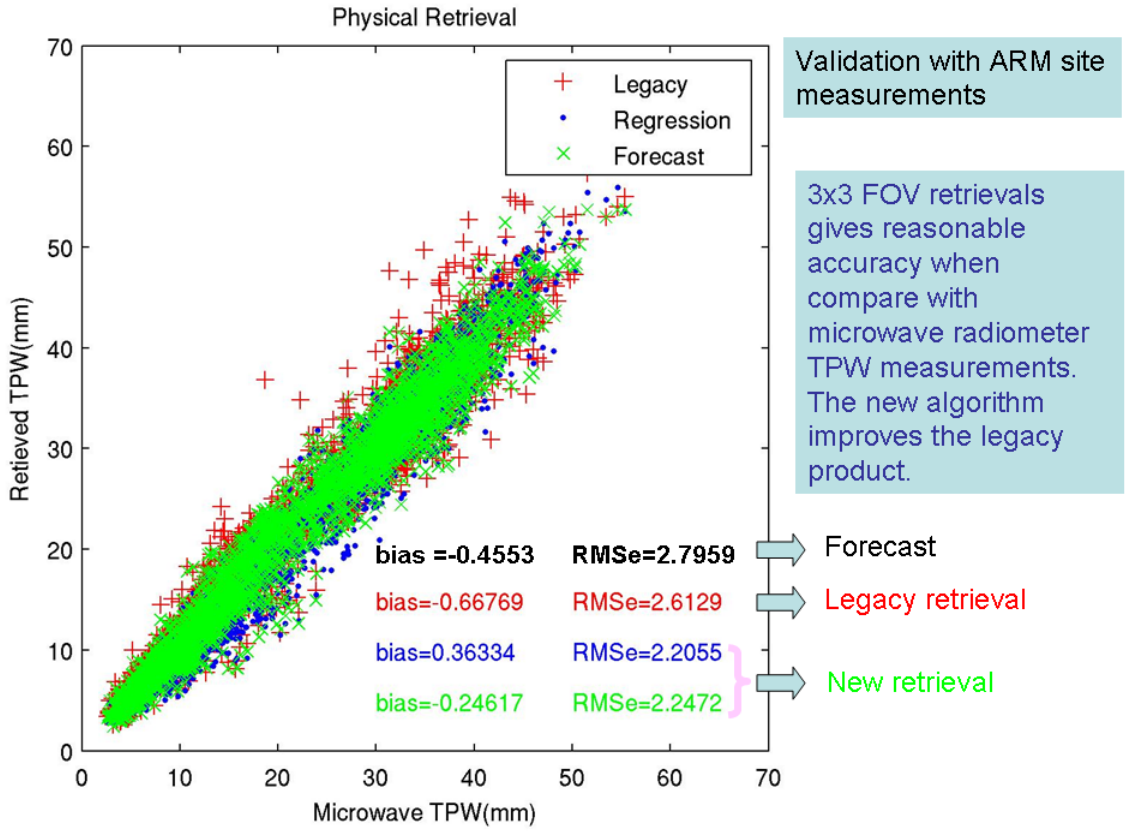

Figure 1.1.1: The scatterplot between GOES Sounder TPW from 3x3 radiances and the microwave TPW at ARM cart site.

Further analysis shows that the improvement of the new sounding algorithm has diurnal and seasonal features. In summer, for example, we found that

(1) the new algorithm with regression as the first guess has the smallest bias over most of the day;

(2) the new algorithm with forecast as the first guess has negative bias at night and positive bias in the day;

(3) the legacy algorithm has a large positive bias at night and a small bias in the day.

Figure 1.1.2 shows the diurnal root mean square (RMS) difference and bias between microwave radiometer TPW and GOES Sounder TPW retrievals at Lamont, Oklahoma during summer months (June, July, August) from 2003 to 2005. Generally, new retrievals with regression as first guess have the smallest RMS difference, but there is still significant bias. The reason for this is unclear, and further investigation is necessary.

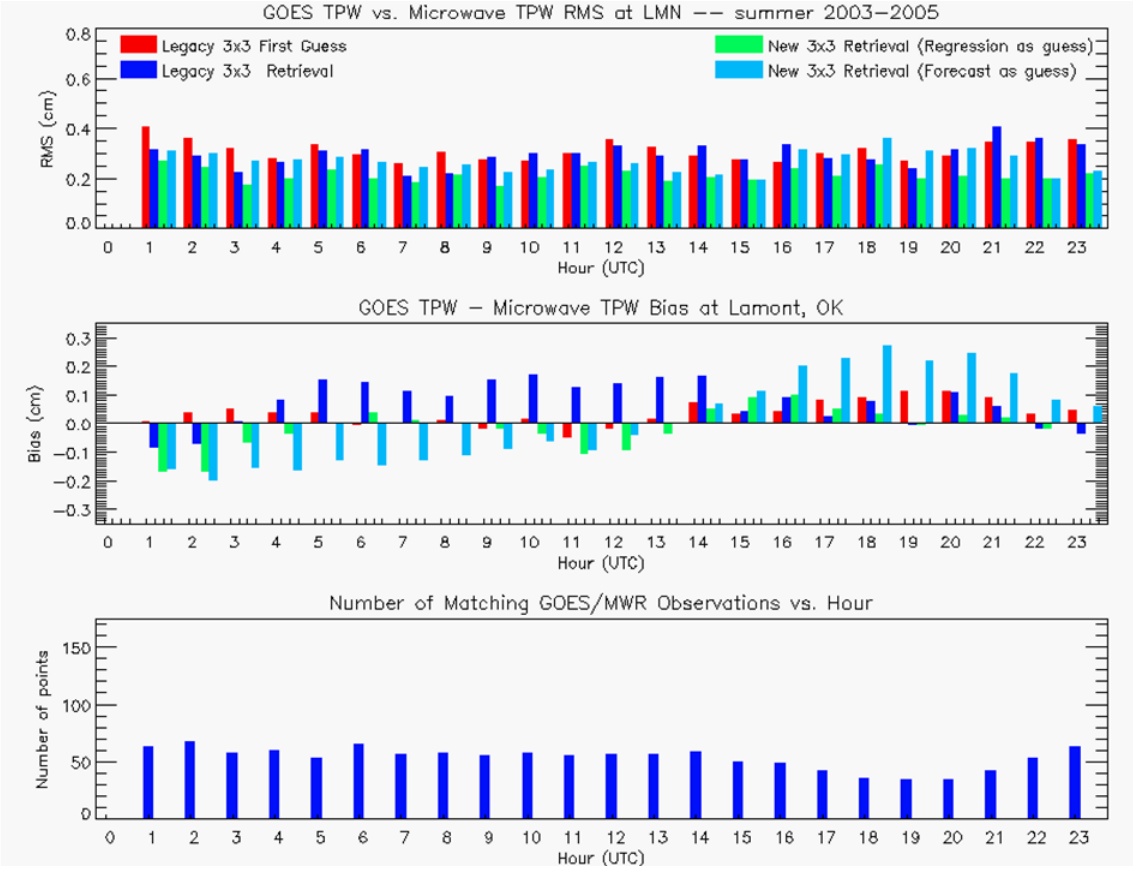

Figure 1.1.2: The diurnal root mean square (RMS) difference and bias between microwave radiometer TPW and GOES Sounder TPW retrievals at Lamont, Oklahoma during summer from 2003 to 2005.

We are currently implementing the new algorithm with regression as first guess in the CIMSS merged processing system. This software will be provided to NESDIS/STAR/ FPDT for testing in early 2007. The new algorithm will also be refined for better single FOV sounding retrievals.

SFOV sounding improvement with ancillary information

Evaluation on single FOV and 3x3 FOV soundings

The single FOV retrieval algorithm has been implemented into NOAA/NESDIS operational processing. A study has been conducted to determine: (1) if a single FOV retrieval has the same or improved accuracy as the 3x3 FOV retrieval, and (2) what the advantage is of using a single FOV retrieval over 3x3 FOV retrieval.

We found that 3x3 FOV retrievals are more accurate, while single FOV (10 km spatial resolution) retrievals preserve the moisture spatial gradient better. In FY07 we will investigate using TC and SC filtering to reduce noise in the single FOV sounding product.

GOES Sounder synergy study (e.g., GOES Sounder and GPS)

Historically, we have used radiosonde observations (RAOB) as "truth" when evaluating sounding retrievals, limiting the validation to 00 UTC and 12 UTC. With Global Positioning System

(GPS) TPW measurements, we can evaluate GOES Sounder moisture retrievals for each GOES measurement. In addition, the combination of GPS and GOES Sounder radiances offers an opportunity to improve the moisture sounding product.

To test the effectiveness of using GPS, the collocated GOES-12 Sounder radiances and RAOB matchup data set is used for regression retrieval. 90% of the data set is used as training while the remaining 10% is used for testing. We studied two configurations for the predictors for moisture profile retrievals: GOES-12 Sounder radiances without GPS; and GOES-12 Sounder radiances with assumed TPW values with GPS. The assumed GPS TPW has an error of approximately 8% in the testing. Figure 1.1.3 shows the moisture mixing ratio regression retrieval RMS (against RAOB) from the above two configurations. Including the GPS TPW as a predictor reduces the RMS of the moisture profile retrieval.

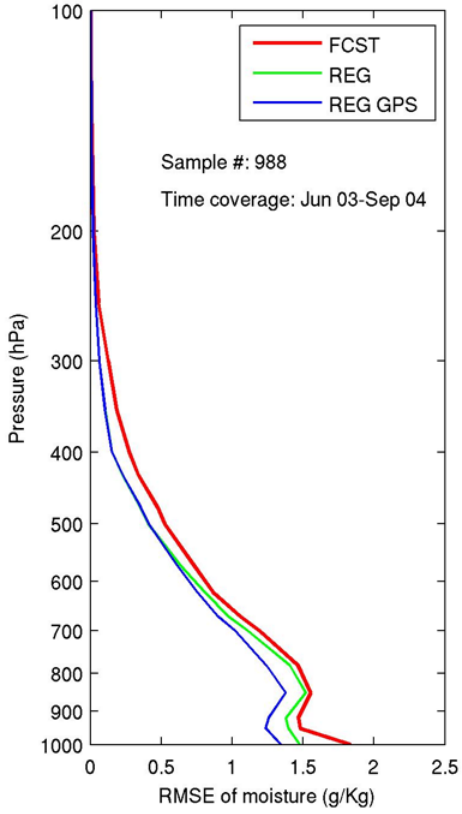

Figure 1.1.3: The moisture mixing ratio regression retrieval RMS (against RAOB) between the two configurations (with and without GPS).

Ozone improvement using Ozone Monitoring Instrument and other ozone measurement data

A new algorithm for the GOES Sounder total column ozone (TCO) retrieval has been developed to include bias correction. A 1, improvement was found applying the new algorithm over the old version (Li et al. 2001). Ozone Monitoring Instrument (OMI) data from the Earth Observing System (EOS) Aura platform were used to validate the new algorithm. Good agreement was found between OMI and GOES-12 Sounder single SFOV TCO. Figure 1.1.4 shows results from the OMI ozone algorithm. The improved GOES Sounder TCO products are now available in real-time for various applications. A manuscript on the new GOES Sounder ozone product has

been submitted to *Geophysical Research Letters* for publication (Li et al. 2007). More applications of hourly GOES ozone product will be studied in FY07. A manuscript on the new GOES Sounder ozone product has been submitted to *Geophysical Research Letters* for publication (Li et al. 2007). More applications of hourly GOES ozone product will be studied in FY07.

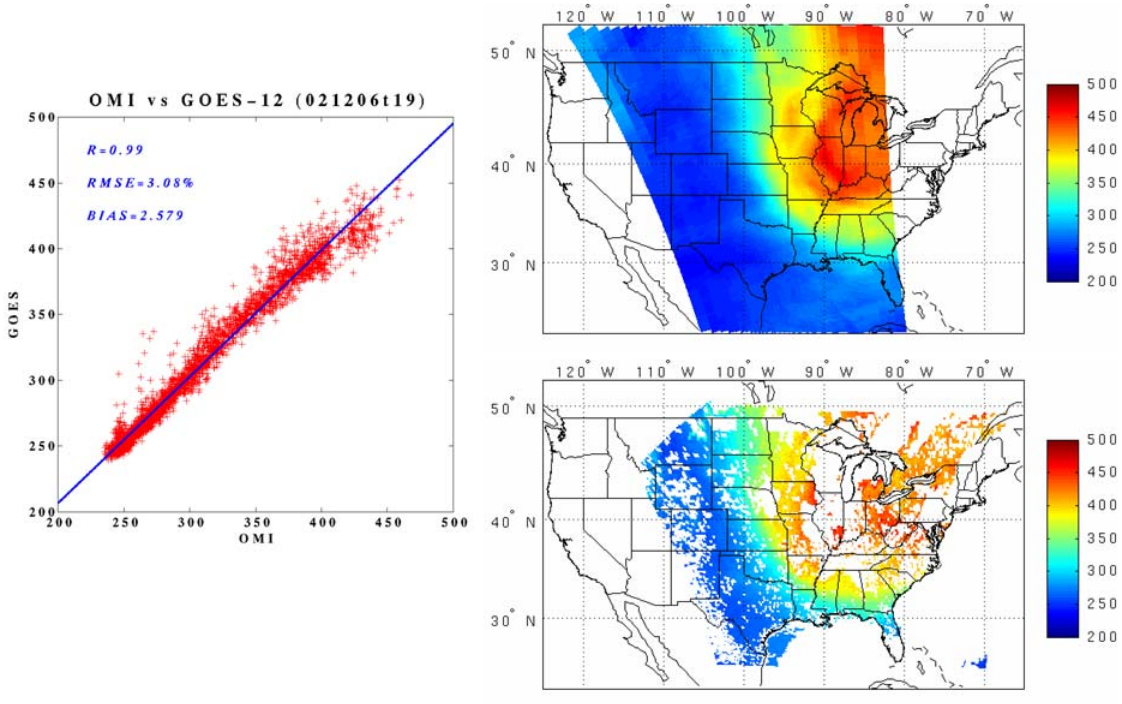

Figure 1.1.4: (Lower Right) OMI ozone; (Upper Right) GOES-12 Sounder ozone at 19 UTC, February 12 of 2006; and (Left): the scatterplot between OMI ozone measurements and GOES-12 Sounder ozone retrievals.

The improved GOES Sounder TCO retrieval algorithm (Li et al. 2007, GRL) was then compared to infrared data from the Spinning Enhanced Visible and InfraRed Imager (SEVIRI). The retrieved TCO also had very good agreement with that from OMI ozone product. We sent our SEVIRI ozone results to EUMETSAT and Dr. Johannes Schmetz, head of Meteorological Division, and Marianne Koenig at EUMETSAT, corresponded with Jun Li and Tim Schmit concerning this work. They have seen artificial ozone gradients in their SEVIRI product that follow coastlines, especially along desert areas. In the CIMSS SEVIRI ozone research product, the surface artifacts are mitigated by properly handling surface emissivity in the retrieval. Dr. Schmetz indicated that Phil Watts at EUMETSAT will revise the SEVIRI ozone product produced at EUMETSAT and will send CIMSS scientists data on the improved results.

Publications and Conference Reports

Knox, J. A., and C. C. Schmidt, 2006: GOES single FOV total column ozone: development and initial results. *Proceeding of 14th Conference on Satellite Meteorology*, Jan.29 – Feb.02, 2006,

Atlanta, GA, AMS. Paper 8.4

Li, Z., J. Li, and W. P. Menzel, 2006: Using time continuity for sounding retrieval from GOES data. *Proceeding of 14th Conference on Satellite Meteorology*, Jan.29 – Feb.02, 2006, Atlanta, GA, AMS. Paper p1.12

Li, Jinglong, Jun Li, C. C. Schmidt, J. P. Nelson III, and T. J. Schmit, 2006: High temporal resolution GOES Sounder Single field of view ozone improvements, *Geophysical Research Letters*, 34, L01804, doi:10.1029/2006GL028172.

Schreiner, A. J., S. A. Ackerman, B. A. Baum, and A. K. Heidinger, 2006: A simple technique for detecting low level cloudiness, *Monthly Weather Review* (submitted)

Schmidt, C. C., Jinlong Li and Jun Li, 2006: Estimating ozone with the GOES sounder and comparable sensors, *Proceeding of SPIE 6277*, 13 – 17 August 2006, San Diego, CA.

Bedka, Sarah T., Jun Li, W. F. Feltz, T. J. Schmit, J. P. Nelson III, and W. P. Menzel, 2006: Evaluation of GOES-12 Sounder SFOV and 3x3 retrievals of TPW over the ARM-SGP site, poster presentation at the *4th GOES-R Users' Conference* held from 01 to 03 May 2006 in Broomfield, CO.

Li, J., 2006: GIMPAP 2006 research activities at CIMSS – GOES Sounder retrieval science, *GIMPAP Review Meeting*, 11 August 2006, NOAA Science Center (presentation available upon request).

Li, Z., J. Li, T. J. Schmit, and W. P. Menzel, 2006: GOES Sounder single FOV soundings, presented at *NOAA/NESDIS Cooperative Research Program (CoRP) Third Annual Science Symposium – NPOESS, GOES-R and Beyond: New Observations and Applications to Benefit Society*, 15 – 16 August 2006, Fort Collins, CO (presentation is available upon request).

Li, Jinlong, Jun Li, C. C. Schmidt, T., J. Schmit, and W. P. Menzel, 2006: Study of total Column Ozone Retrieval from the current GOES Sounder, poster presentation at the *4th GOES-R Users' Conference* held from 01 to 03 May 2006 in Broomfield, CO.

1.2 Global Observing System Instrument Intercalibration – Mat Gunshor

Proposed Work

CIMSS proposed to work with new domestic and international instruments as they were developed and checked out following launch as part of the ongoing effort to continually characterize calibration of operational geostationary satellites. Anticipated new instruments in 2006 included Meteosat Second Generation-2 (MSG-2 or Meteosat-9), and a new high spectral resolution polar orbiter--the Infrared Atmospheric Sounding Interferometer (IASI) from EUMETSAT. Data from the latter instrument did not become available in 2006.
CIMSS also proposed to continue comparisons with the current suite of geostationary imagers, including AIRS. This included investigation of new methods of compensating for AIRS spectral gaps; and presentation of intercalibration theory, methods, and results at various conferences

Summary of Accomplishments and Findings

Characterization of new domestic and international instruments

Data from Japan's Multi-functional Transport Satellite (MTSAT-1R) will be incorporated into a number of NOAA operational products (such as Sea Surface Temperature). To ensure that the satellite delivers quality data, CIMSS monitored the calibration status of MTSAT during 2006 and results of the analyses have been relayed to John Paquette of NESDIS/OSDPD/SSD.

CIMSS also interacted with the instrument design team at Raytheon (including engineers at Space Systems/Loral) to assess the calibration accuracy of MTSAT, address problems discovered, and alleviate user concerns. For example, users reported anomalies in the MTSAT 3.7 micron channel calibration, which manifested as very bright pixels along scan lines. A static lookup table, provided by colleagues in Japan, is used to convert counts to brightness temperature. The lowest temperature in the table for each channel is 130K. In certain scenes, such as cold cloud tops, the 3.7 micron channel is measuring the coldest count possible. A brightness temperature of 130K in that band is visually incongruous with the rest of the image (the next count value corresponds to a brightness temperature of 201K in that band). It appears this effect is only noticeable in the 3.7 micron band, though it exists in all MTSAT bands. CIMSS recommended that users be made aware of this phenomenon and suggested that perhaps such fields of view should be output as missing values in their products. A calibration fix for the 3.7 micrometer shortwave channel was developed by Space Systems/Loral and implemented by the Japanese Meteorological Agency (JMA).

Calibration changes implemented by the Japanese Meteorological Agency (JMA) during the year improved the 4 micrometer imagery, especially in the range of warm temperature values. This was verified by comparisons to the Advanced Very High Resolution Radiometer (AVHRR) on NOAA-18 and AIRS co-located data.

CIMSS also worked with industry colleagues who developed the infrared instrument to produce two reports on MTSAT that were published in SPIE meeting proceedings. Multiple comparisons between MTSAT and AIRS were completed as part of the supporting analyses for these reports.

Figure 1.2.1 shows how the calibration change resulted in brightness temperatures approximately 9 degrees warmer. This appears to be a vast improvement for this band, putting it within approximately 1K of AIRS. Other MTSAT bands appear to be calibrated within the family of other geostationary sensors.

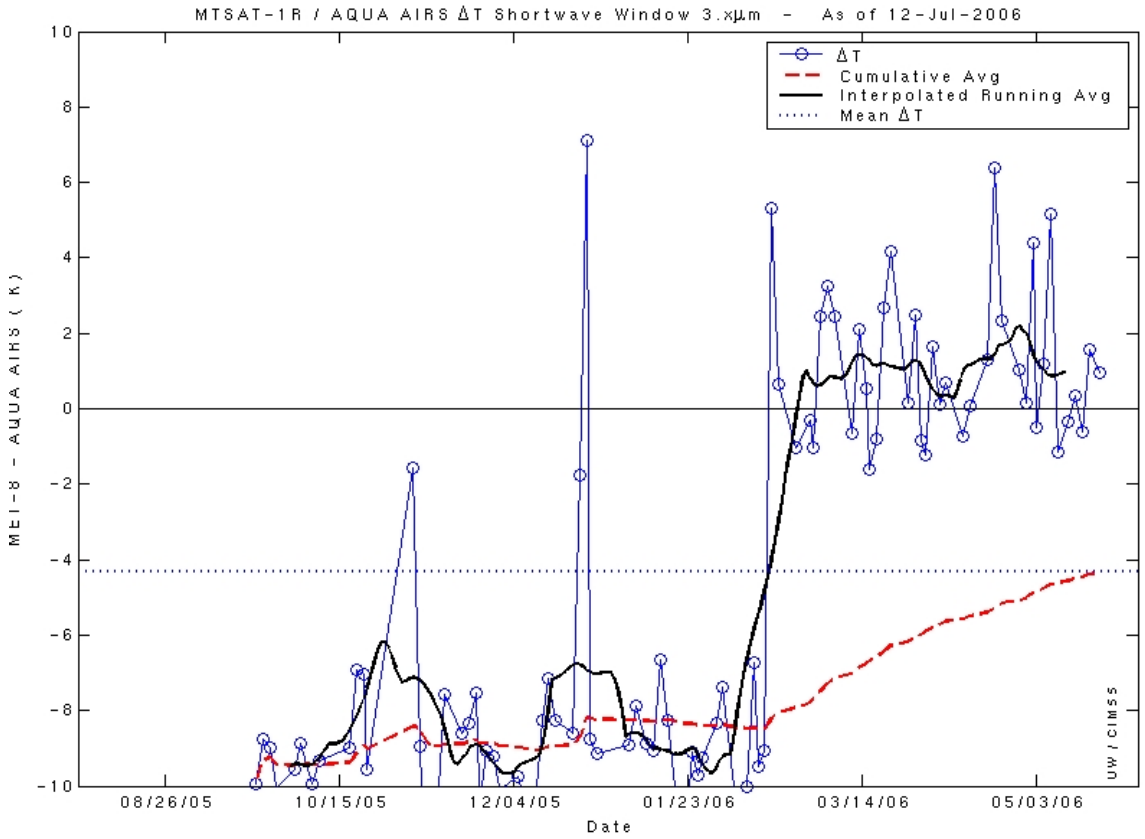

Figure 1.2.1: Time series of MTSAT-AIRS intercalibration for the 3.7μm band.

Comparison of the current suite of geostationary imagers

Due to the difference in emissivity between land and water, there is additional variance in the intercalibration results for satellites whose subpoint is over land. This was tested by comparing GOES-12 at its subpoint over South America with a second set of GOES-12 data collected off the South American coast. The variance of the means in the infrared window channel for cases collected over water was less than that for cases collected over land.

China's FY-2C geostationary imager has a major problem around satellite midnight that appears as a defect in the visible and shortwave bands, and makes even the longwave bands unusable. The problem appears to be stray light reflected off part of the satellite into the optics. China does not produce products during those hours, but they still disseminate the radiance data. It is recommended that these radiances not be used with 2 or 3 hours before or after satellite midnight. FY-2C appears to be reasonably well calibrated during other times.

The GOES-12 imager 4 micrometer spectral band has several poor space-look values that affect Experimental GOES Cloud-Top Pressure (CTP) images derived around 06 UTC near the equator. A GOES Incident Report (GIR) was generated to address this issue, and the intercalibration project provided an initial analysis of GOES-12 imagery supporting the GIR.

GOES, NOAA AVHRR, HIRS intercalibration results were presented at the "Achieving Satellite Instrument Calibration for Climate Change" (ASIC^3) workshop in Lansdowne, VA from 16-18 May 2006. Observations and recommendations concerning current intercalibration status and impediments to progress were included.

A poster titled "Intercalibration of the newest geostationary imagers via high spectral resolution AIRS data" was presented at the 14th Satellite Meteorology and Oceanography Conference in Atlanta, GA (30 January-2 February, 2006). This poster highlighted recent work on intercalibration using AIRS data. Some improvements to techniques for filling AIRS spectral gaps have been made, making the process more consistent and extending the spectral coverage beyond the AIRS endpoint on the shortwave side. Testing indicates that the improved techniques work well in clear sky fields of view but not as well in a cloudy field of view. To address this problem, a cloudy spectrum was used to fill the gaps in cloudy fields of view. This is work in progress and the results, as well as the technique, are still being analyzed.

For a short period from late September through early October, METEOSAT (MET)-9, or METEOSAT Second Generation (MSG)-2, replaced METEOSAT-8 as the operational geostationary imager servicing Europe at 0 degrees longitude. During this time eight cases of AIRS/MET-9 were collected and processed for intercalibration. These preliminary results showed that MET-9 was behaving as expected with respect to calibration.

GOES-11 has replaced GOES-10 as the operational GOES-West. Processing software was upgraded so that when GOES-11 became the operational GOES-West it would replace GOES-10 in the intercalibration routine processing package. This software was tested while GOES-11 was still moving and data were collected by the University of Wisconsin's SSEC Data Center. A comparison of the GOES-11 data with AIRS showed good intercalibration results. The 11μm band comparison is shown in Figure 1.2.2 with an outline of the AIRS granule at simultaneous sub-point overpass on the GOES image. The CIMSS team compared the average of a subset of overlapping fields of view, which revealed the mean temperature difference between GOES-11 and AIRS to be just 0.2K in this case (GOES-11 being cooler). The other infrared bands yielded results also in family for the GOES Imagers.

Publications and Conference Reports

Puschell, Jeffrey J.; Osgood, Roderic; Auchter, Joseph; Hurt, W. Todd; Hitomi, Miyamoto; Sasaki, Masayuki; Tahara, Yoshihiko; Tadros, Alfred; Faller, Ken; Mclaren, Mark; Sheffield, Jonathan; Gaiser, John; Kamel, Ahmed and Gunshor, Mathew. In-flight performance of the Japanese Advanced Meteorological Imager. In: Earth Observing Systems XI, Proc. SPIE Int. Soc. Opt. Eng. 6296, 62960N (2006).

Puschell, Jeffrey J.; Osgood, Roderic; Auchter, Joseph; Hurt, W. Todd; Hitomi, Miyamoto; Sasaki, Masayuki; Tahara, Yoshihiko; Tadros, Alfred; Faller, Ken; Mclaren, Mark; Sheffield, Jonathan; Gaiser, John; Kamel, Ahmed and Gunshor, Mathew. Update on in-flight performance of the Japanese advanced meteorological imager. In: Multispectral, Hyperspectral, and Ultraspectral Remote Sensing Technology, Techniques, and Applications, Proc. SPIE Int. Soc. Opt. Eng. 6405, 64050V (2006).

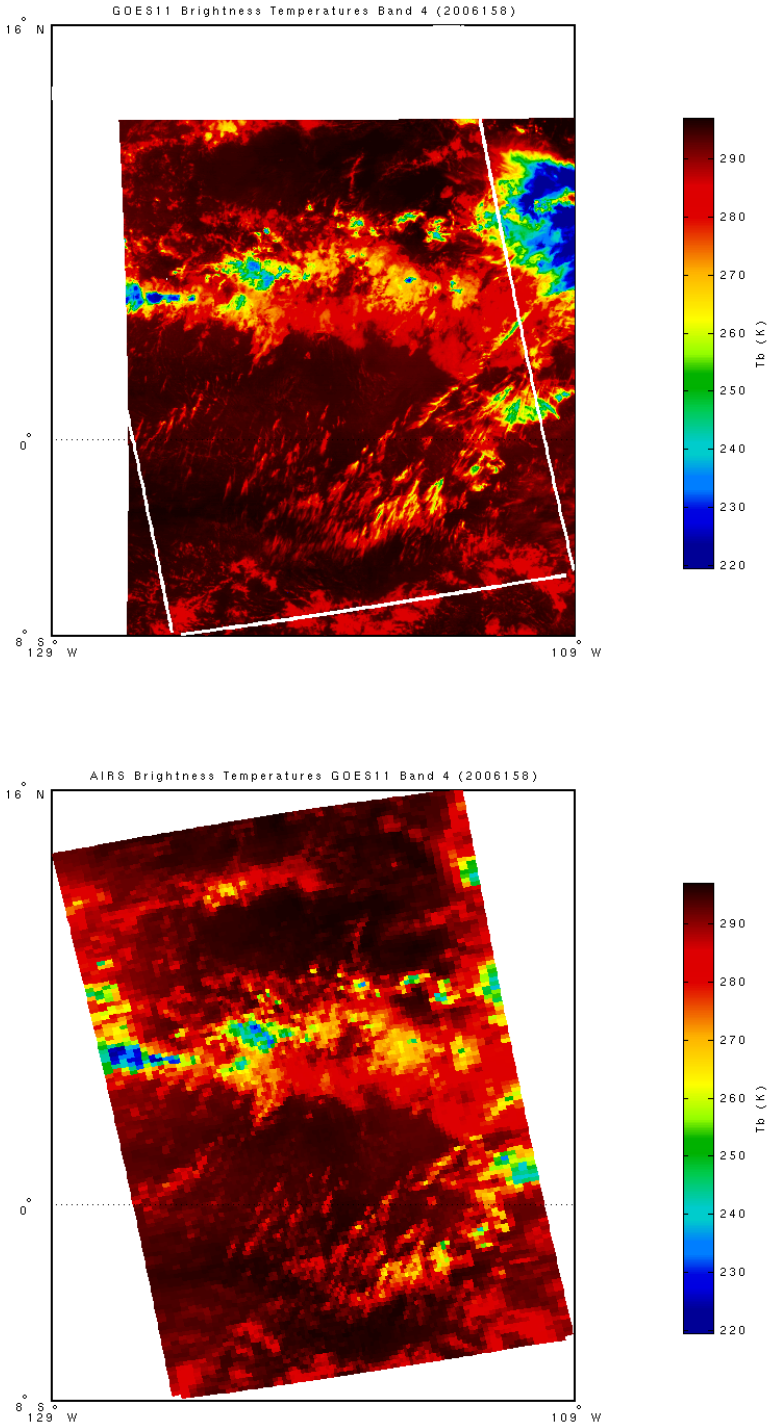

Figure 1.2.2: Infrared Window GOES-11 data from 7 June 2006 (top) compared to AIRS convolved with GOES-11 spectral response (bottom).

1.3 GOES Winds Research – Chris Velden

Proposed Work
The CIMSS automated satellite-derived winds tracking algorithm is continuously evolving. In order to advance the algorithm, new science and research ideas need to be developed and tested at CIMSS.

Summary of Accomplishments/Findings over the past 12-months includes:

(1) The CIMSS winds-tracking software continues to be modified to facilitate easy adaptation to new instruments. Satellite-specific parts of the software were identified and isolated, thereby minimizing the effort required for adding new satellites and sensors. For this reporting period, a specific example is the adaptation of the code to process newly operational GOES-11 data. In addition, the algorithm linkages necessary to ingest and process the newly launched GOES-13 data have been successfully integrated, in anticipation of the science checkout period in December 2006.

(2) The accuracy of GOES winds is highly dependent on image-to-image navigation/registration. Landmarking techniques are usually employed to deduce precise navigation, however, these landmarks are not always available for certain scans (such as GOES rapid-scanning of hurricanes over the ocean) or when clouds obscure the landmarks. We analyzed the impact of various navigation parameter errors on image navigation accuracy. Methods that employ the Earth edge and image center were tested for GOES imagery. Navigation that is based on earth center determination from earth edge measurements does not rely on landmarks, which means that it is adversely affected by excessive cloud cover. Employing these methods, navigation performance within one pixel has been realized at the Chinese National Satellite Meteorological Center for their spinning FY2B. An image center time series analysis indicates that, for the three-axis stablized GOES-9 during the Western Pacific observation mission, the image navigation accuracy is significantly reduced by errors in the forecast of spacecraft attitude. The biases in the roll and pitch can be almost eliminated by introducing the attitude signal derived directly from earth center information. Results of these navigation improvements were tested for impact on GOES winds (Table 1.3.1).

	CIMSS Landmark Navigated		S/C Roll, Pitch Auto corrected		S/C Roll, S/C Roll, Pitch corrected. S/C Yaw , PMA and RMA interactive corrected	
AMV Tracing Method	RAW	AQC	RAW	AQC	RAW	AQC
Matching Distance	100Km	100Km	100Km	100Km	100Km	100Km
Homogeneous Comparisons						
Samples	246	113	246	113	246	113
Speed Bias	0.51	2.15	-0.03	1.59	-0.08	1.27
VRMS	8.73	6.29	8.64	5.70	8.53	5.51
Average Vector Relocation Distance (Km)						
Match with Uncorrected Images	3.21	5.45	26.64	26.34	27.16	26.62

Table 1.3.1: Validation of new image navigation routine using GOES wind vector errors as a metric for accuracy. Comparisons of vector accuracy between CIMSS landmark method and the new method (landmarks not needed) show the new method to be competitive.

A significant advantage of the new method is that it does not rely on landmarks, and can be used for attitude forecasts and applied to regional scans such as GOES local area rapid scans. Combined with imager star sensing data, it is possible to build up an automatic image navigation system, and the Interactive Image Navigation test demonstrates this possibility. This new navigation technique can be applied to the GOES "IMC ON" mode, which is important since this will be the normal operational mode (GOES-E/W). The technique will need slight modifications to create a pixel-level look up table. Operational GOES winds may improve by using this look up table since it should improve frame-to-frame co-registration.

(3) Vector height assignments continue to be a leading cause of uncertainty in our satellite-derived wind algorithm. We are exploring the possibility of using GOES image pairs for cloud height assignments. Both stereo and shadow techniques are being tested in a few selected case studies. Matching software is being written and tested, and the algorithm's performance will be validated against collocated rawindsondes.

(4) Another area of vector height assignment research being investigated is the proposal that the vectors represent a mean *layer* of motion, rather than a single level. To test this hypothesis, GOES-12 Operational winds (IR and WV) are compared to collocated rawinsonde data at both individual levels and layers of varying thickness. RMS differences are calculated for groups of vectors categorized by assigned pressure. In general, upper-level winds agree best with a mean layer motion of ~100 hPa in thickness. Mid- and lower-level winds correspond best to a broader layer-- ~150 hPa thick. Mid-level WV winds can be represented by a very broad layer. Assigning the upper- and mid-level winds to a tropospheric *layer* can increase GOES wind-sonde agreement by ~1-2 m/s. In comparison, the *level** of best fit only increases agreement by ~0.5 -1 m/s. To conclude, the vector representation error can be larger than the height assignment error. To evaluate this idea further, we plan to stratify the GOES wind type/properties (i.e., height assignment methods).

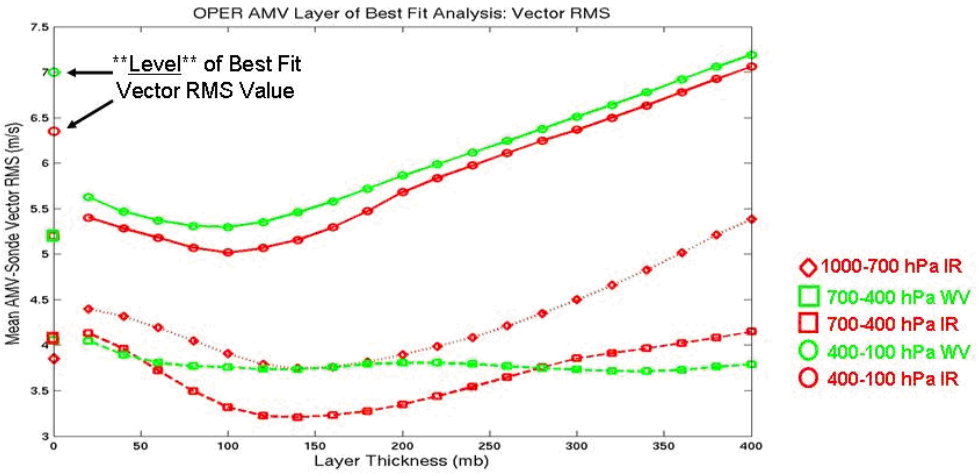

Figure 1.3.1: GOES-12 Operational winds (IR and WV, for selected tropospheric layers) are compared to collocated rawindsonde data at both individual levels and layers of varying thickness.

(5) CIMSS is also supporting elements of a tropical cyclone (TC) predictability study in

conjunction with scientists at the Naval Research Lab. Special GOES-12 rapid-scan wind datasets were processed during major hurricane events in the 2005 and 2006 Atlantic hurricane seasons. Produced at hourly intervals using 5-min rapid scans, these datasets are being tested for forecast impact in global models using variational assimilation methods. We anticipate that the GOES winds will cover important areas of the model initial analyses identified by targeting techniques as potential high impact regions. See Figure 1.3.2 for an example from a = data impact experiment using data from Hurricane Katrina. A web site with the GOES-12 datasets displays can be found at: http://cimss.ssec.wisc.edu/tropic/tropex/archive/g12winds.html

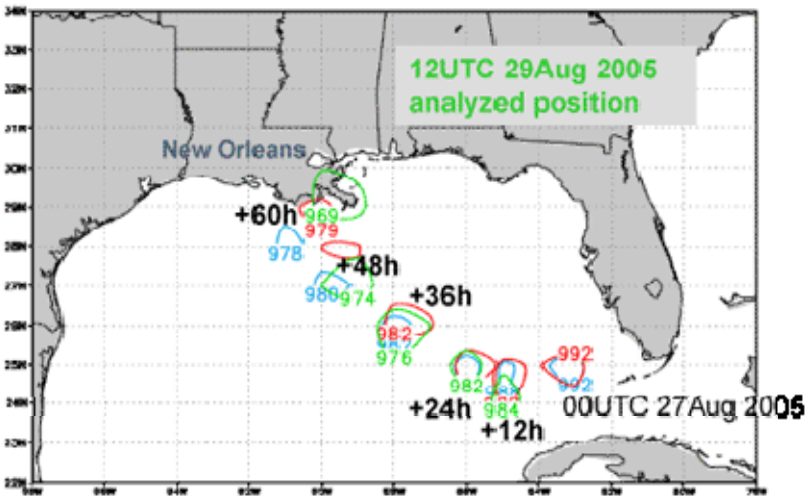

Figure 1.3.2: Forecast and analyzed positions of Hurricane Katrina from 00UTC 27 Aug – 00UTC 30 Aug 2005. Forecasts from the Navy global model assimilating the GOES RS-winds are shown by the red circles, and are an improvement over the forecasts that did not assimilate the winds (gray circles).

(6) The data assimilation community continues to struggle with effective integration of satellite-derived winds into current variational analysis schemes. As a result, observing system experiments show the winds offer only a modest positive impact on NWP forecasts. One of the strong messages from the recent International Winds Workshop (IWW) in Bejing (attended by the PI) was that the data assimilation community could use more information on vector characterization and quality. During this reporting period we have tested a new regression-based quality indicator referred to as the "Expected Error" (EE). This index is designed to be attached to every vector record in order to indicate confidence in the form of an expected vector RMSE. Our analyses suggest the EE is a better indicator of quality than the existing operational QI (Quality Indicator). We are in the process of examining this new EE for data assimilation screening properties and, eventually, for observation weighting in NWP applications.

Publications

Lu, F. and C. Velden, 2006: Attempts to improve GOES image navigation. *Proceedings of 8th WMO IWW*, Bejing, China.

Berger, H., and C. Velden, 2006: New quality indices for GOES derived winds and their potential effect on NWP data impact experiments. *Proceedings of 8th WMO IWW*, Bejing, China.

Berger, H., and C. Velden, 2006: Efforts to improve the assimilation and analysis of satellite-derived winds. *Proceedings of 2nd WMO International THORPEX Science Workshop*, Munich, Germany.

Langland, R. and C. Velden, 2006: Impact of GOES rapid-scan wind observations on NOGAPS north Atlantic hurricane forecasts. *Proceedings of 2nd WMO International THORPEX Science Workshop*, Munich, Germany.

1.4 Tropical Cyclone Research – Chris Velden

Proposed Work
CIMSS continues to develop new diagnostic fields derived from GOES data and analyses for applications to Tropical Cyclones (TCs).

Summary of Accomplishments/Findings over the past 12-months includes:

(1) The CIMSS Tropical Cyclones group continues to develop diagnostic fields derived from GOES winds analyses for applications to TCs. These products include analyses of vertical wind shear, vorticity, upper-level divergence, vertical wind shear tendency, steering currents, and surface-adjusted cloud-drift winds. All of these products are featured on the CIMSS Tropical Cyclones web site (http://cimss.ssec.wisc.edu/tropic/tropic.html), which has become an extremely popular outreach site for both the general public and forecasters during TC events. We continue to upgrade these products and develop new ones. Changes are often based on community and user feedback. Also, GOES datasets and products are continuously requested and provided to the user community for expanding scientific research on TCs.

(2) The research on identifying the Saharan Air Layer (SAL) from GOES and other satellite data, and its influence on TC intensity has been described in previous reports and led to a major paper on the topic (see Dunion and Velden, *BAMS*, March 2004). The SAL is also detectable using AVHRR split-window approaches. Data from 23 years was processed using a dust mask algorithm developed by Amato Evan (UW-AOS student thesis). Monthly means were calculated during this period over the North Atlantic Ocean basin. TC activity over this basin during these same periods was also calculated. A remarkable correlation is indicated between active SAL and inactive TC activity. The trends support the correlations and the findings/hypotheses in the *BAMS* paper. A paper on these findings has been published in *GRL*. We also aim to explore the AVHRR algorithm for applications to our GOES-based SAL algorithm.

(3) We continue to upgrade the Advanced Dvorak Technique (ADT) algorithm, which is now used by several of NOAA's tropical cyclone analysis centers. The algorithm upgrades have focused on two primary areas: 1) refinement of the rules to allow more rapid intensity changes, and 2) statistical evaluation of the performance in specific cases to better understand the behavior and areas of weakness. Several new schemes are being tested.

(4) The CIMSS TC group continues to explore an integrated approach to satellite-based TC intensity estimation through a weighted consensus of ADT, and AMSU methods derived at CIMSS and at CIRA. The approach has first identified the strengths and weaknesses of each individual method, which is then used to assign weights for a consensus algorithm designed to better estimate TC intensity. This new approach was tested in near real time during the 2006 hurricane season. A statistical analysis is underway. For more information, see: http://cimss.ssec.wisc.edu/tropic/satcon/satcon.html

Publications

Olander, T., and C. Velden, 2006: The Advanced Dvorak Technique (ADT): Continued development of an objective scheme to estimate tropical cyclone intensity using geostationary satellite IR information. Accepted in *Wea. and Fore*., to appear in forthcoming issue.

Evan, A. T., J. Dunion, J. A. Foley, A. K. Heidinger and C. S. Velden, 2006: New evidence for a relationship between North Atlantic tropical cyclone activity and African dust outbreaks. *Geophys. Res. Lett*., 33, L19813, doi:10.1029/2006GL026408.

Herndon, D. and C. Velden, 2006: Upgrades to the UW-CIMSS tropical cyclone intensity algorithm. Ext. Abstracts 27th Conference on Hurricanes and Tropical Meteorology, Monterey, CA.

Herndon, D. and C. Velden, 2006: Satellite-based Tropical Cyclone Current Intensity Consensus (SATCON). Ext. Abstracts 60th Interdepartmental Hurricane Conference, Mobile, AL.

1.5 Biomass Burning - Elaine Prins, Chris Schmidt

Proposed Work

The following biomass burning tasks were proposed for 2006:

1) continue the GOES Wildfire ABBA trend analysis throughout the western hemisphere to assess spatial, diurnal, seasonal and interannual changes in biomass burning,
2) collaborate with the user community in environmental applications of the WF_ABBA data base,
3) continue collaborations with the atmospheric modeling community to assimilate the GOES Wildfire ABBA fire product into aerosol/trace gas transport models,
4) work in collaboration with Dr. R. Rabin (NOAA/NSSL) and Dr. P. Bothwell (NOAA/NWS, Storm Prediction Center) on fire weather applications in the continental U.S, and
5) support a global geostationary fire detection system in association with GTOS GOFC/GOLD and CGMS.

Summary of Accomplishments and Findings

Continue the GOES Wildfire ABBA trend analysis throughout the western hemisphere

Over the past year the CIMSS biomass burning team continued GOES Wildfire ABBA (WF_ABBA) trend analyses throughout the Western Hemisphere and provided the WF_ABBA database (2000 – present) to the user community via an ftp site at CIMSS and an on-line database (http://www.nrlmry.navy.mil/flambe/index.html). Figure 1.5.1 provides a summary of GOES WF_ABBA fire detection from 2000 through 2007 by latitude. As in previous years peak burning was observed from 0 to 20°S along the Brazilian arc of deforestation.

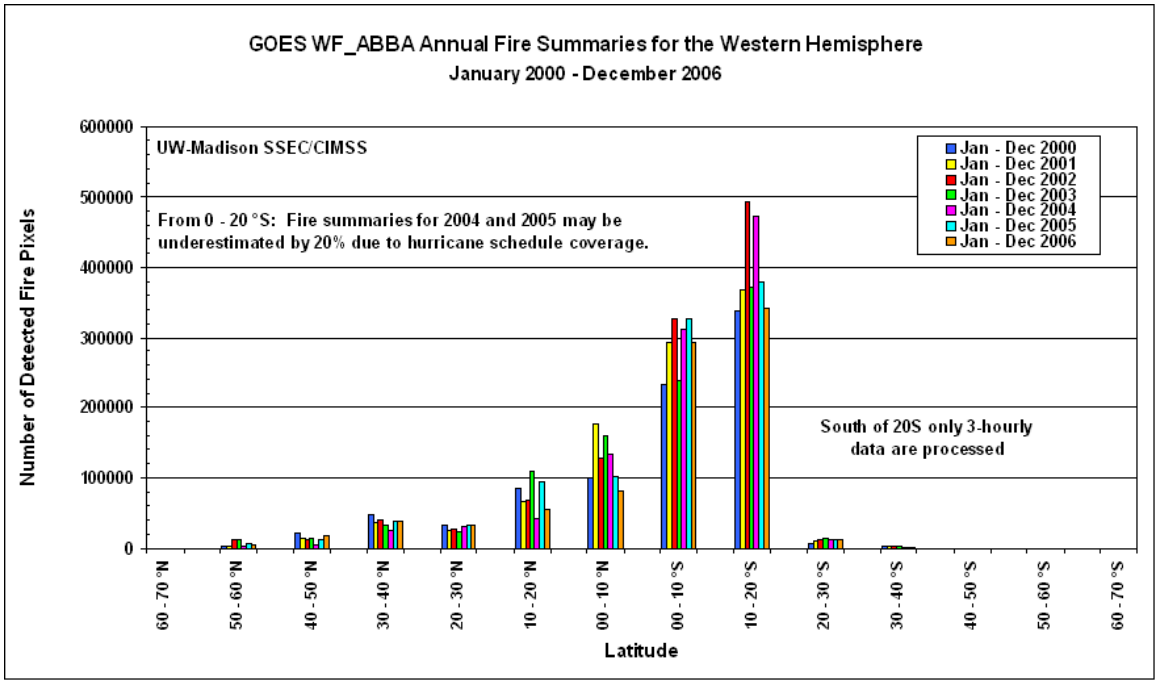

Figure 1.5.1: GOES WF_ABBA annual fire summaries for the Western Hemisphere from January 2000 through December 2006.

Throughout most of the Western Hemisphere there was a reduction in the number of GOES-observed fires. Figure 1.5.2 is a plot showing how burning during 2006 differed from 2005. Fire pixel locations that were only detected in 2005 are shown in yellow, while fire pixels detected during 2006 are shown in red. Nothing is plotted for fire pixel locations that were observed in both years. In North America (30-70 °N), the total number of detected fire pixels increased by approximately 10%. There was increased burning in the plains of Canada, Southern California, Idaho, Nevada; and in Texas and Oklahoma. In Central America (10-30 °N), there was a decrease of nearly 30%. The number of fire pixels detected in South America was approximately 10% less than observed in the previous year. There was a noticeable reduction in Colombia and Venezuela and along the arc of deforestation in Brazil and in the new frontier in Acre, Brazil. The primary regions in South America that showed enhanced burning were in north central Brazil and in eastern Bolivia.

The reduction in observed fire activity in South America in 2006 was observed even though coverage of South America was reduced by nearly 20% during 2004 and 2005 associated with GOES RSO and SRSO schedules for hurricane monitoring. In order to better account for the impact of satellite coverage and monitoring schedules for trend analyses and model data assimilation efforts, CIMSS has written code to determine coverage information for each half-hourly time period processed with the WF_ABBA since January 2000. Summary coverage files have been produced for 2000 through 2006.

Collaborate with the user community in environmental applications of the WF_ABBA data base and transport model assimilation of the GOES Wildfire ABBA fire product

Collaborative research efforts included a variety of institutions and applications ranging from fire weather in the U.S. to land-use and land-cover change in South America (e.g. Georgia Institute of Technology; UC-Irvine; Brazil INPE/CPTEC; Universidade Federal do Acre, Brazil; NCAR-Atmospheric Chemistry Division (4 efforts); NASA GSFC; UMD-College Park; NRL/FNMOC;

UA-Huntsville; US EPA; NASA Langley; Max Planck Institute; Harvard University; Sonoma Technology - USFS Blue Sky program, NOAA/NSSL, Oklahoma State University). Most of the collaborations focused on emissions modeling and data assimilation. These collaborations have resulted in three peer reviewed publications in the past year (Nepstad et al., 2006; Wang et al., 2006, Freitas et al., 2006).

For the past two years, GIMPAP biomass burning funding has partially supported a graduate student (Mr. Jay Hoffman) to address the differences between GOES and MODIS active fire products and the implications for data fusion and model assimilation. Each satellite/algorithm has unique capabilities for fire detection/characterization. In addition to the challenges of detection and parameterization of fires, each satellite fire product provides different information about fire activity. One of the largest problems faced by the modeling community is the assimilation of active fire products. To produce an accurate multi-satellite fire product, it is necessary to discriminate between fires detected by multiple satellites and fires detected by only one satellite. Some variations are expected due to orbit, instrument, and algorithm differences; however other differences can be attributed to fire characteristics. To improve user confidence, Mr. Hoffman's thesis employed new methods to identify collocated fire pixels and he applied statistical tools to characterize and better understand the differences between the Geostationary Operational Environmental Satellite (GOES) Wildfire Automated Biomass Burning Algorithm (WF_ABBA) and MODerate resolution Imaging Spectroradiometer (MODIS) fire products for enhanced applications in model assimilation.

Work in collaboration with NOAA/NSSL and NOAA/NWS/SPC on fire weather applications in the continental U.S.

CIMSS worked in collaboration with Dr. Robert Rabin (NOAA/NSSL) and Dr. Steve Stadler (Oklahoma State University, State Geographer of Oklahoma) to utilize GOES WF_ABBA fire data in combination with ancillary data sets (NDVI, soil moisture, population densities) to assess and evaluate the wildfire activity in the Great Plains during the past year and compare with the previous year. There was enhanced fire activity in eastern Kansas in April 2005 (highlighted in yellow in Figure 1.5.2) that was not detected during the following year. In the winter and spring of 2006 there was increased wildfire activity in Texas, Oklahoma, and western Arkansas (highlighted in red in Figure 1.5.2). Initial results were presented at the Southwest Association of American Geographers Meeting in Norman, OK, on 26-28 October, 2006. Further studies are being done to evaluate this data set relative to ancillary data sets. Results will be presented at the annual meeting of the Association of American Geographers in San Francisco, CA in April 2007.

Support a global geostationary fire detection system

On an international level, CIMSS has played an active role on the GTOS (Global Terrestrial Observing System) GOFC/GOLD (Global Observation of Forest and Land cover Dynamics) fire monitoring and mapping implementation team, and has provided input to CGMS on the development and implementation of a global geostationary fire-monitoring network. A specific goal of the GOFC/GOLD fire program is to develop and foster the implementation of a near real-time operational global geostationary fire monitoring network using current (GOES, MSG, MTSAT, FY-2C) and future geostationary platforms (INSAT-3D, Russian GOMS-N2/Electro, Korean COMS). This effort supports Global Earth Observation System of Systems (GEOSS) activities and the Group on Earth Observations (GEO) 2006 work plan. The GEO plan calls for the initiation of "a globally coordinated warning system for fire and monitoring for forest conversion, including the development of improved information products and risk assessment models (DI-06-13)" and the expansion of "the use of meteorological geostationary satellites for

the management of non-weather related hazards (DI-06-09)." CIMSS coordinated and co-chaired the GOFC/GOLD 2nd Workshop on Geostationary Fire Monitoring and Applications held at the EURopean Organization for the Exploitation of Meteorological SATellites (EUMETSAT) in Darmstadt, Germany on 4-6 December 2006. Over 45 representatives from 18 different countries in Europe, Africa, Asia and the Americas participated in the workshop. The primary goals of this workshop were to assess progress made since the last workshop, and to discuss ongoing activities and plans for the development, implementation, validation and application of regional and global geostationary fire products. The number of countries and research groups involved in geostationary fire monitoring has significantly grown in the last 2 years with applications in a variety of areas (hazards, air quality monitoring, climate change, and industrial applications). The GOES Biomass Burning Monitoring Team at CIMSS gave 4 presentations at the workshop.

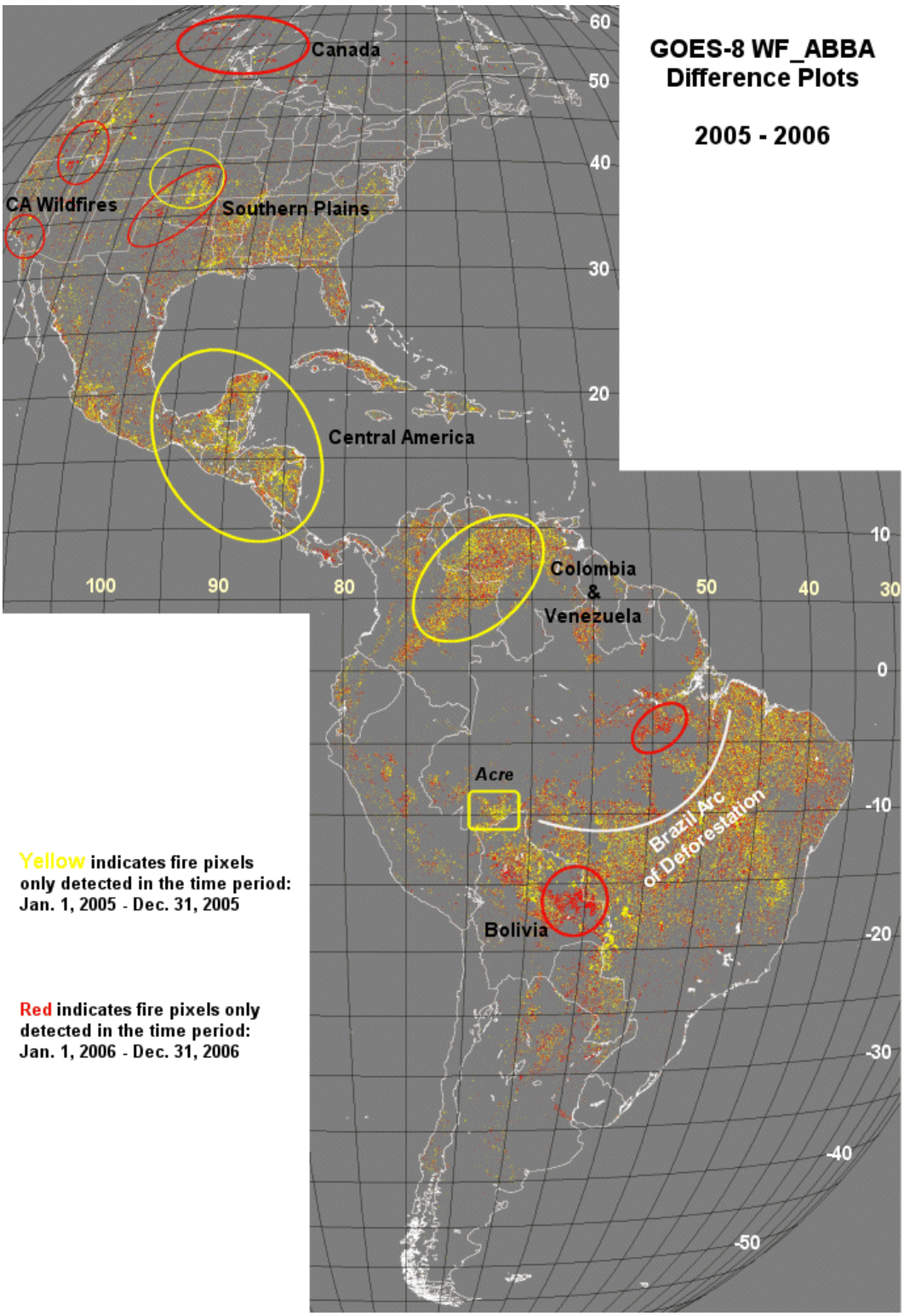

Figure 1.5.2: GOES-12 WF_ABBA filtered fire pixel difference composite for the Western Hemisphere. The yellow markers indicate fires that were only detected from 1 January– 31 December 2005. The red markers indicate fire pixels that were only identified from 1 January through 31 December 2006.

Publications and Conference reports

Freitas, S., K. longo, R. Chatfield, D. Latham, M. F. Silva Dias, M. Andreae, E. Prins, J. Santos, R. Gielow, and J. Carvalho Jr., 2006: Including the sub-grid scale plume rise of vegetation fires in low resolution atmospheric transport models, *Atmos. Chem. Phys. Discuss.*, 6, 11521-11559.

Nepstad, D., S. Schwartzman, B. Bamberger, M. Santilli, D. Ray, P. Schlesinger, P. Lefebvre, A. Alencar, E. Prins, G. Fiske, A. Rolla, 2006: Inhibition of Amazon deforestation and fire by parks and indigenous lands, *Conservation Biology*, 20,1,65-73.

Wang, J., S. A. Christopher, U. Nair, J. S. Reid, E. M. Prins, J. Szykman, J. Hand, 2006: Mesoscale transport of Central American transport to the United States, Part 1: Top down assessment of emission strength and diurnal variation impacts, *Journal of Geophysical Research - Atmospheres*, 111, D05S17, doi:10.1029/2005JD006416.

Hoffman, J. P., 2006: A Comparison of GOES WF_ABBA and MODIS Fire Products, University of Wisconsin-Madison, Department of Atmospheric and Oceanic Sciences, Madison, WI, 2006, 153 p.

Brunner, J., C. C. Schmidt, X. Zhang, and S. Kondragunta, 2006: Estimation of Biomass Burning PM2.5 Emissions Using GOES WFABBA Fire Characterization Data. Poster, Community Workshop on Air Quality Remote Sensing from Space: Defining an Optimum Observing Strategy. Boulder, CO, National Center for Atmospheric Research.

Hoffman, J. P., E. M. Prins, C. C. Schmidt, S. A. Ackerman, and J. S. Reid, 2006: Characterizing and Understanding the Differences Between GOES WF_ABBA and MODIS Fire Products, 2nd GOFC/GOLD Workshop on Geostationary Fire Monitoring and Applications, Darmstadt, Germany, December 4-6, 2006.

Hoffman, J. P., E. M. Prins, C. C. Schmidt, S. A. Ackerman, and J. S. Reid, 2007: Characterizing and understanding the differences between GOES WF_ABBA and MODIS fire products and implications for data assimilation, Submitted to 87th AMS Annual Meeting, San Antonio, TX, January 2007.

Hyer, E., J. Reid, E. Prins, C. Schmidt, 2006: Identifying and Reducing Key Uncertainties in Biomass-Burning Emissions in a Model Based on Active Fire Detection, 2nd GOFC/GOLD Workshop on Geostationary Fire Monitoring and Applications, Darmstadt, Germany, December 4-6, 2006.

Prins, E., C. Schmidt, J. Feltz, J. Brunner, S. Lindstrom, J. Hoffman, 2006: Status and Plans for Global Geostationary Fire Detection and Monitoring With the Wildfire ABBA, 2nd GOFC/GOLD Workshop on Geostationary Fire Monitoring and Applications, Darmstadt, Germany, December 4-6, 2006.

Reid, J. S., E. Hyer, D. L. Westphal, C. Curtis, K. Richardson, E. Prins, C. Schmidt, S. Christopher and J. Wang, 2006: Fire Locating and Modeling of Burning Emissions (FLAMBE): 7 Years of Progress and Prospects, 2nd GOFC/GOLD Workshop on Geostationary Fire Monitoring and Applications, Darmstadt, Germany, December 4-6, 2006.

Schmidt, C., J. Brunner, E. Prins, R. Rabin, 2006: GOES Rapid Scan Wildfire ABBA, 2nd GOFC/GOLD Workshop on Geostationary Fire Monitoring and Applications, Darmstadt, Germany, December 4-6, 2006.

Stadler, S., A. Finchum, R. Rabin, P. Bothwell, E. Prins, J. Brunner, C. Schmidt, 2006: An Exploratory Explanation of Oklahoma's Wildfire Pattern Using Spatial Databases, Southwest Association of American Geographers Meeting, Norman, OK, October 26-28, 2006.

Stadler, S., A. Finchum, B. Battles, R. Rabin, P. Bothwell, E. Prins, 2007: Relationships Between Oklahoma Wildfire, Population Density, And Fuel Availability, Submitted to Annual Meeting of the Association of American Geographers, San Francisco, CA, April 17-21 2007.

Wang, J., S. Christopher, E. Prins, J. Reid, X. Liu, 2006: Transport of Central American Biomass Burning Smoke Aerosols in 1979 – 2005, 14th Conference on Satellite Meteorology and Oceanography, Atlanta, Georgia, 29 January–2 February 2006.

1.6 Further Exploration of GOES IR Data with the Goal of Improving Hurricane Intensity Forecasting – Jim Kossin and Chiou-Jiu Chen

We used a new data archive consists of GOES IR imagery for the period 1983–2005 (described in Knapp and Kossin 2007), and considered two data sets based on this new record: time series of the full 2-D imagery and azimuthally averaged profiles of brightness temperature (Tb). Our goal was to test whether we can add information to the regression model that the SHIPS forecasting model is based on. The SHIPS model employs a number of IR-derived parameters, but the IR data had not yet been fully explored in this context.

We began by performing EOF analyses on the data – both the 1-D profile data and the full 2-D imagery. Only 1-D IR information is currently used in the SHIPS model, and there was unexplored potential for identifying signals in the 2-D fields that may be related to subsequent intensity change. Since the 2-D EOFs capture variance in the azimuthal direction and some percentage of this variance was expected to be due to the variance of the shear vector direction, we first rotated the 2-D images so that all of them were uniformly oriented along the contemporaneous shear vector. EOF analysis was then performed on the time series of the rotated imagery. Once we had the PCs from the various EOF analyses, we performed a variety of tests with them to see if they bring new information to the problem.
The SHIPS data contain 33 variables, including some basic predictors based on GOES-IR imagery. We added the PCs to this predictor pool and performed stepwise regression to determine if the PCs explain additional variance of intensity change. Our main result is that the PCs do not explain more variance by themselves than the present GOES predictors do, and they bring little independent information to the model. The one exception we found was for forecasts issued on major hurricanes (Category 3 to 5). In these cases, adding the PCs measurably increased the explained variance of 24-hour intensity forecasts.

Our next step will be to coordinate with Mark DeMaria (CIRA/NOAA/NESDIS) to provide the GOES-IR predictors for the period 1983–2005 for inclusion into the SHIPS model. This will extend the SHIPS (with the existing GOES predictors) training data considerably, from the present period of 1995–2005.

1.7 Outreach and Education – Margaret Mooney

Proposed Work
Outreach and Education efforts at CIMSS focus on sharing remote sensing data and products with society to enhance science literacy while raising awareness about the benefits of satellite technology. This is accomplished directly through presentations, workshops and the development of educational material and software. It is also accomplished by making data and information freely available on the Internet. For example, the CIMSS Tropical Cyclone web site routinely receives several million hits during any single storm event.

Accomplishments
The first significant outreach event of 2006 took place in January at the annual American Meteorological Society Meeting (AMS) in Atlanta, GA. Along with a presentation and participation in the 15th Symposium on Education, EPO Specialist Margaret Mooney staffed a booth at WeatherFest with Tom Whittaker and Rick Kohrs featuring educational applets developed by Mr. Whittaker and Steve Ackerman.
(http://cimss.ssec.wisc.edu/wxfest/explore.html)

Throughout the four-hour event there were three lines of elementary and middle school children (and parents) waiting to "explore the atmosphere" via highly interactive computer-based activities. Four hundred CD-ROMs featuring the educational applets were distributed at WeatherFest and the Symposium on Education. Also distributed at the symposium were additional CD-ROMs featuring "Satellite Meteorology for Grades 7-12" and fliers announcing the CIMSS summer workshops.

The success at WeatherFest was duplicated at University of Wisconsin-Madison's Science Expeditions in April where over a thousand youths used the educational applets and took home CDs to explore and learn on their own. Other state-based events include a presentation at the annual meeting of the Wisconsin Society of Science Teachers and hosting a "meteorology major" for alumni and their grandchildren at the UW's Grandparents University.
CIMSS conducted a Teacher Workshop on Remote Sensing and Satellite Meteorology for middle and high school educators in June. This two-day event included several hands-on sessions interspersed with lectures by research and operational meteorologists who routinely use satellite products to do their job, such as the Milwaukee/Sullivan NWS Science and Operations Officer.

In July, CIMSS hosted the 14th annual summer workshop on Atmospheric, Earth and Space Science for high school students. This workshop, which has established a legacy in the educational community, became partially self-sustaining in 2006 by initiating a minimal tuition fee to cover funds previously provided through grants. This experiment in program sustainability proved successful with 14 students enrolling, two were granted financial aid scholarships.

In July, CIMSS hosted the 14th annual summer workshop on Atmospheric, Earth and Space Science for high school students. This workshop, which is well known in the educational community, became partially self-sustaining in 2006 by charging a minimal tuition fee to cover funds previously provided through grants. This experiment in program sustainability proved successful: 14 students enrolled and two were granted financial aid scholarships.

Due to the accessibility of information on the Internet and Madison's intellectual vitality, CIMSS workshops accommodate national and international audiences with approximately one-fourth of our

participants traveling from out of state. In 2006, one educator came from Micronesia for the teacher workshop and one high school student flew from Norway for the popular student workshop.

The year concluded with a celebration to honor the 40th anniversary of the first geostationary satellite and the career of Verner E. Suomi on December 6th. The agenda featured formal presentations by Paul Menzel and Steve Ackerman followed by a reception with several informal commemorative speeches. The event also included the unveiling of plans for the Suomi Science Museum to be located off the lobby of the Atmospheric, Oceanic and Space Science building on the UW-Madison campus. The museum will feature informative historical displays and exciting state-of-the art interactive activities. Along with paying tribute to Dr. Suomi's pioneering contributions to the field of satellite meteorology, the museum will highlight the connections between NOAA and CIMSS and successive advancements in remote sensing satellite technology.

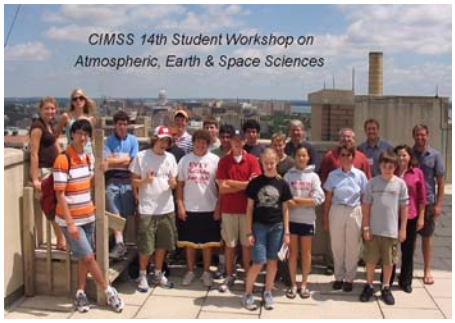

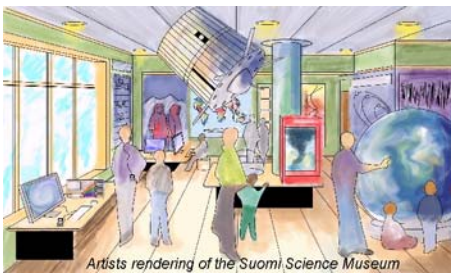
Artists rendering of the Suomi Science Museum

Publications and Conference Reports
15th Symposium on Education, AMS Annual Meeting, January 2006, "Satellite Meteorology Resources for K-16 Educators and Students", Margaret Mooney and S. A. Ackerman

7th International Conference on School and Popular Meteorological and Oceanographic Education, July 2006, "ESIP and CIMSS: Increasing the Use and Usability of Satellite Data in Science Classrooms", Margaret Mooney and S. A. Ackerman

2 CIMSS Support for Polar and Geostationary Satellite Science Topics (PSDI)

2.1 Intercalibration of GOES and POES – Mat Gunshor

Proposed Work
Calibration and instrument intercomparison are the main methods by which individual instruments can be validated against one another between geostationary and polar orbiting platforms. Routine automated intercalibration provides information on how operational geostationary environmental satellites around the globe compare radiometrically. CIMSS has been intercalibrating satellite instruments routinely since 1999 and the methodology is documented in the research journal literature.

The primary task for FY2006 was to continue routine intercalibration using NOAA-15 and -16 AVHRR and HIRS compared with GOES-10, -11 and -12, and Meteosat-5, -7 and -8. The continuation of routine intercalibration requires regular maintenance and periodic archiving. CIMSS proposed to continue to write, update, and maintain a large volume of software directly

related to this project. A web page was to be maintained to communicate results to the user community.

Summary of Accomplishments and Findings

In 2006, the continuation of routine intercalibration continued. Thousands of comparisons were made between polar-orbiting AVHRR and HIRS (on NOAA-15 and -16), and the imagers on GOES-10, -11 and -12, and Meteosat-5, -7, and –8 in the infrared window, water vapor, and 13.3 micrometer channels. As planned, GOES-11 took over as the operational GOES-West and was added to the routine processing suite. The intercalibration webpage at CIMSS was updated to include GOES-11 results and examples. The web page was also updated so that results from no longer operational instruments are part of an archive section. A large volume of software and ancillary data was updated and is maintained on the CIMSS Concurrent Versions System (CVS). The satellite and model data used to process individual calibration cases was periodically archived from the processing disks to make space for new cases.

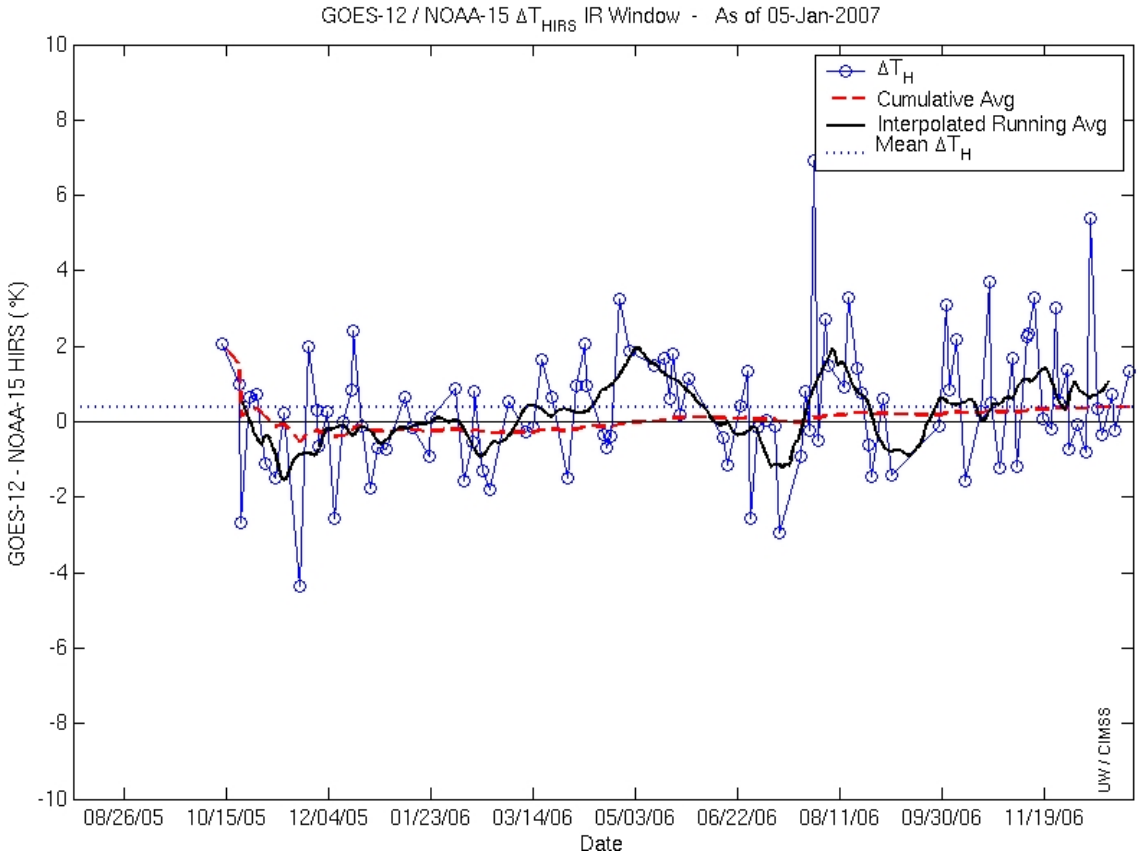

Figure 2.1.1: Time series of GOES-12-NOAA-15 HIRS Intercalibration cases from mid October 2005 through the end of December 2006. Similar plots for GOES-9,-10,-11, and –12 compared to NOAA-15 and NOAA-16 HIRS and AVHRR are updated daily on the CIMSS intercalibration website: http://cimss.ssec.wisc.edu/goes/intercal

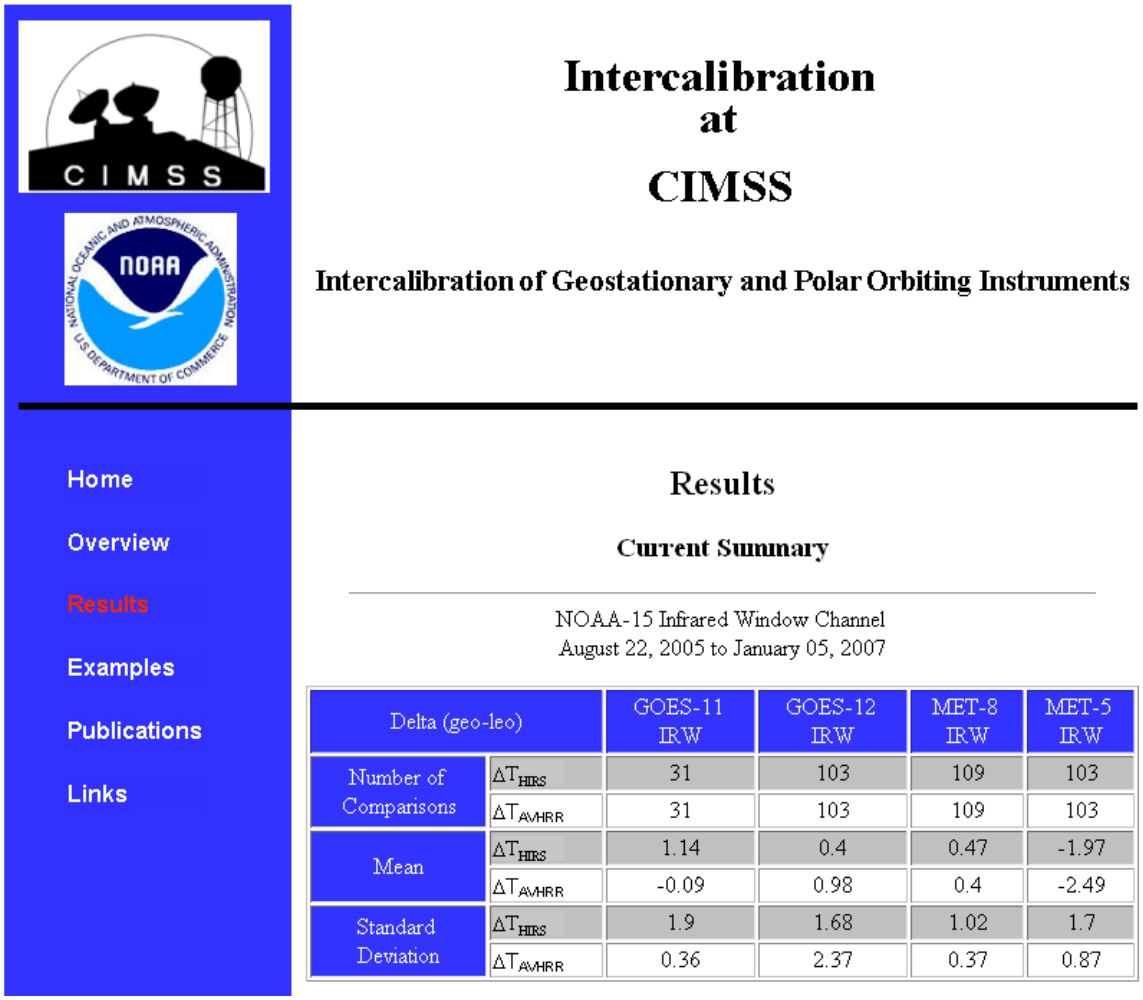

Delta (geo-leo)		GOES-11 IRW	GOES-12 IRW	MET-8 IRW	MET-5 IRW
Number of Comparisons	ΔT_{HIRS}	31	103	109	103
	ΔT_{AVHRR}	31	103	109	103
Mean	ΔT_{HIRS}	1.14	0.4	0.47	-1.97
	ΔT_{AVHRR}	-0.09	0.98	0.4	-2.49
Standard Deviation	ΔT_{HIRS}	1.9	1.68	1.02	1.7
	ΔT_{AVHRR}	0.36	2.37	0.37	0.87

Figure 2.1.2: Snapshot of results posted to Intercalibration webpage on 5 January 2007. Results here show the mean and standard deviation of all cases processed to date.

Publications and Conference Reports
Publications and Conference Reports for Intercalibration are considered part of the research arm of Intercalibration at CIMSS and are funded and reported under CIMSS GIMPAP Intercalibration.

2.2 GOES Wildfire Algorithm - Elaine Prins, Chris Schmidt

Proposed Work
The UW-Madison biomass burning team proposed several tasks for 2006:

(1) To continue producing half-hourly WF_ABBA fire products in real time and make them available via the web and anonymous FTP;
(2) To finalize implementation of and improve upon the Rapid Scan WF_ABBA to take advantage of high temporal resolution data for early wildfire detection applications in the U.S.;

(3) To implement automated real-time GOES-9 and Meteosat-8 (formerly Meteosat Second Generation) fire processing capabilities and participate in a Meteosat-8 fire detection demonstration study in cooperation with GOFC/GOLD, EUMETSAT and the EU civil protection and fire service;
(4) To continue to participate in international satellite fire product validation and inter-calibration activities. Results were to be used to reduce false alarms and minimize actual fires eliminated by temporal filtering techniques.

Summary of Accomplishments and Findings
Ongoing support for WF_ABBA realtime processing involves adapting to issues that arise with the various satellites. On or about 1 Feb 2006 the 4 μm channel on the GOES-12 Imager began reading radiances beyond the predefined range for GVAR counts, causing hot pixels to appear as extremely cold (bad data). Figure 2.2.1 shows an example of this behavior. The very hot pixels appeared white when they should appear black. CIMSS discovered the problem and participated in investigating the source. It was eventually determined that the degraded sensor performance was due to a pre-existing issue with a heating element within the optical bench of GOES-12. CIMSS developed a patch and method for tracking when this occurs. During this investigation it was found that similar "rollover" occurred with GOES-11 in 2002 when GOES-11 was run in SRSO-mode during the IHOP campaign.

GOES-10 was decommissioned in early June of 2006. As a result, GOES-11 support had to be implemented at NESDIS before GOES-11 became the operational GOES-West. GOES-11 support was successfully implemented at NESDIS before GOES-11 became operational. At the same time, the aforementioned "rollover patch" was implemented at NESDIS.

In FY2006 CIMSS continued to support WF_ABBA validation work. Wilfrid Schroeder validated GOES and MODIS fire detections against high resolution ASTER scenes as part of a project at NESDIS/Ops. It was found that the false-positive rates for both MODIS and GOES were comparable at around 2%. It was also found that analysts did not necessarily improve the error of omission and error of commission rates. CIMSS provided data and expertise in support of this work.

Aside from Mr. Schroeder's work CIMSS has also been developing innovative ways to look at GOES and MODIS fire data comparisons to apply to fire data fusion applications and calibration/validation. For the past two years PSDI biomass burning funding has partially supported a graduate student (Mr. Jay Hoffman) to address the differences between GOES and MODIS active fire products and the implications for data fusion and model assimilation. Each satellite/algorithm has unique capabilities for fire detection/characterization. In addition to the challenges of detection and parameterization of fires, each satellite fire product provides different information about fire activity. Some variations are expected due to differences in orbit, instrument, and algorithm; however other differences can be attributed to fire characteristics. To improve user confidence, Mr. Hoffman's thesis employed new methods to identify collocated fire pixels and applies statistical tools to characterize and better understand the differences between the Geostationary Operational Environmental Satellite (GOES) Wildfire Automated Biomass Burning Algorithm (WF_ABBA) and MODerate resolution Imaging Spectroradiometer (MODIS) fire products for enhanced applications in model assimilation.

An initial version of the Met-8 WF_ABBA is being tested at CIMSS. Met-8 is substantially different from the GOES satellites in a number of ways. One of the most important differences is the remapping performed on the original data. While the goal of providing stable, accurate

navigation is laudable, the data is altered in such a way that fire detection becomes more difficult. Changes have been required to adapt the WF_ABBA to those circumstances. A working version of WF_ABBA support for MTSAT-1R is currently in testing and due to the different style of sensor (CCD array) and down-sampling performed by the satellite operator, the WF_ABBA requires modifications for that satellite as well.

The rapid-scan WF_ABBA is in testing phase at CIMSS. The goal of this product update is to process all data downloaded from supported satellites. There are implementation challenges to making this run reliably in real time while handling changes to data schedules, data drop-outs, and other occurrences that can derail real-time processing. The RSO WF_ABBA also will result in a great number of detected fires--as many as 50% based on early studies. These fires are typically short-lived fires or fires temporarily obscured by clouds. The impact of the larger dataset on the match rate to other products from satellites such as MODIS has yet to be examined. Figure 2.2.2 shows examples of the "classic" WF_ABBA and the RSO WF_ABBA from a typical day during the spring of 2006. The increased number of detected fires is readily apparent.

Publications and Conference Reports

Peer-Reviewed Publications/Thesis

Hoffman, J. P., 2006: A Comparison of GOES WF_ABBA and MODIS Fire Products, University of Wisconsin-Madison, Department of Atmospheric and Oceanic Sciences, Madison, WI, 2006, 153 p.

Conferences Presentations/Papers/Posters

Hoffman, J. P., E. M. Prins, C. C. Schmidt, S. A. Ackerman, and J. S. Reid, 2006: Characterizing and Understanding the Differences Between GOES WF_ABBA and MODIS Fire Products, 2nd GOFC/GOLD Workshop on Geostationary Fire Monitoring and Applications, Darmstadt, Germany, December 4-6, 2006.

Hoffman, J. P., E. M. Prins, C. C. Schmidt, S. A. Ackerman, and J. S. Reid, 2007: Characterizing and understanding the differences between GOES WF_ABBA and MODIS fire products and implications for data assimilation, Submitted to 87th AMS Annual Meeting, San Antonio, TX, January 2007.

Prins, E., C. Schmidt, J. Feltz, J. Brunner, S. Lindstrom, J. Hoffman, 2006: Status and Plans for Global Geostationary Fire Detection and Monitoring With the Wildfire ABBA, 2nd GOFC/GOLD Workshop on Geostationary Fire Monitoring and Applications, Darmstadt, Germany, December 4-6, 2006.

Schmidt, C., J. Brunner, E. Prins, R. Rabin, 2006: GOES Rapid Scan Wildfire ABBA, 2nd GOFC/GOLD Workshop on Geostationary Fire Monitoring and Applications, Darmstadt, Germany, December 4-6, 2006.

Schroeder, W., Czsisar, I., 2006: GOES Active Fire Product Validation Using High Resolution Data, 2nd GOFC/GOLD Workshop on Geostationary Fire Monitoring and Applications, Darmstadt, Germany, December 4-6, 2006.

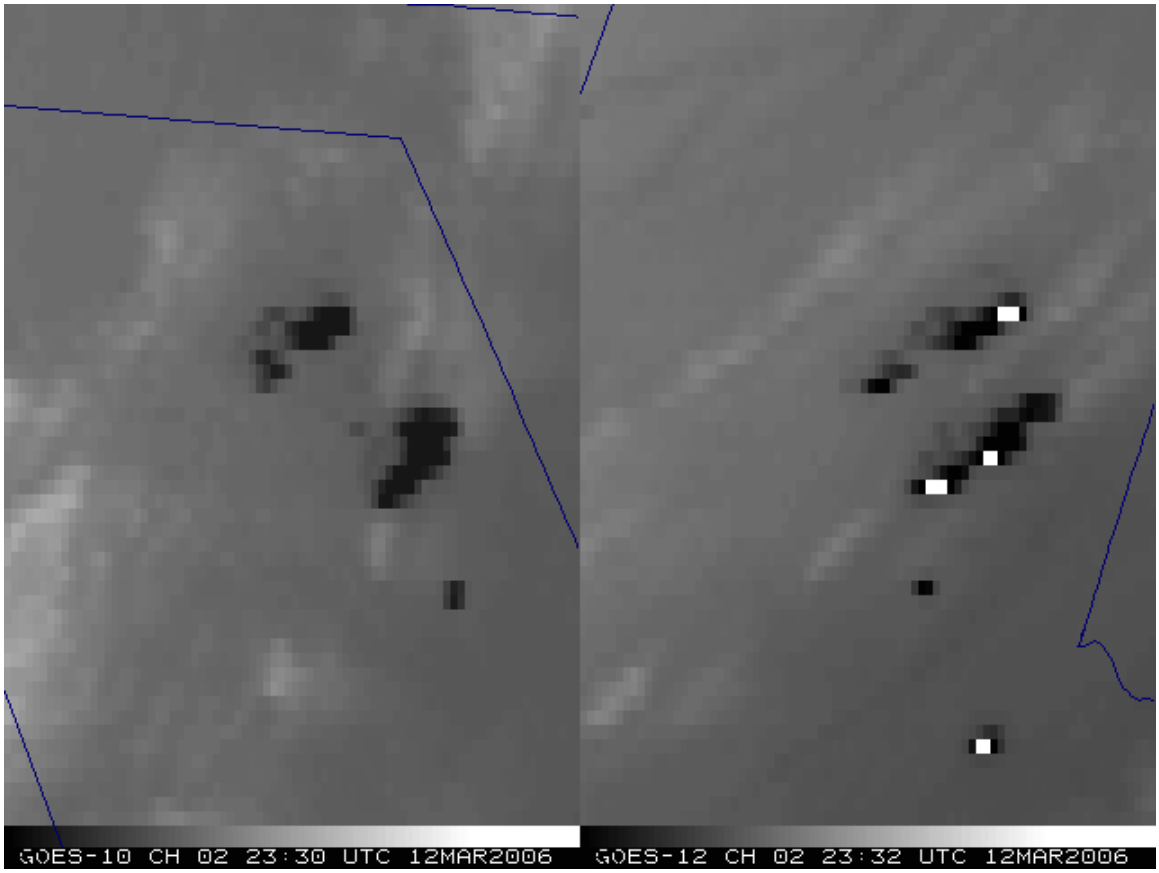

Figure 2.2.1: GOES-10 versus GOES-12 on 12 March 2006 at approximately 23:30 UTC. The white pixels on the GOES-12 image are "rollover" pixels where the satellite-reported radiance ran over the top of the pre-defined GVAR scale. The fires shown were in Texas and were very hot and spread very quickly.

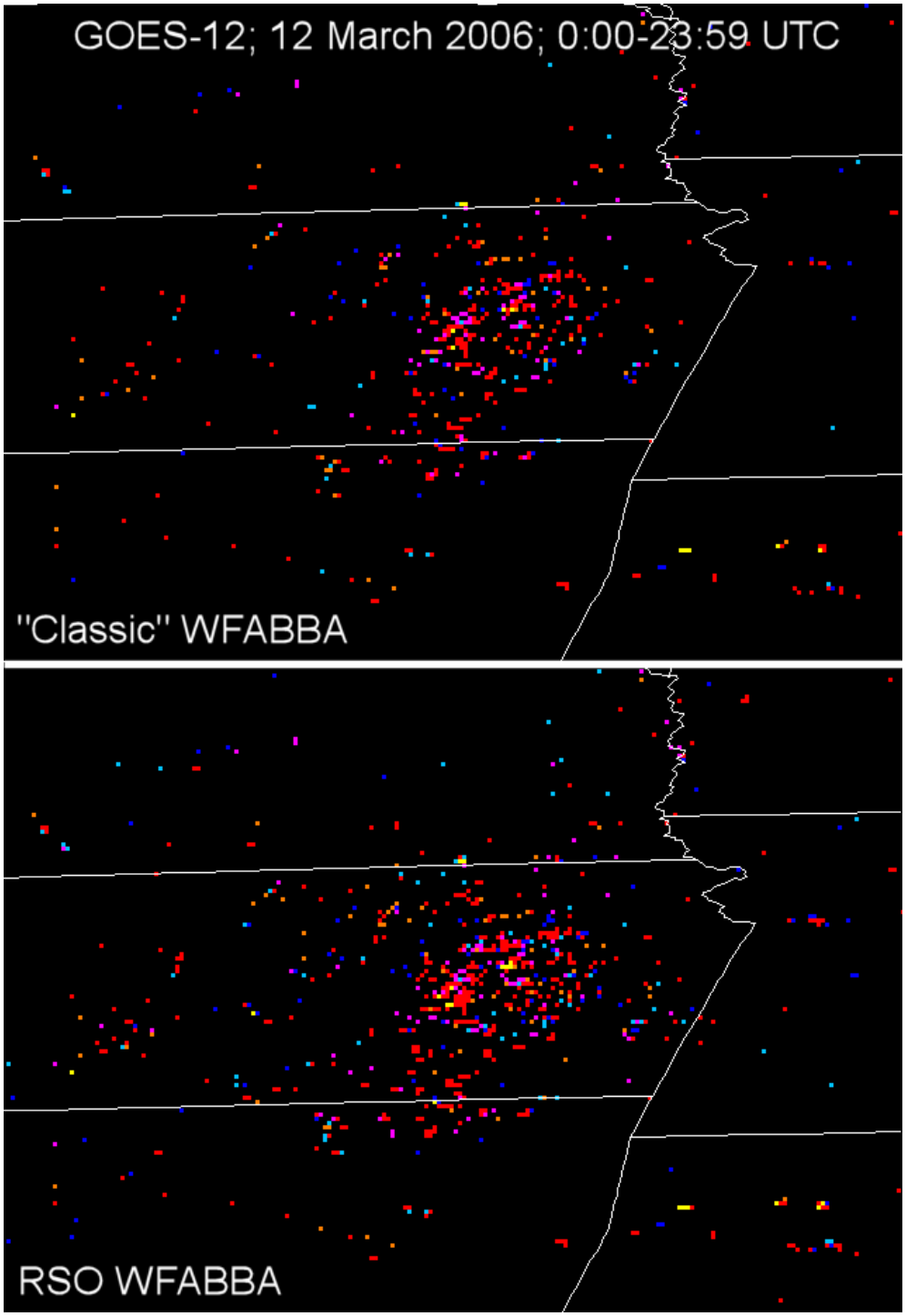

Figure 2.2.2: GOES-12 WF_ABBA for all day on 12 March 2006. The top image is the "classic" half-hourly WF_ABBA, and the bottom half is the RSO WF_ABBA with all available data from that day processed. The RSO WF_ABBA detected roughly 50% more individual fires. The images in this figure cover agricultural burning in Kansas.

2.3 Geostationary Winds Support – Chris Velden

Proposed Work

CIMSS has supported the research and development of the automated satellite winds tracking software for the last 25 years. Under this funding, the CIMSS winds research team helps maintain and advance the winds algorithm science modules and capabilities. This includes any new science advances, validation, and developments for the science community. The algorithm upgrades are then made available to colleagues at NOAA/NESDIS for operational consideration/implementation.

Summary of Accomplishments/Findings

(1) We provided code science advances/upgrades to USAF/AFWA (NESDIS operational national backup). CIMSS is providing software assistance and upgrades to AFWA as their GOES winds production is now operational. The goal is to keep the algorithm version reasonably close to the NOAA/NESDIS operational version for output consistency.

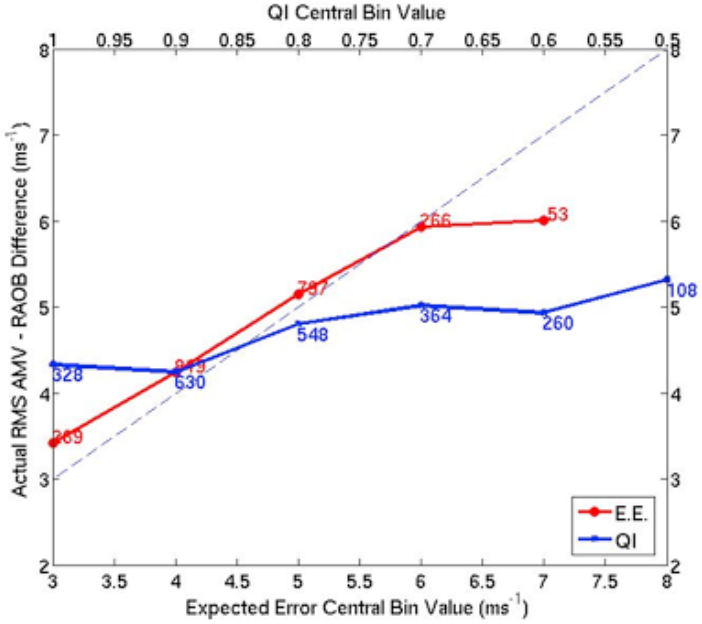

Figure 2.3.1: Comparison of the new Expected Error (EE, solid red curve) quality indicator for GOES winds with the current operationally employed AMV Quality Indicator (QI, solid blue curve) for operational GOES-E IR winds during August - September 2005. Actual RMS differences between collocated GOES – RAOB are used to assess each parameter as a quality indicator. As the curves show, the EE relationship is a better predictor of measured GOES – RAOB differences than the QI. The 1-1 line (dashed blue) is plotted for reference. The numbers in red and blue represent respectively: the number of winds in the EE-bins and in the QI-bins

(2) The implementation and testing of new QC software obtained from John LeMarshall (JCSDA) continues. This code appends a new vector "expected error" (EE), which will be useful for data assimilation purposes. The code has been rewritten from its original format into code compatible with GOES winds algorithm versions currently in place at

CIMSS and operationally at NOAA/NESDIS. Testing has yielded reasonable EE values (see Figure 2.3.1), and it appears this indicator may have more value than the currently employed QI index. The EE will be tested operationally by NESDIS in the coming months.

In addition to the above accomplishments, CIMSS is a responder to Winds POP action items, as well as an active member of the WMO-sponsored International Winds Workshops. Four CIMSS scientists working on GOES winds research attended the recent IWW in Bejing, China. Through these venues, ideas are continuously exchanged between the CIMSS PIs, the NESDIS winds specialists, and the international winds community.

Publications

Berger, H., and C. Velden, 2006: New quality indices for GOES derived winds and their potential effect on NWP data impact experiments. *Proceedings of 8th WMO IWW*, Bejing, China.

Berger, H., and C. Velden, 2006: Efforts to improve the assimilation and analysis of satellite-derived winds. *Proceedings of 2nd WMO International THORPEX Science Workshop*, Munich, Germany.

2.4 GOES Spectral Response Studies – Mat Gunshor

Proposed Work

CIMSS scientists were to prepare for quantitative use of GOES Sounder and Imager radiances through the generation of transmittance files calculated from Spectral Response Functions (SRF) in conjunction with a line by line radiative transfer model (LBLRTM). The primary goal of this research is to maintain a high level of accuracy in the calculations and resulting products obtained from the GOES series of Sounders and Imagers. A secondary goal was to maintain existing GOES expertise in this area and apply it to other instruments, such as international imagers (e.g., Meteosat, FY-2C) and polar-orbiting instruments (e.g., NOAA, MODIS). For example, Meteosat Second Generation (MSG)-2 test data were expected to become available in spring 2006. Transmittance files and weighting functions needed to be generated so that scientists could properly utilize those data

The first objective for 2006 was to calculate the Planck Function Coefficients (PFC) needed to convert radiances into temperature for the GOES Imager and Sounder, make them available for implementation into McIDAS, and distribute them to the user community via the Internet. Calculations needed to be made for the GOES-N, O, and P; and be updated as necessary for the current operational GOES (10, 11, & 12) instruments.

The second objective was to create and test GOES Sounder and Imager transmittance files in binary format for the Pressure Layer Optical Depth (PLOD) fast forward model to facilitate incorporation into McIDAS and other software packages. Weighting functions need to be generated and made available to the user community along with the coefficient files.

Summary of Accomplishments and Findings

Calculate PFCs for the GOES Imager and Sounder

Weighting functions for the MTSAT bands were calculated and compared to forward model calculations done for GOES-9. This was done to help assess the impact of replacing GOES-9 with MTSAT in operational product generation.

We received feedback from NWS forecast offices that real-time GOES weighting functions would be useful as a forecaster educational tool and, potentially, as a forecasting tool. A major undertaking this year has been providing real-time GOES weighting functions over the CONUS. The weighting functions are calculated based on radiosonde data using the Pressure-Layer Fast Algorithm for Atmospheric Transmittances fast forward model. A real-time web page displaying weighting functions for the Geostationary GOES Imager (all infrared bands) and Sounder (water vapor infrared bands) has been created (Figure 2.4.1). The interactive web page updates radiosonde data at 00 UTC and 12 UTC, and weighting function plots are available for four days. Several Alaskan and Hawaiian stations have been added as well (http://cimss.ssec.wisc.edu/goes/wf).

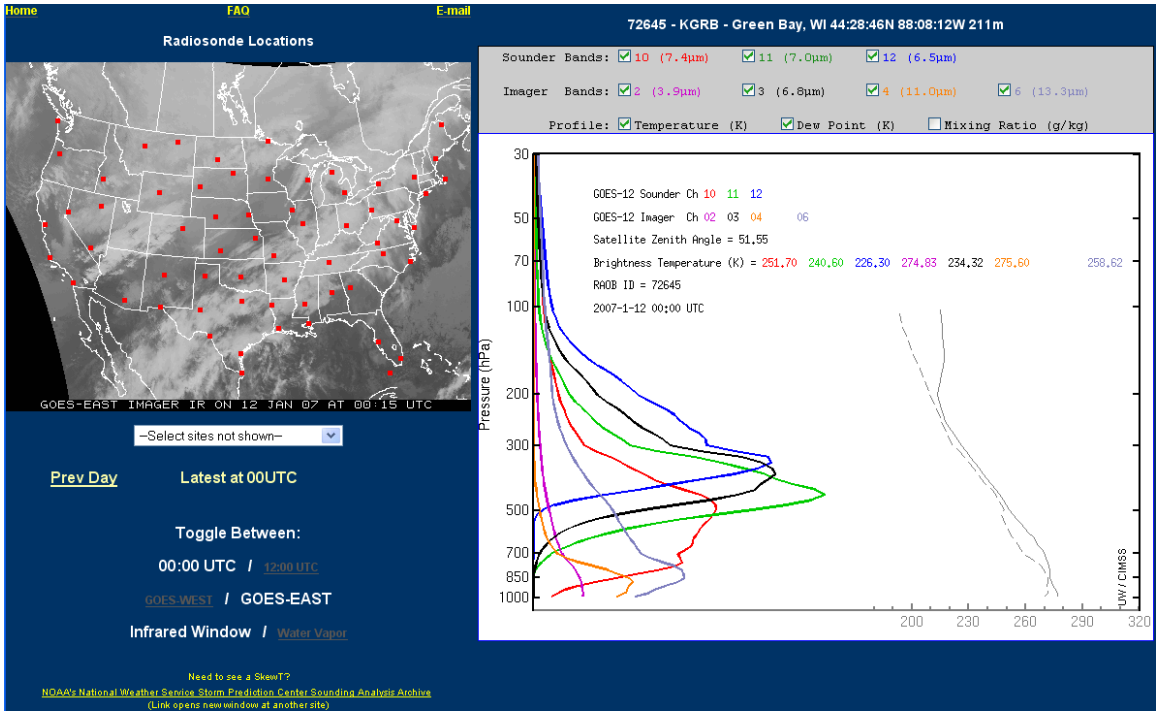

Figure 2.4.1: Snapshot of the CIMSS Realtime GOES Weighting Function web page. Visitors can choose what bands to look at, as well as choosing to plot temperature and dew point. The most recent 5 days are kept online and visitors can also choose between GOES-East and GOES-West, 00 and 12 UTC raobs, and from a wide range of U.S. stations.

Create and test GOES Sounder and Imager transmittance files PLOD fast forward model
MSG-2 and MSG-3 spectral response functions were obtained and converted into the PLOD transmittance coefficient file format; and Planck Function Coefficients were sent to appropriate personnel for incorporation into McIDAS. Similar work was completed for the GOES-O spectral response functions.

2.5 GOES Quality Assessment – James P. Nelson III

Proposed Work
Work supported through this project is vital to maintaining and improving the integrity of all the GOES Imager and Sounder research products that CIMSS makes available to the meteorological

community via the following Web sites: http://cimss.ssec.wisc.edu/goes/rt/ and http://cimss.ssec.wisc.edu/goes/realtime/

The most recent CIMSS Product Systems Development and Implementation (PSDI) proposal covered 1 May through 31 December 2006. Our goals and tasks for FY2006 were:

- To continue development on software for a web-based display of temperature and moisture retrieval quality statistics compared with data from nearby radiosondes,
- To activate new radiosonde/RAOB collocation files associated with new retrieval algorithms,
- To develop software to evaluate retrieval quality against high-resolution numerical model data for both point and gradient comparisons,
- To continue monitoring GOES Imager and Sounder product systems hardware,
- To enhance code documentation and appearance,
- To add more software and data files to our Concurrent Versions System (CVS) repository,
- To improve software portability to other platforms.

Summary of Accomplishments and Findings

During 2006, we have made progress in several areas related to this project. New software has been written to archive approximately 40GB daily of CIMSS temperature and moisture retrievals, cloud retrievals and related data. This software makes it much easier to add or remove files from the ongoing archive, which is vital for retrospective research. More files have been added to the SSEC CVS repository, which contains various Imager and Sounder software and associated ancillary files. Use of CVS greatly enhances the stability and integrity of CIMSS GOES software and ancillary files.

Use of the standard UNIX "make" and "tar" utilities continues to increase, which aids software development and maintenance. Together, these utilities are extremely useful for organizing development on a program-by-program basis, and will be valuable when preparing to migrate software from CIMSS to NESDIS operations. A minor but important software upgrade was performed to update the freely-available "Grace" software to its latest revision. Grace will be an important component of the work to display statistics on the Web showing temperature and moisture retrieval quality compared to nearby radiosondes.

On 12 January 2006, some files were provided to scientists in Washington, D.C. to aid in their investigation of how the single field of view retrieval algorithm handles missing GOES Sounder data. On 21 June 2006, GOES-11 replaced GOES-10 as the operational western geostationary satellite, and software updates were performed to make that transition at CIMSS. In June and July 2006, the latest version of the McIDAS-X software was installed on a number of our UNIX workstations. In the latter part of 2006, work began toward purchasing additional computing hardware that will significantly enhance retrieval processing capabilities at CIMSS. Finally, work was done to provide data to scientists at the Universities of California-Davis, North Carolina State and Stanford. Satisfying external data requests is vital for healthy interaction with other scientists and institutions, and it is felt that this work also falls under the umbrella of science maintenance and quality control.

An ongoing emphasis in our work is to search for generic, robust solutions to our problems. When a problem arises, rather than simply getting a given piece of software to run again as soon as possible, we often times attempt to *improve* the software in some way at the same time. Even

cosmetic improvements to software are useful, because the software should then be easier to interpret for the next generation of scientists who will need to interface with the code. Software improvement is a very gradual process, but incrementally over time the sum of improvements made should result in overall improvements to our Imager and Sounder software.

2.6 GOES N Checkout – Tim Schmit and Mat Gunshor

Proposed Work

As with previous GOES post-launch checkouts, there are several goals for the GOES-13 Science Test. First, we planned to investigate the quality of the GOES-13 data. This was to be accomplished by comparison with data from other satellites as well as by calculating the signal-to-noise ratio. The second goal was to generate products from the GOES-13 data stream and compare them to those produced from other satellites. These products may include several Imager and Sounder products: temperature/moisture retrievals, Total Precipitable Water (TPW), Lifted Index, Cloud-top pressure, and atmospheric motion vectors. The third goal was to investigate the impact of recent instrument and other hardware changes. For example, we planned to investigate the better navigation, improved calibration and operation of the satellite through eclipse periods.

Summary of Accomplishments and Findings

Investigate GOES-13 Data Quality

'Bad' early GOES-13 Sounder visible data have been identified and flagged, and preliminary Imager and Sounder noise analyses have been conducted. In general, the GOES-13 Sounder Signal-to-Noise ratio is much better, especially for the longest wave channels, due mostly to colder detector temperatures (Figure 2.6.1).

Generate and Compare GOES-13 Products

The first GOES-13 Imager and Sounder images have been acquired (Figure 2.6.2), and the first GOES-13 versus GOES-11 or -12 comparisons (in both the visible and infrared spectral regions) have been made. In addition, sample products from the GOES-13 Sounder have been generated and compared with similar products from other satellites (Cloud-top pressure, Lifted Index and TPW). Clear Sky Brightness Temperatures (CSBT) and Cloud-top pressure have also been generated from GOES-13 Imager data. These and other results are posted online at the following locations:

- http://cimss.ssec.wisc.edu/goes/g13_report/
- http://cimss.ssec.wisc.edu/goes/blog/category/goes-13/
- http://rammb.cira.colostate.edu/projects/goes_n/

In general during the test, GOES-13 was operated in a mode similar to the GOES-East or -West Imager and Sounder schedules. However, other valuable data were also acquired during special schedules that were run during the tests. These data made possible the generation of loops of full disk images every 30 minutes, 5-minute imaging loops, the longest duration loop ever compiled of 30-second Imager data, imagery showing hot spots due to fires, and space-views with the Sounder for noise determination.

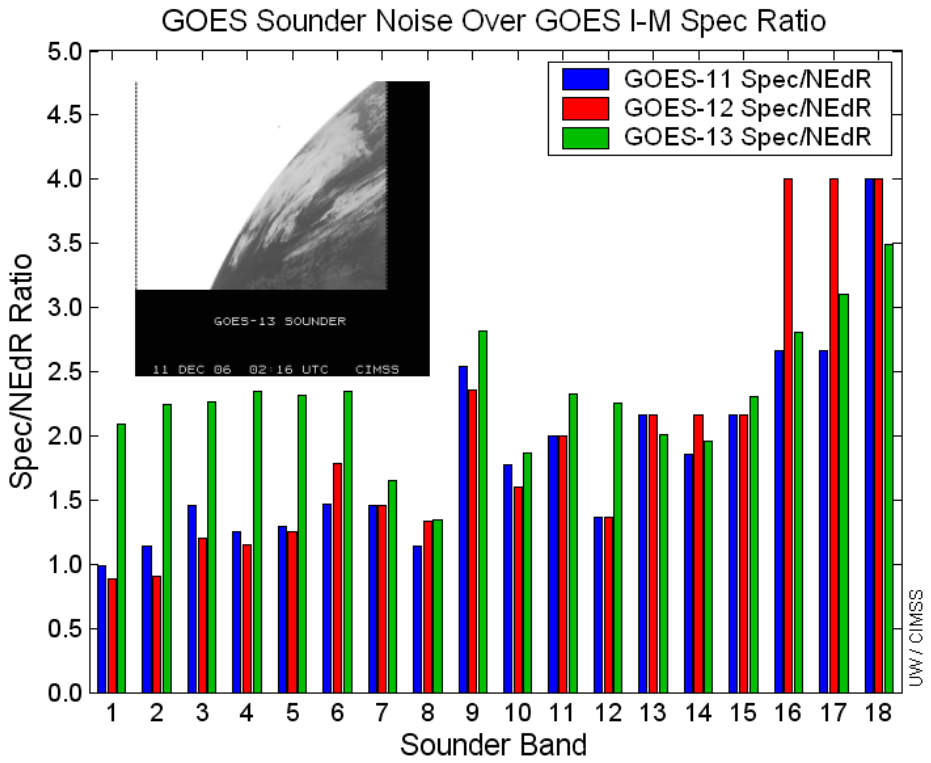

Figure 2.6.1: GOES-11, -12 and -13 Sounder noise comparison using data obtained from special scans during the NOAA Science Test.

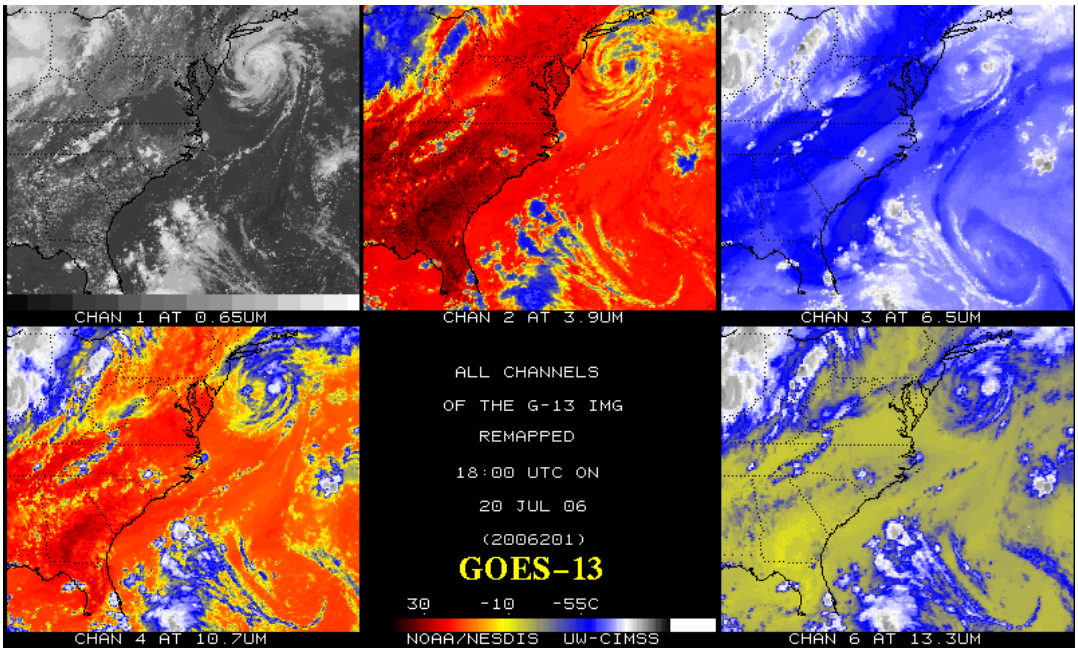

Figure 2.6.2: The first calibrated infrared data that was taken on 20 July, 2006 from the Geostationary Operational Environmental Satellite (GOES)-13 Imager.

Investigate the Impact of Instrument and other Hardware Changes
A preliminary eclipse and Keep Out Zone (KOZ) analysis has been conducted

2.7 Cloud-Drift and Water Vapor Winds in the Polar Regions from MODIS –Jeff Key

Project Goals
Geostationary satellite radiance measurements have been used to generate cloud-drift winds in the low- and mid-latitudes of the western hemisphere for more than two decades. Fully automated cloud-drift wind production from the Geostationary Operational Environmental Satellites (GOES) became operational in 1996, and wind vectors are routinely used in operational numerical models of the National Centers for Environmental Prediction (NCEP). Unfortunately, GOES is of little use at high latitudes due to the poor viewing geometry.

The objective of this project is to generate wind vectors over the polar regions from polar-orbiting satellites. Of primary interest is the MODIS instrument on NASA's Terra and Aqua satellites. We have developed an experimental wind product that can be used in numerical weather prediction systems, and have helped transition the product to NESDIS operations. Under this PSDI funding we continue to evaluate, improve, and extend the product suite.

The project Principal Investigator at CIMSS is Chris Velden. Dave Santek is performing the analyses and oversees the implementation and modification of McIDAS (Man computer Interactive Data Access System) and heritage wind generation software for use with MODIS. Steve Wanzong also assists in code modification and testing. Jeff Key, NOAA/NESDIS, works on the project in collaboration with CIMSS scientists, and is the NESDIS point of contact for the project.

Accomplishments
Over the past year we have continued the real-time generation of the MODIS polar winds product from both Terra and Aqua. The data are made available to users via anonymous FTP. MODIS data are acquired from the NOAA Real-Time System, which is a NOAA computer at NASA's Goddard Space Flight Center. The experimental MODIS wind product is routinely generated by CIMSS for scientific research. The product transitioned to NESDIS operations in November 2005. We continue to work with our STAR and OSDPD colleagues on code differences and any discrepancies that arise between the CIMSS and OSDPD winds.

We have begun to generate a mixed satellite product. Until recently, MODIS winds were only generated from the Terra and Aqua satellites separately. The mixed satellite system uses data from both, which improves the time resolution. It does, however, introduce other potential problems (e.g., parallax). The mixed satellite winds are currently being evaluated.

Ten numerical weather prediction centers worldwide now use the MODIS winds in their operational systems: the Joint Center for Satellite Data Assimilation (JCSDA), the European Centre for Medium-Range Weather Forecasts (ECMWF), the NASA Global Modeling and Assimilation Office (GMAO), the U.K. Met Office, the Canadian Meteorological Centre (CMC), the Japan Meteorological Agency (JMA), the U.S. Navy's, Fleet Numerical Meteorology and Oceanography Center (FNMOC), Deutscher Wetterdienst (DWD; Germany), MeteoFrance, and

the National Center for Atmospheric Research (NCAR). MeteoFrance and NCAR began operational use during the past year.

Two of the investigators (Velden and Key) took part in the 8th International Winds Workshop held in Beijing in April 2006.

Publications (since project inception)

Key, J., D. Santek, C.S. Velden, J.M. Daniels, W. Bresky, and W.P. Menzel, 2005, Polar winds from satellite imagers for numerical weather prediction and climate applications, *Proceedings of the 8th Conference on Polar Meteorology and Oceanography*, American Meteorological Society, San Diego, California, 10-13 January 2005.

Velden, C., and many co-authors, 2005: Recent innovations in deriving tropospheric winds from satellites. *Bull. Amer. Meteor. Soc*., 86, 205-223.

Key, J., D. Santek, C.S. Velden, N. Bormann, J.-N. Thepaut, L.P. Riishojgaard, Y. Zhu, and W.P. Menzel, 2002, Cloud-drift and Water Vapor Winds in the Polar Regions from MODIS, *IEEE Trans. Geosci. Remote Sensing*, 41(2), 482-492.

Santek, D., J. Key, and C. Velden, 2003, Real-time Derivation of Cloud Drift and Water Vapor Winds in the Polar Regions from MODIS Data, *Proceedings of the 12th Conf. on Satellite Meteorology and Oceanography*, American Meteorological Society, Long Beach, CA, 9-13 February 2003.

Bormann, N., J-N. Thépaut, J. Key, D. Santek, and C. Velden, 2002, Impact of polar cloud track winds from MODIS on ECMWF analyses and forecasts, *Proceedings of the 15th Conf. on Numerical Weather Prediction*, American Meteorological Society, San Antonio, TX, 12-16 August, 2002.

Key, J., D. Santek, C.S. Velden, and W.P. Menzel, 2001, Cloud-drift and water vapor winds in the polar regions from MODIS, *Proceedings of the 11th Conference on Satellite Meteorology and Oceanography*, American Meteorological Society, Madison, Wisconsin, 15-18 October 2001, 320-323.

Key, J., C. Velden, and D. Santek, 2001, High-latitude cloud-drift and water vapor winds from MODIS, *Proceedings of the Sixth Conference on Polar Meteorology and Oceanography*, American Meteorological Society, San Diego, 14-18 May 2001, 351-354.

2.8 GOES Gridded Cloud Products – Tony Schreiner

Proposed Work

This was the final year of a two-year project to determine the quality of the GOES Sounder Effective Cloud Amount (ECA) reformatted to a Lambert Conformal Grid over the CONtinental United States (CONUS) in GRIB-2 format. In the first year, we:

- Examined the quality of the analyses and performed quality checks on the meteorological "reasonableness" of the gridded product, and
- Validated the gridded cloud product against the GOES Sounder cloud product, making sure the derived gridded product was not degraded when transformed from the native product to the Lambert Conformal projection.

During 2006 we proposed to:

- Assist in making this an operational product.
- Reconfirm that the Lambert Conformal gridded version produced operationally is qualitatively the same as the native product.

Summary of Accomplishments and Findings

The gridded cloud amount product became available as an hourly NESDIS operational product on 1 November 2006. Figure 2.8.1 is an example of the native product (a Lambert Conformal gridded projection in GRIB-2 format). The color enhancement from tan to blue to yellow infer thin to opaque clouds, respectively.

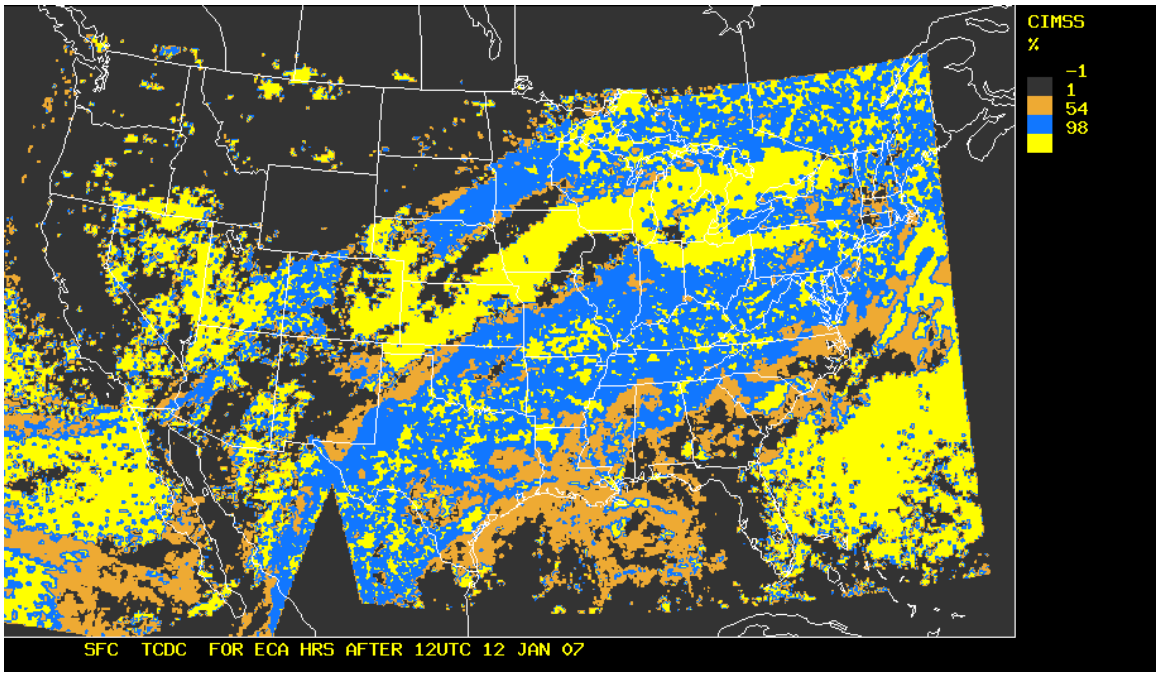

Figure 2.8.1: GOES-11 & -12 Sounder Effective Cloud Amount (ECA) derived image Lambert Conformal gridded projection for 12 January 2007 at 1200 UTC.

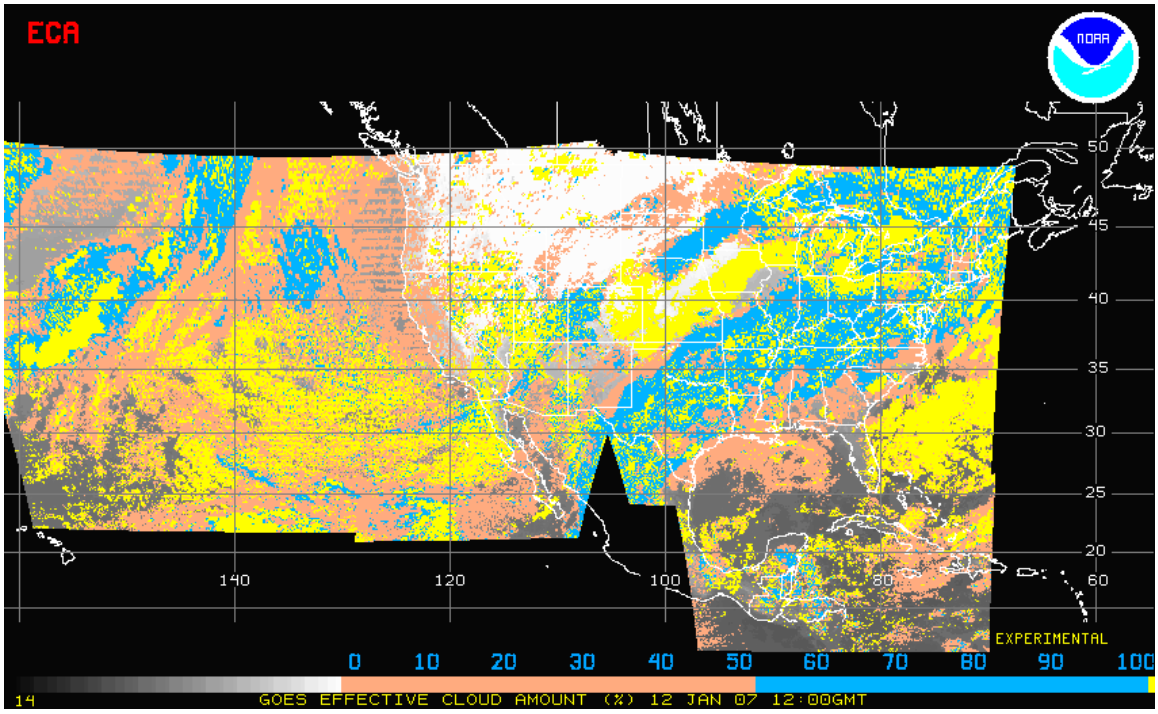

Figure 2.8.2: GOES-11 & -12 Sounder Effective Cloud Amount (ECA) image (Mercator projection in GRIB-2 format) for 12 January 2007 at 1200 UTC.

Figure 2.8.2 is an example of the operational product (a Mercator projection of the derived image processed by the NOAA/NESDIS/OSDPD group). The colored regions from salmon to light blue to yellow indicate thin to opaque clouds, respectively.

Our results indicated that the operational product is essentially the same as the native product

2.9 AVHRR CLAVR-x – Andy Heidinger and William Straka III

Proposed Work
Our proposed activities for CLAVR-x focused on supporting the operational transition of CLAVR-x multi-layer cloud properties products. In addition to supporting this effort, we also undertook efforts to make CLAVR-x ready for METOP AVHRR data which provides the first ever global 1 km AVHRR data.

Summary of Accomplishments and Findings
The most significant accomplishment was that the CLAVR-x met its goal of becoming operational in December 2006. Most of the work done by CIMSS during this period involved solving minor issues that arose in the transition of the CLAVR-x system to the OSDPD operational platform. For the first time, CLAVR-x cloud products are visible from the OSDPD web page.

In addition to meeting this operational milestone, we also worked on CLAVR-x to prepare for processing of METOP data. METOP data represents the first ever global 1 km AVHRR data-set.

To ensure optimal performance of CLAVR-x at this higher resolution, several of the ancillary datasets have been switched with newer versions that are now available at higher resolutions. In addition, Hal Woolf from CIMSS generously provided a special version of his fast radiative transfer model that provides a consistent interface for all AVHRR instruments from TIROS-N through the METOP series. The first image shown below illustrates an early look at the CLAVR-x cloud products generated from global 1km METOP AVHRR data.

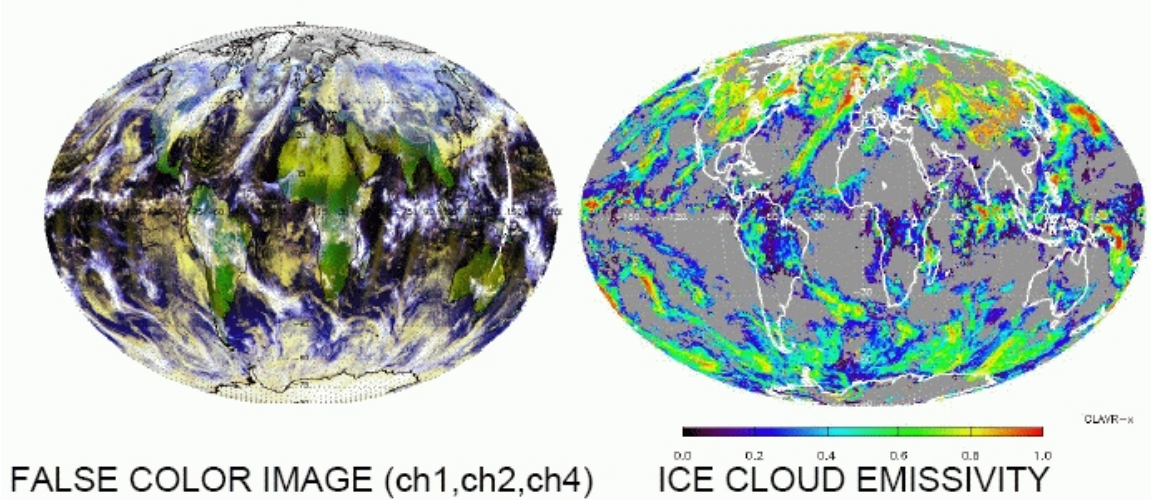

Additionally, we have collaborated with other groups to develop improved methods of verifying the performance of our cloud properties. For example, analysis of the CLAVR-x cloud properties has proceeded through the comparison of cloud properties to various ground-based sensors. This includes a comparison of both AVHRR pixel-level and 0.5 degree data, which are the two datasets available operationally.

In the image shown below, a comparison was done with data from every 4th data during 2004 for both NOAA-15 and NOAA-16. 2004 was chosen for a variety of reasons. First, it is the only complete year of data from ARM. Also, this same year was used in a comparison with the GOES-R AWG Cloud Properties group. The data were then compared with data from the ARM at the Southern Great Plains site, using the Active Remotely-Sensed Cloud Locations (ARSCL) data set. This dataset is a dataset that contains cloud boundaries from the micro-pulse laser and millimeter Cloud Radar. The comparison shows that ice cloud top heights of single layer clouds are within 3 km. The average difference is 2.1 km, with a RMS of 1.6. Most of the large deviations were contained to clouds which CLAVR-x detected to be greater than 14 km. The stringent requirements forced there to be very few data points for the entire year.

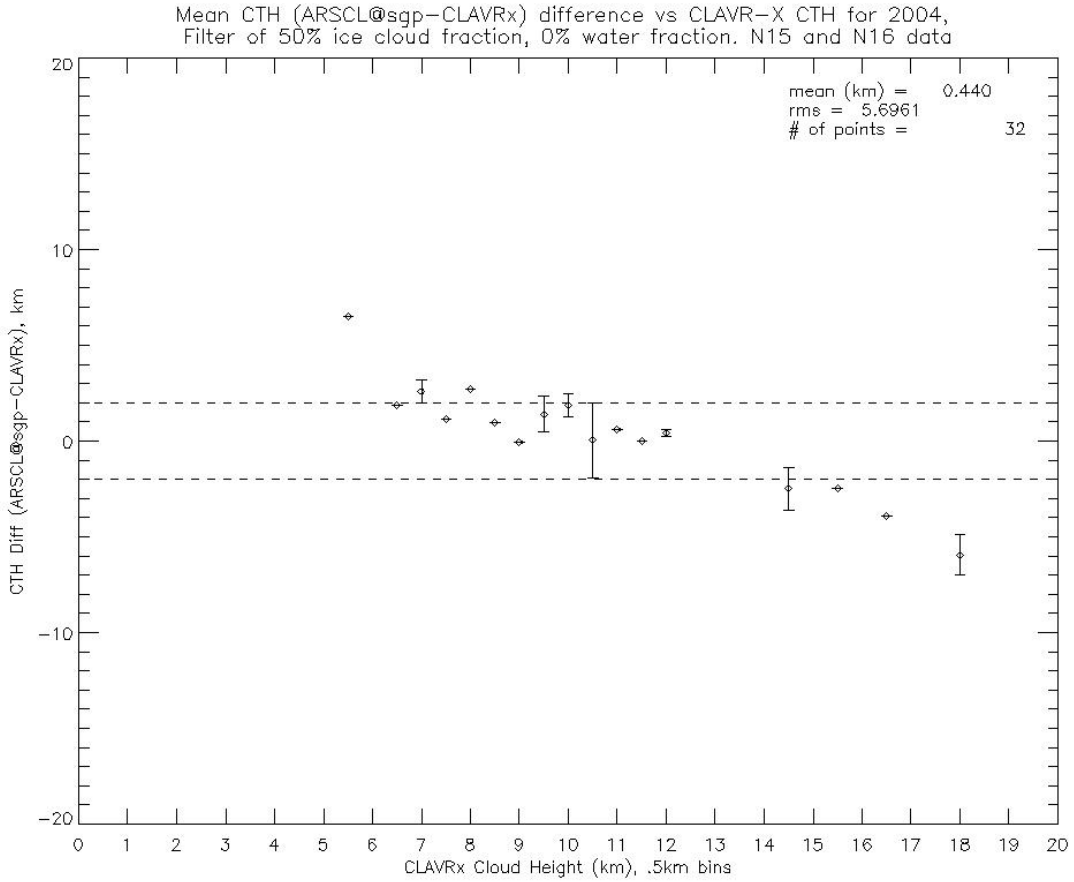

In addition to looking at cloud properties using data from US sensors, we expanded to looking at data from CLOUDNET, which is a European version of ARM. The study was presented at the AMS Cloud Radiation Conference in Madison, WI. This study showed that while some cloud top quantities, such as cloud top height, agree well when measured from ground based instruments and satellites, there are others, such as lwp, that do not agree well with ground-based measurements. The likely cause of the differences is caused by ice cloud contamination in the CLAVR-x pixel as well as the viewing zenith angle, which is not constant for polar-orbiting satellites. While this study looked at a small sample of data, these two factors seem to be the primary causes of such spread between ground- and satellite-based calculations of cloud properties. A comparison with data from the SEVIRI imager over the CLOUDNET site showed that there was fairly consistent agreement between various algorithms currently being used for cloud microphysical properties.

As more ground-based data becomes available, future studies may be able to show how the viewing angle is responsible for the spread of the data and how its influence can be parameterized. This includes looking at data from other CloudNet and other ground-based sites as data becomes available. In addition, tools are being developed for comparing CLAVR-x and CALIPSO/CloudSat data.

Publications/Presentations

Heidinger, Andrew; Baum, B. A. and Yang, P.. Consistency of cloud ice properties estimated from MODIS, AVHRR and SEVIRI. Conference on Atmospheric Radiation, 12th, and Conference on Cloud Physics, 12th, Madison, WI, 9-14 July 2006.

Hutchison, Keith; Lisager, B.; Jackson, J. M.; Roskovensky, J. K.; Heidinger, A. K.; Pavolonis, M. J.; Kopp, T. J. and Frey, R. A.. The VIIRS cloud mask. Symposium on Future National Operational Environmental Satellites, 3rd, San Antonio, TX, 14-18 January 2007 (preprints).

Evan, Amato T.; Heidinger, Andrew K. and Knippertz, Peter. Analysis of winter dust activity off the coast of West Africa using a new 24-year over-water advanced very high resolution radiometer satellite dust climatology. Journal of Geophysical Research, Volume 111, 2006.

Straka, William C. III and Heidinger, Andrew K.. Comparison of the Advanced Very High Resolution Radiometer (AVHRR) and Moderate Resolution Imaging Spectroradiometer (MODIS) cloud properties using PATMOS-x. Conference on Satellite Meteorology and Oceanography, 14th, Atlanta, GA, 29 January-2 February 2006.

Vicente, Gilberto A. and Heidinger, A. K.. Operational cloud detection systems in the NPOESS GOES-R era. Symposium on Future National Operational Environmental Satellites, 3rd, San Antonio, TX, 14-18 January 2007.

2.10 GOES Surface and Insolation Project Processing (GSIP) – Andy Heidinger and William Straka III

Proposed Work

GOES Surface and Insolation Project Processing (GSIP) is a flexible fortran-90 GOES imager processing system. While originally developed by Andy Heidinger, subsequent development of the GSIP system has occurred in NESDIS. The work at CIMSS is focused on solving some remaining technical challenges. These challenges include increasing the speed of the code, and verifying and optimizing the cloud algorithms. In addition, CIMSS is tasked with validating the GSIP products over the ocean as requested by the coral bleaching group in NESDIS.

Summary of Accomplishments and Findings

During this reporting period, we have made corrections to the cloud property algorithms and have made a few modifications to the routine, such as the addition of outputting the various cloud mask tests at test sites as well as changing in order to read in the AREA files faster than before. This was done via a simple C subroutine, developed by Michael Pavolonis, which reads in the entire chunk of binary data rather than each individual element.

There have been various comparisons and analysis done using the data from GSIP. In addition to the continued comparisons with the SURFRAD sites, readers and comparisons are being performed at the ARM Southern Great Plains site in Oklahoma. Another analysis, which was presented at the AMS Cloud Physics conference, was performed on cloud top effective radius and total column optical depth estimated from GSIP and compared to an experimental effective radius retrieval for optically thick, convectively generated ice clouds in which the scattering properties of droxtals are assumed. This was developed by the NOAA Regional and Mesoscale Meteorology (RAMM) team. It was found that the algorithm used in GSIP produced lower effective radii over the course of the day. The diurnal trend of this comparison showed that there was a high bias that

existed regardless of the time of the day. However, the R-squared values are lower earlier in the day compared to later in the day. This suggests that the retrievals are more similar with active convective clouds in the afternoon, or that there is a significant difference in the scattering geometry between morning and afternoon with the two retrieval methods. This is something that will be investigated as these algorithms continue to be developed. It is quite difficult to say which method is "better" because many assumptions about ice scattering are necessary. More importantly, both provide information about diurnal trends in effective radius.

The GSIP cloud mask routine has been used by the biomass burning group in order to do general qualitative comparisons with their basic opaque cloud mask/climatology in order for them to proceed on the GOES WF_ABBA reprocessing effort. The Biomass Burning group has expressed some interest in expanding the qualitative of the limited case studies into a quantitative analysis at a later point.

GSIP was originally being augmented to read and analyze data from SEVIRI (MET-08 and MET-09). This was being done to analyze prototype algorithms for the Advanced Baseline Imager (ABI) and new GOES imagers. However, this was scraped in order to make way for a better algorithm test bed, which is currently in development.

However, analysis of the algorithms from GSIP is still ongoing. Future work will be focused on analysis from ocean surface instruments (buoys) as well as continued analysis from ARM and other ground-based instruments. This will continue until such time that the new geostationary test bed (GEOCAT) becomes operational.

Publications and Conference reports
Straka, W.C., D. T. Lindsey, A. K. Heidinger. A Study of Cloud Top Microphysical Characteristics in High Plains Thunderstorms, Preprints, 12th Conference on Cloud Physics, Madison, WI, Amer. Meteor. Soc., CD-ROM, JP2.17

3 Ground Systems Research

3.1 Global Fire Detection - Elaine Prins, Chris Schmidt

Proposed Work
CIMSS proposed to participate in cost-sharing activities with NASA and other NOAA programs to adapt the GOES WF_ABBA to MSG (Met-8), FY-2C, MTSAT-1R, INSAT-3D, and GOMS Electro N2 over the next 2 years. The goal is to create a global consistent fire product utilizing the capabilities of each of these unique systems and a common fire detection algorithm, the GOES Wildfire Automated Biomass Burning Algorithm. During the first year, development focused on adapting the WF_ABBA to Met-8, MTSAT-1R, and preliminary studies for FY-2C.

Summary of Accomplishments and Findings

Adaptation of the WF_ABBA to Met-8
CIMSS development and implementation of a global geostationary fire monitoring network began in June 2006. Initial efforts focused on adapting the GOES WF_ABBA to Met-8 SEVIRI. The WF_ABBA required a number of modifications to read the SEVIRI data and compute viewing parameters. In addition the oversampling in both the north/south and east/west with SEVIRI and subsequent re-sampling/re-gridding of the data has implications for both fire

detection and sub-pixel characterization. Some of the issues have been addressed in the code, but others remain. The Met-8 WF_ABBA has been applied to a number of test cases in Africa and Europe and the code is being adjusted to better identify isolated single-pixel fire events. In terms of sub-pixel characterization, the Met-8 WF_ABBA is being modified to compute fire radiative power (FRP) in addition to Dozier estimates of instantaneous sub-pixel fire size and temperature. The accuracy of these estimates is in question due to the re-gridding/re-sampling protocol. At the GOFC/GOLD 2nd Workshop on Geostationary Fire Monitoring and Applications held at the EURopean Organization for the Exploitation of Meteorological SATellites (EUMETSAT) in Darmstadt, Germany on 4-6 December 2006, the participants agreed that in order to generate accurate sub-pixel fire characteristics, the user community must have access to the pre-gridded oversampled Met-8 SEVIRI data.

Figure 3.1.1 shows an example of the Met-8 WF_ABBA applied to SEVIRI data in Western Africa on 3 December 2005 at 1300 UTC. The dark hot spots seen in the highlighted region of the Met-8 3.9 micron image represent fires primarily associated with agricultural burning. The Met-8 WF_ABBA fire product does a fairly good job of identifying the fires in the image, although there are a few isolated single fire pixels that were not identified by the algorithm.

Adaptation of the WF_ABBA to MTSAT-1R

A preliminary version of the MTSAT-1R WF_ABBA has been developed and applied to a case study in Southeast Asia. The low saturation temperature (~320 K) in the 4 micron band poses a significant problem for fire detection within 3 to 4 hours of local noon. Figure 3.1.2 shows an example of this in Australia on 13 January 2007 at 03:33 UTC in the early afternoon local time. All of southern Australia is saturated, making it impossible to identify fires in this region. Additional modifications must be made to the MTSAT-1R WF_ABBA to address the effects of the low saturation value. It may be necessary to block out large regions during peak solar heating.

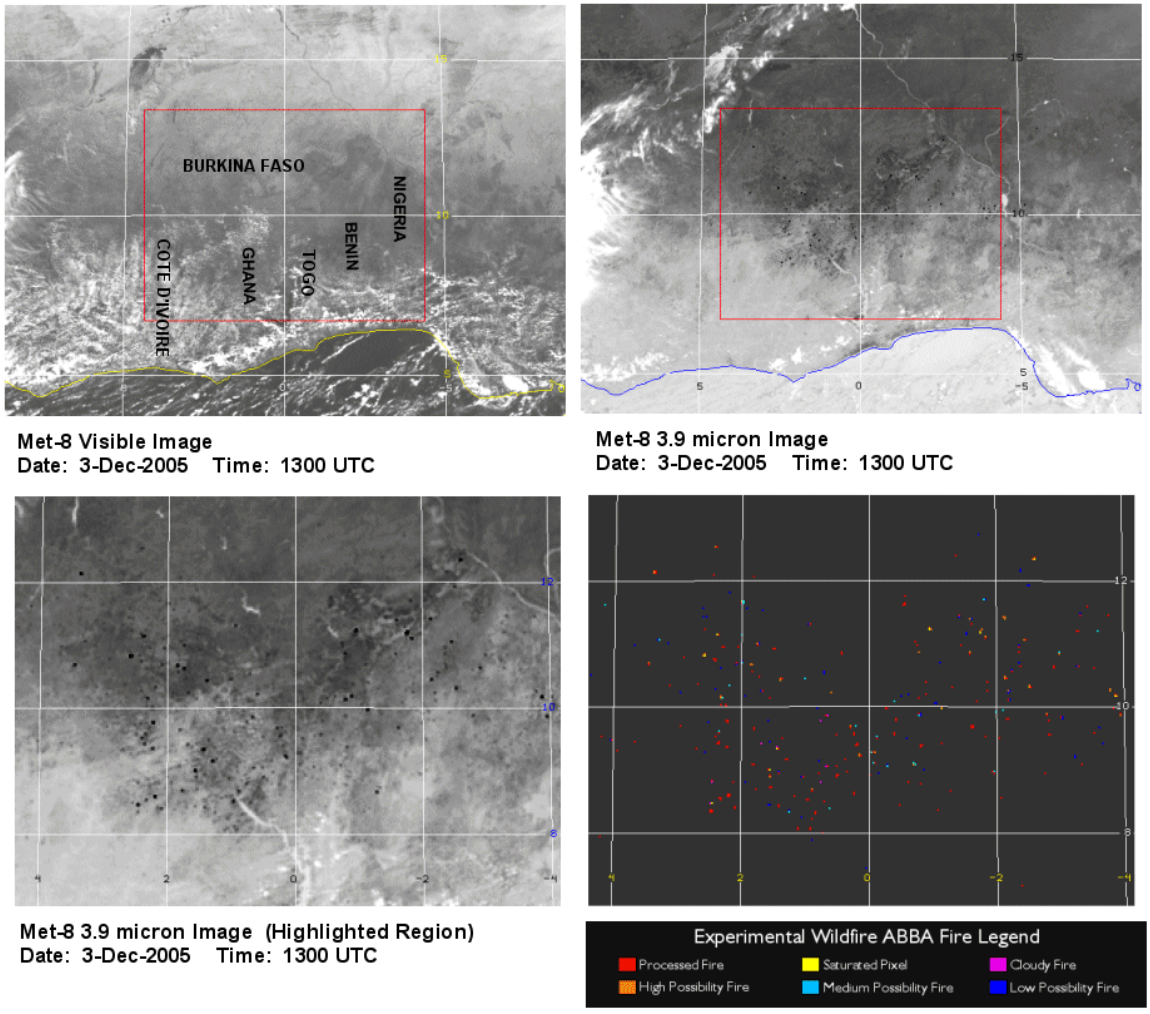

Figure 3.1.1: Application of the WF_ABBA to Met-8 SEVIRI data in Western Africa on 3 December 2005 at 1300 UTC. The dark hot spots in the highlighted 3.9 micron data primarily represent agricultural burning.

Adaptation of WF_ABBA to FY-2C

CIMSS has begun to collaborate with Dr. Liu Cheng of the National Satellite Meteorological Center of the China Meteorological Administration to better understand the sensitivity of the FY-2C 4.0 micron channel to sub-pixel hot spots. Previous comparisons of GOES-9, MTSAT-1R and FY-2C 4.0 micron imagery showed that even when the region of interest is closer to the FY-2C satellite sub-point than it is to GOES-9 and MTSAT-1R, the FY-2C does not seem to identify the fire pixels as readily as the other two platforms. Additional studies will be done to investigate this issue.

With the substantial differences between the global geostationary instruments, it will be necessary to provide additional metadata to the user regarding processing regions, block-out zones (associated with biome types, regions of saturation, etc.), and opaque clouds. The generation of metadata will be incorporated into the WF_ABBA code for each platform.

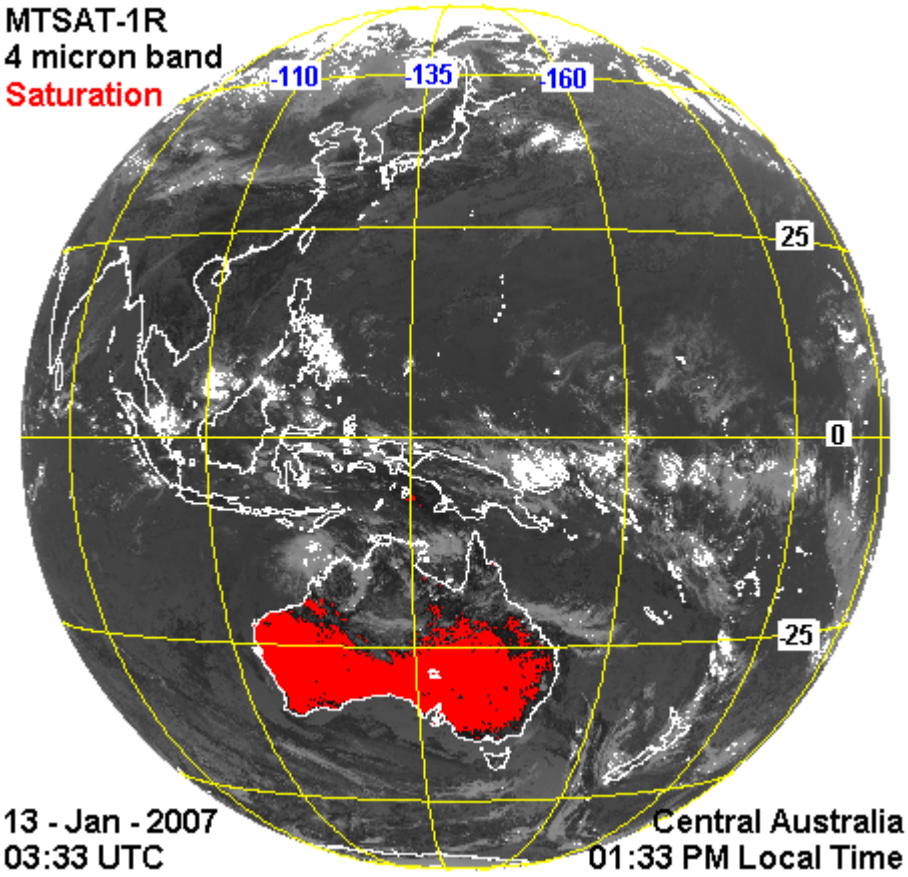

Figure 3.1.2: MTSAT-1R 3.9 micron data observed on 13 January 2007 at 03:33 UTC. The low saturation temperature (~ 320 K) in the 4 micron band results in nearly complete saturation of southern Australia.

Publications and Conference reports

Prins, E., C. Schmidt, J. Feltz, J. Brunner, S. Lindstrom, J. Hoffman, 2006: Status and Plans for Global Geostationary Fire Detection and Monitoring With the Wildfire ABBA, 2nd GOFC/GOLD Workshop on Geostationary Fire Monitoring and Applications, Darmstadt, Germany, December 4-6, 2006.

4 GOES R Risk Reduction

4.1 Algorithm Development – Allen Huang and Chris Velden, Team Leaders

4.1.1 GOES-R Risk Reduction Algorithm Development (ABI fire detection) – Elaine Prins and Christopher Schmidt

Proposed Work

The UW-Madison CIMSS biomass burning team proposed the following tasks for 2006. Research and development activities in 2006 will center primarily on active fire product development and validation. Development will focus on active fire detection and sub-pixel characteristics for emission estimates, including the investigation of fire radiative power. This

effort will involve the use of multiple data sources (geo and leo) that take advantage of the strengths of each system to create improved fused fire products. This risk reduction activity will ensure enhanced future fire detection, monitoring and characterization. Initially CIMSS will investigate GOES ABI fire monitoring capabilities by simulating ABI with MODIS, MSG (METEOSAT Second Generation), and MTSAT-1R (Multi-functional Transport SATellite) multispectral data.

Summary of Accomplishments and Findings

UW-Madison GOES-R Risk Reduction biomass burning algorithm development efforts began in April 2006 and focused on simulation of GOES-12 Imager and GOES-R ABI data from higher spatial resolution MODIS data to better understand the differences between current and future geostationary fire detection and characterization capabilities. MODIS observations of the large destructive fires in Southern California in October 2003 were used to simulate GOES-12 Imager and GOES-R ABI 3.9 and 11 µm data and fire characterization capabilities. In order to more accurately simulate Imager and ABI data, appropriate point spread functions were applied in the simulation process. Figure 4.1.1 shows the spatial response and sampling differences between GOES-R ABI and GOES-I/M Imagers. The figure shows the spatial response of each instrument with each grid point representing 1km^2 at the sub-satellite point. The scanning pattern represents an approximation of the size and sampling for both sensors overlaid on the MODIS 3.9 µm image of the Verdale fire. GOES-R is expected to have minimal oversampling compared to the current GOES, which oversamples by a factor of 1.75 in the East/West direction. The red boxes on the point spread function plots represent the nominal 4 km and 2 km fields of view for GOES-12 and GOES-R respectively.

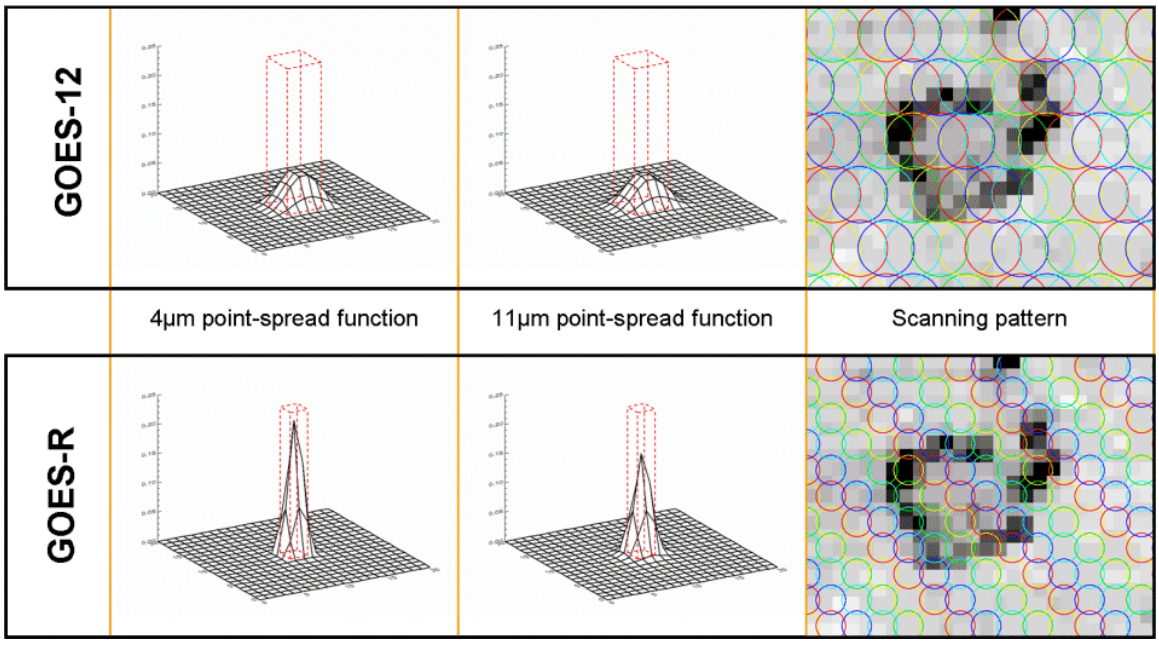

Figure 4.1.1: GOES-R ABI and GOES-I/M spatial response and sampling differences.

A modified version of the GOES Wildfire Automated Biomass Burning Algorithm (WF_ABBA) was applied to the simulated GOES-12 Imager and GOES-R ABI data to determine Dozier estimates of instantaneous sub-pixel fire size and temperature. GOES-12 and GOES-R were assumed to be located directly over the fires to limit issues introduced by remapping data. Fire

Radiative Power (FRP) was derived from the Dozier output. Saturation in the 3.9 μm band on GOES-12 inhibited determination of FRP for 20% of the fire pixels. Only 4% of the ABI fire pixels were saturated. ABI was also able to characterize more of the variability in fire intensity due to the increased spatial resolution. The mean fire pixel FRP was 46 Wm^{-2} for GOES-R ABI and 24 Wm^{-2} for GOES-12. This is primarily due to the fact that several of the hotter fires were included in the average for GOES-R ABI, but were not included in the GOES-12 Imager calculation due to saturation. This difference shows the substantial improvement in fire characterization with GOES-R ABI allowing for more realistic estimates of emissions.

Initial efforts to simulate GOES-R ABI data from higher spatial resolution MODIS consisted of applying simple averaging or point spread functions to higher resolution MODIS data in the native MODIS projection. In order to create more realistic GOES-R ABI data sets that can be used to develop improved fire detection and sub-pixel characterization, it is necessary to take into consideration point spread function and oversampling issues, variations in pixel size with view angle, diffraction, band-to-band co-registration, and other factors. These are issues which strongly impact fire detection and sub-pixel characterization. UW-Madison is investigating ways to simulate more realistic ABI data utilizing MODIS, Met-8 SEVIRI and GOES data. For a given region of interest the MODIS and coincident GOES/Met-8 data can serve as bookends over a period of time with GOES and Met-8 providing the diurnal signature. At the bookends, the MODIS data can be made to look more like the SEVIRI/GOES data at a higher ABI resolution and then nudged over time (between the bookends) with guidance from the GOES/MET-8 data. Since fires can often appear as an on/off type feature, the diurnal GOES/Met-8 data can be used to introduce variation in fire location and intensity over time. It would also be possible to use an educated random fire generator for certain biomes.

CIMSS is modifying existing McIDAS code to create enhanced more realistic simulated data sets for all ABI IR channels that have similar MODIS channels. Although the band widths for ABI and MODIS can be quite different, this type of simulation would provide “real world” proxy data that can be used in conjunction with model simulated data, with applications in various product development activities. The McIDAS remapping software is being modified to take into consideration factors such as point spread function and oversampling, view angle dependencies, diffraction, etc. CIMSS is focusing on simulating GOES ABI from MODIS data collected on 24 April 2004 in Central America and on 27 October 2003 in Southern California. These case studies include excellent examples of diurnal variability in fire activity in both clear and cloudy situations. Figure 4.1.2 shows an initial example of generating simulated GOES-R ABI 3.9 micron data in a geostationary projection from MODIS data collected at 2055 UTC on 27 October 2003 in Southern California.

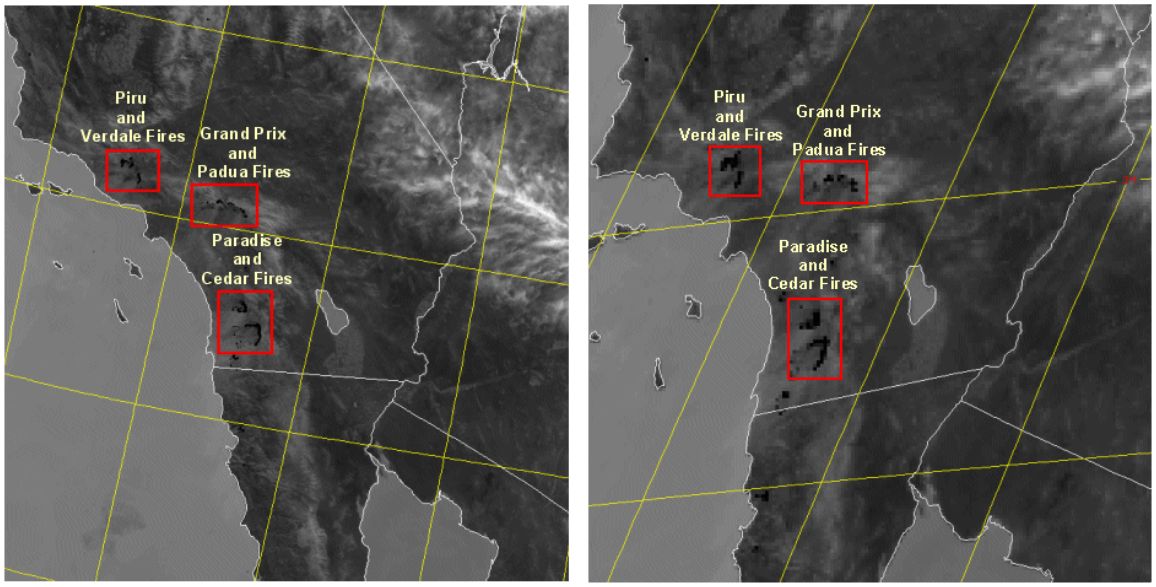

Original MODIS 4 micron image (1 km)

Date: 27-October-2003
Time: 20:55 UTC

Simulated GOES-R ABI 4 micron image (2 km)

Date: 27-October-2003
Time: 20:55 UTC

Figure 4.1.2: Original MODIS and GOES-R ABI simulated 4 micron image for 2055 UTC on 27 October 2003.

In order to characterize sub-pixel fires, accurate estimates of surface emissivity are needed for the short (4 micron) and long-wave (11 micron) infrared window bands. Currently the WF_ABBA emissivities are assigned based on the AVHRR GLCC version 2 dataset available from the USGS using a table that relates emissivities to land cover types in the GLCC dataset. CIMSS is investigating application of the dynamic SeeBor dataset which contains monthly estimates of spectral band emissivities derived from MODIS data. Figure 4.1.3 shows a comparison of the current WF_ABBA 4 micron static emissivity map and the SeeBor 4 micron emissivity map for July 2005. The red highlighted regions in the current emissivity map represent fire detection block out zones primarily associated with urban areas. There are noticeable differences between these two emissivity data sets especially along biome transition zones. Additional analyses will be done to determine the impact on fire characterization utilizing the SeeBor dynamic emissivity maps.

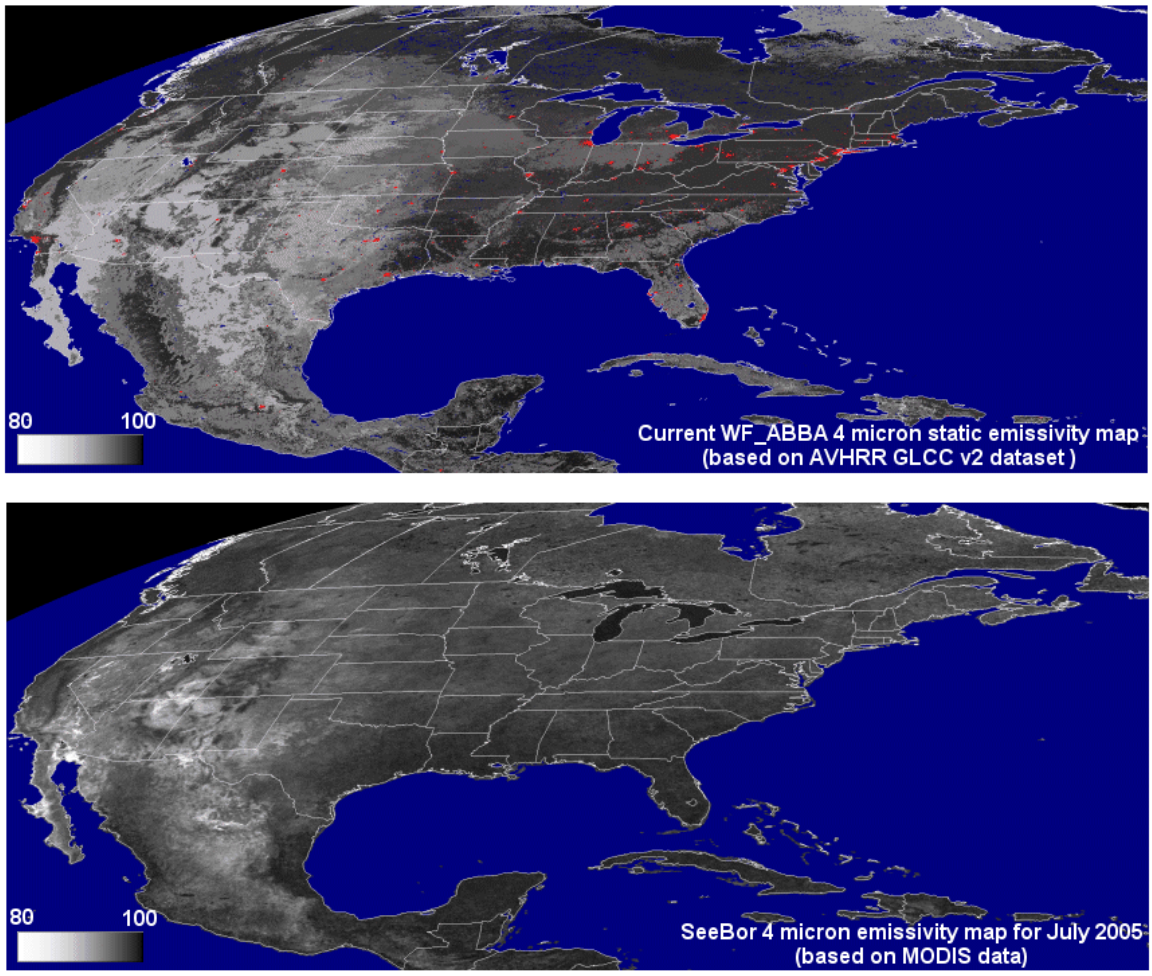

Figure 4.1.3: Comparison of the current static WF_ABBA 4 micron emissivity data set and the SeeBor 4 micron data set for July 2005.

NOAA/NESDIS has indicated that 2 km MTSAT-1R JAMI data will be made available for specific case studies. Obtaining access to this data set provides a wonderful opportunity to investigate the lower thresholds for GOES-R fire detection and monitoring capabilities from a large detector array with a spatial resolution similar to ABI. UW-Madison CIMSS provided input to NOAA/NESDIS regarding priorities for MTSAT-1R 2 km data coverage of fire activity.

Publications and Conference Reports

Peer-Reviewed Publications

Prins, E., C. Velden, J. Hawkins, F. J. Turk, J. Daniels, G. Dittberner, K. Holmlund, R. Hood, A. Laing, S. Nasiri, J. Puschell, J. M. Shepherd, J. Zapotocny, 2006: 13th AMS Conference on Satellite Meteorology and Oceanography, Meeting Summary on Next Generation Environmental Sensors and Emerging Applications in Satellite Meteorology and Oceanography, *BAMS*, 87, 5,.633 – 637.

Conference Papers/Posters
Schmidt, C. C. and E. M. Prins, 2006: Comparison of Current and Future GOES Fire Characterization, Fourth GOES-R Users Conference, May 1-3, 2006, Broomfield, CO.

4.1.2 GOES-R Risk Reduction Algorithm Development Tropical Cyclone Project – J. P. Kossin and C. S. Velden

Proposed Work
We proposed to perform an important subset of the testing and validation portions of retrieval development by examining retrieval algorithm performance and impacts in the unique and challenging environments around tropical cyclones (TCs). Another goal of the proposed work was to demonstrate the potential of high-temporal-resolution ABI imagery to delineate structure changes in the TC upper-levels and form upper-level fields of parameters related to intensity change (e.g., divergence, potential vorticity, and inertial stability).

Summary of Accomplishments and Findings
Comparison of in situ data with retrieved products in clear regions of the tropical cyclone (TC) environment
Two hurricane cases (Fran and Ivan 2004) were selected for the in situ measurement and retrieval data comparison. The selection was based on the large number of available high altitude aircraft dropsondes that were available for these storms, and their good spatial and temporal overlap with available data from the AQUA Atmospheric Infrared Sounder (AIRS) instrument. The dropsondes were released from Gulfstream-IV aircraft tasked specifically for hurricane reconnaissance, and many were released into relatively clear regions that typically surround the cirrus canopy above the storms. The dropsonde data were gathered from archives at the NOAA Hurricane Research Division, with assistance from Dr. Michael Black (NOAA/AOML).

AIRS L1B radiances were used to retrieve the vertical temperature profiles through IMAPP (International MODIS/AIRS Processing Package) AIRS level 2 retrieval software (version 1.2). Since the AIRS retrieval algorithm is presently only applicable to clear sky conditions, AIRS pixels with clear sky condition were selected for this phase of the study. MODIS has its own cloud mask algorithm and MODIS products have 1 km × 1 km cloud mask information on MYD06 datasets. AIRS has 90 × 135 pixels on one granule and each pixel has a diameter around 13 km at nadir. AIRS do not produce cloud mask information. One AIRS pixel has several hundred MODIS 1 km × 1 km pixels. Since the MODIS and AIRS instruments are both available on a common platform (EOS-AQUA), and they observe the earth simultaneously, MODIS cloud mask information can be used to determine the AIRS pixel cloud mask.

The MODIS cloud mask includes four categories – “confidently clear”, “probably clear”, “probably cloudy”, and “confidently cloudy” – and each MODIS pixel has its own cloud mask as mentioned above. To identify clear regions, we summed the numbers of “confidently clear” and “probably clear” collocated MODIS pixels. If this sum was over 65% of the total number of collocated MODIS pixels, the AIRS pixel was assumed to be clear. A total of eighteen clear pixels were selected with these criteria.

ECMWF reanalysis data were also collected to compare the vertical temperature profiles with the in situ measurements using dropsonde during hurricane period and the contemporaneous AIRS retrieved soundings. The ECMWF data (0.5° × 0.5°) were interpolated to the resolution of the AIRS pixels (13 km at nadir) around the TC environment.

The differences between the in situ temperature and moisture measurements and ECMWF analysis or AIRS retrievals were calculated as a simple arithmetic difference (ECMWF or AIRS minus dropsonde). These differences are shown in Figure 4.1.4, along with the RMS error of the AIRS and ECMWF soundings, and give an indication of the performance characteristics of the AIRS retrievals in the hurricane environment.

This work was performed by members of the CIMSS retrieval team (Yong-Keun Lee and Elisabeth Weisz). The data we collected will be combined with data being constructed at CIRA/CSU, who are applying the data to a different problem.

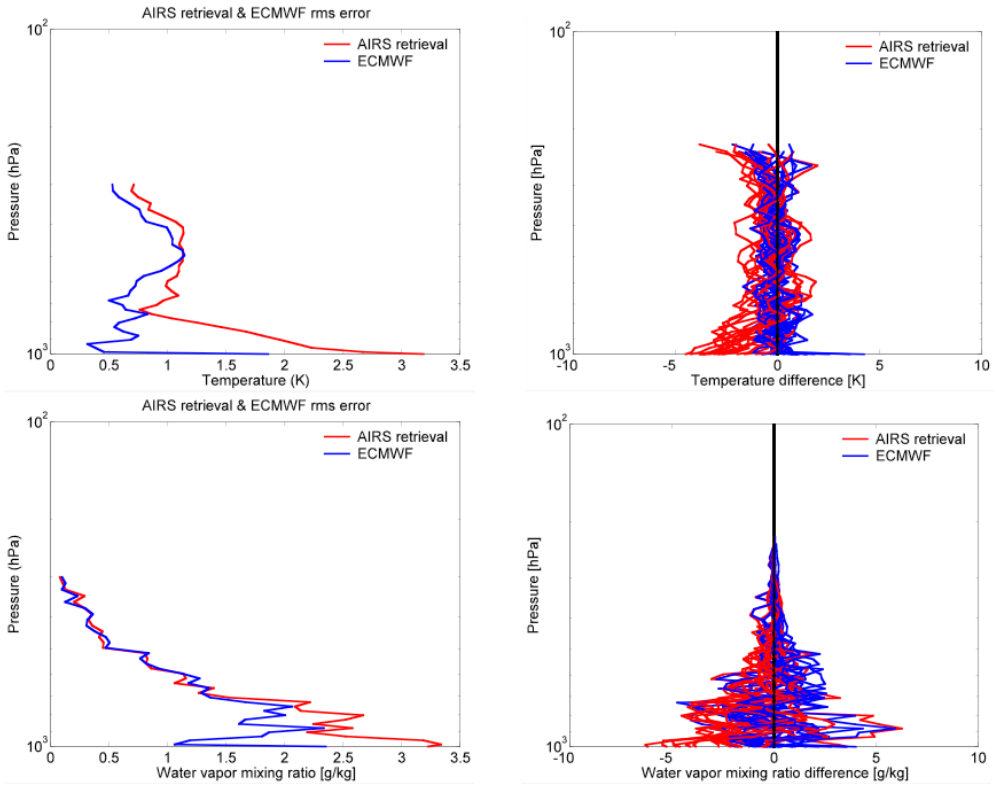

Figure 4.1.4: Sounding error. Left panels: RMS error of temperature (top) and moisture (bottom). Red (blue) shows error in AIRS retrievals (ECMWF profiles). Right panels: Differences (error) of the soundings defined as ECMWF or AIRS minus dropsonde.

Atmospheric Motion Vectors with GOES-R spatial and temporal resolution

A second objective of our GOES-R risk reduction work has been to demonstrate what will be achievable with the availability of the ABI. One way to do this was to employ currently existing GOES observing strategies that mimic what will be possible with ABI. Specifically, in regards to tropical cyclones, the upper-level outflow is thought to be important toward understanding intensity change. Atmospheric motion vectors (AMVs), derived from special GOES five-minute rapid-scan (r/s) imaging operations, can be effective at simulating what will be available on a routine basis once GOES-R is launched.

As a demonstration of this capability, GOES-11 AMVs were derived from 5-min. r/s imagery during a special observing period as NASA's Tropical Cloud Systems and Processes (TCSP)

experiment was taking place in July of 2005. Hurricane Emily traversed the sampling domain and provides a good case study, as the intensity fluctuated during the period of observation. Upper-level divergence is one parameter often associated with intensity change. Divergence from a particular analysis, calculated on spherical coordinates, is shown in Figure 4.1.5. The wind observations (in ms^{-1}) are also plotted. The divergence was only calculated for points that have at least two observations within 0.25 degrees of the analysis point in order to avoid spurious divergence features created by the analysis scheme. The analysis in Figure 4.1.5 captures some of the upper-level divergence over the hurricane (100 kts max wind at the analysis time). This divergence precedes Emily strengthening to 130 kts over the subsequent twenty-four hours.

We are in the process of creating time series of upper-level quantities derived from the GOES r/s AMVs over Emily. From these we hope to denote trends and potentially associations with the hurricane's structure and intensity fluctuations. High-resolution data such as this will be routinely possible from the GOES-R ABI, and our intent is to see what we can observe and learn from current GOES capabilities (special observing modes) in advance of this deployment.

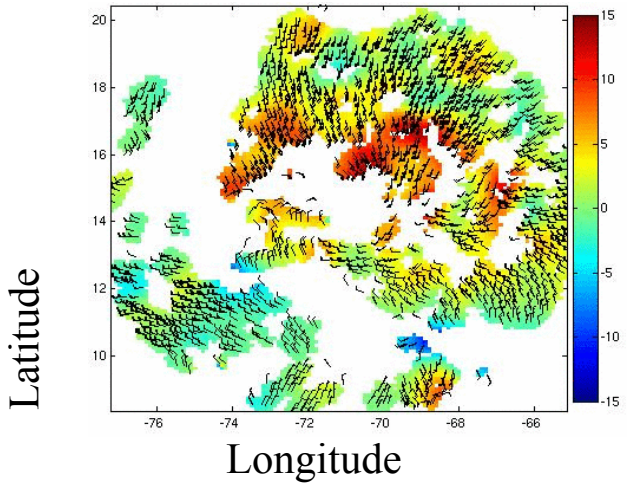

Figure 4.1.5: Divergence (10^5 s^{-1}) analysis centered on hurricane Emily valid 16z on 15 July, 2005.

4.1.3 GOES-R Risk Reduction Algorithm Development Sounding Algorithm Development - Jun Li

Proposed Work

- Evaluate AIRS clear, cloud-cleared and cloudy retrieval sounding algorithms
- Develop IASI clear sounding retrieval algorithm
- Conduct synergistic IASI/AVHRR sounding retrieval and evaluate its performance

Summary of Accomplishments and Findings

Handling surface emissivity in sounding retrieval

Emissivity knowledge is very important in ABI (Advanced Baseline Imager) sounding retrieval. Due to the limited spectral information, it is unlikely to derive the surface emissivities together with sounding from ABI infrared measurements. It is necessary to have emissivity prior information for ABI sounding products. Usually there are two ways for emissivity prior information: using ecosystem classified global emissivity database, or using emissivity spectrum

derived from hyperspectral infrared sounder from polar orbiting satellites. Since the hyperspectral IR derived emissivity spectrum is spectrally close to the ABI measurements, it can be used in ABI sounding retrieval.

Progress has been made on the retrieval of emissivity spectrum from hyperspectral IR radiance measurements. AIRS (Atmospheric Infrared Sounder) radiances are used for this study. The eigenvectors of hyperspectral IR emissivity are derived from a lab measured hyperspectral IR emissivity spectrum. In the retrieval process, the emissivity spectrum is expressed as a linear combination of the first 6 eigenvector, and the 6 eigenvector coefficients are retrieved simultaneously with temperature and moisture soundings. The retrieved hyperspectral emissivity spectra then can be spatially, temporally, and spectrally interpolated for ABI sounding retrieval. Simulated AIRS radiances show the simultaneous retrieval of emissivity spectrum and sounding in a physical way is promising, it is a new approach in sounding retrieval. Figure 4.1.6 shows the Root means square error (RMSE) of emissivity retrieval (upper panel), temperature profile retrieval (lower left) and water vapor Relative Humidity (RH) profile retrieval (RH in range of 0 ~ 100%). 32 simulated AIRS radiance spectra over desert region are used, realistic desert emissivity spectra are used in the simulation. The algorithm is being tested with AIRS real measurements. Results will be reported in next quarterly report.

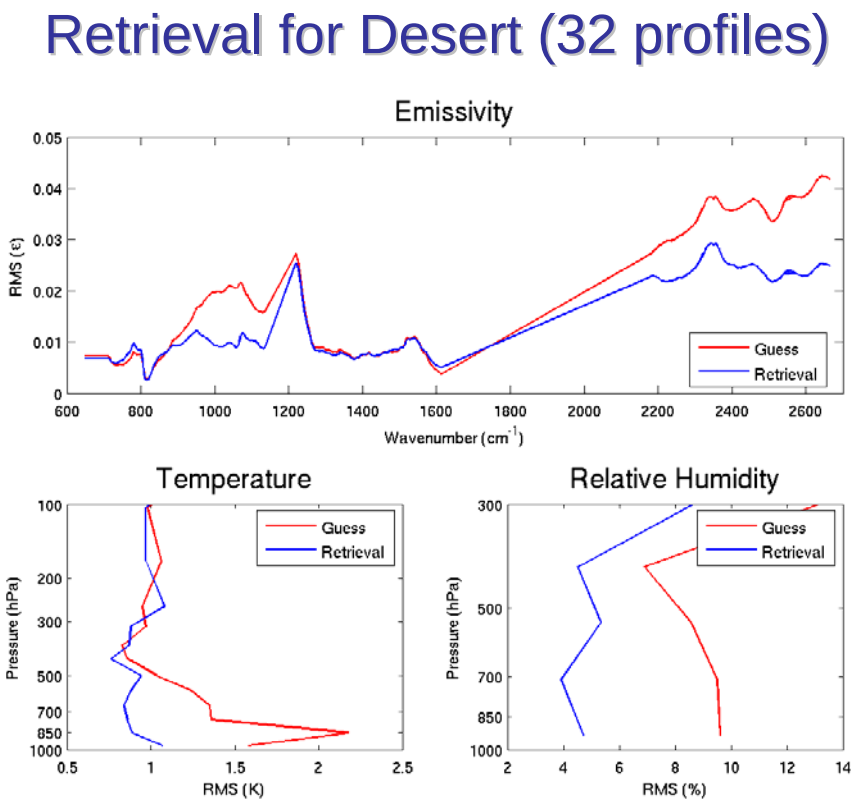

Figure 4.1.6: Root means square error (RMSE) of emissivity retrieval (upper panel), temperature profile retrieval (lower left) and water vapor Relative humidity (RH) profile retrieval (RH in range of 0 ~ 100%). 32 simulated AIRS radiance spectra over desert region are used, realistic desert emissivity spectra are used in the simulation.

Using time continuity in sounding retrieval

Time Continuity (TC) is the unique aspect of GOES observations. Use time continuity in sounding retrieval will assure the optimal process of GOES-R measurements. In order to test the impact time continuity on retrieval, a simple test is performed to the disk GIFTS simulated radiances: (1) using static training data set – time independent set (TIS), and (2) using the known dynamic training data set before the satellite observations – time dependent data (TDD). Figure 4.1.7 shows the water vapor mixing ratio retrieval RMSE from TIS and TDD. Retrievals are improved using TDD that contains the time continuous information. The next step is to use the measurement continuity in retrieval process.

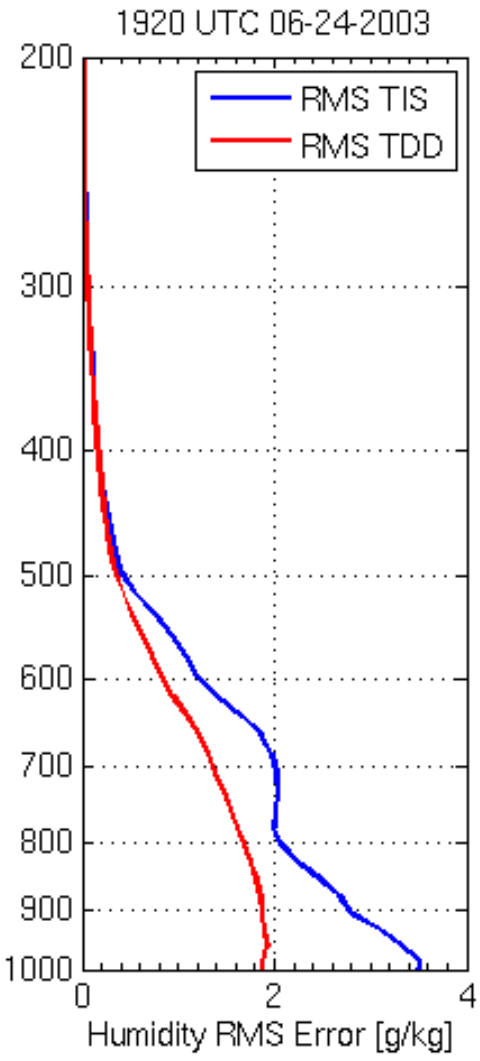

Figure 4.1.7: The water vapor mixing ratio retrieval RMSE (root mean square error) from TIS and TDD, GIFTS simulated disk clear sky radiances are used in the retrieval. Retrievals are improved using TDD that contains the time continuous information.

Cloudy sounding retrieval algorithm tested with AIRS

Simulation with GIFTS radiances shows that the above-cloud sounding approach is effective. We have tested the cloudy sounding algorithm using the AIRS (Atmospheric InfraRed Sounder) radiance measurements. Results are promising when compare the above-cloud sounding retrievals with ECMWF analysis. Specifically, the cloud-top pressure (CTP) retrievals from AIRS single footprint agree very well with the operational MODIS CTP product. Note that MODIS CTP product uses sounding profiles from global forecast, while AIRS above-cloud sounding approach retrieves CTP and above-cloud sounding simultaneously. Figure 4.1.8 shows the AIRS CTPs (13.5 km spatial resolution at nadir) from above-cloud sounding approach (left panel) and the operational MODIS CTP product (5 km spatial resolution at nadir) (right panel).

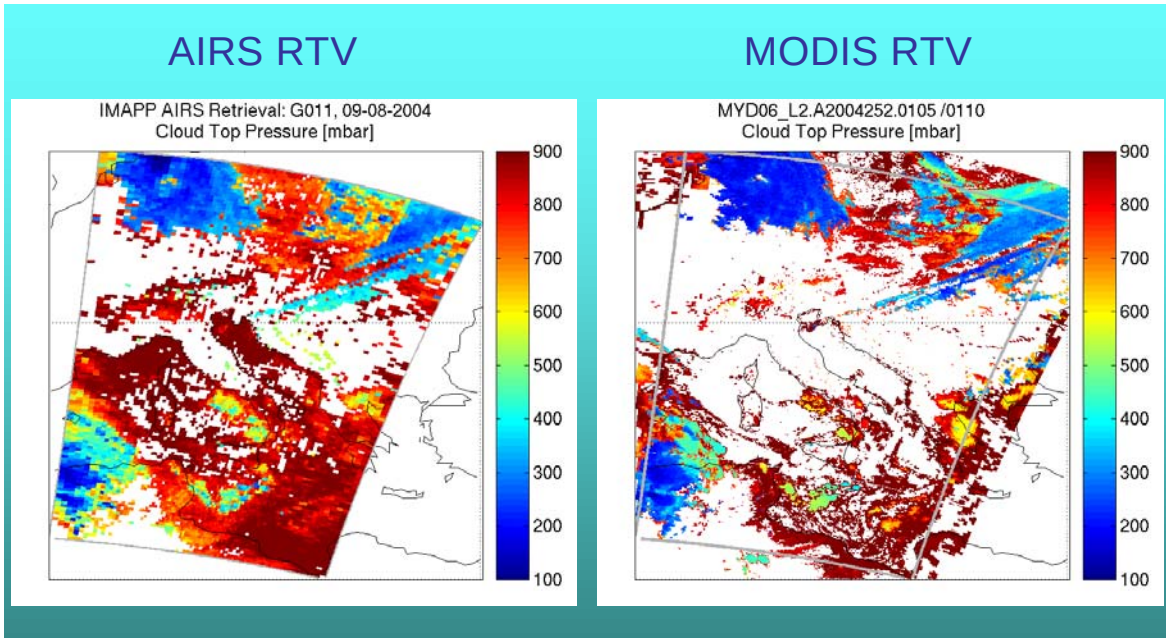

Figure 4.1.8: AIRS CTPs (13.5 km spatial resolution at nadir) from above-cloud sounding approach (left panel) and the operational MODIS CTP product (5 km spatial resolution at nadir) (right panel).

4.1.4 GOES-R Risk Reduction Composite Algorithm Development - Jun Li

Proposed Work

In addition to the simulated trace gases spectral data, IASI data will also be used to explore the composition retrieval for their total and layer concentration profile. The advantages of the temporal resolution of geostationary hyperspectral will also be addressed to demonstrate the optimal processing strategy to extract the desirable information on trace gases.

Summary of Accomplishments and Findings

Total column ozone retrieval algorithm development with ABI/SEVIRI

The algorithm has been developed for Advanced Baseline Imager (ABI), and the algorithm has been tested using the Spinning Enhanced Visible and Infra-Red Imager (SEVIRI) onboard Meteosat-8. Simulation shows that ozone from SEVIRI is worse than that from the current GOES Sounder due to lack of stratospheric CO2 absorption spectral bands in SEVIRI. However,

with help of temperature profile from forecast, the SEVIRI/ABI provides ozone with similar accuracy of the current GOES Sounder (Jin et al. 2006, submitted to IEEE TGARS) but with much large spatial coverage (disk). Preliminary results show that the total column ozone retrievals from SEVIRI agree well with ozone measurements from Ozone Monitoring Instrument (OMI) onboard the Earth Observing System's Aura platform. Figure 4.1.9 shows the OMI (upper) and SEVIRI (lower) total column ozone measurements in clear skies from 15 to 16, February 2006 over Europe. OMI provides global ozone once every day while SEVIRI provides ozone in disk coverage every 15 minutes. In addition, SEVIRI with 15-minute temporal resolution depicts the ozone transportation and evolution very well.

We also collaborated with Dr. Johannes Schmetz, Head of Meteorological Division and Marianne Koenig at EUMETSAT on our ABI/SEVIRI ozone retrievals. Currently EUMETSAT SEVIRI ozone product has artificial gradients which follow coastlines, especially along desert areas. In CIMSS SEVIRI ozone research product, the surface artifacts are mitigated due to properly handling the surface emissivity in the retrieval. Phil Watts at EUMETSAT will revisited the SEVIRI ozone product produced at EUMETSAT and will send us their results according to Dr. Johannes Schmetz.

The ozone algorithm will be improved with better cloud detection and handling large local zenith angle.

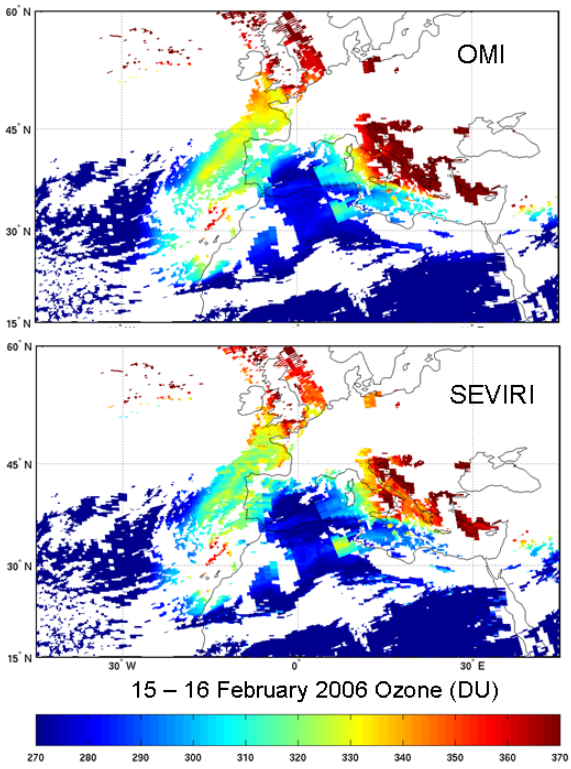

Figure 4.1.9: The scatter plot of OMI (upper) and SEVIRI (lower) total column ozone measurements in clear skies over Europe from 15 to 16 on 15 February 2006. SEVIRI agrees well with OMI.

Improvement on dust detection with ABI/SEVIRI

Dust detection has been improved over ocean. An IR-based dust detection and property retrieval algorithm has been developed for ABI, SEVIRI data are tested (Li et al. 2007, International Journal of Remote Sensing, in press). However, the algorithm has defect over ocean. The dust

diction technique has been improved over ocean by employing separate ocean and land surface emissivities. Results (not shown) agree better now with the composite color image over ocean.

4.1.5 GOES R Risk Reduction Winds – Chris Velden

Proposed Work
The primary goals of the GOES-R Risk Reduction work on wind algorithms are to focus on innovative methods to derive vector fields from the increased spectral capabilities that will be offered by GOES-R. We accomplish this by using both real and simulated satellite data.

Summary of Accomplishments/Findings over the past 12-months include (but are not limited to):
Our initial GOES-R winds focus concentrated on demonstrating the initial concept to target and track features from simulated GOES-R moisture retrievals. Several steps are involved in producing the clear sky profiles of winds. Mesoscale models are used to generate simulated atmospheric profiles with detailed horizontal and vertical resolution. Top of atmosphere (TOA) radiances are determined using these profiles along with the GIFTS forward radiative transfer model. Single field of view vertical temperature and water vapor retrievals are calculated from the TOA radiances. Moisture profiles from the retrievals are analyzed on constant pressure surfaces, and converted to images. Three successive analyses (images) are used to generate targets and clear sky AMV using existing tracking techniques.

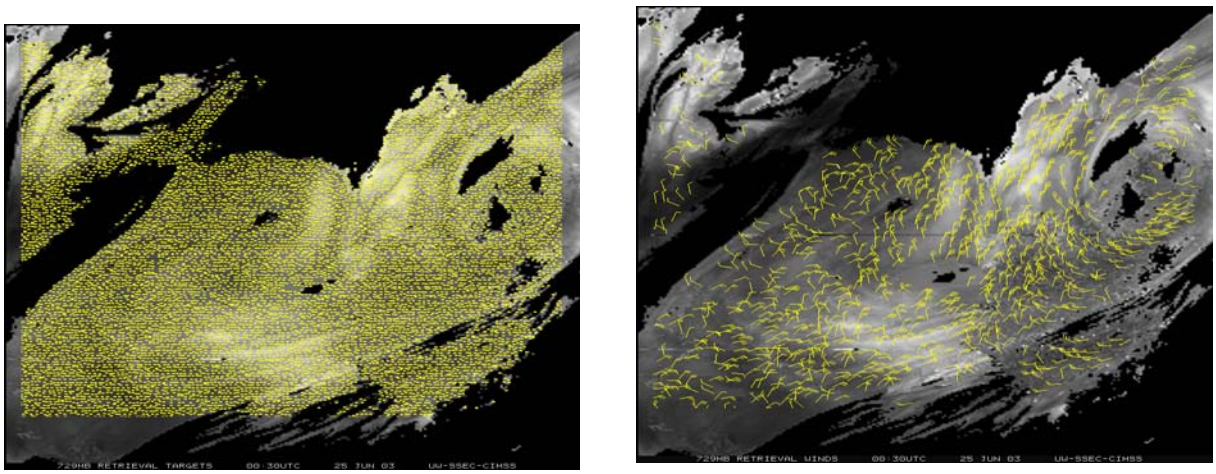

Figure 4.1.10: Plot of targets (left) and traceable wind vectors (right) at 729mb, derived from tracking simulated retrievals of water vapor from 3 successive 30-min. analyses.

As an example, a WRF model simulation was initialized at 0000 UTC, 24 June 2003, and run for 30 hours, with output every 30-minutes. 101 pressure levels were available for each time period (3 successive 30-min fields were employed for attempts at feature tracking) and retrieved moisture fields were derived and converted to images for input to the CIMSS automated tracking software. Winds were calculated at every available pressure level. A representative level is shown in Figure 4.1.10.

Figure 4.1.10 shows a prominently cloud-free environment, allowing good water vapor observations and winds coverage. Note the low level circulation defined by the winds in the

northeast section of the image. Figure 4.1.11 below shows the vertical density of the resultant lower-tropospheric wind field achieved in this simulation.

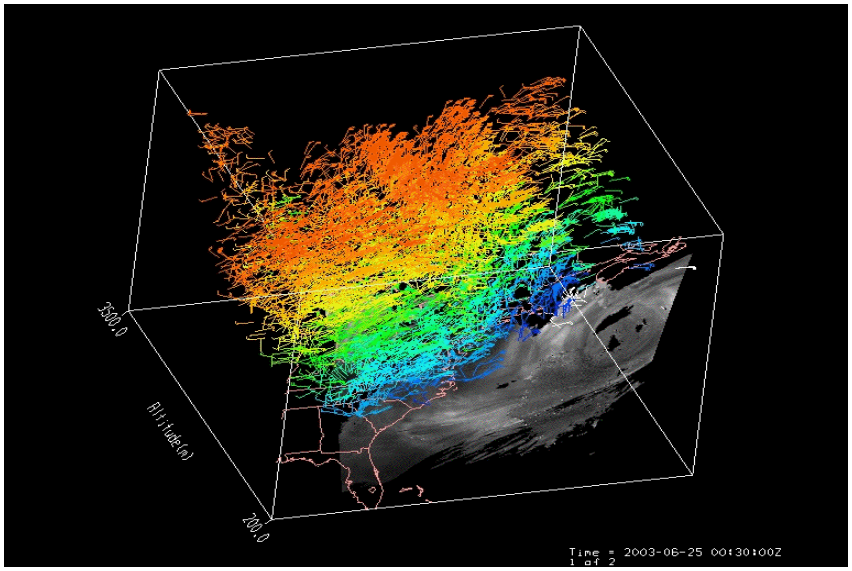

Figure 4.1.11: IDV display of winds from the simulated retrievals illustrating the vertical density. Orange wind barbs are at the top level of 683mb. Blue wind barbs are at the lowest level of 986mb.

In this case, the only quality control routine applied to the wind set was the automated objective Quality Indicator (QI). The final wind field is validated by comparing it to the actual WRF model wind field, and to the winds generated using the WRF model mixing ratios as input to the CIMSS automated tracking routines. A comparison of all collocated vectors is shown in the table below.

100km Vector Match Distance	Winds with QI > 50
Simulated Retrieval Wind Count	13812
WRF Wind Count	851968
Match Count	13812
Speed Bias (m/s)	1.3
Vector RMS (m/s)	6.7

100km Vector Match Distance	Winds with QI > 50
Simulated Retrieval Wind Count	13812
Model Q-tracked Winds Count	32737
Match Count	13741
Speed Bias (m/s)	0.3
Vector RMS (m/s)	8.4

100km Vector Match Distance	Winds with QI > 50
Model Q-tracked Winds Count	32737
WRF Wind Count	851968
Match Count	32737
Speed Bias (m/s)	0.7
Vector RMS (m/s)	4.9

The comparison results show that the retrieval winds are slightly faster than the WRF model winds, but with lower biases. The RMS error values are fairly consistent, and closely represent values from operational winds production. Although this product is in its infancy, and too early to draw conclusions from the statistics on one case study, the results are encouraging.

The next dataset being investigated (FULLDISK) dwarfs the previous case in the number and size of files. WRF simulations run on a full-disk domain simulating the expected GOES-R coverage are broken up into "cubes" to simulate HES sounding blocks. These cubes are written as Unidata network Common Data Form (NetCDF) files. Each NetCDF file contains the moisture field information. New data staging code using Jython stitches the cubes together into a McIDAS AREA file as preparation for the winds retrievals. Jython is an implementation of Python integrated with the Java platform.

The Winds Group is now working on data received from the Retrievals Team for retrieved moisture fields from the FULLDISK case. Staging of the FULLDISK case study in preparation for winds demonstration is now underway. The work on demonstrating multi-level winds from simulated hyperspectral sounder retrieved moisture fields will be wrapped up with the completion of the FULLDISK case. Future efforts will be focused on ABI winds risk reduction.

The trials in this study were limited to simulated hyperspectral data sets. The results indicate that method/algorithm improvements are needed to exploit this new capability. However, the proof of concept has been demonstrated, and the method is next applied to real data using the GOES sounder moisture retrievals as a next step.

Geostationary Operational Environmental Satellite (GOES) East and West sounders provide real-time retrievals of temperature and moisture in cloud-free regions on an hourly basis. The single field-of-view product has spatial resolution of about 10 km. The vertical profiles can be converted to images of temperature or moisture at all or selected pressure levels, which then serve as input image sequences for satellite wind retrieval algorithms. By their nature, the sounder generated moisture fields on constant pressure surfaces will overcome the existing problem of determining heights of the wind vectors. This work is an attempt to deduce winds from real GOES-derived dew point temperature (*Td*) images using the CIMSS automated feature-tracking algorithm. In the same manner as the method employing simulated data above, the potential applicability of GOES sounder moisture fields for deriving winds is tested.

In late 2005, NOAA/NESDIS implemented a new integrated GOES Sounder product processing system that derives atmospheric products such as clear sky radiances, temperature and moisture profiles, cloud-top pressure, and surface skin temperature at the full GOES sounder resolution of about $10km^2$. These products not only have better geographical coverage, but also provide improved depiction of gradient information, which allow for constant pressure level moisture analysis fields of significant contrast to be extracted and used as input to our wind retrieval algorithm.

The GOES full resolution sounder product processing system provides hourly Single-Field-Of-View (SFOV) retrievals of the atmospheric state in clear sky regions at nominal spatial resolution of 10 km. The atmospheric profiles of temperature and moisture are derived using a nonlinear physical retrieval algorithm. First, the GOES sounder radiances are navigated and calibrated, and it is determined if a pixel is cloudy or clear. For each cloud-free pixel, a first guess temperature profile is obtained from a space-time interpolation of fields provided by NWS (National Weather Service) forecast models; currently the GFS (Global Forecast System) model is used. Hourly

surface observations and sea surface temperature from AVHRR help provide surface boundary information. Sounder radiances are then used with a forward radiative transfer model to simultaneously retrieve temperature and moisture profiles as well as surface skin temperature. At this time, relative humidity (RH) and dew point temperature (Td) are provided at the same pressure levels as temperature, occupying 31 pressure levels between 1000 and 10mb.

GOES sounder vertical profiles are converted to a set of images representing moisture on constant pressure levels by extracting the variable of interest (i.e., Td) from each profile at the desired available constant pressure level. Hourly images (3) are then used to attempt winds retrieval. Winds are derived for 20 pressure levels between 1000mb and 100mb. An example of GOES sounder winds from 5 December 2003 are shown in Figure 4.1.12. The vertical distribution of the derived wind vectors is fairly even throughout the altitude range of 0-15 km.

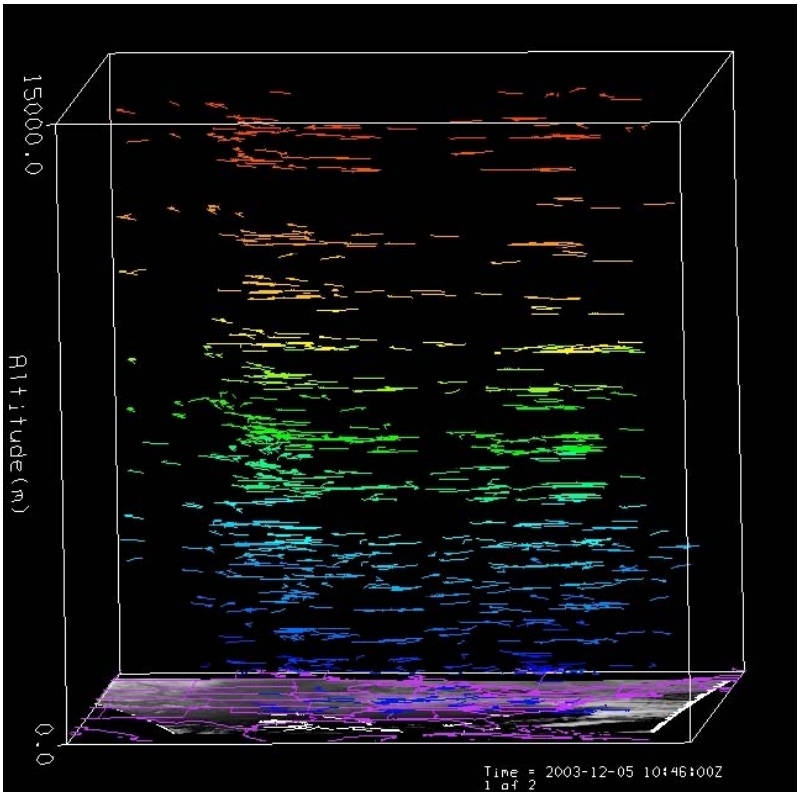

Figure 4.1.12: Vertical distribution of winds from the GOES sounder-derived moisture (Td) constant-pressure fields on 5 December 2003, 12 UTC.

Publications

Velden, C., S. Wanzong, I. Genkova, D. A. Santek, J. Li, E. R. Olson, and J. A. Otkin, 2007: Clear-sky atmospheric motion vectors derived from the GOES sounder and simulated hyperspectral moisture retrievals. AMS Annual meeting, GOES-R Symposium.

Wanzong, S., and C. Velden, 2006: Wind vector calculations using simulated hyperspectral satellite retrievals. 8th International Winds Workshop, Bejing, China.

Genkova, I., and C. Velden, 2006: Satellite wind vectors from GOES sounders moisture fields. 8th International Winds Workshop, Bejing, China.

4.1.6 GOES-R Risk Reduction Algorithm Development - Cloudy sky radiative transfer models – Tom Greenwald

Proposed work

The objective of this work is to develop state-of-the-art radiative transfer forward and adjoint models for rapidly calculating top-of-atmosphere radiances in cloudy conditions and to utilize the latest cloud optical property databases. The proposed work for this year included:

- Verify accuracy of the GIFTS fast model in cloudy conditions
- Compare GIFTS fast model to the SOI (Successive Order of Interaction) RT model in terms of accuracy and speed (referred to as our "bake-off")
- Release version 1 of the fast forward model
- Build an adjoint for the fast model
- Improve and refine forward models

Summary of accomplishments and findings

- Using over 75,000 WRF simulated cloud profiles, a comparison was made between the GIFTS fast model and the SOI model in terms of their errors due solely to multiple scattering. Results indicted (see Figure 4.1.13) that the SOI model is significantly more accurate for cirrus clouds (optical depth < 3.6) but is about 60% slower than the GIFTS model.
- Version 1 of the GIFTS fast model (written in Fortran 95) was released in February.
- An adjoint version of the clear sky part of the fast model (PLOD) was built and tested.
- Developed a new fast model that allows for multiple cloud layers, called FIRTM-AD (Texas A&M group – see publication below)
- Improvements and enhancements were made to the GIFTS fast model, including incorporating the latest cloud optical property database developed by Dr. Bryan Baum, incorporating the land surface emissivity database, improving integration of the thermal source function, and numerous code modifications.

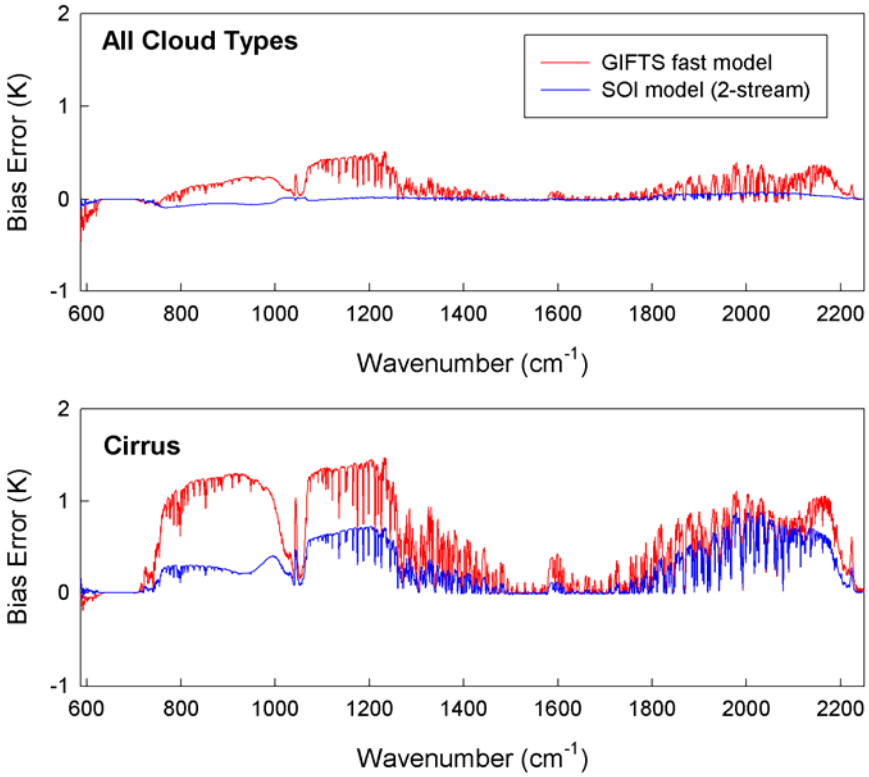

Figure 4.1.13: Accuracy of the GIFTS fast model and the two-stream SOI model for top-of-atmosphere brightness temperatures at an observation zenith angle of 55° based on (top panel) for all WRF simulated cloud profiles and (bottom panel) cirrus only profiles.

Publications and conference reports

Greenwald, T., H.-L. Huang, D. Tobin, P. Yang, L. Moy, E. Olson, J. Otkin, B. Baum, H. Woolf and X. Xu, 2006: CIMSS Forward Model Capability to Support GOES-R Measurement Simulations, Fourth GOES-R Users Conference, Broomfield, Colorado.

Zhang, Z., P. Yang, G. Kattawar, H-L. Huang, T. Greenwald, J. Li, B. Baum, 2006: A Fast Infrared Radiative Transfer Model Based on the Adding-Doubling Method for Hyperspectral Remote Sensing Applications, *J. of Quantitative Spectroscopy & Radiative Transfer*, provisionally accepted.

4.2 GOES-R Risk Reduction Validation / Demonstration – Dave Tobin

Proposed Work

The demonstration effort proposed for 2006 involves an independent assessment of the capabilities of the derived geophysical data and products. CIMSS participates in this demonstration program by: 1) comparing radiances and derived products with independent correlative measurements from ground-based networks, comprehensive test sites, and field campaigns; 2) comparing radiances and derived products with independent satellite retrieval products from instruments on different platforms; and 3) by performing selected forecast model impact case studies.

Once an algorithm is developed and then implemented with the Data Processing and Archive System, efforts will focus on assessing: 1) the computational efficiency of the algorithm with respect to production requirements, and 2) the accuracy of the products with respect to product requirements. As stated above, the accuracy assessment will make use of comparisons with independent data sources and other validation approaches. Where appropriate and necessary, the algorithm may be developed and implemented for an existing sensor (not GOES-R) such that the demonstration may take place in the pre-launch phase. The proposed demonstration activities for 2006 were:

- Write the first draft of the Product Verification Plan, which will document how we will demonstrate the production and assess the accuracy of the HES-like products.
- Demonstrate and assess the accuracy of the GIFTS L0-L1 algorithms and L1 products using both simulated and real GIFTS data hosted by the GIPS.
- Demonstrate and assess the initial accuracy of a baseline T/q retrieval algorithm hosted by the GIPS. This will be demonstrated by implementing the baseline algorithm for aircraft (S-HIS or NAST-I), AIRS, and/or IASI and assessing the accuracy of the products by comparisons to independent validation data.

Summary of Accomplishments and Findings

Major accomplishments in this area during 2006 were related to the GIFTS L0-L1 algorithm. With the completion of the fabrication of GIFTS in early 2006 and subsequent thermal vacuum and ground based measurement characterization testing, we have been able to demonstrate both the accuracy and processing feasibility of the GIFTS L0-L1 processing algorithms.

GIFTS has 3-sigma (not-to-exceed) overall radiometric calibration requirements of 1K for a range of typical scene brightness temperatures. This accuracy is required for remote sensing applications and is also relevant to satellite inter-calibration efforts. An accurate high spectral resolution sensor in Geo orbit offers the ability to inter-calibrate with numerous LEO sensors to accurately determine, understand, and remove inter-satellite biases.

The GIPS processing algorithms have been refined to work with the real GIFTS data. Major steps in this process during 2006 have involved the implementation of a spectral phase alignment process (which accounts for missed metrology laser fringe counts during interferometer scan turn-arounds), construction of a bad pixel mask, and implementation of a new spectral resampling algorithm. Previous quarterly reports have detailed the progress on some of these aspects of the GIPS.

A focus of the GIPS processing has been the Atmospheric Variability Experiment (AVE) conducted during the GIFTS Ground Based Measurement (GBM). During the GBM, GIFTS was configured to view the atmosphere using a ZnSe chamber window and a 45 degree fold mirror. During AVE, GIFTS data was collected on a regular interval and coincident radiosonde launches were performed to capture the evolution of the boundary layer over approximately 12 hours. Additionally, coincident AERI data was collected, allowing detailed comparisons of GIFTS and AERI radiance spectra. Figure 4.2.1 shows a sample comparison of GIFTS and AERI clear sky spectra. Refinement of the GIPS processing algorithms is on-going under separate funding. In particular, we are refining and implementing a radiometric non-linearity correction for the GIFTS data.

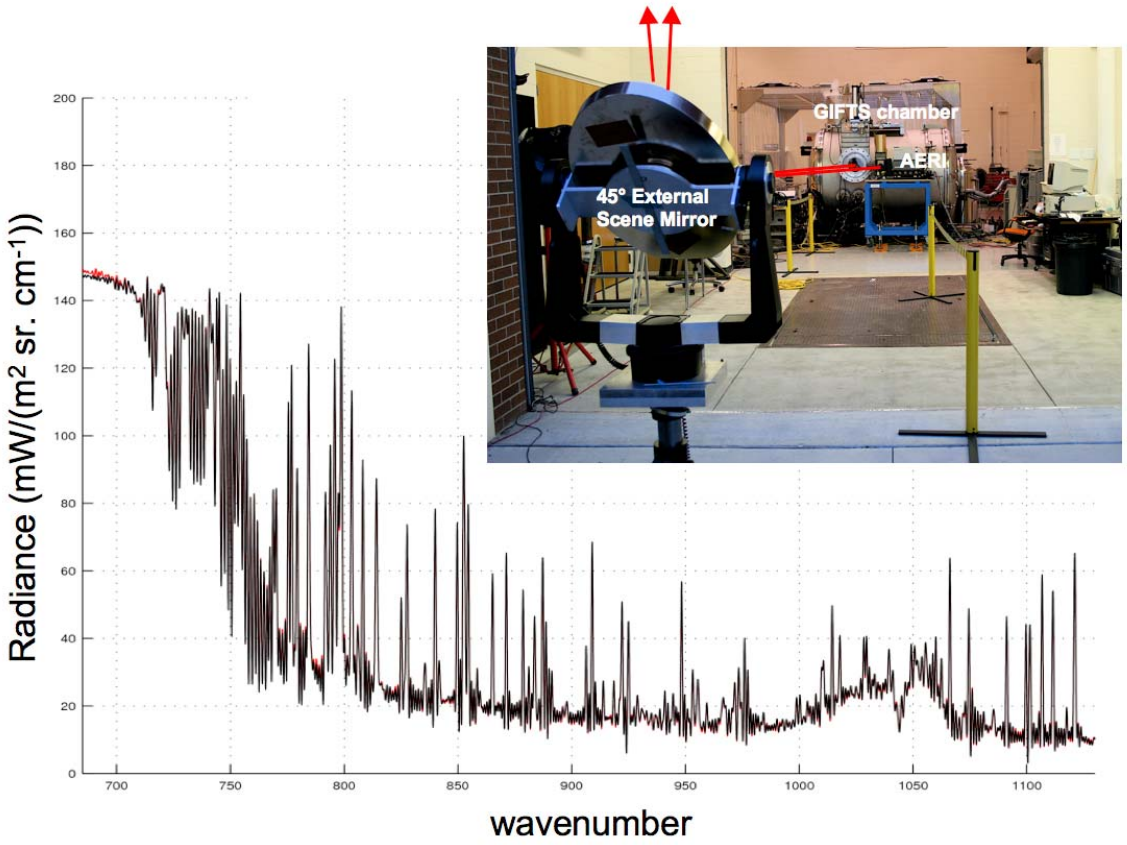

Figure 4.2.1: Comparisons of GIFTS (black) and AERI (red) clear sky zenith viewing radiance spectra collected during the GIFTS Ground Based Measurement Campaign in September 2006.

Regarding Level 2 algorithm demonstration, an initial Level 2 AIRS temperature and water vapor profile retrieval algorithm has been delivered by the Algorithm Developers for implementation in the Data Processing system. Work is underway within the Data Processing group to implement this algorithm. Demonstration efforts will be conducted in the next quarter to evaluate the accuracy of the resulting products, primarily via comparison with ARM site matchup validation data. Additionally, an alternative algorithm has been used to produce temperature and water vapor profiles.

No notable progress was made towards the creation of a Product Verification Plan this year. Under NASA support, a GIFTS Measurement Concept Validation Plan was produced in 2001 (*Tobin, D. C., C. Velden, N. Pougatchev, S. Ackerman, GIFTS Measurement Concept Validation Plan, GIFTS Project Document GIFTS-MCVP-02-002, 12 February 2001*). We had previously planned to build upon this document and the existing GIFTS Product Evaluation Plan to create a draft Product Verification Plan for GOES-RRR algorithms and processing in the GOES-R pre-launch time frame.

Publications and Conference Reports

Reference software implementation for GIFTS ground data processing, R. K. Garcia, H. B. Howell, R. O. Knuteson, G. D. Martin, E. R. Olson, and M. J. Smuga-Otto, Proc. SPIE Int. Soc. Opt. Eng. 6301, 63010Y (2006)

Techniques used in improving the radiance validation of Atmospheric Infrared Sounder (AIRS) observations with the Scanning High-Resolution Interferometer Sounder (S-HIS), Kenneth H. Vinson, David C. Tobin, Henry E. Revercomb, Robert O. Knuteson, Fred A. Best, William L. Smith, Nick N. Ciganovich, Steven Dutcher, Scott D. Ellington, Raymond K. Garcia, H. Benjamin Howell, Daniel D. LaPorte, Joe K. Taylor, Paul van Delst, and Mark W. Werner, Proc. SPIE Int. Soc. Opt. Eng. 6405, 640505 (2006)

Geosynchronous Imaging Fourier Transform Spectrometer (GIFTS) thermal vacuum testing: aspects of spectral characterization, David C. Tobin, Henry E. Revercomb, Joe K. Taylor, Fred A. Best, Robert O. Knuteson, William L. Smith, John Elwell, Greg Cantwell, Gail Bingham, Joe Tansock, Robert A. Reisse, and Daniel K. Zhou, Proc. SPIE Int. Soc. Opt. Eng. 6405, 64050G (2006)

The geosynchronous imaging Fourier transform spectrometer (GIFTS): noise performance, Joe K. Taylor, Henry E. Revercomb, David C. Tobin, Fred A. Best, Robert O. Knuteson, John D. Elwell, Gregory W. Cantwell, Deron K. Scott, Gail E. Bingham, William L. Smith, Daniel K. Zhou, and Robert A. Reisse, Proc. SPIE Int. Soc. Opt. Eng. 6405, 64050J (2006)

Performance verification of the Geosynchronous Imaging Fourier Transform Spectrometer (GIFTS) on-board blackbody calibration system, Fred A. Best, Henry E. Revercomb, David C. Tobin, Robert O. Knuteson, Joseph K. Taylor, Donald J. Thielman, Douglas P. Adler, Mark W. Werner, Scott D. Ellington, John D. Elwell, Deron K. Scott, Gregory W. Cantwell, Gail E. Bingham, and William L. Smith, Proc. SPIE Int. Soc. Opt. Eng. 6405, 64050I (2006)

4.3 GOES-R Risk Reduction Preparation for Data Assimilation – Allen Huang and Xiaolei Zhou

Proposed work

- Expand on the sensitivity study of the GOES-R HES measurements to the actual demonstration of GOES-R high temporal and spectral resolution HES data in the assimilation and analysis system.
- Prepare for data assimilation by demonstrating how to quantify the measurement and product information content provided by simulated HES.
- Optimize the use of GOES-R simulated measurements and explore ideal assimilation and analysis approaches.
- Refine currently available forward and backward operators required by the assimilation system.
- Adapt preprocessing tools such as cloud detection, optimal channel selection, dynamic measurement noise estimation, measurement noise filtering and radiances and sounding products error characterization for the demonstration of AIRS, IASI and simulated HES.
- Document and share preprocessing tools and results from these experiments with other GOES-R Risk Reduction data assimilation teams to assist their HES data assimilation studies.

Summary of accomplishments and findings

Impact of "clear-channel" radiances on storm-scale prediction

We completed a paper entitled "identifying cloud-uncontaminated AIRS spectra from cloudy FOV based on cloud top pressure and weighting functions" (accepted for publication in Mon. Wea. Rev.). In 2007, we'll apply and test a similar algorithm to GIFTS radiances at storm scales.

Consistency between horizontal resolution and vertical resolution

We are conducting an EOF analysis of observed and modeled vertical profiles of the atmospheric temperature and water vapor. Channel selection is not a new topic, but no existing literature focuses on developing a channel selection algorithm that captures the maximum vertical variability derivable from high-spectral resolution radiance data. Preliminary work was completed in 2006. In 2007 we hope to complete a journal paper on this subject.

Applying the sensitivity results of radiance for model's forecast verification and data assimilation

We are writing a journal paper entitled "verifying mesoscale forecasts using the advanced infrared sounder (AIRS) observations and adjoint sensitivity results of radiance." The results of the adjoint sensitivity of radiance are compared and contrasted with the vertical structures of RTM weighting functions, while highlighting the advantages of the adjoint sensitivity study. An error analysis of mesoscale forecasts is then carried out for a mesoscale test case using the AIRS observations and the adjoint sensitivity results. It is shown that such an error analysis may provide useful insights in determining the forecast skill of a model and which AIRS channels may provide the most important information for improving the relevant forecasts. We'd like to conduct a similar study for a storm case next year.

4.4 GOES-R Risk Reduction Nowcasting – Ralph Petersen

Proposed Work

The proposed work focuses on identifying areas of convective instability 3-6 hours in advance of storm development based on the moisture data from current and future GOES satellites. Study areas include: 1) continued development and testing of the Lagrangian model, 2) development of visualization tools to view predicted DPIs in formats identical to the current observational products, 3) use AIRS soundings as a surrogate for GOES-R HES data in assessing the impact of higher vertical resolution on resolving the pre-convective environment, 4) improved utilization of satellite sounders by projecting GOES sounder products ahead in time and space to provide new nowcasting products, 5) assessment of the relative benefits of using moisture retrievals versus radiances in nowcasting and NWP assimilation systems over land, and 6) interaction with NWS/WFOs, NSL and NCEP/SPC to evaluate new objective nowcasting products. Tests using AIRS data to assess the impact of improved GOES sounder vertical resolution on NWP have been de-emphasized following the decision to eliminate HES from the GOES-R series. Experiments using AIRS data in nowcasting are still planned, however. The removal of HES and reduction in program funding also eliminated the proposed collaboration with ORA/ERSL.

Summary of Accomplishments and Findings

Development and testing of Lagrangian model; and improved utilization of satellite sounders to provide new nowcasting products

Efforts this year concentrated on improving the representativeness of the wind data being used to initialize the Lagrangian forecast parcels and to test the system using additional case studies.

Much emphasis has been place on the 13 April 2006 hail event over southern Wisconsin that was not captured in conventional operational NWP guidance, but was evident in detailed nowcasts made 6-hours in advance of the event. In an effort to make the stability calculations more exact and to incorporate the effects of localized diurnal heating evident in GOES data, the nowcasting system is being expanded to include multi-layer predictions of Equivalent Potential Temperature (2e) and vertical differences (the rigorous definition of convective instability). In order to support real-time operational evaluation of the nowcasting products, the model codes are also being transferred from an older developmental platform to a much faster and more reliable Linux-based system.

Develop visualization tools to view predicted DPIs

Work continued to improve tools for anticipating development of severe thunderstorms, especially hard-to-forecast isolated severe events. Recent efforts focused on developing visualization tools and web presentation capabilities that allow operational forecaster to easily integrate consistent images of the DPI observations and nowcasts, and rapidly identify the most important features. A prototype nowcast web page showing the 13April 2006 WI hail event nowcasts is available at http://cimss.ssec.wisc.edu/model/ncstR_13Apr06/nowcast.html. It includes hourly animations of DPI-like images of mid- and high-level precipitable water and derived vertical moisture gradients (key indicators for convective instability), along with verification satellite imagery. In addition, the production of nowcast product images has been modified to use a contemporaneous image from the previous hourly nowcast run as a 'first-guess'. This process increases resolution and retains past nowcast data in new products.

Tests focused on the 13 April 2006 Wisconsin hail storms, which tracked from south of Madison to west of Milwaukee and caused millions of dollars of property damage. Although the standard NWP guidance from the NAM model showed no evidence for this storm development, the nowcast system (see Figure 4.4.1) indicated that the low-level moisture observed over central Indiana in the initial DPI data would transport to an isolated band across south-central Wisconsin within six hours. Simultaneously, an overlaying narrow area of mid-level dryness was shown to move into the same area from south-western Minnesota. Derived vertical moisture differences show an initial development of isolated instability (dark blue to bright red area) over central Iowa at the time of a tornado sighting there, followed by rapid development of instability over extreme southern Wisconsin six hours into the nowcast, when and where the hail storms developed. The results clearly show both the value of the multi-layer moisture data from GOES and the ability of the nowcast system to retain and project isolated moisture extremes in anticipation of hard-to-forecast convective events.

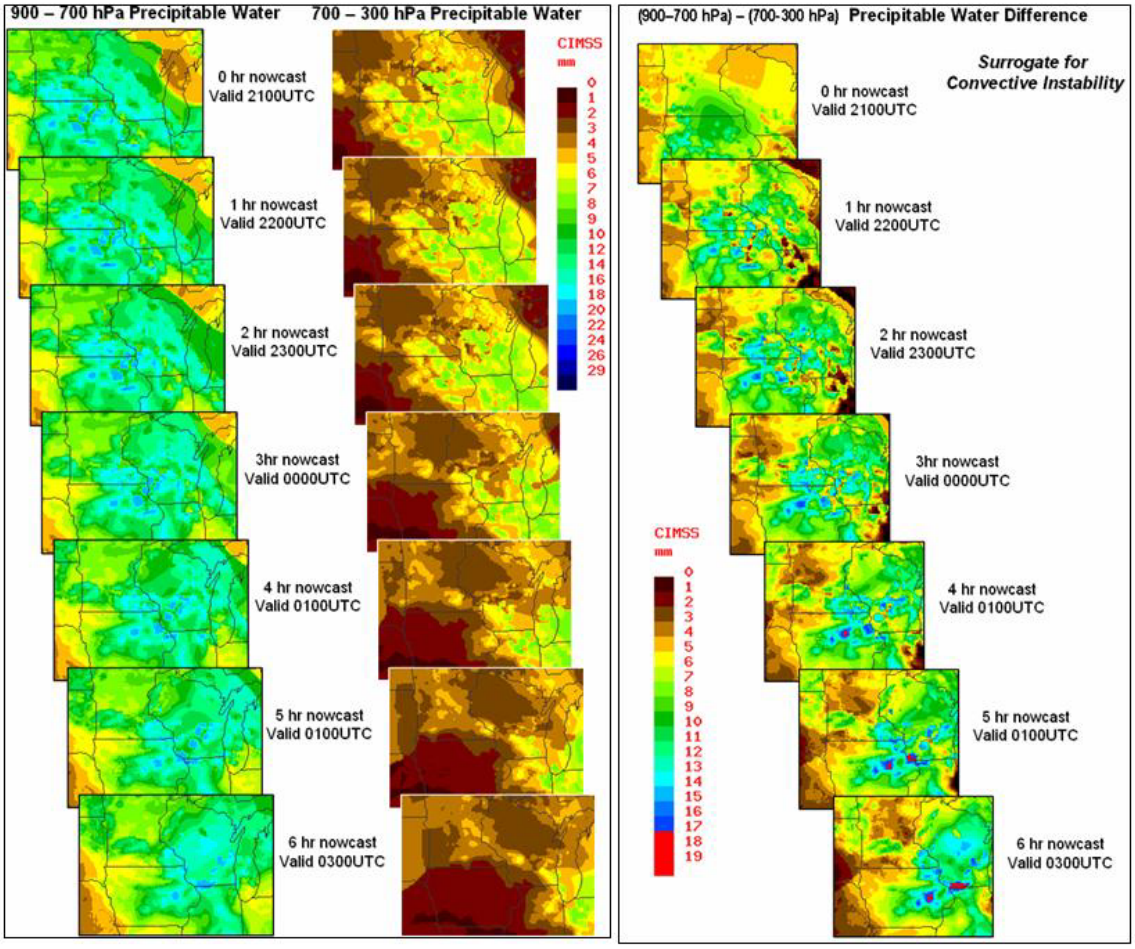

Figure 4.4.1: NAM model NWP guidance (left) and Nowcast product output (right) for severe hail case study over southern Wisconsin.

Use AIRS soundings as a surrogate for GOES-R HES data in assessing the impact of higher vertical resolution on resolving the pre-convective environment

This work, including the incorporation of AIRS sounder products into the NCEP-based WRF/GSI system to accelerate the use of HES in conventional NWP, was scheduled to become more active later in the year. Due to lack of funding at ERSL and the cancellation of HES, many of the resources intended for this work are being redirected to pre-ABI related activities. However, examination of AIRS data for a previously studied severe thunderstorm case showed that POES observations alone could not replace the enhanced spatial and temporal resolution provided by GOES. In this case, the important mesoscale moisture features that were critical to the location and timing of the convective development were entirely missing in the AIRS data – either 'lost' in the data gaps between orbits or 'masked' by cirrus outflow which formed after the initial convection developed prior to the 12-hourly AIRS overpasses (See Figure 4.4.2).

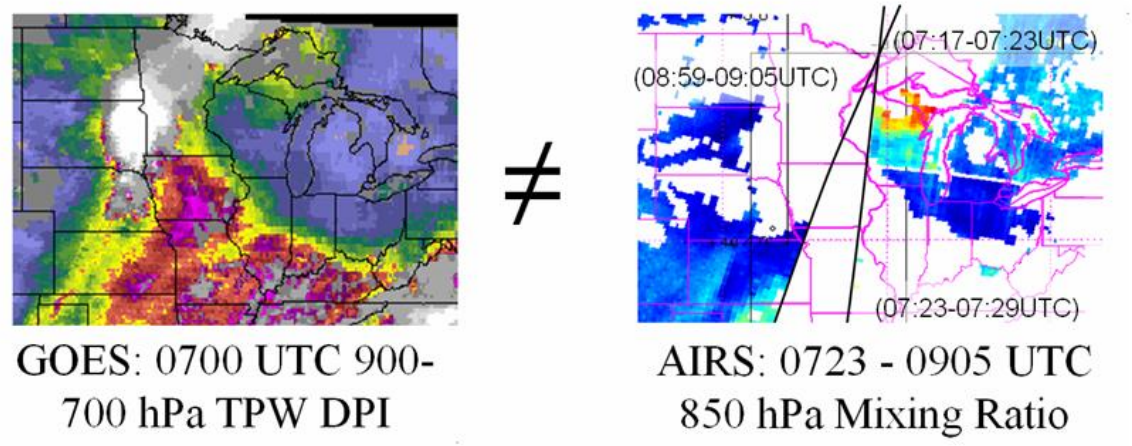

Figure 4.4.2: Severe thunderstorm case illustrating that POES observations alone (right) can not replace the enhanced spatial and temporal resolution provided by GOES (left).

AIRS data for the 13April 2006 hail case have also been processed with both the standard AIRS processing and CIMSS processing. Preliminary results show major improvement in CIMSS data over land. Limited tests of the utility of these higher-vertical resolution data in nowcasts are planned for the coming year.

Interact with NWS/WFOs, NSL and NCEP/SPC to evaluate new objective nowcasting products
Initial discussions have begun with NWS/Green Bay (GRB) and NWS/Sullivan. GRB has offered to host an overview seminar this winter based on the fully functional web page and real-time model output. The seminar would include discussions of how to best quantify the usefulness of the products, and how to improve presentation methods for next year's severe storm season. Based on review of the case study results discussed above, GRB has further offered to expand the seminar participation to include NWS offices at Sullivan, LaCrosse, Minneapolis and Marquette for expanded testing and evaluation.

Publications and Conference Reports

Petersen, R. A., 2006: Travels with Charlie: An invited paper on the future direction of international aviation meteorology presented at the WMO Commission on Aeronautical Meteorology. Geneva, Switzerland

Petersen, R. A. and R. Aune, 2006: An objective nowcasting tool that optimizes the impact of GOES Derive Product Imagery in very-short-range forecasts. AMS Satellite Conference. Atlanta, GA

Petersen, R. A. and R. Aune, 2006: An objective nowcasting tool that optimizes the impact of GOES Derive Product Imagery in very-short-range forecasts. GOES Users' Conference. Boulder, GA

Petersen, R. A. and R. Aune, 2006: An objective nowcasting tool that optimizes the impact of GOES Derive Product Imagery in very-short-range forecasts. *Proceedings of SPIE Optics and Photonics 2006 -- Volume 6301*: Atmospheric and Environmental Remote Sensing Data Processing and Utilization II. San Diego, CA

4.5 GOES-R Risk Reduction Ground System Design and Studies – Bob Knuteson

Proposed Work
The CIMSS GOES-R Risk Reduction activities related to ground data processing design and system studies in 2006 had three major objectives; 1) the evaluation of on-orbit algorithms for the L0 to L1 calibration of the Geostationary Imaging Fourier Transform Spectrometer (GIFTS) as a risk reduction activity for the GOES-R Hyperspectral Environmental Suite (HES) sounder, 2) the preliminary design of ground processing architectures suitable for the large data volumes and high throughput requirements of the GOES-R sensors (ABI and HES), and 3) the demonstration of advanced computing technology in the areas of data storage and retrieval, cluster computing, high speed networks and distributed computing specifically applied to the data anticipated in the GOES-R time frame. Significant progress was made in each of these areas which can now be transitioned into the implementation needed for NOAA Algorithm Working Group integration and for the future ground data processing system for GIFTS or any other geostationary hyperspectral infrared sounder.

Summary of Accomplishments and Findings
Significant progress was made in each of the task areas in 2006. Highlights are provided below:

- A 24 hour simulation of "full-disk" Earth emitted radiances was developed under this risk reduction activity in order to support the large scale simulation studies required for the ABI and HES sounder. This dataset has since become one of the proxy datasets that will be used by the Algorithm Working Groups. A paper on the 24 hour full disk simulation was presented at the AMS annual meeting in January 2006. The full simulation was completed mid-year and is available upon request. In addition to the WRF model fields, the dataset includes top of atmosphere radiances for a broad continuous spectral region of the infrared at high enough spectral resolution to allow the simulation of numerous infrared sensors including the ABI and GIFTS. In addition, interferograms were created from this dataset simulating the GIFTS on-orbit observations. This "raw" sensor data has been used in a successful demonstration of the scalability of the GIFTS Information Processing System (GIPS) software under another NOAA grant for the Office of Systems Development (McKenzie). It is anticipated that future simulated datasets of this type will be supported by the AWG proxy data team using the approach developed under this risk reduction task.

- A draft GIFTS L0-L1 Algorithm Theoretical Basis Document (ATBD) was prepared in conformance to the NOAA STAR documentation guidelines and is available from the UW-Madison SSEC web site. A paper was presented at the 2006 AMS annual meeting on this topic. The draft GIFTS L0-L1 ATBD is intended to be an evolutionary document that describes both the theoretical equations for the target algorithms and the detailed performance tradeoffs that need to be considered in software implementation of the algorithms. In 2006, real data from the GIFTS thermal vacuum testing was used to evaluate existing algorithms and modify or extend them for application to the actual thermal vacuum test data. Data sets with both laboratory blackbody and sky-viewing scenes were identified from tests run by NASA at Space Dynamics Laboratory in Logan, Utah between May and September 2006. Simply acquiring these datasets for evaluation is a significant task due to the relatively large data volumes involved and the need to develop new tools for working with the data files as provided by NASA. The GIFTS

ATBD has been used in the GIPS software development project mentioned previously. While there is a need for continuing refinement of these algorithms it is suggested that further ATBD changes be funded by a GIFTS specific ground system development activity rather than under GOES-R risk reduction. This is consistent with the mature level of this algorithm development.

- Designs of the system level concept for processing of GOES-R data in an efficient and reliable manner have been captured in the form of data flow diagrams (see diagrams below). The primary technologies that are being leveraged for the future system designs are cluster computing and intelligent storage systems combined with high speed networks for efficient parallel processing of sensor fields of view. This approach of parallel mass computing reflects the needs of the GOES-R program where the future sensors are anticipated to collect multiple fields of view simultaneously with nearly two orders of magnitude increase in sensor data rates. The UW-Madison SSEC has also performed some computing and cost estimation studies which are summarized below for the GIFTS sensor as it is currently configured for flight. Further work to refine these system designs will be deferred until the status of the geostationary hyperspectral sounder is clarified.

- A preliminary design study for GOES-R Level 2 processing was conducted assuming the use of simulated Earth observations in a high performance computing environment. A diagram showing an example data flow is provided below. Numerous technical details have been identified in an assessment of the existing UW-Madison SSEC software code base which will be used in the development of a prototype implementation of the water vapor winds processing. The activities under this risk reduction task are being coordinated with the AWG Algorithm Integration Team (AIT) leader (W. Wolf). It is anticipated that further CIMSS work in this task area will be supported directly by the AWG AIT under separate funding.

- A forward looking demonstration, called Origami, was developed during the task period in order to link distributed computing methods, client-server data distribution, and database management to visualization tools with a user friendly web interface. The Origami demonstration was extremely successful in illustrating how existing modern infrastructure technologies, e.g. storage area network, database engines, cluster computing, and open data access protocols, can be coupled with the next generation UW-Madison SSEC visualization tools (the IDV which is built upon VISAD) to create a development environment suitable for the GOES-R era. While the Origami demonstration was intended to highlight the integration of modern technologies, it also shows how large scale computing resources can be coupled in a seamless manner to three dimensional visualization of model and observed state parameters in a manner that can be scaled up to any size problem. The scalability of a computing system suitable for GOES-R that has the features contained by the existing McIDAS system for the current GOES sensor plus the additional functionality required for the GOES-R series is the ultimate goal of this work. A diagram of the Origami concept is provided below and was presented at the Fall AGU meeting in December 2006. Future progress in this area will be limited by available funding but continuing the exploration of this work under GOES-R risk reduction is highly recommended.

Diagrams developed under GOES-R Risk Reduction funding for ground data processing system design and study are provided below:

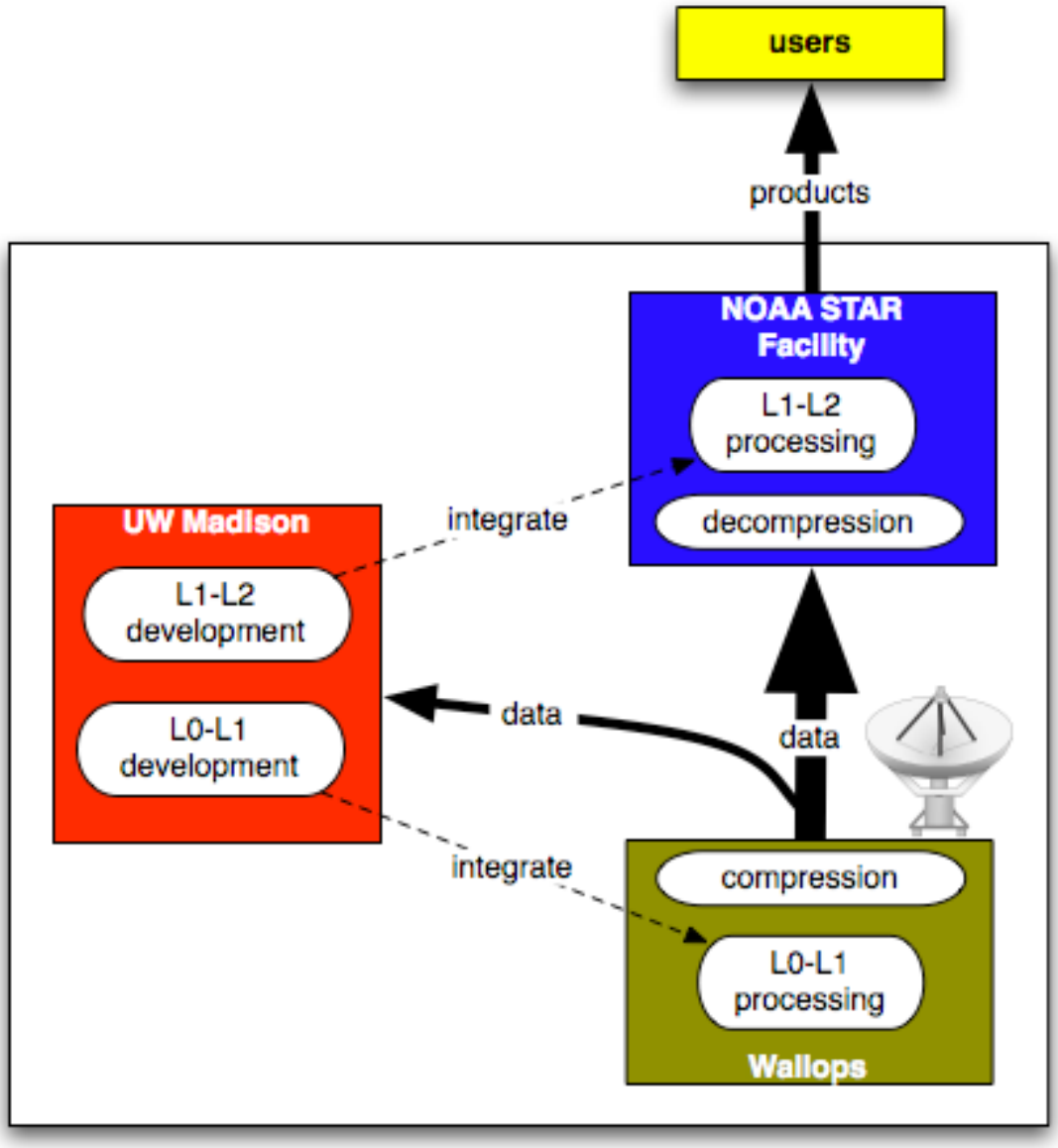

Figure 4.5.1: Ground Segment Concept Proposed by UW-Madison CIMSS.

Figure 4.5.1 shows the proposed concept for a ground system for GOES-R which combines the efforts of NOAA OSD, NOAA STAR, and the cooperative institutes. This diagram is suitable for ABI and other sensors. In particular, the UW-Madison CIMSS has estimated the system elements for the NASA GIFTS sensor assuming that it would be processed under this concept. A preliminary computing estimate for a L0-L1 (raw downlink to calibrated radiances) near real-time cluster processing system is about 150 dual cores or 75 quad core machines using current commodity hardware. Most of the CPU time needed is for easily parallelizable computations such as FFTs, which can be performed independently on every pixel in a cube of incoming data, making compute cluster computing the natural low-cost solution for deploying a ground system. Higher level data processing (beyond calibrated radiances) is believed to require a system of similar size.

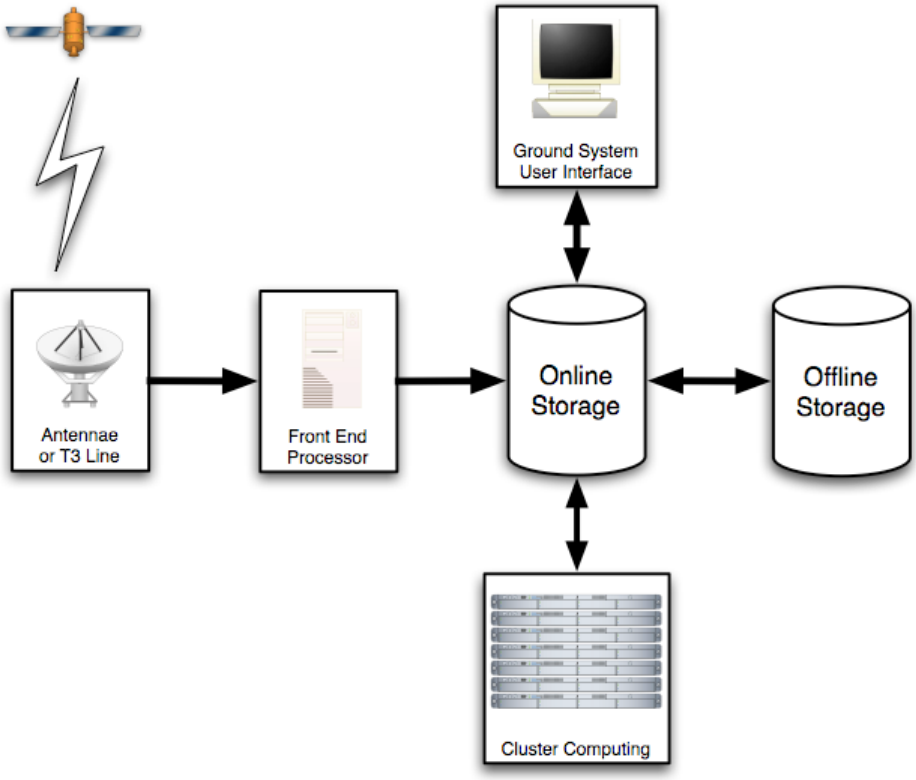

Figure 4.5.2: Ground Data Processing System Concept for UW-Madison CIMSS Development System.

Figure 4.5.2 illustrates the elements required in any ground data processing system independent of sensor or product. This diagram in particular is intended to identify the design concept of the development system which is suggested be located at UW-Madison CIMSS for support of the GOES-R algorithm development and subsequent data processing. Detailed cost estimates for a system designed to process GIFTS on orbit data in an on-demand mode are available by contacting the investigators.

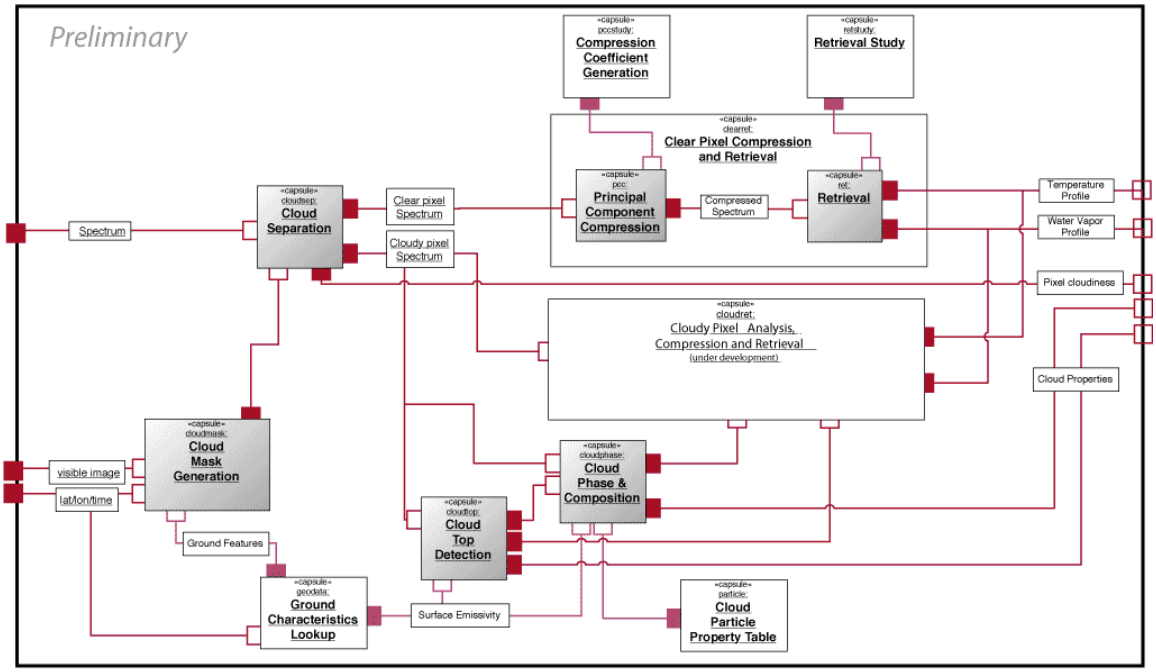

Figure 4.5.3: Data Flow Diagram for Level 2 Products from GOES-R.

Figure 4.5.3 shows a possible module and dependency graph for processing calibrated spectra into retrieved T/WV profiles and cloud mask. Refining the individual algorithms identified in this diagram is an active area of research of the Algorithm Working Group. This style of diagram makes use of Unified Metadata Language (UML) which provides a consistent framework for the definition of interfaces between software modules. This example is of the temperature and water vapor profile product but serves as an illustration of the type of diagram that needs to be created by the Algorithm Integration Team for each GOES-R product.

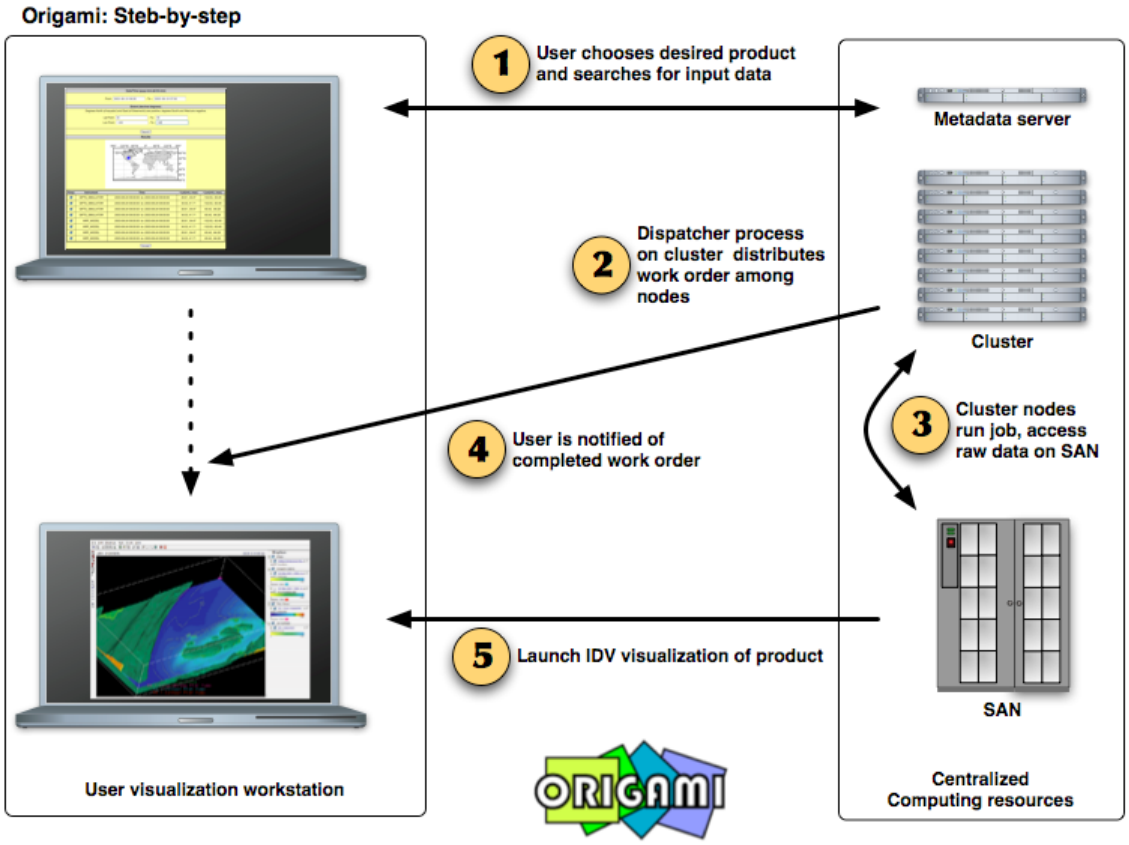

Figure 4.5.4: Origami Demonstration Conceptual Diagram.

The Origami demonstration is a lightweight on-demand processing model for computing subsets of online or archived GOES-R data for algorithm development and product validation. The demonstration shows how to couple scalable computing resources (cluster compute nodes and storage area networks) with fully three dimensional visualization tools using with a simple web browser based user interface. The technologies used within the Origami demo are key elements for any future GOES-R ground data processing system and moreover provide a bridge both to the past GOES (McIDAS) systems and to data from external systems like POES/NPOESS polar data and NMC model fields.

Publications and Conference Reports

Knuteson, R., R. Garcia, E. Olson, H. Revercomb, M. Smuga-Otto, D. Tobin, 2006: Preliminary Evaluation of the GIFTS Calibration Algorithm Using the GIPS, AMS Annual Meeting in Atlanta, Georgia, January 2006

Olson, E., J. Otkin, R. Knuteson, M. Smuga-Otto, R. Garcia, W. Feltz, H.L. Huang, C. Velden, L. Moy, 2006: Geostationary Interferometer 24-Hour Simulated Dataset for Test Processing and Calibration, AMS Annual Meeting in Atlanta, Georgia, January 2006

Smuga-Otto, M., R. Garcia, R. Knuteson, G. Martin, B. Flynn, D. Hackel, 2006: Integrating a High-Throughput Parallel Processing Framework and Storage Area Network Concepts into a Prototype Interactive Scientific Visualization Environment for Hyperspectral Data, poster paper American Geophysical Union (AGU) Fall Meeting, San Francisco, December 2006.

5 GOES R Instrument Studies – Jun Li

Proposed Work

(1) Conduct research on GOES-R (and beyond) imager and sounder requirements and instrument trade-offs to balance the spectral coverage/resolution, spatial resolution, temporal resolution, radiometric resolution, and other instrument characteristics for instrument optimization;
(2) Demonstrate what the GOES-R systems may look like and make the GOES-R systems more understandable to the public and end-users;
(3) Study the impact of GOES-R sensor characteristics, system characteristics and scan strategy on the science products and their applications;
(4) Study the improvements/advantages and benefits from the GOES-R (and beyond) systems over the current GOES systems in forecasting and nowcasting various weather and environmental events.
(5) Investigate the continuity of current GOES Sounder products with ABI and perform tradeoff studies on GOES-R sounding options.

The specific goals for 2006 were:

- Support HES (Hyperspectral Environmental Suite) critical reviews.
- Study the impact of GOES-R instrument changes/refinement on science products.
- Continue to do trade-off studies to support HES design and requirement.
- Study the impact of GOES-R sensor characteristics, system characteristics, and GOES-R scan strategy on science products and their applications.

Summary of GOES-R Instrument Studies Accomplishments in 2006

Study the impact of GOES-R instrument changes/refinement on science products
Advanced Baseline Imager (ABI) continuation of the current GOES Sounder products
The ability of the ABI to support continued production of current GOES Sounder operational products is important since it will fly before the HES. Initial simulation shows that ABI can provide similar moisture information to the current GOES Sounder with a fast coverage rate. However, a hyperspectral IR sounder is needed if advanced temperature and moisture sounding products are required.

The needed 'continuity' products (radiances, TPW, LI, skin temperature, clouds, and winds) from today's sounder can be provided by the ABI even though the ABI is not a sounder. In order to simulate the ABI's ability to continue the current GOES Sounder products, the following clear sky retrieval simulation was carried out:

- Near-Global Radiosonde Observations (RAOBs)
  - 600 independent sounding retrievals
- Retrieval algorithm is based on regression (first guess) followed by physical (final)
- HES spectral coverage assumed
  - 675 – 1200 with spectral resolution of 0.625 cm**-1
  - 1689 – 2150 with spectral resolution of 1.25 cm**-1
  - 2150 – 2400 with spectral resolution of 2.50 cm**-1
  - Noise from Performance and Operational requirements Document

- Current GOES Sounder spec noise is assumed for GOES-N class sounder
- ABI 9 infrared (IR) spectral bands are used, the noise is assumed to be
  - K @300 K for all IR bands except the 13.3 um band
  - K @300 K for 13.3 um band

Figure 5.1 shows the temperature and relative humidity retrieval RMSE from various ABI fields of regard compared to the GOES-N class sounder and HES.

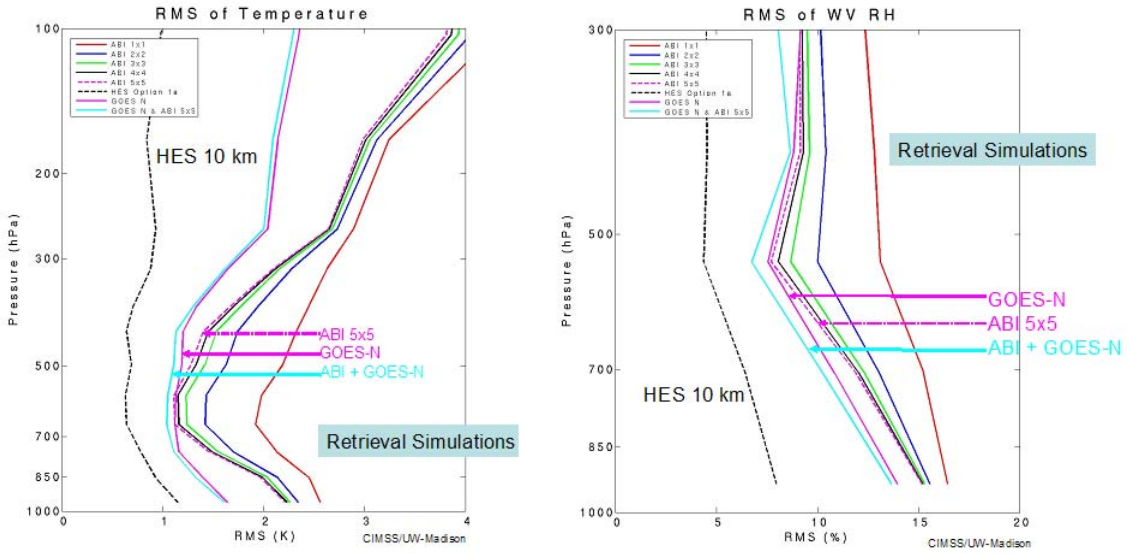

Figure 5.1: RMSE for various ABI fields of regard, the GOES-N class Sounder, and HES. *Left:* temperature retrieval. *Right:* relative humidity retrieval.

Initial simulation shows that ABI 5 by 5 measurements contain moisture information similar to the GOES-N class sounder. This is due to the fact that the ABI has water vapor absorption bands similar to the GOES-N class sounder even though the spectral coverage is a little different. Due to the lack of CO_2 channels, however, the ABI does not provide good temperature information. The combination of forecast and ABI for temperature soundings is being studied.

ABI simulation results were presented by Jun Li and Tim Schmit at the GOES-R conference held on 13 September 2006 at NOAA science center in DC.

Given an ABI, it is not cost effective to procure additional GOES-N class sounders in the GOES-R era to generate currently used sounder products. Because the GOES-N class sounders have a slow scan rate and broad spectral resolution, the resources would be better spent on the deployment of a high spectral sounder (even one in demonstration mode).

A geostationary hyperspectral infrared (IR) sounder would provide high spatial and temporal coverage that is unique for regional weather forecasting. Currently only the Atmospheric Infrared Sounder (AIRS) on NASA's polar orbiting Aqua satellite provides hyperspectral IR measurements (the European IASI has just been launched). The animation below (see Figure 5.2) shows the hourly AIRS measurements (an IR window image) within an approximate geostationary disk coverage area. A geostationary hyperspectral sounder will provide full hourly disk coverage rather than the partial coverage available with polar orbiting sounders, and will do

so with a spatial resolution better than 10 km, as opposed to the 14 km resolution of AIRS. The GIF loop animation can be obtained from:

http://www.ssec.wisc.edu/~cyliu/tmp/GOES_simulation/AIRSonDisk/AIRSonDisk.gif

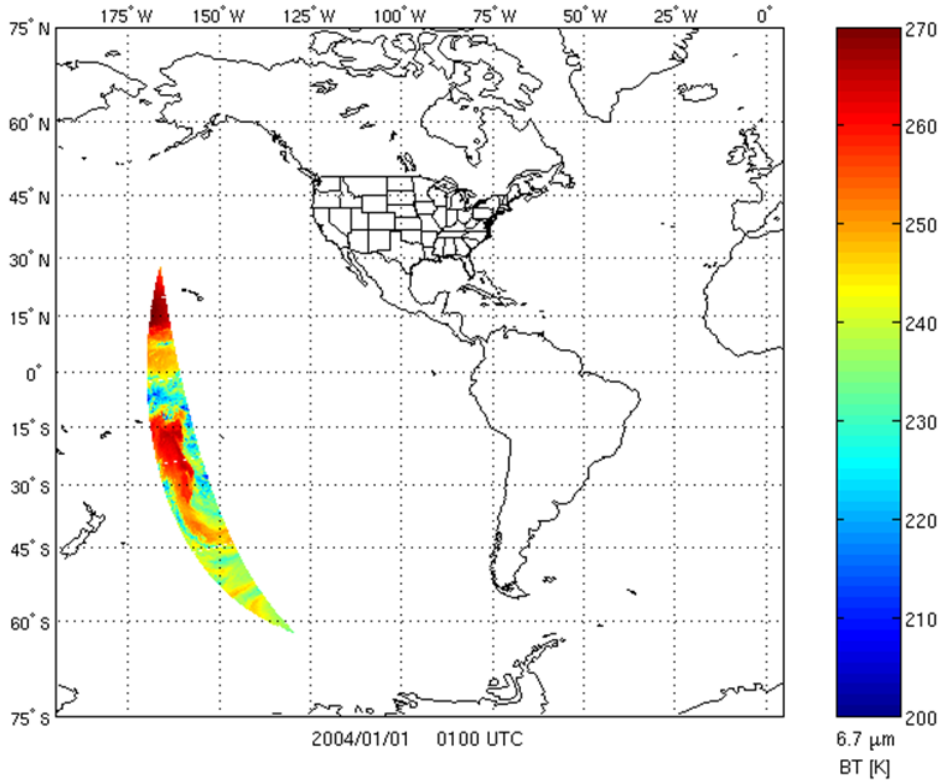

Figure 5.2: An AIRS water vapor channel brightness temperature (BT) image over GOES disk coverage within one hour.

ABI data set for compression

ABI compression datasets are available via FTP, and GOES-12 Imager full disk images have been added to the CIMSS ABI compression study dataset archive. The GOES-12 Imager data were added to a growing set of data that researchers are using to examine data compression techniques to benefit current and future GOES imager data storage and dissemination. Other data sets provided so far include MODerate-resolution Imaging Spectroradiometer (MODIS) data which have had their bit-depths reduced to presumed ABI parameters, unaltered MODIS data, and Meteosat-8 full disk images.

In addition, a database of convective turbulence MODIS imagery has been collected for ABI simulations. Examples of convective cases are collected from MODIS data for ABI simulation. To see what has been done to date, visit:

http://www.ssec.wisc.edu/~jordang/ConvGW/index.html

Trade-off Studies

Summary of HES (Hyperspectral Environmental Suite) spectral coverage study
We continued to investigate HES spectral coverage by performing trade-off studies per Atmosphere-Ocean-Land Technical Advisory Panel (AOL TAP) request. These studies included: 1) comparison of current GOES Sounder temperature, moisture, and ozone data quality to that of the GOES-R Minimum Mission (MM) capability, 2) study of the three proposed HES options, and 3) evaluation of the likely impacts from relaxed longwave CO_2 region noise, reduction to the HES longwave window region, and relaxed H_2O region spectral resolution coupled with an increased signal-to-noise ratio (SNR).

HES capability and LWCO2 (longwave CO2 band) cutoff studies using AIRS
We used both simulated and real hyperspectral radiances for HES trade-off studies. Usually, there are two ways to perform trade-off studies; using simulated or real data (e.g., AIRS, IASI). The advantage of using simulated data is that the truth is known and the information can be well identified, the disadvantage is that the realistic surface (e.g., emissivity) and atmospheric (e.g., trace gas, clouds) conditions are difficult to handle in simulation. On the other hand, AIRS data contain real surface and atmospheric conditions, but truth is not available. We use collocated best estimated radiosonde profiles ("truth") and AIRS radiances at the ARM CART site for HES spectral trade-off studies and sounding capability demonstration. Approximately 500 matches representing a variety of atmospheric conditions have been collected.

AIRS is representative of the capability of HES to retrieve vertical structure. The AIRS moisture retrieval profile is compared with the best estimate profile (true) at the ARM CART site. Figure 5.3 shows the AIRS brightness temperature spectrum, AIRS sounding retrieval profiles and best estimated profiles for temperature and water vapor at the ARM CART Site. The retrieval starts with a smoothed first guess (red), and the vertical structures of temperature and moisture are captured by AIRS measurements. Those vertical structures are very important for short range and regional forecast.

In addition, AIRS data are used to study the atmospheric variability at the ARM CART Site. By looking at the BT spectral variability, $LWCO_2$ cutoff can be estimated based on the users' requirements on temperature profile product. We also used NASTI full spectral coverage with high spectral resolution for HES trade-off studies.

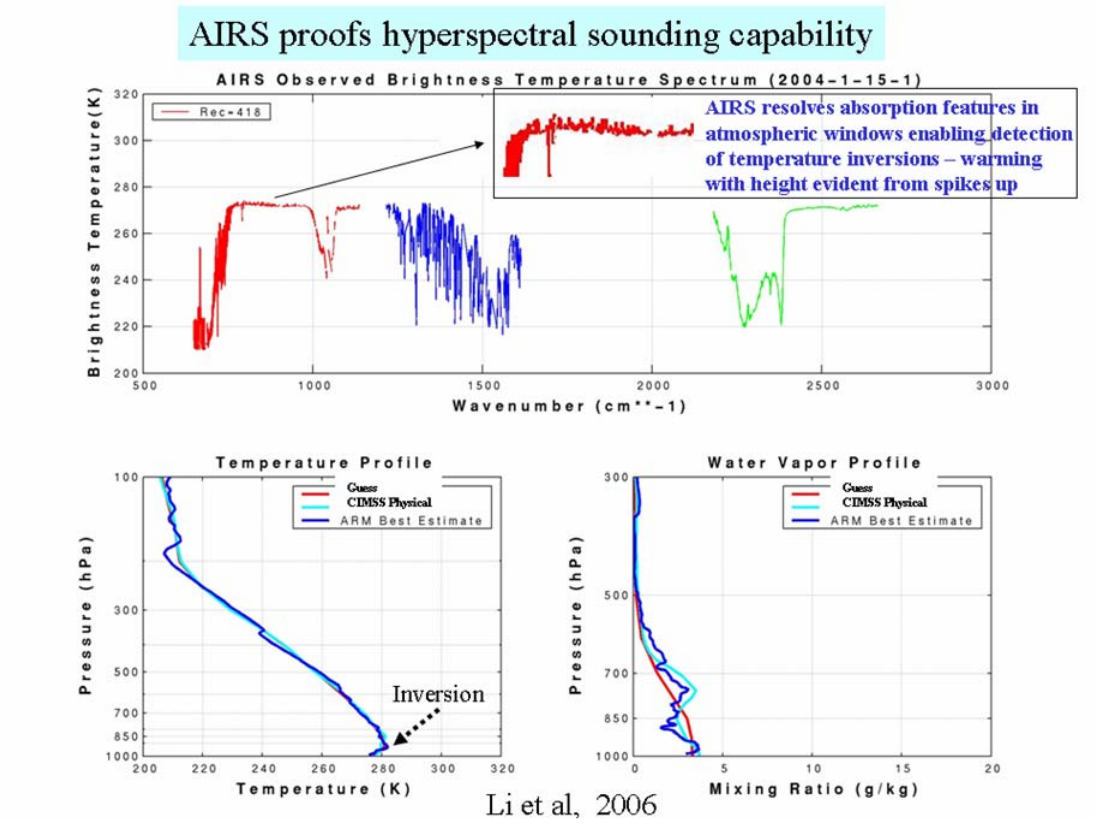

Figure 5.3: (Top) The AIRS brightness temperature spectrum; (Bottom left) AIRS temperature sounding retrieval (light blue, CIMSS version) and best estimated profile (truth) at ARM Cart Site (dark blue); (Bottom right) AIRS water vapor sounding retrieval (light blue) and best estimated profile (truth) at ARM Cart Site (dark blue).

HES Minimum Mission (MM) studies

Clear sky simulation revealed that significant degradation of temperature and moisture retrieval quality would result under minimum mission (MM) capabilities as compared to the HES 2-band (650 – 1200, 1650 – 2250 cm^{-1} with 0.625 cm^{-1} spectral resolution) option. The shortwave and longwave sides of the H2O band are nearly equivalent in moisture information content – either will serve HES well for moisture retrievals. Additionally, the ozone profile retrieval would benefit significantly from inclusion of the 9.6 μm band in the longwave region.

Study of HES three options

The following three proposed HES options were studied:

Option 1 (wavenumber in cm^{-1}) (spectral resolution in cm^{-1})

a. (675-1200) (0.625) + (1689-2150) (1.25) + (2150-2400) (2.5)
b. (675-1200) (0.625) + (1210-1645) (1.25) + (2150-2400) (2.5)

Option 2

(675-1000) (0.625) + (1689-2150) (1.25)

Option 3

a. (675-1080) (0.625) + (1689-2150) (1.25)
b. (675-1000) (0.625) + (1689-2150) (1.25) + (2150-2250; 2350-2400) (2.5)
c. (675-1080) (0.625) + (1689-2150) (1.25) + (2150-2250; 2350-2400) (2.5)

Clear sky simulation shows that, in the bulk sense, there is no significant difference among the three options for temperature and moisture retrieval. Option 1 is slightly better, however.

Study of relaxing H2O region spectral resolution but increasing SNR
Simulation shows it is comparable (although the simulations aren't exact -- the noise and spectral resolution are treated separately and the spectral degradation is larger than that proposed). Stated another way, the improved noise seems to offset the poorer spectral resolution. On the other hand, we should keep in mind that once we give up on spectral resolution, it's gone. But, instrument noise may come in better than spec. So, ideally, we should leave things as they are. From H2O vertical resolution point of view, finer spectral resolution in the water vapor region is critical for structure retrieval.

HES end-formulation
CIMSS HES trade-off results are presented at the 3rd GOES-R Users' Conference held in Broomfield, CO from 01 to 03 May 2006. Figure 5.4 illustrates HES end-formulation coverage compared with the current GOES Sounder coverage. The HES end-formulation coverage includes coverage in all current GOES Sounder bands. This project also supported CIMSS scientist (Hank Revercomb) to attend HES reviews.

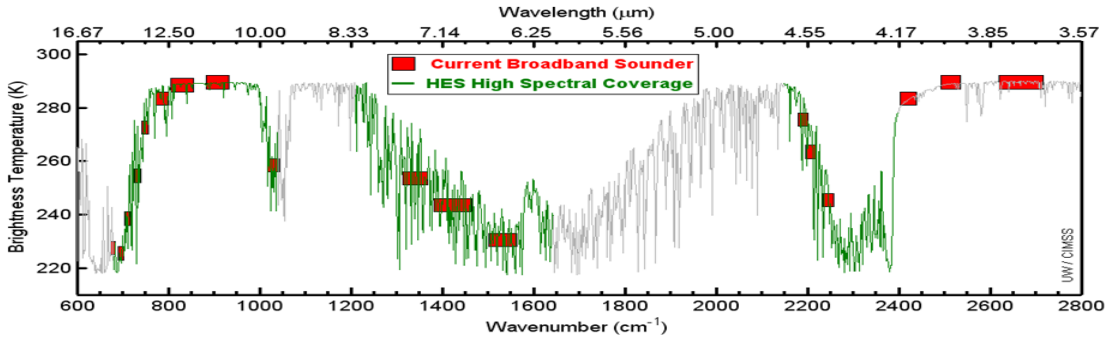

Figure 5.4: Spectral coverage of HES (end of formulation) along with the current GOES Sounder coverage**.**

Study the impact of GOES-R sensor characteristics, system characteristics, and GOES-R scan strategy on science products and their applications

HES point spread function impact on sounding product
The Point Spread Function (PSF) causes blurring error as reported in our 2005 report. In 2006 we studied the impact of blurring on temperature and moisture retrieval using MODIS 1 km IR data for 1915 UTC on 06 Sept. 2002. Only clear simulated footprints with 10 km spatial resolution are included in the retrieval test. Figure 5.5 shows the BT difference (BTD) between 100% Ensquared Energy (EE) and 90%, 80%, and 70% EE, respectively, for the MODIS 11 IR spectral bands. It can be seen that BT blurring is not random; it varies spectrally. The BTD in the window bands is larger than that in the absorption bands.

The BTD impact on temperature and moisture retrieval is also quantified with MODIS IR data. We found that 90%, 80% and 70% EE will cause approximately 0.07, 0.10 and 0.15 K additional temperature retrieval error, respectively.. For the water vapor relative humidity (RH), 90%, 80% and 70% EE will cause approximately 0.4%, 0.6% and 0.8% additional retrieval error, respectively.

In addition, the AOL TAP requested that we study the effect of Detector Optical Ensquared Energy (DOEE) blurring. A study using the MAS (MODIS Airborne Simulator) 50 meter spatial resolution data showed that the blurring error difference between 88% and 84% is small, 88% is slightly better than 84%.

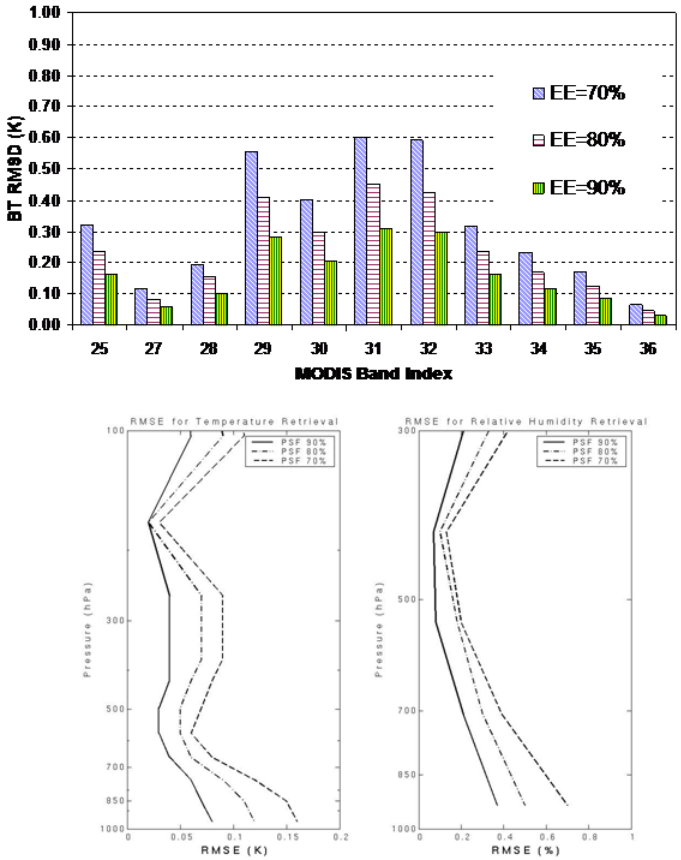

Figure 5.5: (Top) The Brightness Temperature Difference between 100%Ensquared Energy (EE) and 70%, 80%, 90%EE, respectively, for the MODIS 11 IR spectral bands; (Bottom left) additional temperature retrieval error due to 90%, 80% and 70% EE, respectively; (Bottom right) additional relative humidity (RH) retrieval error due to 90%, 80% and 70% EE, respectively.

Impact of a two-satellite system versus one-satellite system

The impact on science of a two-satellite system for ABI and HES (e.g., ABI/HES synergy) was studied using ECMWF forecast analysis data. Results show that effective synergy of ABI and HES radiances (for cloud-clearing applications) requires that the ABI and HES are close within a distance of less than 0.5 degree in geostationary orbit. Figure 5.6 shows the brightness temperature difference (BTD) for ABI 11.2 and 7.4 μm due to a .5 degree viewing angle difference between satellites. The BTD in this simulation ranges from -.2K to +.2K, and

introduction of clouds and other effects would likely make the differences larger. The possibility of correcting for different viewing angles was also studied. A partial correction for this difference is possible, but it is difficult because of its high dependence on water vapor conditions.

ABI/HES cloud-clearing requires that the ABI and HES are close with a distance of less than 0.5 degree in geostationary orbit. However, synergy between the level 2 product from one instrument and the radiances from the other instrument doe not require this proximity. In addition, direct cloudy sounding through combination of ABI clear radiances and HES cloudy radiances is not constrained to a one-satellite system.

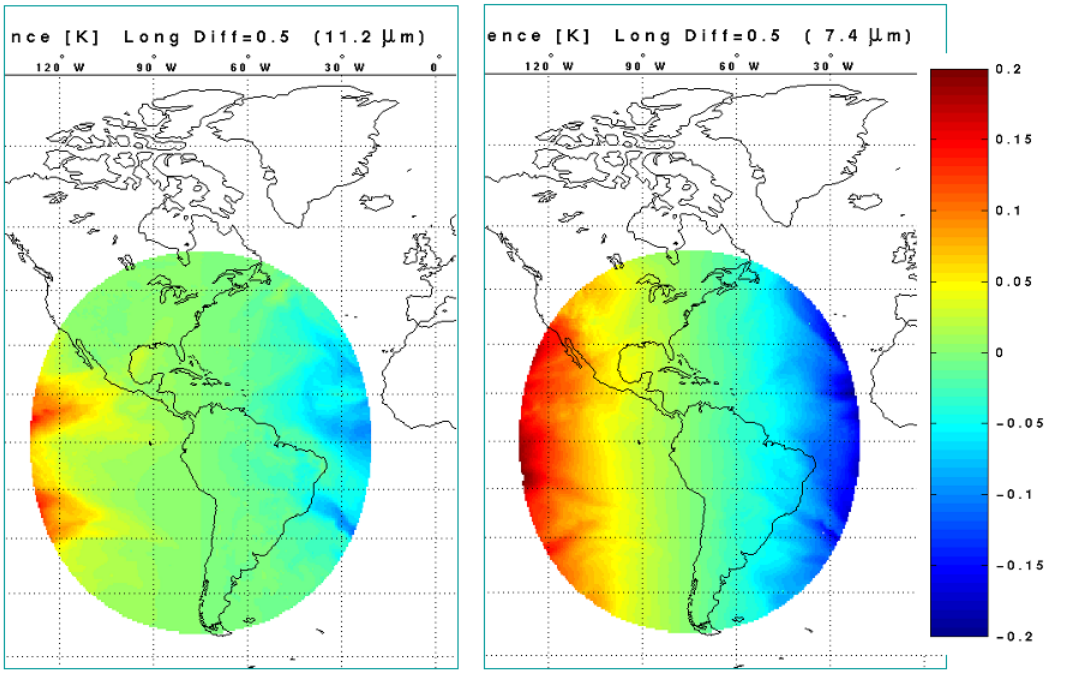

Figure 5.6: The Brightness Temperature Difference for ABI 11.2 and 7.4 µm due to the viewing angle difference within a two-satellite system.

Pros of one-HES (central)

- Fewer HES cost less
- Eliminate merged "seam" in central U.S.
- Eliminate the "notch" in the north-central U.S.
    - "notch" will be bigger if GOES-W is at 137W
- Better satellite view angle of CONUS
- Slightly better retrievals over CONUS
- Allows radiances for regional applications
- May still combine with ABI product information
    - if its within a time window
    - if parallax is corrected for
- Assures fully capable HES

- LW and SW CO_2, O_3, Windows, CW (Costal Water), etc.

Cons of one-HES when compared with two-HES

- Poorer satellite view (of 65 degree) of Hawaii
- May be important for CW application
- Can NPOESS monitor frequently enough?
- Less coverage on the (east-west) edges to combine with ABI
- NWS "hemispheric coverage" reduced and ocean coverage is reduced significantly
- Poorer view of hurricane genesis areas in Atlantic and Pacific
- Poorer view of cloud edges during convective initiation (ABI could be used.)
- Can't use combined radiances for cloud-clearing
- Significant problems time-sharing with HES-CW

Figure 5.7 shows the BT (clear sky calculations from ECMWF analysis) coverage from two-HES (left panel) and one-HES (right) with local zenith angle of 62.5 degree.

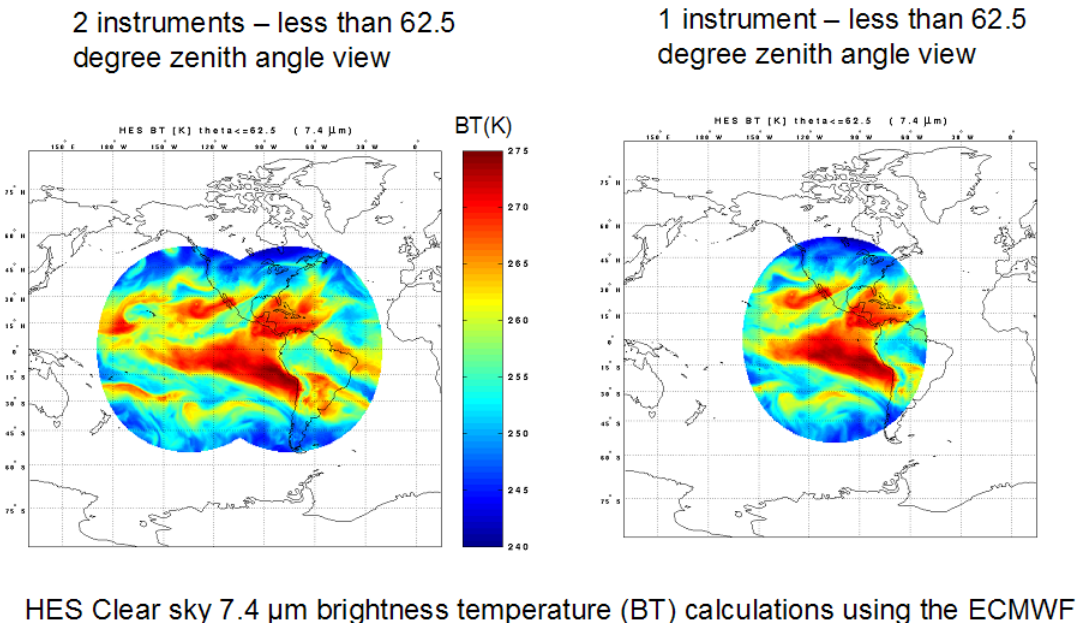

Figure 5.7: The BT (clear sky calculations from ECMWF analysis) coverage from: *Left:* two-HES, and *Right*: one-HES with local zenith angle of 62.5 degree.

Publications and Conference Reports

Li, J., P. Zhang, T. J. Schmit, J. Schmetz, and W. P. Menzel, 2007: Quantitative monitoring of a Saharan dust event with SEVIRI on Meteosat-8, *International Journal of Remote Sensing* (in press).

Li, Z., J. Li, T. J. Schmit, W. P. Menzel, 2007: Current and future environmental satellite imagers on scene classification, *Remote Sensing Environment* (in press).

Zhang, P., J. Li, T. J. Schmit, E. Olso, and W. P. Menzel, 2006: Impact of point spread function on infrared radiances from geostationary satellite, *IEEE Trans. On Geoscience and Remote Sensing*, 44, 2176 - 2183.

Wang, F., J. Li, T. J. Schmit, and S. A. Ackerman, 2007: Trade studies of hyperspectral infrared sounder on geostationary satellite, *Applied Optics*, 46, 200 – 209.

Jun Li attended GOES-R AWG meeting and gave summary of GOES-R trade-off study work at sounding team from 16 to 18 November 2005 in Washington DC

Jun Li attended MODIS science team meeting and gave a presentation on imager/sounder synergism from 4 to 6 January 2006 Baltimore, MD

Tim Schmit and Paul Menzel presented CIMSS GOES-R trade-off work at HES trade-off meeting held on 22, December 2005 (telcom).

Jun Li attended AMS annual meeting held from 29 January to 02 February 2006 in Atlanta, GA, and gave a poster presentation titled "Synergism of ABI and HES for atmospheric and cloud products"

Tim Schmit attended AMS meeting held from 29 January to 02 February 2006 in Atlanta, GA, and gave an oral presentation of the ABI.

Chian-Yi Liu attended AMS meeting held from 29 January to 02 February 2006 in Atlanta, GA, and gave a poster presentation titled "Cloud-clearing of AIRS radiances using MODIS".

Work from this project was also presented by James J. Gurka of OSD at the AMS 2006 Annual meeting.

Jun Li attended GOES-R Users' conference held from 01 to 03 May 2006, Broomfield, CO, and gave a poster presentation entitled "Synergism of ABI and HES for atmospheric sounding and cloud property retrieval"

Tim Schmit attended GOES-R Users' conference held from 01 to 03 May 2006, Broomfield, CO, and gave an oral presentation entitled "Advanced Baseline Imager (ABI)"

Jinlong Li attended the GOES-R Users' conference held from 01 to 03 May 2006, and gave a poster presentation entitled "Trade-off study for the hyperspectral IR sounder for a geostationary satellite"

Mathew Gunshor attended the GOES-R Users' conference held from 01 to 03 May 2006, and gave a poster presentation entitled "Simulated Datasets for Next Generation Geostationary Imager Studies".

Michael J. Pavolonis attended the GOES-R Users' conference held from 01 to 03 May 2006 in Broomfield, CO, and gave a poster presentation on "Using Aircraft-based NAST Interferometer Data to Perform HES Trade-off Studies".

Paul Menzel gave an oral presentation entitled "Hyperspectral Environmental Suite (HES) Sounder" at the GOES-R Users' conference held from 01 to 03 May 2006.

Timothy J. Schmit attended the EUMETSAT conference held in Helsinki, Finland from June 12 to 15, and gave a presentation on GOES-R.

Jun Li attended the International (A)TOVS Science Conference (ITSC-15) held from 4 to 10 October 2006 in Maratea, Italy, and gave a presentation entitled "GOES IR Sounder – future perspective from current applications".

6 Data Compression Studies – Bormin Huang

Proposed Work
The proposed work for 2006 included: 1) Study lossless compression techniques for future GOES data processing, 2) Study noisy transmission impacts on data decompression, and 3) Design error-resilient compression codes.

Summary of Accomplishments and Findings
The PI (Bormin Huang) was invited to serve as session chairs in several international IEEE compression-related conferences and contributed one invited book chapter.

Lossless compression techniques
Investigated or developed state-of-the-art transform-, predictor-, and clustering-based compression methods to benchmark the achievable lossless compression ratios on the NAST-I interferometer data (Figure 6.1). Studied different preprocessing techniques. Improved various entropy coding methods (such as adaptive arithmetic coding, static arithmetic coding, adaptive Huffman coding, static Huffman coding, prefix coding, etc.) to boost their compression gains.

Study Noisy Transmission Impacts
Performed error propagation and correction studies with state-of-the-art channel codes (LDPCs and Turbo codes) for noisy channel transmission (Figure 6.2).

➢ **Results for AIRS grating data with 10 complete granules (NOT the lower-noise 1501-channel subset.)**

Granule	9	16	60	82	120	126	129	151	182	193	Avg.
JPEG2000 with BAR	2.73	2.8	2.62	2.87	2.74	2.63	2.88	2.64	2.57	2.64	**2.71**
MWT with BAR	2.65	2.71	2.52	2.76	2.65	2.54	2.8	2.5	2.46	2.54	**2.61**
CALIC with BAR	2.44	2.51	2.33	2.61	2.46	2.35	2.64	2.38	2.31	2.38	**2.44**
JPEG-LS with BAR	2.77	2.82	2.67	2.87	2.76	2.68	2.87	2.67	2.63	2.69	**2.74**
MST with JPEG-LS	2.84	2.9	2.75	2.94	2.84	2.75	2.94	2.73	2.69	2.77	**2.82**
Lossless PCA	3.19	3.19	3.18	3.2	3.16	3.17	3.22	3.14	3.1	3.16	**3.17**
OOMP	3.21	3.3	2.78	3.1	3.26	2.81	2.81	2.79	2.74	3.33	**3.01**
PLT	3.03	3.08	2.97	3.08	3.02	2.95	3.09	2.93	2.88	2.98	**3.00**
PVQ	2.23	2.25	2.01	2.37	2.13	2.07	2.38	2.03	1.96	2.04	**2.15**
DPVQ	2.85	2.88	2.75	2.94	2.8	2.76	2.91	2.73	2.64	2.73	**2.80**
PPVQ	3.35	3.36	3.3	3.39	3.31	3.29	3.38	3.26	3.22	3.27	**3.31**
FPVQ	3.35	3.36	3.3	3.38	3.31	3.29	3.38	3.26	3.22	3.28	**3.31**
AVQLP	3.35	3.37	3.33	3.4	3.32	3.32	3.42	3.26	3.21	3.29	**3.33**

➢ **Results for NAST-I Michelson interferometer data with 2 scenes.**

	JPEG2000 with BAR	2D CALIC with BAR	2D JPEG-LS with BAR	Lossless PCA	PPVQ
Scene 1 (Winter US East Coast)	4.35	3.98	4.13	4.87	4.48
Scene 2 (Summer Italy Coast)	4.55	4.05	4.3	5.32	4.82
Average	**4.45**	**4.02**	**4.22**	**5.10**	**4.65**

Figure 6.1: Compression ratios for AIRS grating data and NAST-I interferometer data.

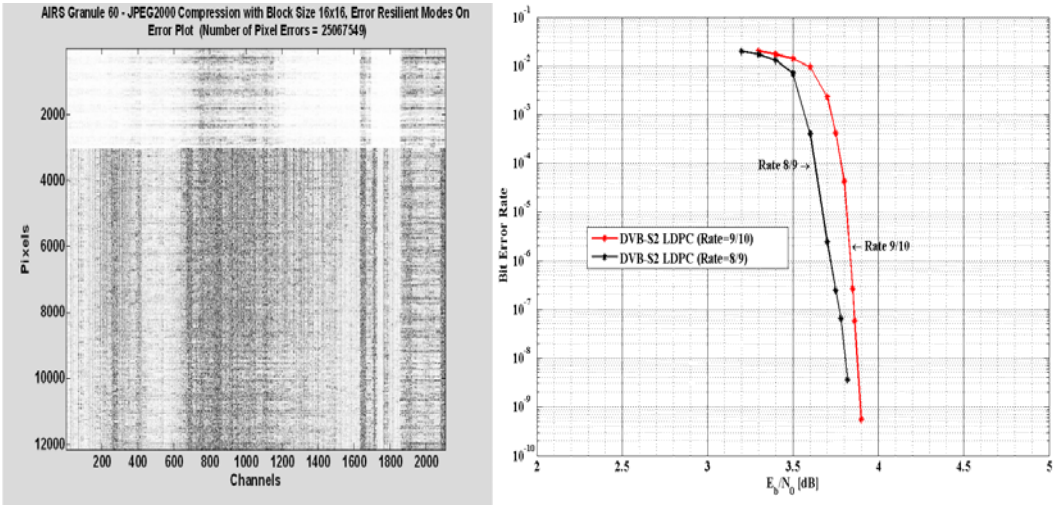

Figure 6.2: Error plot with error resilient modes on (left). Signal to noise ratio as a function of bit error rate (right).

Design error-resilient reversible variable-length codes (RVLC).
Developed error-resilient compression schemes for AIRS and NAST-I data, including reversible variable-length codes (RVLC). Made the DSP-and non-DSP versions of 3D Wavelet-RVLC compression code publicly available (Figure 6.3).

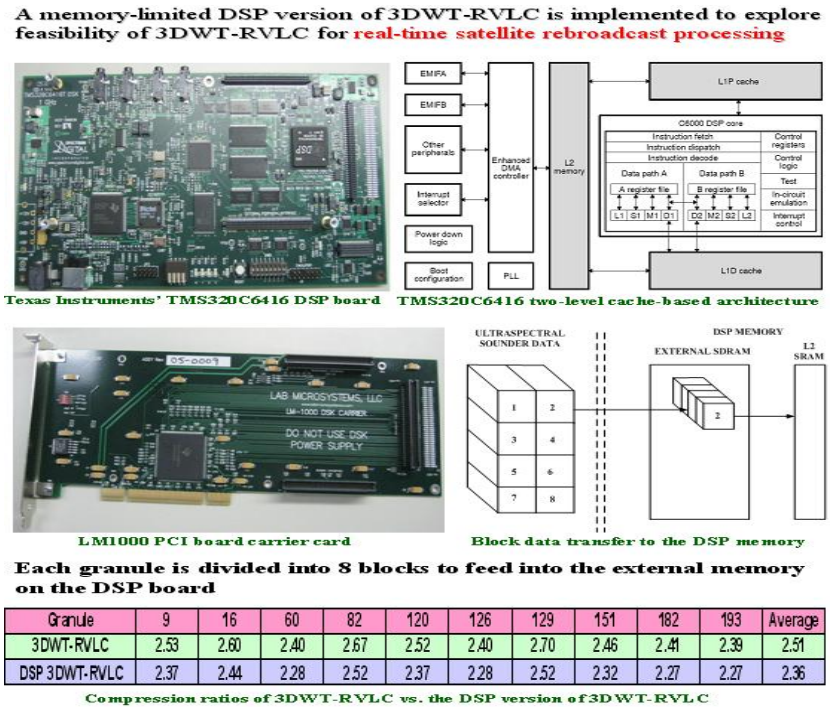

Granule	9	16	60	82	120	126	129	151	182	193	Average
3DWT-RVLC	2.53	2.60	2.40	2.67	2.52	2.40	2.70	2.46	2.41	2.39	2.51
DSP 3DWT-RVLC	2.37	2.44	2.28	2.52	2.37	2.28	2.52	2.32	2.27	2.27	2.36

Compression ratios of 3DWT-RVLC vs. the DSP version of 3DWT-RVLC

Figure 6.3: DSP implementation of the CIMSS error-resilient 3DWT-RVLC code.

Publications

Book Chapter

B. Huang, A. Ahuja, H.-L. Huang, Lossless Compression of Ultraspectral Sounder Data, *Hyperspectral Data Compression*, edited by G. Motta and J. Storer, Springer, 2006.

Journal and Conference Papers

B. Huang, and Y. Sriraja, "Predictor-guided lookup tables for lossless compression of hyperspectral imagery," *IEEE Signal Processing Letters (accepted)*.

B. Huang, A. Ahuja, and H.-L. Huang, "Optimal compression of high spectral resolution satellite data via adaptive vector quantization with linear prediction," *Journal of Atmospheric and Oceanic Technology (accepted)* .

B. Huang, A. Ahuja, and Y. Sriraja, "Burst error studies with DVB-S2 and 3D wavelet reversible variable-length coding for ultraspectral sounder data compression," *IEEE ICCT 2006*.

B. Huang, Y. Sriraja, and A. Ahuja, "Optimal code rate allocation with turbo product codes for JPEG2000 compression of ultraspectral sounder data," *IEEE ICCT 2006*.

B. Huang, A. Ahuja, Y. Sriraja, and H.-L. Huang, “Lossless Compression Studies for Real-time Rebroadcast of Data from NOAA's Future Advanced GOES Sounders”, *Proc. SPIE,* 6405, pp. 640560-1~640560-12, 2006.

B. Huang, and A. Ahuja,“MST-Embedded JPEG-LS: Application to lossless compression of ultraspectral sounder data”, *Proc. SPIE,* 6365, pp. 636518-1~636518-6, 2006.

B. Huang, and Y. Sriraja, “Lossless compression of hyperspectral imagery via lookup tables with predictor selection”, *Proc. SPIE,* 6365, pp. 636515-1~636515-8, 2006.

B. Huang, and A. Ahuja, “Real-Time DSP implementation of 3D wavelet reversible variable-length coding for ultraspectral sounder data compression," *IEEE IGARSS 2006*.

B. Huang, and Y. Sriraja, “Lossless multiwavelet compression of ultraspectral sounder data," *IEEE IGARSS 2006*.

A. Ahuja, and B. Huang, “Real-Time DSP implementation of bias-adjusted reordering with 3D wavelet reversible variable-length coding for ultraspectral sounder data compression," *IEEE FIEOS 2006*.

B. Huang, Y. Sriraja, H.-L. Huang, and M. D. Goldberg, “Improvement of burst error correction using a look-up table with low density parity check coding for compressed ultraspectral sounder data,” *IEEE Int. Conf. Advanced Comm. Tech.,* vol. 2, pp. 1172-1176, 2006.

B. Huang, and A. Ahuja, “Adaptive linear prediction for compression of ultraspectral sounder data”, *Proc. SPIE,* 6300, pp. 630002-1~630002-7, 2006.

B. Huang, A. Ahuja, Y. Sriraja, C. Wang, and M. D. Goldberg, “Burst error performance of 3DWT-RVLC with low density parity check codes for ultraspectral sounder data compression ”, *Proc. SPIE,* 6300, pp. 63000B-1~63000B-10, 2006.

B. Huang, Y. Sriraja, and A. Ahuja, “An optimal unequal error protection scheme with turbo product codes for wavelet compression of ultraspectral sounder data”, *Proc. SPIE,* 6300, pp. 630009-1~630009-9, 2006.

B. Huang, Y. Sriraja, and S. C. Wei, “Lossless compression of ultraspectral sounder data using a marker-based resilient arithmetic coder”, *Proc. SPIE,* 6300, pp. 63000C-1~63000C-9, 2006.

S. C. Wei, B. Huang, and A. Ahuja “Lossless compression of ultraspectral sounder data using a generalized prediction-based lower triangular transform ”, *Proc. SPIE,* 6300, pp. 630003-1~630003-8, 2006.

T. J. Schmit, B. Huang, Y. Sriraja, and H.-L. Huang “Lossless compression of ultraspectral sounder data using a generalized prediction-based lower triangular transform ”, *Proc. SPIE,* 6300, pp. 630003-1~630003-8, 2006.

A. Ahuja, and B. Huang, “Comparison of minimum spanning tree reordering with bias-adjusted reordering for lossless compression of ultraspectral sounder data,” *Proc. SPIE,* 6233, 859-866, 2006.

B. Huang, A. Ahuja, Y. Sriraja, H.-L. Huang, and M. D. Goldberg, "Lossless compression studies for NOAA GOES-R Hyperspectral Environmental Suite," *86th AMS Annual Meeting, Atlanta, Georgia, 2006*.

7 Hyperspectral Data Processing Demonstration – Bob Knuteson

Proposed Work
This project is intended to develop a software prototype implementation of algorithms developed under GOES-R risk reduction funding for use on hyperspectral data. The NASA Geostationary Imaging Fourier Transform Spectrometer (GIFTS) project, of which UW-Madison Space Science and Engineering Center is a partner, was selected as a realistic example of a future hyperspectral geostationary sounder. During the 2006 reporting period, the emphasis of this project was placed on the development of parallel processing software known as the GIFTS Information Processing System (GIPS). The GIPS software as developed under this project is being used directly in an assessment of the ground data processing requirements for a future hyperspectral sounder. This project is closely coordinated through NOAA OSD with a contractor to integrate the GIPS software onto selected target hardware for performance profiling. Status of this project is reported to NOAA in regular coordination teleconferences with public release of demonstration code and documentation made periodically via the UW-Madison SSEC web page.

It should be noted that the GOES-R Risk Reduction project provided several key inputs to this project:

(1) a draft ATBD for the GIFTS level 0 to 1 algorithms for the conversion of raw counts into physical units which was used to design and implement the GIPS science modules,
(2) top of atmosphere simulated GIFTS interferograms from a 24 hour Earth simulation, and
(3) real observations from the GIFTS Engineering Development Unit at Utah State Space Dynamics Laboratory (SDL) including both laboratory and sky viewing data made in coordination with a NASA project at UW-Madison SSEC.

Summary of Accomplishments and Findings
Significant progress was made in 2006 under this project in the following two main areas:

- GIPS software released publicly from UW-Madison SSEC, along with a large simulated Earth test dataset, has been used by a contractor identified by NOAA in a scalability demonstration which successfully confirmed the software design concepts used in the prototype software implementation. This small scale demonstration using simulated GIFTS data (created by UW-Madison SSEC for this purpose) on realistic cluster computing hardware has been used to estimate the hardware requirements needed for real-time processing in an operational environment. Since the technology of cluster computing is rapidly maturing this demonstration provides confidence that the ground data processing for hyperspectral sounders (of the class of GIFTS) can be accomplished in a cost effective manner and at low risk.

- The GIPS software used in the demonstration of simulated Earth observations has been adapted for use with real GIFTS observations from the thermal vacuum testing performed for NASA at Utah State Space Dynamics Laboratory. Two key datasets were identified for this software testing. The larger test (> 1TB) is a laboratory "day-in-the-life"

measurement where the instrument optics temperature is varied to simulate the thermal stresses of on orbit conditions while viewing a fixed external blackbody target. The smaller test (<100GB) is unique in that the GIFTS was made to view the downwelling atmosphere under clear sky conditions over a 10 hour time period. This data contains atmospheric spectral lines so is particular useful for verification of the spectral calibration across the 128 by 128 focal plane arrays (LW and SMW). Testing on the smaller dataset (collected in September 2006) was mainly completed by the end of 2006 with a software release anticipated in late January 2007. Subject to continued funding this project should move on to the next level; a demonstration of GIFTS data processing on a sufficiently large cluster computing system to show real-time processing rates can be achieved and thereby confirm the estimates made previously.

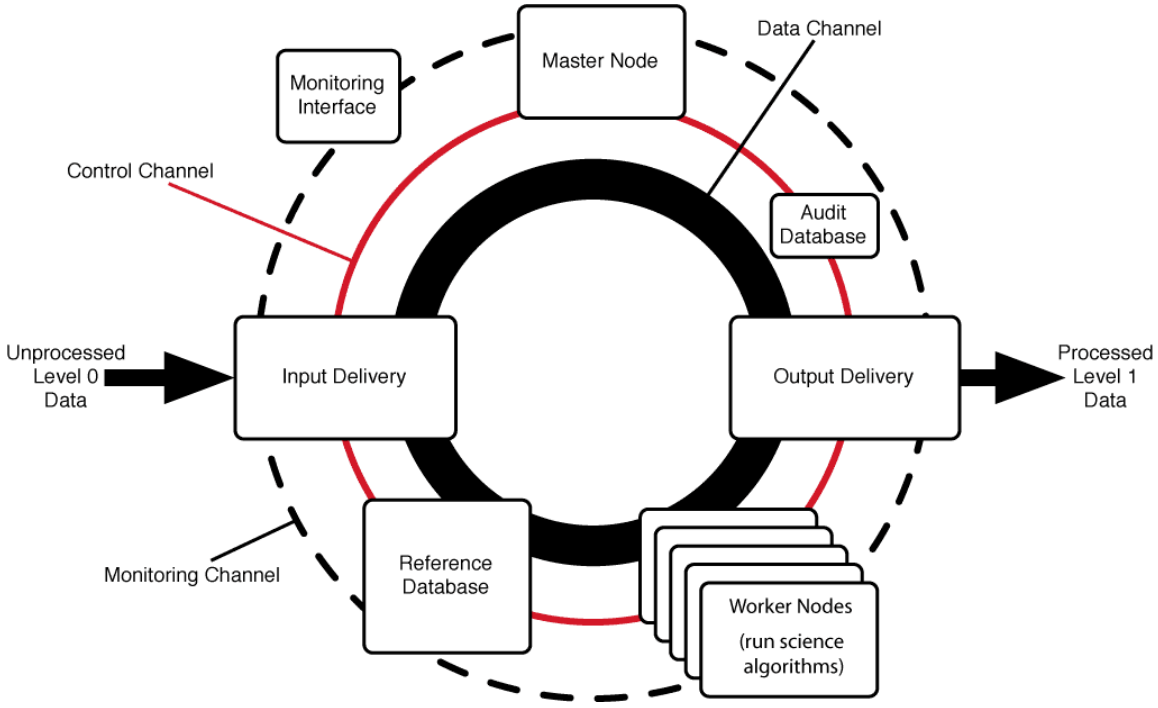

Figure 7.1: GIPS Concept Diagram.

The UW-Madison SSEC "Target diagram" represents the highest-level abstraction of our GIPS L0-L1 system design, in this case for raw-to-calibrated-radiance processing. It provides a unifying framework and common vocabulary for discussions on system architecture options and details. The various communication channels are represented as rings so as not to imply preference for any specific type of interconnect technology – this decision can be made later, and individualized to the specific needs of the concrete system. Further, components such as the Input, Output Delivery and the various Databases can be located across one or more physical machines as appropriate.

Publications and Conference Reports

Garcia, R. K., H. B. Howell, R. O. Knuteson, G. D. Martin, E. R. Olson, and M. J. Smuga-Otto, 2006: Reference Software Implementation for GIFTS Ground Data Processing, Proceedings of SPIE Vol. 6301, Atmospheric and Environmental Remote Sensing Data Processing and

Utilization II: Perspective on Calibration/Validation Initiatives and Strategies, A. Huang, H. Bloom, Eds. 63010Y (Sep. 1, 2006).

8 GOES R Algorithm Working Group (AWG)

8.1 GOES R Algorithm Working Group: Proxy Data Set Development – Allen Huang, Jason Otkin and Tom Greenwald

Proposed Work

The main focus of this project is to provide state-of-the-art proxy data sets, models, software tools, and their associated documents and/or user guides in support of a broad range of GOES-R AWG application and development team activities. The accomplishments from this project will directly enable most of the AWG team members to use the common GOES-R datasets and software tools. This will allow the various AWG teams to concentrate on their own area of expertise and allow better sharing of results between groups. In addition, the refined and up-to-date databases will include: 1) global infrared surface emissivity, 2) ice and water cloud microphysical properties, 3) aerosol/dust microphysical properties, and 4) community models (such as NWP, infrared radiative transfer, and infrared emissivity models).
In addition, ABI-like datasets (for most ABI bands) will be generated from MODIS imagery. Some of the steps to simulate the spatial, geometric and radiometric features include: acquiring the MODIS hdf format images, selecting bands with similar central wavenumbers, de-striping the IR bands with an algorithm developed at CIMSS, averaging to appropriate ABI resolution, etc.

Summary of Accomplishments and Findings

Eight WRF model simulations (at 4 km grid spacing) of an intense extratropical cyclone over the North Atlantic Ocean were performed using different combinations of cloud microphysical and PBL parameterization schemes. Cloud data from each simulation was subsequently compared to MODIS-derived cloud information in order to assess the ability of the WRF model to realistically simulate the observed cloud features. Preliminary results are encouraging. Figure 8.1.1 directly below shows frequency distributions for the MODIS-derived and WRF-simulated cloud water paths. The table legend is organized from the simulation with the most sophisticated parameterization schemes (SEIF_ETA) to the least sophisticated schemes (PLIN_YSU). Overall, it is clear that the various WRF model simulations captured the observed cloud water path distribution very well. It is also evident that the most sophisticated schemes consistently outperformed the least sophisticated schemes.

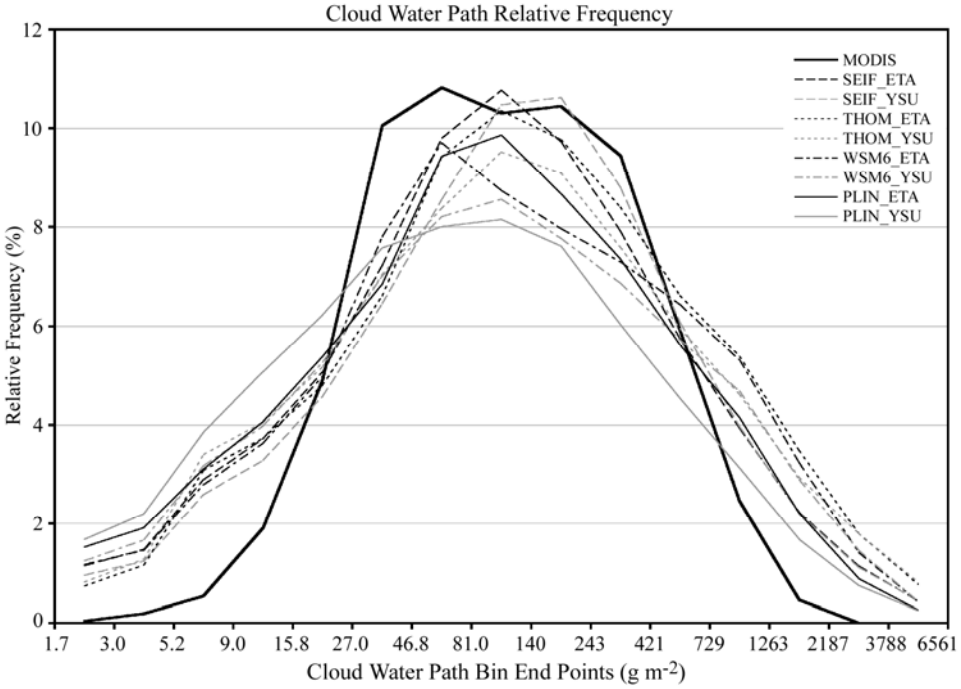

Figure 8.1.1: Plots of frequency distributions for the MODIS-derived and WRF-simulated cloud water paths.

Besides comparing the synthetic ABI radiances to observations we have also begun to examine the quality of the synthetic radiances by determining the errors in our 2-cloud-layer radiative transfer model (FIRTM2) due to multiple scattering, which is one of the dominant errors in our forward model system. We used the SOI RT model (developed here at UW-Madison) as the reference model in 32-stream mode with delta scaling. The SOI model and FIRTM2 were both given identical gas and cloud properties and calculations were performed for two different fixed zenith angles of 0^o and 55^o for a section of the WRF model domain for the North Atlantic case described above. The sub-domain consisted of 300x300 grid points and covered a wide range of cloud types (see figure directly below). Preliminary results show that bias errors in FIRTM2 for all cloud types and for a wide range of zenith angles were less than 0.4 K for all ABI channels considered here (8-16). RMS errors were less than 1 K (see figure below). The biggest errors occurred for cirrus (visible optical depth < 3.6) at the largest zenith angle, with bias errors of over 1 K and RMS errors of up to 1.5 K for the window channels (see figure below). These enhanced errors for cirrus are likely caused by the assumption of isotropic scattering in FIRTM2.

Other accomplishments included:

- Supplied the adjoint model for PLOD (predicts layer gas optical depths) to UW-Madison sounding team member Dr. Jun Li for testing purposes in his impact study of the retrieval of cloud and atmospheric properties.

- Began work on the adjoint model for the 2-cloud-layer model, FIRTM2, which is needed by the sounding group.

- Began work on the Users' Guide for the forward model code.

- Prepared for 1st dissimilation of proxy models and datasets for AWG members in the end of January 2007.

- Simulated the GIFTS and ABI channels 8-16 at geosynchronous orbit for the full disk (8 km grid spacing). Figure 8.1.2 shows examples of top-of-atmosphere radiances for two of the ABI channels that are similar to channels on current GOES imagers.

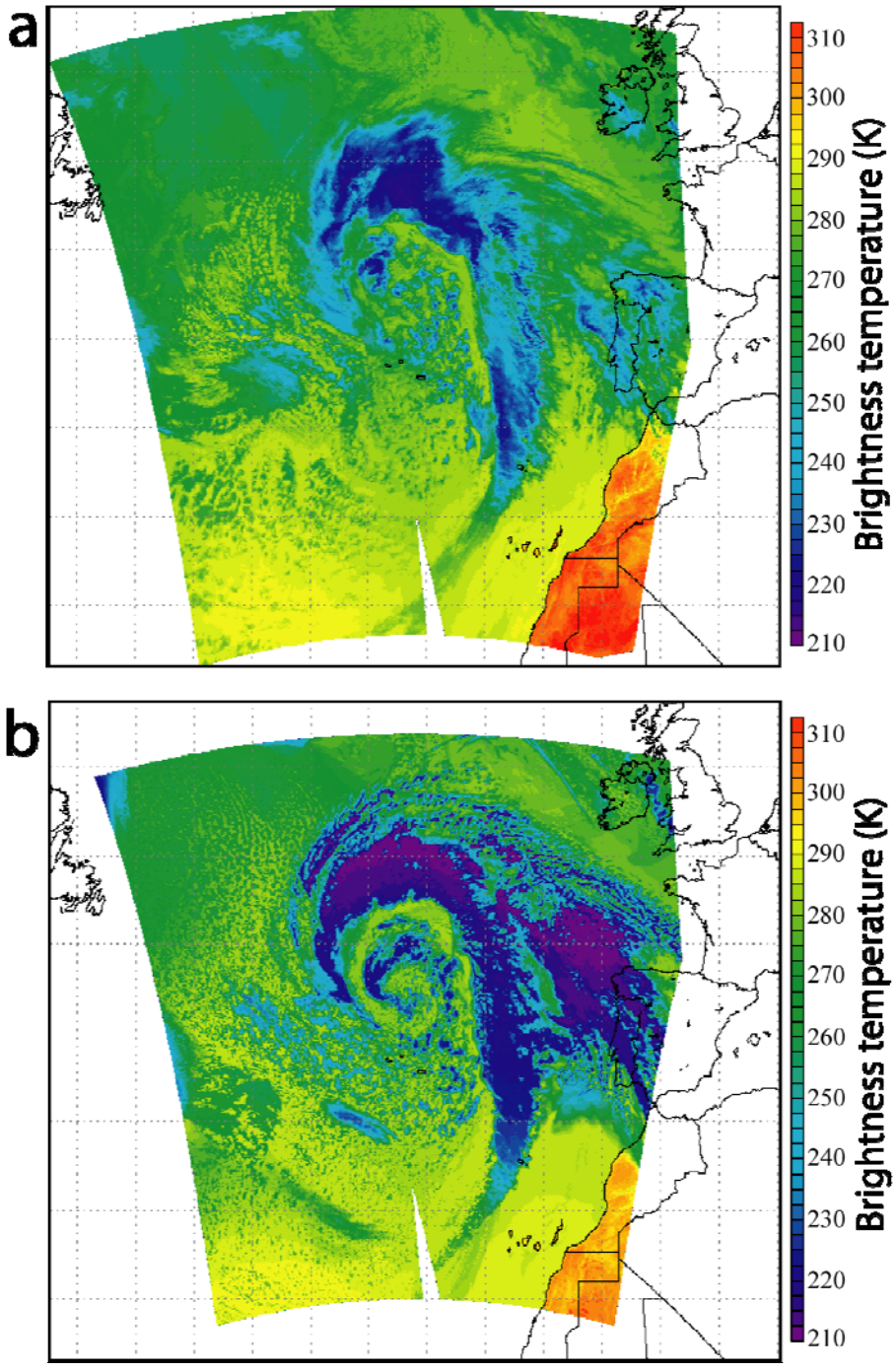

Figure 8.1.2: Composite of top-of-atmosphere brightness temperatures for MODIS band 29 (8.5 μm) (a) actually measured and (b) simulated. Overpass times were 1410 and 1550 UTC.

- The 5 km resolution global land surface IR emissivity databases were converted to netCDF and the size of the databases were greatly reduced by using instead emissivities at 10 spectral tie points. Obtaining surface emissivities between these tie points is done through linear interpolation.

- Successfully ported the forward radiative transfer model code onto our new 32-node 64-bit Opteron cluster using two different compilers in order to expand its portability to other systems. Examining the quality of the top-of-atmosphere radiance data files helped to uncover coding errors in the forward model code. Several improvements were made to the code as well as the addition of other input options.

Publications and conference reports
Greenwald, T., H.-L. Huang, D. Tobin, J. Otkin, E. Olson, M. Gunshor, and P. Yang, 2007: Evaluation of simulated GOES-R ABI and hyperspectral radiance measurements, Third Future National Operational Satellites Symposium, San Antonio, Texas, January14-18.

8.2 GOES R Algorithm Working Group: Sounding Retrieval Algorithm – Jun Li

Proposed Work
Work proposed for year one of the Algorithm Working Group (AWG), as documented in Dr. Goldberg's letter dated 21 March 2006, focused on evaluation and development of Version 1 of Hyperspectral Environmental Suite (HES) retrieval algorithms. The content of Version 1 was to include:

- Direct cloudy sounding approaches,
- Advanced Baseline Imager/ Hyperspectral Environmental Suite (ABI/HES) cloud clearing approaches, and
- Efficient radiative transfer Jacobian computation.

Summary of AWG 2006 Accomplishments and Findings

Version 1.0 of clear and direct cloudy sounding software is ready for demonstration by the Algorithm Integration Team (AIT)
The single field-of-view (FOV) hyperspectral sounding algorithm version 1.0 uses an efficient statistical retrieval approach, and includes both clear sky sounding and above-cloud direct sounding approaches. Software and testing data are available to the AIT, and will be online very soon. A generic hyperspectral IR sounder instrument (650 – 2400 cm^{-1} with a spectral resolution of 0.625 cm^{-1}) is assumed in the version 1.0 algorithm. The algorithm has been applied to one day's full disk hyperspectral IR proxy data (generated by the CIMSS AWG proxy team) at 10 km spatial resolution and 1 hour temporal resolution. Output includes:

(1) clear sky derivation of temperature and moisture soundings at 101 vertical pressure levels (from the top of the atmosphere to the surface);

(2) partial cloudy derivation of effective cloud top pressure (CTP), cloud optical thickness (COT), and temperature and moisture soundings at 101 vertical pressure levels, when COT <1.0;

(3) cloudy derivation of CTP, COT, and temperature and moisture soundings above the CTP levels, when COT >1.0.

Figure 8.2.1 shows that the 500 hPa water vapor (g/kg) retrievals are close to the truth; and the hyperspectral IR radiances provide more retrieval coverage at 200 hPa than at 500 hPa (since there are less clouds higher than 200 hPa).

Figure 8.2.2 shows the temperature cross section (true and retrieved) along the 44^{o} latitude.

Figure 8.2.3 is the same as Figure 8.2.2 but for water vapor mixing ratio. The retrievals are close to "truth" in clear skies and in above-cloud regions.

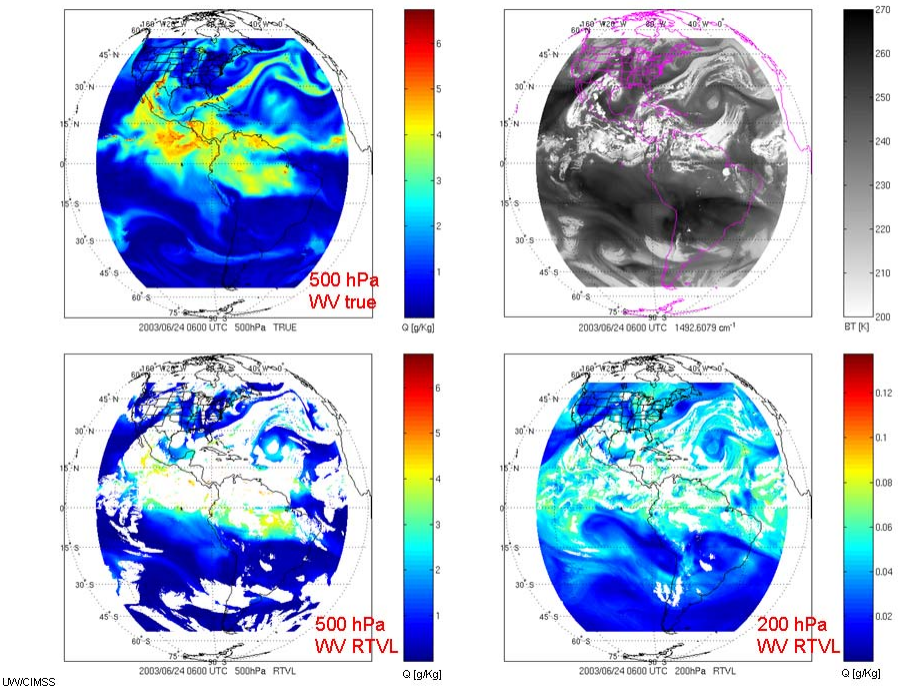

Figure 8.2.1: *Upper Left*: 500 hPa water vapor mixing ratio from the WRF model (truth); *Upper Right*: simulated BT image of an water vapor absorption channel; *Lower Left*: 00 hPa water vapor mixing ratio retrieval image; and *Lower Right*: 200 hPa water vapor mixing ration retrieval image.

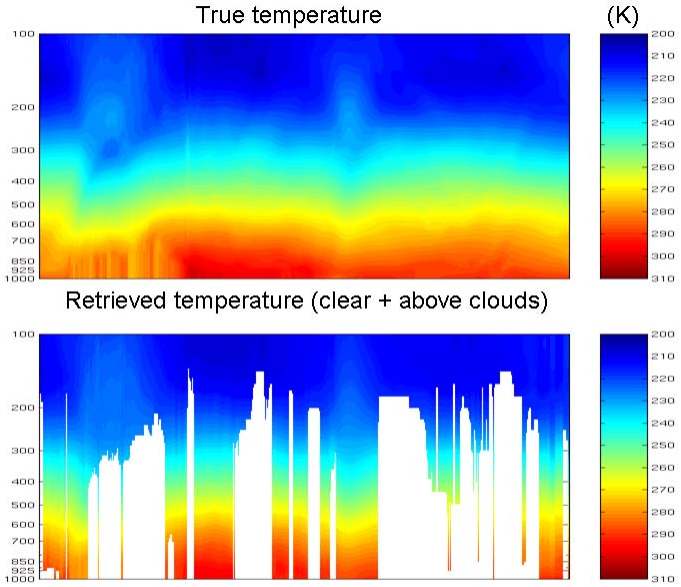

(Note: this is a loop, GIF animation is available to show the evolution, contact: Jun.Li@ssec.wisc.edu)

Figure 8.2.2: The temperature cross section along the 44^{o} latitude. (Top: "Truth"; Bottom: clear plus above clouds retrieval)

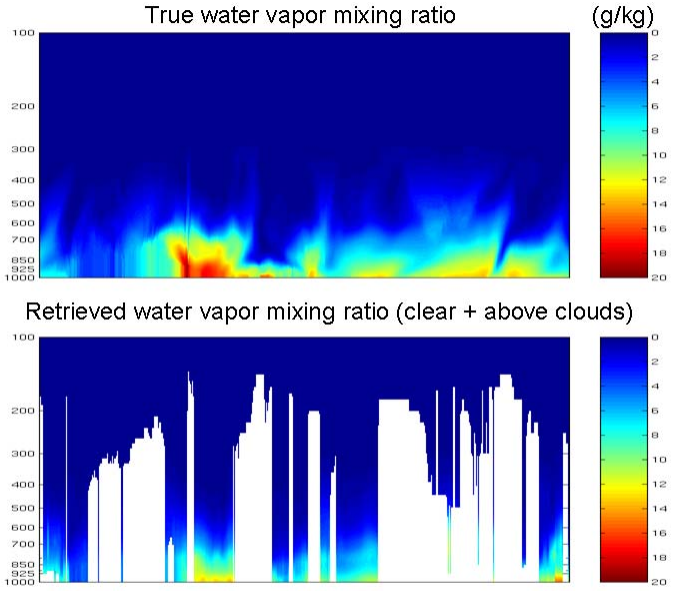

(Note: this is a loop, GIF animation is available to show the evolution, contact: Jun.Li@ssec.wisc.edu)

Figure 8.2.3: The water vapor mixing ratio cross section along the 44^{o} latitude. (Top: "Truth"; Bottom: clear plus above clouds retrieval)

The direct sounding approach in both clear and cloudy skies has been tested with Atmospheric InfraRed Sounder (AIRS) measurements. Additionally, preliminary simulation results using near global radiosonde observations with this version 1.0 retrieval algorithm were presented by Jun Li and Tim Schmit at the AWG GOES-R meeting on 13 September 2006 and AWG sounding telcon meeting on 04 December 2006. Both simulation and real AIRS testing show that the algorithm is reliable and a viable candidate for generating a hyperspectral IR sounding product.

An algorithm for simultaneously retrieving sounding data and the emissivity spectrum has been developed under GOES-R Risk Reduction. The AWG sounding software will be updated to include this new emissivity algorithm.

ABI/HES cloud-clearing approach studied

The ABI/HES cloud-clearing approach has undergone initial testing with MODIS/AIRS, and is ready for further demonstration with IASI/AHVRR (Infrared Atmospheric Sounding Interferometer/Advanced Very High Resolution Radiometer). In the future it can be applied to ABI and geostationary hyperspectral IR data processing. The MatLab version of imager/sounder cloud-clearing is available now, and it can be rewritten to Fortran if needed.

Improvement has been made on efficient Jacobian calculation

Improvements have been made to the efficient Jacobian algorithm (Li 1994) used for radiative transfer calculations. The new algorithm enables derivation of radiance or brightness temperature for a given IR spectral band with respect to profiles in temperature, moisture, and any trace gas; surface skin temperature; and surface emissivity. The boundary layer moisture retrieval is improved by approximately 0.5% (mixing ratio) using the refined Jacobian. A manuscript on Jacobian improvement is under preparation.

ABI continuation of legacy GOES Sounder products

Since the ABI acquisition process starts earlier than the geostationary hyperspectral sounder acquisition process, it is important that legacy GOES Sounder products used by the NWS can be generated from ABI data. Many legacy products (radiances, TPW, LI, skin temperature, clouds, and winds) can be provided from ABI data, but temperature sounding information is limited because ABI has only one infrared CO2 absorption band. We are evaluating the combination of forecast radiances with ABI radiances to enable ABI production of current GOES-N sounder products. The operational MODIS (MoDerate Resolution Imaging Spectrometer) sounding algorithm (Seemann and Li 2003, JAM) was selected to demonstrate the feasibility of this approach for ABI moisture profile retrieval, and we have started testing of the ABI stand alone sounding algorithm.

Publications and Conference Reports

Jun Li; GOES-R Sounding Retrieval Algorithm Development; GOES-R Users' Conference, 1-3 May 2006 Broomfield, CO; Poster Presentation.

Jun Li and Tim Schmit; ABI Continuation of Current GOES Class Sounder Products, GOES-R AWG meeting, 13 September 2006, NOAA Science Center, Silver Spring, MD; Presentation

Jun Li; GOES Sounder Applications and Future Needs; International (A)TOVS Science Conference (ITSC-15), 4-10 October 2006, Maratea, Italy; Presentation.

- A proceeding paper on this presentation will be available.

8.3 GOES R Algorithm Working Group: Sounding Validation – Dave Tobin

Proposed Work
This work was proposed in March 2006 and does not reflect the more recent decision to exclude HES from the GOES-R payload. We planned to provide essential validation datasets and analysis in 2006 for assessing candidate HES temperature and water vapor sounding algorithms. The primary focus was to be on the production and use of highly accurate temperature and water vapor profiles from the Atmospheric Radiation Measurement (ARM) sites and from aircraft campaigns.

Even though the decision has been made to exclude HES from the GOES-R payload, achieving temperature and water vapor soundings with high accuracy and optimal vertical resolution remains a major goal of atmospheric scientists. High accuracy and vertical resolution are required for critical applications, such as nowcasting the onset of severe weather over the CONUS. Representative validation data and highly accurate analyses are required to assess the candidate sounding algorithms that will be investigated by the AWG. The ARM sites are perhaps the best sites in the world for providing atmospheric state, cloud, and radiation observations for this type of validation activity. Also, high spectral resolution infrared radiance observations collected by the Scanning-High resolution Interferometer Sounder (S-HIS) and the NPOESS Aircraft Sounder Testbed-Interferometer (NAST-I) from high altitude aircraft are useful for sounding algorithm assessment.

Our plan remains to produce and provide ARM site and aircraft based datasets for the AWG sounding algorithm validation, and to use the datasets to assess the algorithms. This requires assembly of validation data sets including best estimates of the surface, atmospheric temperature and water vapor profiles and cloud observations from an array of ARM site observations, and coincident satellite observations (AIRS, MODIS, and GOES). Supplemental aircraft datasets will include the S-HIS and/or NAST-I radiance observations and coincident validation data. During the first year we planned to:

- Coordinate dataset needs with Sounding AWG chair and members
- Assemble ARM and aircraft datasets
- Perform sounding algorithm validation analyses

This activity will be continued in future years as required to select, assess and refine AWG sounding algorithms.

Summary of Accomplishments and Findings
The proposed efforts regarding Sounding Algorithm Validation were proposed in March 2006 and therefore did not reflect the more recent decision to exclude HES from the GOES-R payload. The AWG strategy and necessary actions for producing and assessing GOES-R soundings in the no-HES framework is still uncertain. Therefore, efforts this year focused on the generic preparatory work of developing sounding validation datasets from ARM, with relatively little sounding validation work for the AWG.

ARM site atmospheric state best estimates have been produced to compile a sounding algorithm dataset. The effort is described in detail in Tobin et al., 2006. This AWG effort leverages heavily on support from EOS Aqua. In addition to datasets produced for the Southern Great Plains (SGP) and Tropical Western Pacific (TWP) ARM sites, datasets are now also assembled for the arctic North Slope of Alaska (NSA) site. Conditions for this site pose a difficult challenge for advanced

sounding due to cloud conditions, cold and dry atmospheres, and a variety of surface types. Drawing upon radiosondes launched at EOS Aqua ARM site overpass times, ensembles of validation profiles were compiled for each site during five "phases" of dedicated radiosonde launches spanning approximately four years. Additional phases are now being planned for CY2007. Figure 8.3.1 shows an assessment of AIRS team version 4 temperature and water vapor retrievals for one phase of dedicated soundings at the NSA site. The results reflect the difficulty in performing retrievals for the NSA site conditions characterized by low yields and RMS performance exceeding standard retrieval goals (1K/1km temperature and 20%/2km water vapor). These datasets are also used to assess other candidate retrieval algorithms, and soundings produced using a combined AIRS/MODIS algorithm are being assessed.

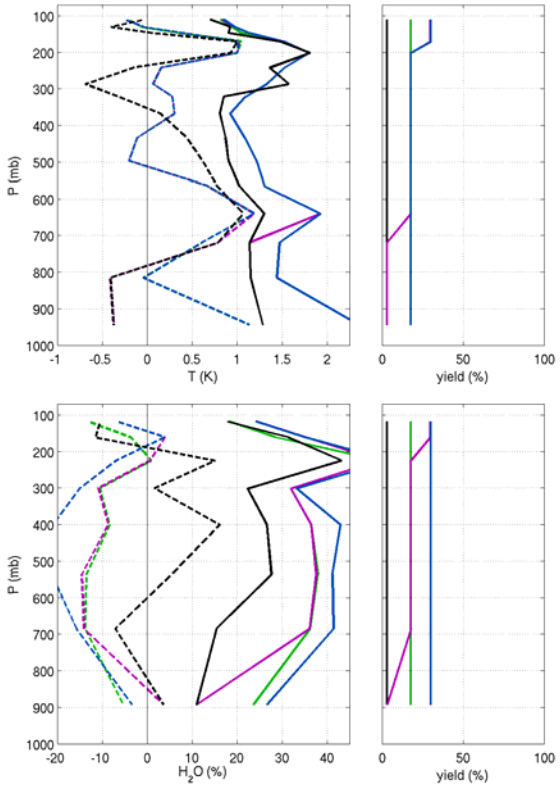

Figure 8.3.1: Validation of AIRS version 4 atmospheric profile retrievals using ARM NSA site profiles. Top left panel: 1 km layer temperature differences (AIRS-ARM); Top right panel: temperature retrieval yield; Bottom left panel: percent difference in 2 km layer water vapor amounts (100(AIRS-ARM)/ARM); Bottom right panel: water vapor retrieval yield. Each panel includes the bias (dashed curves) and RMSE (solid curves) for four selections of quality control flags (QC1, black; QC2, green; QC3, purple; QC4, blue) as discussed in Tobin et al. 2006. Water vapor statistics are computed with percent differences weighted by the ARM water vapor amounts.

Publications and Conference Reports

Tobin D. C., et al., (2006), Atmospheric Radiation Measurement site atmospheric state best estimates for Atmospheric Infrared Sounder temperature and water vapor retrieval validation, *J. Geophys. Res.*, 111, D09S14, 10.1029/2005JD006103.

8.4 GOES R Algorithm Working Group GOES R Winds – Chris Velden

Proposed Work
The development and automated processing of wind vectors from satellites has its heritage at CIMSS. The work plan research objectives seek to continue this heritage by adapting current methods and algorithms to NOAA's next generation of geostationary satellites, starting with GOES-R. The ABI will provide both traditional and new spectral channels that the CIMSS winds team will employ to test, process and validate using simulated and proxy datasets provided by other members of the GOES-R AWG project. We plan to use locally-available hardware resources initially for software testing, with a phased transition to a collaborative testbed environment as it comes online. The proxy data will leverage off of existing imagery from GOES and MSG/SEVERI. We will also employ ABI simulated imagery for select case studies. The algorithm development, testing and validation will focus on heritage algorithms currently being used in NESDIS operations today to generate winds from satellite imagery. We will leverage and adapt current algorithms/software to expected ABI characteristics, focusing first on ABI heritage channels (VIS, IR-W, WV) for winds testing. We will then turn our attention to the new spectral capabilities afforded by the ABI for wind derivation. All software development will follow accepted AWG standards, and will be accompanied by documentation. This work will insure the readiness of the CIMSS/NESDIS automated winds algorithm for eventual operational implementation upon the deployment of GOES-R ABI.

Summary of Accomplishments/Findings
This study has only been activated for the past 5 months. We have begun to adapt and optimize the CIMSS/NESDIS automated feature tracking algorithm for deriving atmospheric motion vectors from sequential satellite imagery for applications to the GOES-R ABI. In addition, we are assembling proxy datasets to use as simulated ABI imagery. This project includes software code modifications, and will soon include testing on proxy datasets, validation, and documentation.

Publications
Velden, C., S. Wanzong, I. Genkova, D. A. Santek, J. Li, E. R. Olson, and J. A. Otkin, 2007: Clear sky atmospheric motion vectors derived from the GOES sounder and simulated GOES-R hyperspectral moisture retrievals. Ext. Abstracts Third Symposium on Future National Operational Satellites, AMS Annual Meeting.

8.5 GOES R Algorithm Working Group: Cloud Properties – Andy Heidinger and William Straka III

Proposed Effort
This project includes all of the CIMSS efforts relating to the GOES-R Algorithm Working Group (AWG) Cloud Application Team. The task of the team is to develop a set of consensus cloud algorithms and all documentation for delivery to the NESDIS/STAR integration teams. Our effort also includes development of a cloud product test bed and new algorithms where appropriate.

Summary of Accomplishments and Findings
The major accomplishment this year has been the development of the Geostationary Earth Orbiting Cloud Algorithm Test-bed (GEOCAT). GEOCAT serves as the main tool for the GOES-R AQG cloud application team. It consolidates the core functions of reading, calibrating

and navigating data from various geo platforms and allows for the simultaneous generation of multiple products from multiple algorithms. We have developed GEOCAT and are now implementing some core algorithms such as the cloud mask. We are also validating the performance of the radiative models used within GOECAT. Recently we added a new CIMSS derived surface emissivity data-base and new higher spatial resolution surface type data-base to make better use of the spatial and spectral information from the ABI on GOES-R.

We are also developing and improving analysis techniques to help come to consensus on algorithmic approaches for the GOES-R cloud products. Analysis of the cloud top pressure using an algorithm developed and used operationally here at CIMSS was compared with one developed at NASA. To date we have compared the GOES-12 CIMSS cloud heights with those from NASA LaRC. The comparisons were done using the cloud boundary information (ARSCL) provided by the lidar/radar sensors at the ARM CART site. The figure shown below gives one example of the type of analysis being done for this effort. The analyses have indicated strengths and weaknesses in both methods that will be factored into the final GOES-R algorithm. Once our GOES-R algorithms are available, we will be able to compare them to their predecessors using the same analysis.

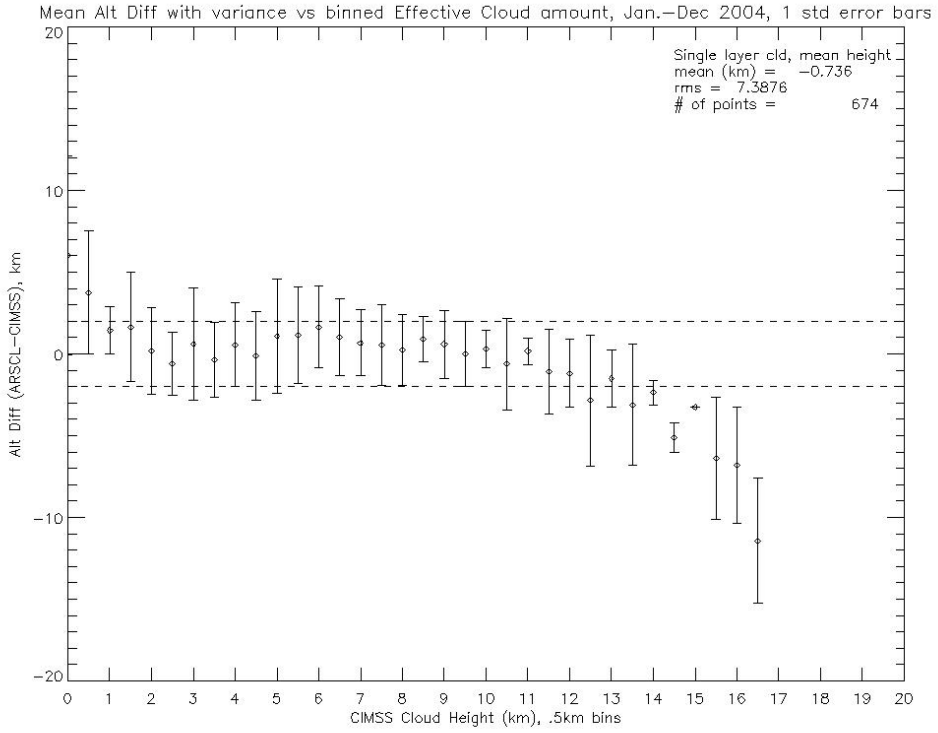

Publications/Presentations:
Heidinger, Andrew and Michael Pavolonis: The GOES-R AWG Cloud Application Team. Fourth GOES Users Conference, Broomfield, CO, May 2006.

8.6 GOES R Algorithm Working Group: Aerosols – Steve Ackerman

Proposed Work

- Develop and begin testing an appropriate strategy for the AWG Aerosol algorithm, with focus on dust, smoke and volcanic aerosols.
- Collaborate with Cloud and Aviation AWG groups.

Summary of Accomplishments and Findings.
Figure 8.6.1 shows the development strategy for AWG aerosol detection algorithm. We have applied this strategy for dust detection via ABI, using MODIS data as a proxy and are continuing development using MODIS and SERVI observations. Candidate Algorithms exist for AVHRR, GOES (imager and sounder), MODIS and SERIVI that make use of visible, near-infrared, and infrared channels, with some emphasis on the IR channels so that daytime and nighttime approaches are similar. Improvements are being made to make detection thresholds a function of several parameters (e.g. viewing and illumination geometry, surface type, and atmospheric profile). The approaches require ancillary data, such as surface type (e.g. water, land, desert). The overall strategy is:

- Start with current AVHRR, MODIS and aerosol (e.g. volcanic ash, dust and heavy smoke) detection algorithm and modify accordingly to ABI characteristics.
- Identify optimum method for aerosol properties and height estimation (likely 1-D variational approach)
- Identify test data sets (MODIS/AIRS/SEVERI/) and apply algorithm to test data. Coordinate algorithm with cloud and aviation AWG groups.

Figure 8.6.2 is a MODIS 0.86 micron reflectance and an IR window channel image of a dust storm over off the coast of Africa on March 8, 2006 at approach 12UTZ. Figure 8.6.3 shows the results of the dust algorithm as well as the MODIS cloud mask applied to the scene. This approach has been applied to several MODIS scenes and will soon be applied to SERVI data. We are trying to coordinate efforts as best we can with the AWG cloud group and the Aviation working group on volcanic aerosol detection. In that regard, we are exploring approaches to retrieving dust optical properties using a 1-DVAR approach developed by a visiting scientist in collaboration with CIMSS scientists.

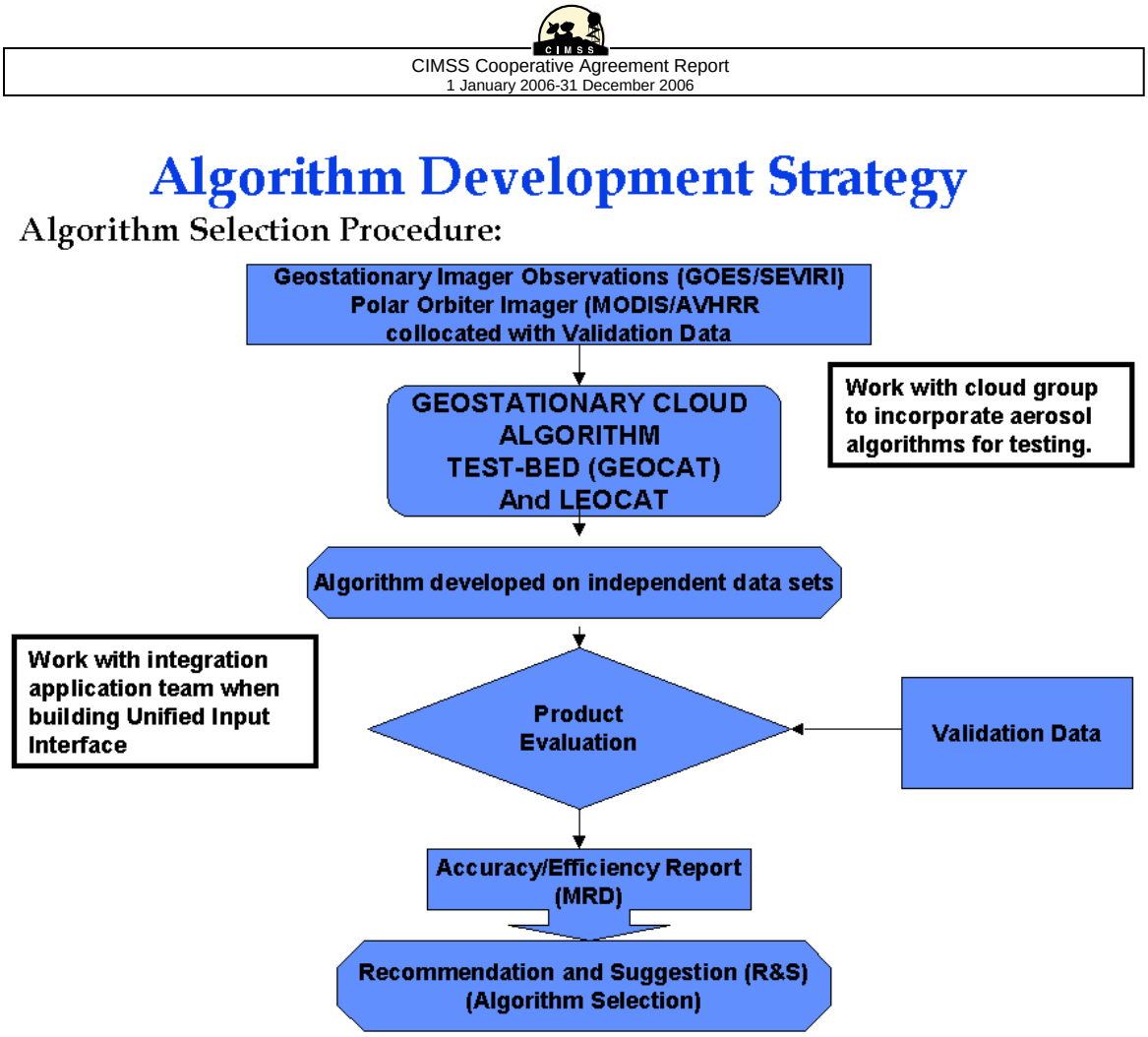

Figure 8.6.1: Development strategy for the AWG aerosol detection algorithm

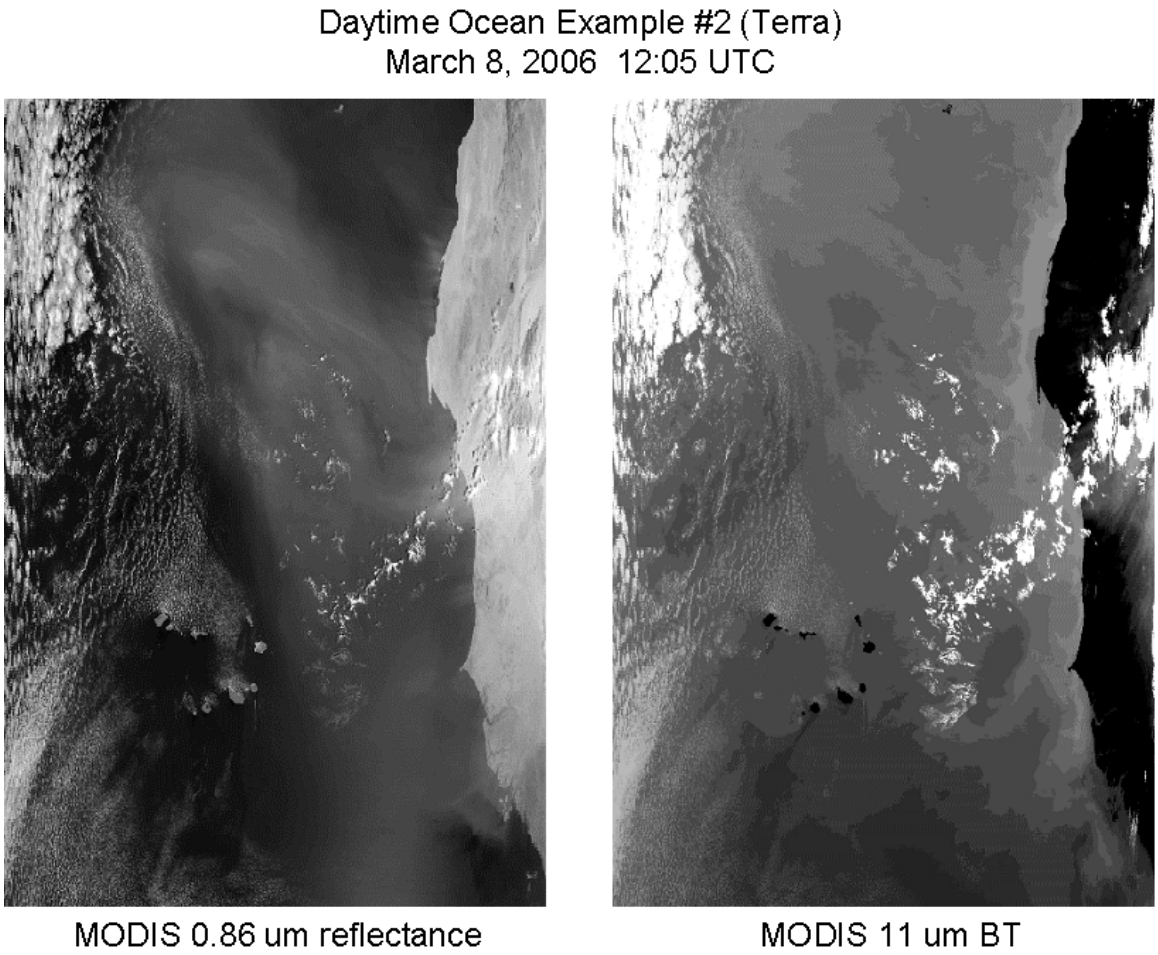

Figure 8.6.2: MODIS 0.86 micron reflectance (left) and an IR window channel (right) image of a dust storm over off the coast of Africa on March 8, 2006 at approach 12UTZ.

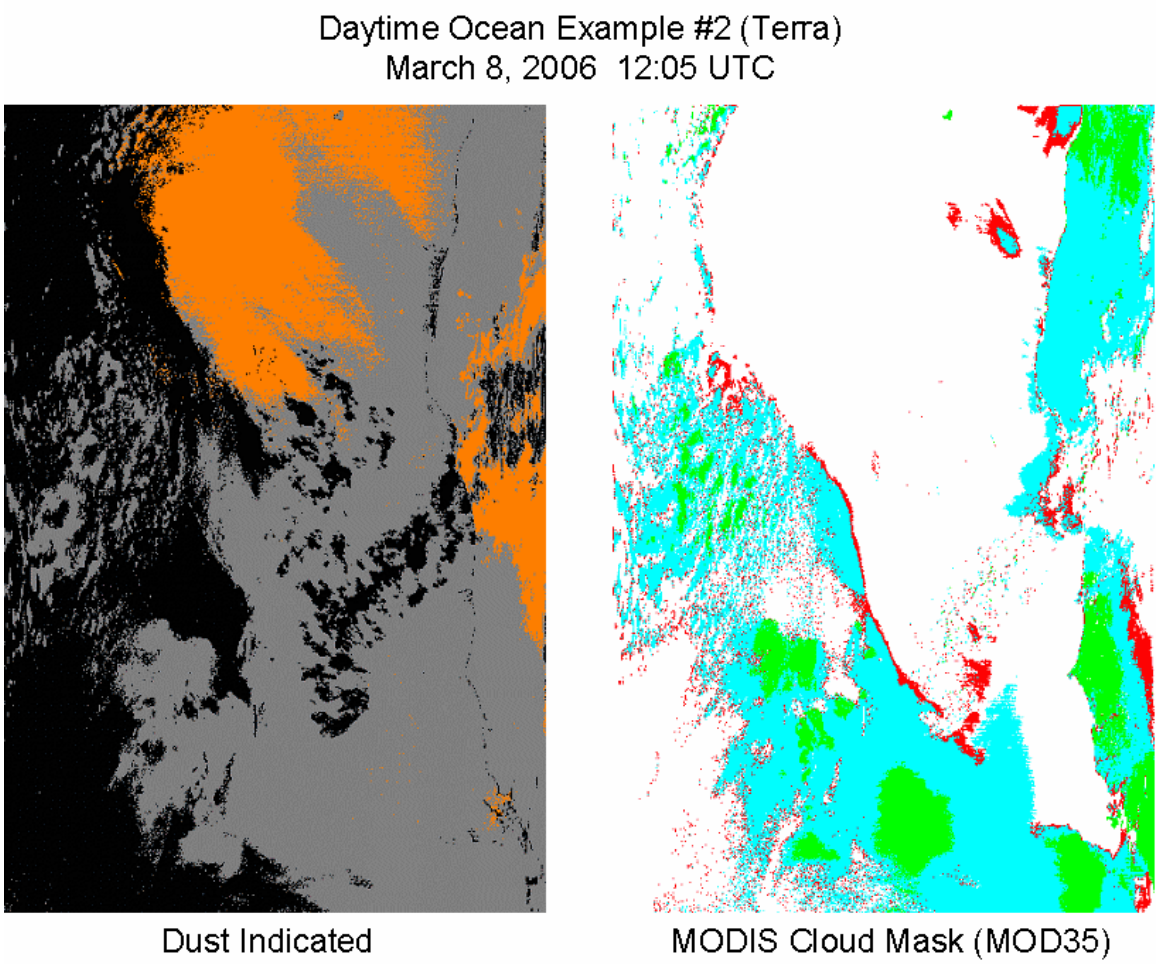

Figure 8.6.3: Preliminary results of the dust algorithm (left) as well as the MODIS cloud mask (right) applied to the scene of Figure 8.6.2.

8.7 GOES R Algorithm Working Group: Ozone – Chris Schmidt and Jun Li

Proposed Work

The Advanced Baseline Imager (ABI) on GOES-R has sufficient spectral coverage, most importantly the 9.6 μm ozone absorption band, to retrieve total column ozone over its coverage area. The legacy GOES I-M Sounder experimental total column ozone (TCO) algorithm from CIMSS can be applied to ABI. ABI ozone will provide high spatial and temporal resolution sampling of ozone features that primarily reflect ozone distribution in the stratosphere and upper troposphere; ABI ozone alone cannot meet requirements for measuring the tropospheric column ozone. ABI ozone will provide continuity with the current ozone capabilities and function as a part of an ABI Sounding package. Development of an ABI ozone algorithm begins with adapting the algorithm to EUMETSAT's Spinning Enhanced Visible and Infra-Red Imager (SEVIRI) which has similar spectral coverage to that proposed for ABI. Alongside using straight SEVIRI data as a proxy the effort will also include using ABI proxy data derived from SEVIRI and MODIS data.

Summary of Accomplishments and Findings

In 2006 CIMSS developed an ozone regression algorithm based off the current GOES I-M algorithm for SEVIRI. Two versions were built, one uses temperature profiles from numerical models to enhance the accuracy of the ozone estimate and the other does not. The model data was necessary to make up for bands that ABI will be missing in the CO2 absorption region. Accuracy when compared to the Ozone Monitoring Instrument (OMI) aboard NASA's Aura platform was good. OMI utilizes ultraviolet data to obtain its ozone measurements and is known to have a high accuracy, making it a good reference comparison. Also included in the algorithm is a bias correction originally developed for GOES I-M that takes into account seasonal and latitudinal biases. On GOES I-M this bias correction reduces the average bias to around 1 Dobson Unit (DU). No adjustments were made for the slight differences in SEVIRI's spectral coverage, and despite that when using real data from 14 February 2006 the bias remained less than 5 DU. With the temperature profile data the %RMSE is around 3-5% and the bias is less than 5 DU. Similar results were achieved in simulation. The SEVIRI algorithm without temperature data was run in simulation and saw a slightly higher bias and a %RMSE around 8%, which was expected based on previous experiences. Figure 8.7.1 shows a scatter plot between the ozone from SEVIRI with temperature data and ozone from OMI which shows how well the regression is working. Of note is that a simplified cloud screen was used for SEVIRI, which did increase the error somewhat.

Figure 8.7.2 is the collocated SEVIRI and OMI ozone clear-sky pixels for 12:00 UTC on 14 February to 12:00 UTC on 15 February 2006. Qualitatively the agreement is very good. There is room for improvement, particularly in the cloud screen used with SEVIRI data.

The next phase includes stress-testing the regression algorithm with real-time SEVIRI data and testing it on ABI proxy data provided by the proxy team, proxy data that will be developed from SEVIRI and MODIS data.

Publications and Conference Reports

Submitted Publications

Jin, X., J. Li, C. C. Schmidt, T. J. Schmit, and J. Li: Retrieval of Total Column Ozone from Imagers Onboard Geostationary Satellites, IEEE Transactions on Geoscience and Remote Sensing, submitted.

Conferences Presentations/Papers/Posters

Schmidt, C. C. and J. Li, 2006: Ozone Estimates with Current and Future GOES, 4th GOES User's Conference, Broomfield, CO, May 1-3, 2006.

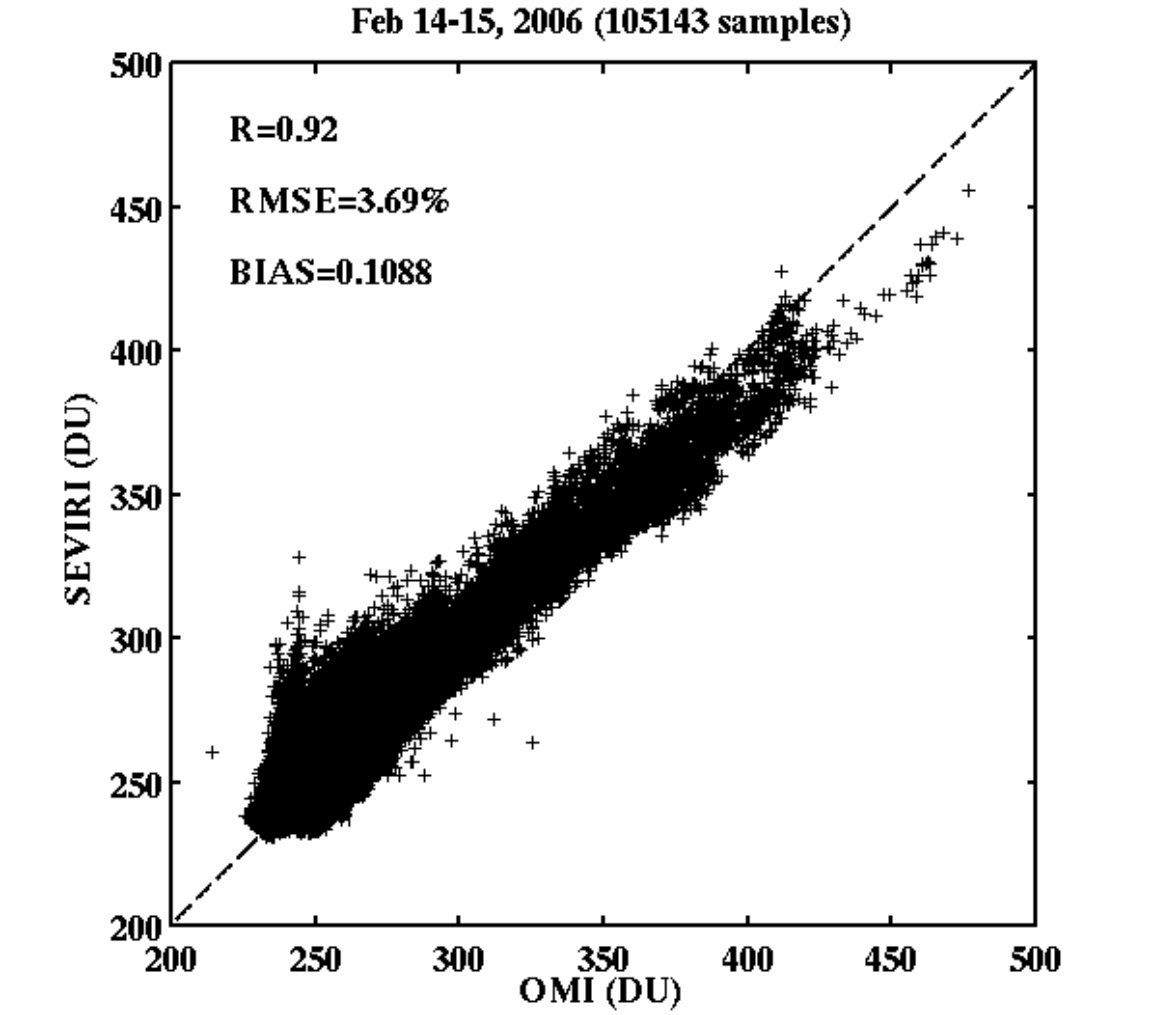

Figure 8.7.1: Scatter plot of collocated OMI ozone measurements and the SEVIRI ozone estimates for clear sky pixels between 12:00 UTC on 14 February and 12:00 UTC on 15 February 2006.

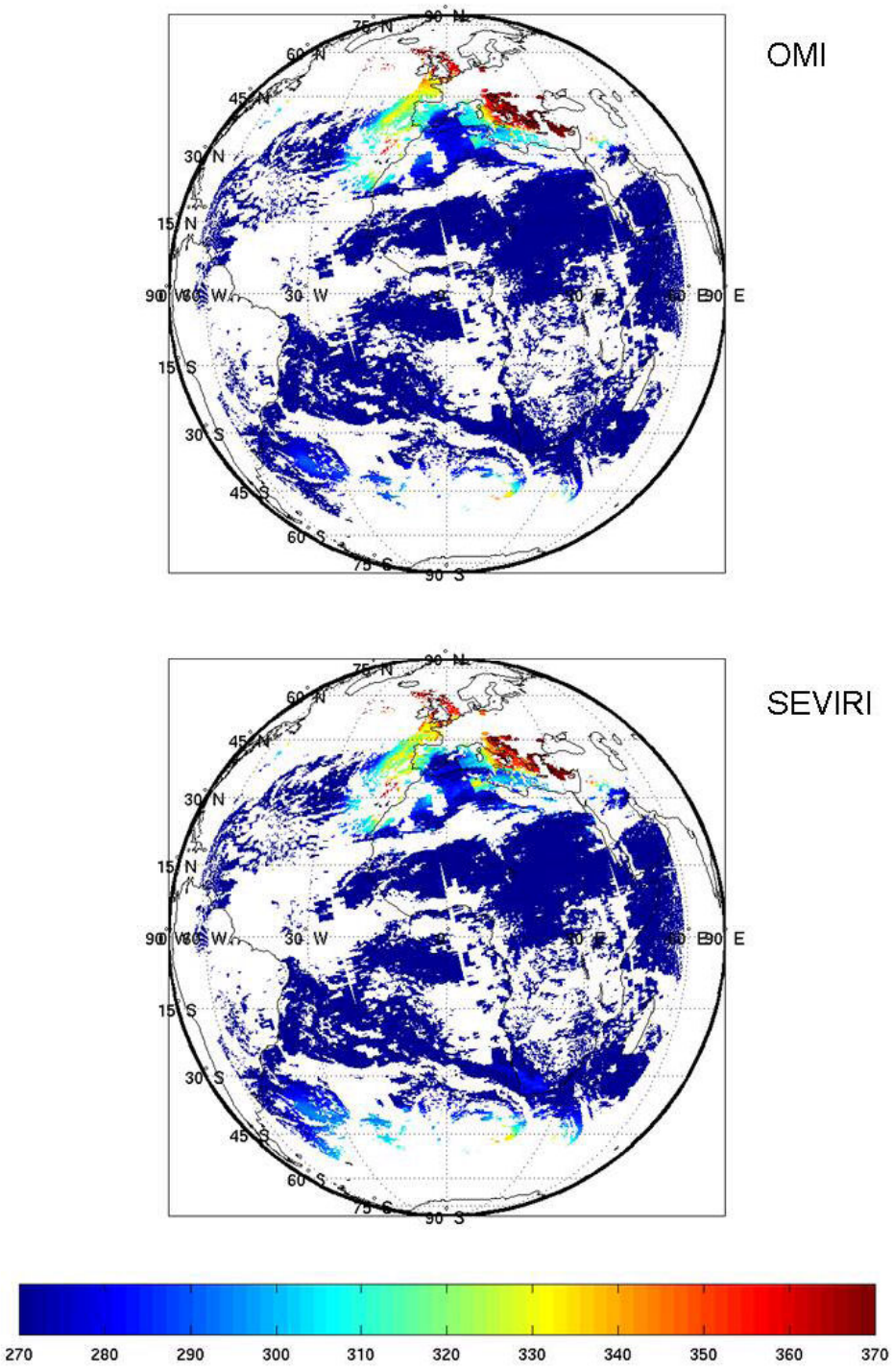

Figure 8.7.2: Mapping of TCO (DU) with OMI (upper panel) and collocated SEVIRI (low panel) clear sky pixels between 12:00 UTC on 14 February and 12:00 UTC on 15 February 2006.

8.8 GOES R Algorithm Working Group: Fire Detection – Elaine Prins

The primary focus of this effort is to evaluate the current GOES Wildfire Automated Biomass Burning Algorithm (WF_ABBA) and adapt the algorithm for application with the GOES-R ABI. This activity builds on historical and current expertise at CIMSS in fire algorithm development for the GOES Imager and the global geostationary fire observation network (MSG, MTSAT-1R, INSAT-3D, etc.). CIMSS will revise the WF_ABBA to address GOES-R ABI observational requirements utilizing the improved fire monitoring capabilities on GOES-R. This will include updating modules that identify and characterize sub-pixel fire activity, demonstrating and validating the prototype GOES-R ABI WF_ABBA using various GOES-R ABI proxy data sets, and providing a version of the algorithm for further evaluation by the AWG science team. This effort will involve collaborating with MODIS and NPOESS VIIRS fire product development experts to maximize future use of multiple data sources (geo and leo) that take advantage of the strengths of each system to create improved fused fire products. This activity will ensure enhanced future geostationary fire detection, diurnal monitoring, and characterization in the GOES-R era.

Summary of Accomplishments and Findings
UW-Madison CIMSS AWG GOES_R ABI fire detection efforts began in September 2006. Over the past four months CIMSS has focused on algorithm design review (ADR), test plan design and validation, and identification of possible proxy data sets.

WF-ABBA Algorithm Design Review
As part of the ADR process, the current WF_ABBA code was evaluated on a line-by-line basis and a flow chart was created to show areas where updates, modifications may be necessary. GOES-RRR funding is being used to investigate some of these areas and determine if updates are needed and/or beneficial for meeting GOES-R MRD requirements. CIMSS presented the GOES-R Algorithm Design Review via telecon on December 8, 2006. The ADR overview included a summary of high risk areas which include the following: (1) unknowns regarding sub-pixel fire characterization requirements; (2) lack of adequate proxy data for algorithm development/testing and the need for access to realistic fire data generated from higher resolution sensors as well as model simulated data; and (3) ABI sampling and re-gridding techniques and protocol for flagging saturated detectors are not entirely known and may impact fire detection and characterization, especially if there is no access to pre-gridded and/or level 1B flagged data in real time. Recent studies utilizing the MSG SEVIRI re-gridded data have shown that re-gridding techniques can affect the fire signature in such a way that it impacts the ability of the WF_ABBA to identify some fires and compromises sub-pixel fire characterization.

WF-ABBA Test Plan Design and Validation
In cooperation with the AWG Land Surface Team, CIMSS provided recommendations for the GOES-R ABI fire test plan and validation efforts. Ground truth validation of a fire algorithm is difficult. Although various fire databases exist for federal, state, native American, and private lands; many fires are not documented. There is no comprehensive database of all fire activity in the U.S. (e.g. wildfires and agricultural burning). CIMSS recommended a two phase approach for testing and validation. Phase 1 requires the availability of ABI simulated imagery and proxy data from models (CIRA) and other satellite sensors (MODIS, GOES, Met-8, MTSAT 2km data, etc.) that provide realistic examples and address issues that effect fire detection with ABI to the extent possible. Ideally the data set should consist of half-hourly data for two weeks in each season in a variety of biomes. Half of the simulated proxy data will be used for algorithm tuning. The remaining will be used for testing. Fires detected with the proposed algorithm(s) will be

compared with the number of known/estimated fires in the simulated proxy data sets. The number of fires in simulated data derived from existing data sets is not entirely known. Algorithms should detect at least 95% of the fires within the ABI detection capability, with a false alarm rate of 5-10% for highest confidence fires. The fire detection success/failure rates will be evaluated for each tested algorithm. In Phase 2 high resolution data (e.g. 30m resolution Terra/ASTER and Landsat 7/ETM+ data) will be used to validate the ABI fire algorithm in a variety of biomes. In addition ABI fire algorithm output will be compared with ground truth information in regional/local case study analyses and field programs.

Identification of Proxy Data Sets

The CIMSS biomass burning group has been working in conjunction with CIRA and the CIMSS AWG proxy data team to identify appropriate proxy data simulated from models and higher resolution satellite sensors (e.g. MODIS). Information regarding measurement ranges for sub-pixel fire temperature and area, 4 micron band saturation, band to band co-registration, oversampling issues, point spread functions, and emissivity were provided to CIRA to assist them in creating realistic proxy fire data sets. We suggested creating a test data set for Central America using 24 April 2004 as guidance for diurnal signals and fire activity in partially cloudy situations. The biomass burning group is also evaluating proxy data sets simulated from MODIS data.

9 Joint Center for Satellite Data Assimilation (JCSDA)

9.1 Assessing Forecast Impact of Multiple Data Types in the GFS – Tom Zapotocny

Proposed Work

Multiple Observing System Experiments (OSEs) are used to quantify the contributions made to forecast quality using both conventional data and remotely sensed satellite data. Concentration in this work is directed at examining the contribution of individual observing systems as well as rawinsondes. This work is a follow-on to earlier work which examined the total contribution of all conventional data and all satellite data in the Global Forecast System (GFS). The positive/negative impact is measured by comparing the analyses and forecasts from an assimilation/forecast system using all the data types to an assimilation/forecast system excluding the particular observing system. Impact is assessed by comparing these results over extended 45 day time periods during the extreme seasons. The assimilation/forecast system used for these experiments is the National Centers for Environmental Prediction (NCEP) Global Data Assimilation System (GDAS)/Global Forecast System (GFS). In 2006 we evaluated:

- GDAS/GFS anomaly correlations to data denials.
- Hurricane Track Forecast Errors to data denials.

The data types denied in this work include Advanced Microwave Sounding Unit (AMSU) data, High Resolution Infrared Radiometric Sounder (HIRS) data, Geostationary wind (GEO Wind) data QuikSCAT (QuikSCAT) data and rawinsonde (RAOB) data.

Summary of Accomplishments

GDAS/GFS Anomaly Correlations to Data Denial

A case study was conducted including data from both hemispheres and the tropics consisting of periods during January-February 2003 and August-September 2003. During these periods, a

T254 - 64 layer version of NCEP's global spectral model was used. All satellite and conventional data routinely used by the GDAS were assimilated via the Spectral Statistical Interpolation (SSI) algorithm except for the observing systems being tested. Figure 9.1.1 presents a summary of the anomaly correlations at day 5 for the five data types plus the control simulation for seven fields covering both hemispheres and the tropics. A particular data type has a positive impact if the anomaly correlation of the control simulation is higher than the anomaly correlation from the denial experiment. From the figure it is clear that the largest positive impact is from AMSU data in both seasons. QuikSCAT data provides the second largest positive impact, with the remainder of the data types providing a nearly neutral impact.

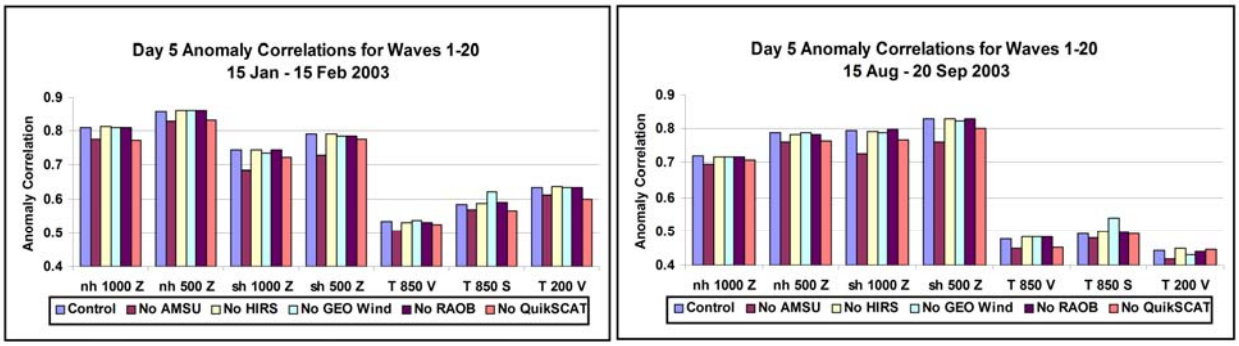

Figure 9.1.1: The day 5 anomaly correlations for waves 1-20 for seven fields covering the tropical belt and each hemisphere. Results are shown for the control simulation and denials of AMSU, HIRS, GEO Winds, Rawinsondes and QuikSCAT data. The 15 January to 15 February 2003 results are shown on the left, while the 15 August to 20 September results are shown on the right.

Hurricane Track Forecast Errors to Data Denials

The hurricane track forecast errors out to 96 hours were examined for both the Atlantic Basin and Eastern Pacific Basin during August-September 2003. In order for a storm (tropical depression, tropical storm or hurricane) to be included in this study, it had to exist in all five runs (the control plus four experimental runs). Figure 9.1.2 presents a summary of the hurricane track forecast error for the four data types plus the control simulation in the Atlantic and East Pacific Basins. A particular data type has a positive impact if the denied track error is greater than the control track error. The Atlantic Basin hurricane track forecast errors (left panel) show that the control run and all experimental runs have similar errors (within about 10 nm) out to 48 hours. However, track errors in the Eastern Pacific increase substantially out to 48 hours when the GEO Winds are removed from the assimilation system. The 96 hour track errors are not completed in the Eastern Pacific because the sample size was too small to be statistically significant.

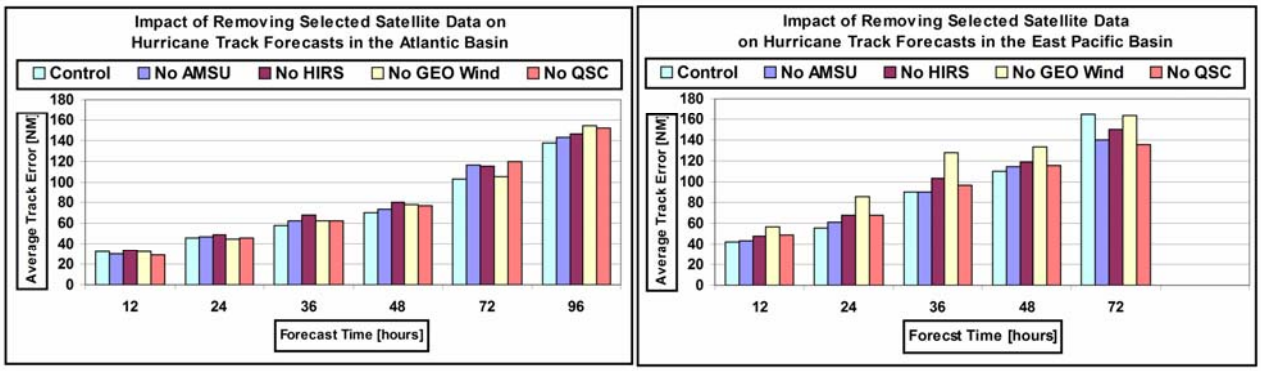

Figure 9.1.2: Average track error (NM) by forecast hour for the control simulation and experiments where AMSU, HIRS, GEO Winds and QuikSCAT were denied. The Atlantic Basin results are shown on the left, while the Eastern Pacific Basin results are shown on the right. A small sample size in the number of hurricanes precludes presenting the 96 hour results in the Eastern Pacific Ocean.

Publications and Conference Reports

Zapotocny, T. H., J. A. Jung, J. F. Le Marshall, R. E. Treadon, 2006: A Two Season Impact Study of Satellite and In-Situ Data in the NCEP Global Data Assimilation System. Accepted for publication in *Wea. and Forecasting* January 2007.

Le Marshall, J., J. Jung, T. Zapotocny, C. Redder, M. Dunn, J. Daniels, and L. P. Riishogjaard, 2006: Impact of MODIS Atmospheric Motion Vectors on Global NWP. Submitted to *Aust. Meteor. Mag*.

AIRS, HIRS and CSBT Experiments, presented at The 4th Workshop on Satellite Data Assimilation. Greenbelt, MD. 31 May – 1 June 2006.

Jung, J. A., T. H. Zapotocny, J. F. Le Marshall, and R. E. Treadon, 2006: NOAA Polar Orbiting Satellite Observing System Experiments using the NCEP GDAS. Preprints 87 Annual AMS meeting, San Antonio Tx. 14-18 January 2007.

Jung, J. A., T. H. Zapotocny, R. E. Treadon, J. F. LeMarshall, 2006: Atmospheric Infrared Sounder Assimilation Experiments using the National Center for Environmental Prediction's Global Forecast System. Presented at 14th Conference on Satellite Meteorology and Oceanography, Atlanta, GA, 28 January-2 February 2006.

Le Marshall, J. F., J. A. Jung, J. Derber, R. Treadon, M. Goldberg, W. Wolf, and T. H. Zapotocny, 2006: Assimilation of Atmospheric Infrared Sounder (AIRS) Observations at JCSDA. Presented at 14th Conference on Satellite Meteorology and Oceanography, Atlanta, GA, 28 January-2 February 2006.

Santek, D., J. A. Jung, T. H. Zapotocny, J. Key, C. Velden, 2006: Mechanisms that Propagate Polar Satellite Derived Atmospheric Motion Vector Information into Lower Latitudes. Presented at 14th Conference on Satellite Meteorology and Oceanography, Atlanta, GA, 28 January-2 February 2006.

Zapotocny, T. H., J. A. Jung, R. E. Treadon, J. F. LeMarshall, 2006: Recent MODIS Assimilation Experiments in the NCEP GDAS. Presented at 14th Conference on Satellite Meteorology and Oceanography, Atlanta, GA, 28 January-2 February 2006.

9.2 Assessing the Forecast Impact of Having One, Two or Three Operational Polar-Orbiting Satellites – Jim Jung and Tom Zapotocny

Proposed Work

Observing System Experiments (OSEs) are used to quantify the contributions made to forecast using both conventional data and remotely sensed satellite data. The positive/negative impact is measured by comparing the analyses and forecasts from an assimilation/forecast system using all the data types to an assimilation/forecast system excluding the particular observing system. Impact is assessed by comparing these results over extended periods during the extreme seasons. The assimilation/forecast system used for these experiments is the National Centers for Environmental Prediction (NCEP) Global Data Assimilation/Forecast System (GDAS/GFS). The case study chosen herein consists of a 51-day period during August-September 2003. During this period, a T254 - 64 layer version of NCEP's global spectral model was used. All satellite and conventional data routinely used by the GDAS are assimilated except for the observing systems being tested.

The relative advantage of having the present compliment of three operational polar orbiting satellites (NOAA-15, 16 and 17) is investigated with respect to having two (NOAA-16 and 17) or one (NOAA-17). These configurations are referred to as 1_NOAA, 2_NOAA, and 3-NOAA, respectively. The baseline experiment, 1_NOAA, uses the Advanced Microwave Sounding Unit (AMSU) and High Resolution Infrared Radiometric Sounder (HIRS) data from NOAA-17 along with the NCEP operational compliment of conventional and satellite data, but excludes data from NOAA-15 and NOAA-16. The 2_NOAA experiment adds NOAA-16 AMSU and HIRS data to the baseline experiment. The 3_NOAA experiment adds NOAA-15 AMSU data as well as NOAA-16 AMSU and HIRS data to the baseline experiment.

Summary of Accomplishments and Findings

The impact of these satellite data on the quality of forecasts made by the GFS for 15 August to 20 September 2003 are explored in detail. The impacts of satellite data on hurricane track forecasts are also evaluated. Figure 9.2.1 presents a summary of the anomaly correlations at day 5 for the mid-latitudes (right) and polar regions (left) during August and September 2003. The 3_NOAA experiment has consistently higher anomaly correlation scores for both regions. The 2_NOAA experiment has lower anomaly correlation scores than the 3_NOAA experiment, but are consistently higher than the 1_NOAA experiment. The anomaly correlation scores are lowest in all cases for the 1_NOAA experiment.

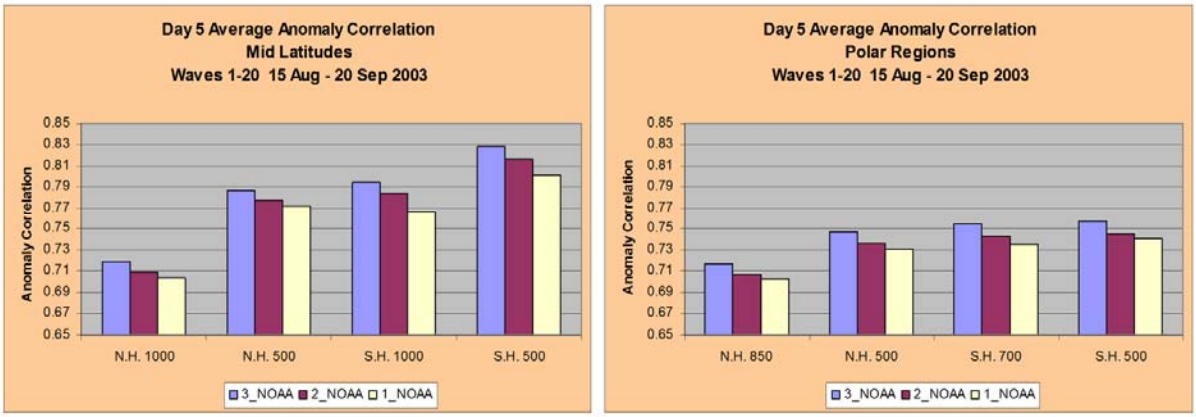

Figure 9.2.1: The 500 hPa geopotential height anomaly correlations for day 5 in mid-latitudes (left) and polar regions (right) during 15 August - 20 September 2003. The blue, red and yellow bars are for the assimilation of 3, 2, and 1 NOAA polar orbiting satellite(s), respectively. The 3_NOAA experiment is currently used in NCEP operations.

For the forecast impact, the 1_NOAA experiment is used as the baseline to compare the 2_NOAA and 3_NOAA 500 hPa geopotential height results shown in Figure 9.2.2. Consistent with the anomaly correlation scores, the 2_NOAA and 3_NOAA experiments both have generally positive impacts with the 3_NOAA having slightly greater impact. In both the 2_NOAA and 3_NOAA experiment the greatest impacts in the 12-hour forecasts are in the Indian Ocean and along the west coast of South America. By 24-hours the greatest positive impacts move to the Indonesian region and in the equatorial region west of South America. The satellite impacts are generally minimal over land, most likely due to the amount of conventional data available and the corresponding limited use of satellite data.

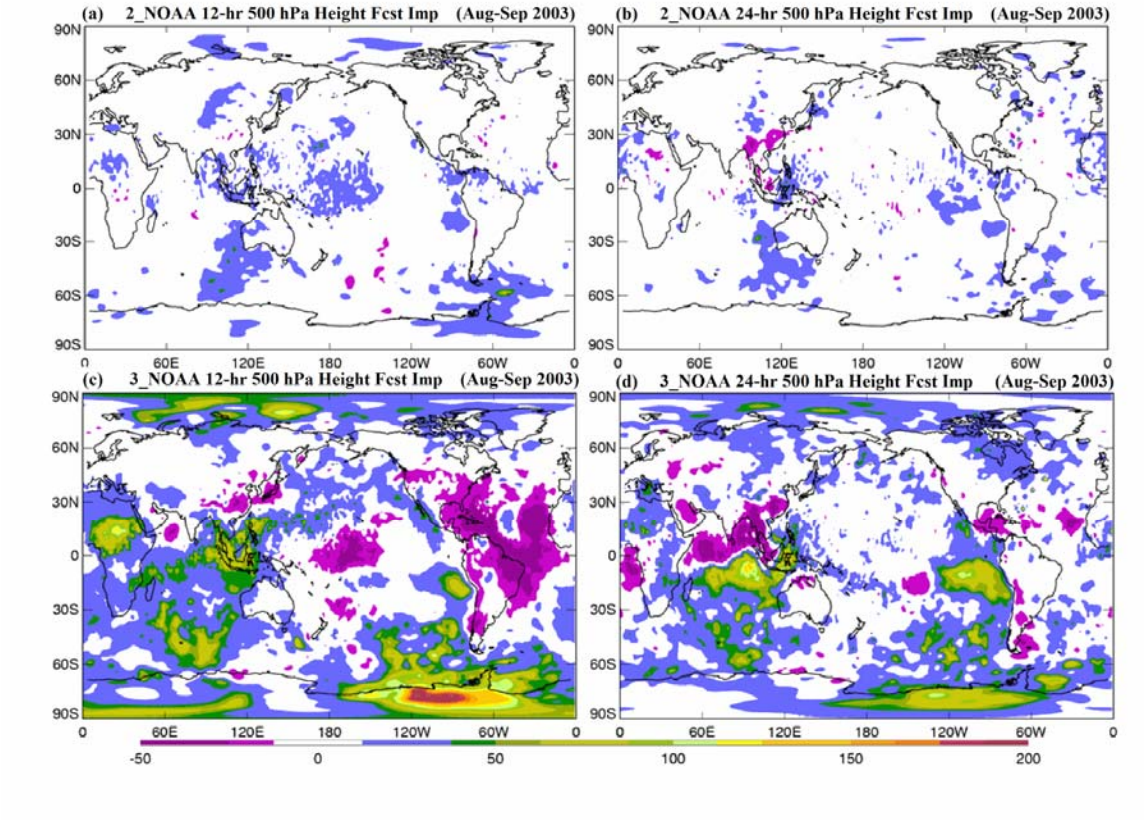

Figure 9.2.2: Geographical distributions of forecast impact from the August-September 2003 time period for 500 hPa geopotential height for forecast hours 12 and 24. The shaded contour interval is 12.5% and limited to minus 50% to 200%. Values outside this range retain the maximum/minimum color values while values closer to zero than ±12.5% are white. The 2_NOAA results are shown in (a) and (b) while the 3_NOAA results are shown in (c) and (d).

The hurricane track forecasts out to 120 hours were examined for the Atlantic Basin during this time period. In order for a storm (tropical depression, tropical storm or hurricane) to be used in these diagnostics, the storm must exist in all three experimental runs. The hurricane track forecast errors show the 3_NOAA experiment generally has the smallest track errors (highlighted red) when compared to the 2_NOAA and 1_NOAA results shown in Table 9.2.1. The 2_NOAA experiment seems to have the greatest track errors. This suggests the greatest improvement in track errors seems to be from the addition of NOAA-15 data. Of the three polar satellites, the NOAA-15 orbit adds the most information in the Western Atlantic and Gulf of Mexico for the 0000 UTC assimilation cycle (orbits not shown).

Table: Atlantic Basin average forecast error (km) during 2003.

12.8	29.3	45.9	61.1	70.9	105.7	153.6	196.1	1_NOAA
14.7	29.6	47.6	65.0	80.4	119.3	156.0	214.7	2_NOAA
12.2	31.8	45.6	59.4	70.6	103.0	137.3	201.4	3_NOAA
38	36	31	30	25	19	17	15	# cases
00-hr	12-hr	24-hr	36-hr	48-hr	72-hr	96-hr	120-hr	Fcst Hr

Table 9.2.1: Atlantic Basin average forecast error (km) during August-September 2003 when including data from multiple NOAA polar orbiting satellites. The highlighted numbers represent the best average forecast. The number of cases and forecast hour are shown in rows 4 and 5.

Publications and Conference reports

Le Marshall, J., J. Jung, J. Derber, M. Chahine, R. Treadon, S. J. Lord, M. Goldberg, W. Wolf, H. C. Liu, J. Joiner, J. Woollen, R. Todling. P. van Delst, and Y. Tahara, 2006: Improving Global Analysis and Forecasting with AIRS. *Bull. Amer. Meteor. Soc.*, 87,747,750.

Le Marshall, J., J. Jung, T. Zapotocny, J. Derber, R. Treadon, M. Goldberg and W. Wolf, 2006: The Application of AIRS Radiances in Numerical Weather Prediction. *Aust. Meteor. Mag.*, 55, 213-217.

Zapotocny, T. H., J. A. Jung, J. F. Le Marshall, R. E. Treadon, 2006: A Two Season Impact Study of Satellite and In-Situ Data in the NCEP Global Data Assimilation System. Conditionally accepted in Weather and Forecasting.

Conference papers and posters

AIRS, HIRS and CSBT Experiments, presented at The 4th Workshop on Satellite Data Assimilation. Greenbelt, MD. 31 May – 1 June 2006.

Jung, J. A., T. H. Zapotocny, J. F. Le Marshall, and R. E. Treadon, 2006: NOAA Polar Orbiting Satellite Observing System Experiments using the NCEP GDAS. Preprints 87 Annual AMS meeting, San Antonio Tx. 14-18 January 2007.

Jung, J. A., T. H. Zapotocny, R. E. Treadon, J. F. LeMarshall, 2006: Atmospheric Infrared Sounder Assimilation Experiments using the National Center for Environmental Prediction's Global Forecast System. Presented at 14th Conference on Satellite Meteorology and Oceanography, Atlanta, GA, 28 January-2 February 2006.

Le Marshall, J. F., J. A. Jung, J. Derber, R. Treadon, M. Goldberg, W. Wolf, and T. H. Zapotocny, 2006: Assimilation of Atmospheric Infrared Sounder (AIRS) Observations at JCSDA. Presented at 14th Conference on Satellite Meteorology and Oceanography, Atlanta, GA, 28 January-2 February 2006.

Santek, D., J. A. Jung, T. H. Zapotocny, J. Key, C. Velden, 2006: Mechanisms that Propagate Polar Satellite Derived Atmospheric Motion Vector Information into Lower Latitudes. Presented

at 14th Conference on Satellite Meteorology and Oceanography, Atlanta, GA, 28 January-2 February 2006.

Zapotocny, T. H., J. A. Jung, R. E. Treadon, J. F. LeMarshall, 2006: Recent MODIS Assimilation Experiments in the NCEP GDAS. Presented at 14th Conference on Satellite Meteorology and Oceanography, Atlanta, GA, 28 January-2 February 2006.

9.3 Assimilating and Determining the Impact of Sea Surface Winds Measured by WindSAT/Coriolis in the Global Forecast System – Tom Zapotocny

Proposed Work

This project investigates the impact passively sensed remote data have on numerical weather prediction (NWP) models. The impact of sea surface wind vectors have previously been estimated with active remote sensing instruments, such as QuikSCAT, and the data have proven to provide a positive impact on forecasts. The future polar system National Polar-orbiting Operational Environmental Satellite System (NPOESS) will be relying on passive techniques from instruments such as the CMIS (Conical scanning Microwave Imager/Sounder). To investigate the capability of such passive techniques for measuring surface wind speed and direction, the WindSAT/Coriolis instrument was placed into polar orbit by the National Aeronautics and Space Administration (NASA) in 2002. These data have now been distributed to the NWP and oceanic sciences community to assess possible implications for the NPOESS program. Initial studies of the impact of WindSAT data were completed using data from January 2004. Recently the focus has shifted to evaluating the WindSAT forecast impacts in real time during the summer and fall seasons of 2006.

Summary of Accomplishments

WindSAT/Coriolis data are available to the Joint Center for Satellite Data Assimilation (JCSDA). These wind vectors have been inserted into the National Centers for Environmental Prediction (NCEP) Global Forecast System (GFS) and forecast impacts have been compared with those from QuikSCAT winds and the operational GFS (control) for the same time. The WindSAT, QuikSCAT and control forecast impact simulations have been completed at the operational resolution of the GFS using both the Spectral Statistical Interpolation (SSI) and Gridpoint Statistical Interpolation (GSI) assimilation algorithms.

Recent progress includes completing these comparisons from late July 2006 to the end of September 2006. Several variations of assimilating the WindSAT data have been tried. They include using a 0.5° superob which is identical to the QuikSCAT superob, a 1.0° superob and a 0.5° superob where data values less than 5 m s^{-1} or greater than 25 m s^{-1} were not used.

Figure 9.3.1 shows the day 5 Northern Hemisphere 500 hPa geopotential height anomaly correlation from many of the experiments described above for the time period 23 August - 23 September 2006. The best (highest) anomaly correlation is achieved from the 0.5° superob with elimination of wind speeds below 5 m s^{-1} and above 25 m s^{-1}. Although not shown, other fields such as 1000 hPa wind also modestly benefit from the addition of WindSAT data.

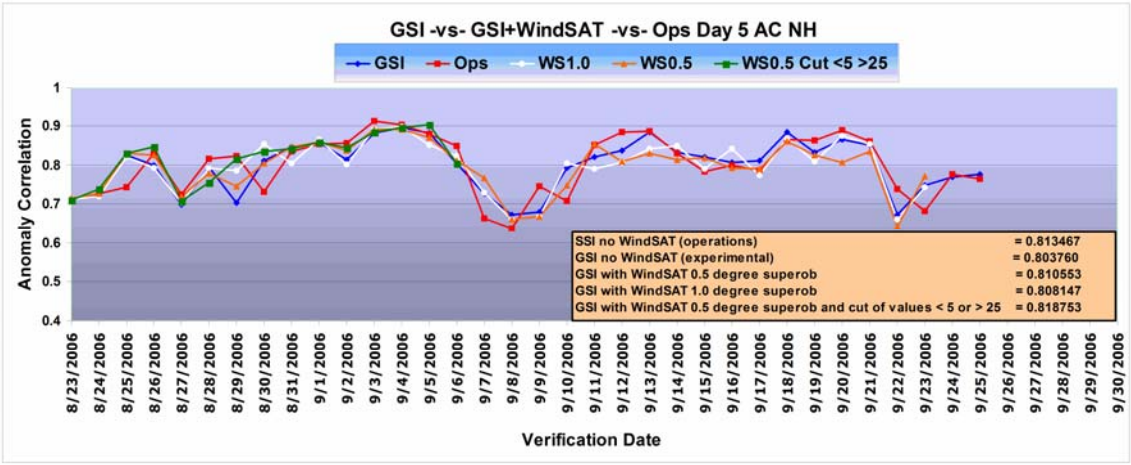

Figure 9.3.1: The day 5 Northern Hemisphere anomaly correlation for the period 23 August – 23 September 2006. Experiments shown include the control simulations without WindSAT data from both the SSI and GSI assimilation algorithms as well as several GSI results with WindSAT data at various levels of superobing. The monthly averaged anomaly correlation is shown in the legend for each experiment.

Publications and Conference reports

Le Marshall, J., L. Bi, J. Jung, T. Zapotocny, and M. Morgan, 2006: WindSat Polarmetric Microwave Observations Improve Southern Hemisphere Numerical Weather Prediction. Accepted in *Aust. Meteor. Mag*.

9.4 Community Radiative Transfer Model – Paul van Delst

Proposed Work

Community Radiative Transfer Model (CRTM) development in 2006 focused on (1) inclusion of additional gas absorption algorithms, (2) updated line-by-line computations and preparation for new sensors, and (3) construction of software test suites. The first task – inclusion of other gas absorption algorithms – was carried out to allow the leveraging of other groups' work that produces fast transmittance models for particular sensors. The last two tasks are ongoing as new satellite instruments are launched; and new functionality is added to, or new algorithms are implemented in, the CRTM. In addition to CRTM development, the investigation of the impact of CRTM results in the NCEP/EMC Global Data Assimilation System (GDAS) was undertaken via changes to the radiance data bias correction scheme. A new bias correction scheme was devised and, while initial results were mixed, is still being investigated.

Summary of Accomplishments and Findings

Inclusion of Additional Gas Absorption Algorithms

The gas absorption computation is one of the main components of the CRTM and, currently, CompactOPTRAN is the only choice of algorithm. To include other algorithms – such as OPTRANv7, SARTA(for AIRS), and RTTOV(for IASI) – in the CRTM, a new design of the gas absorption (AtmAbsorption) modules in the CRTM was necessary. NOAA/NESDIS scientists Yong Han and Yong Chen proposed an initial design to allow multiple AtmAbsorption algorithms to be used simultaneously in a CRTM run.

During this initial design phase, Roger Saunders of the Met Office visited the Joint Center for Satellite Data Assimilation (JCSDA) in March-April 2006 to investigate the integration of the RTTOV gas absorption code into the CRTM. Paul van Delst undertook a reciprocal visit to the Met Office in August-September 2006 as an NWP-SAF Visiting Scientist. During this time some of the new CRTM AtmAbsorption design changes were implemented in the code to allow for the initial integration of the RTTOV gas absorption software into the CRTM forward, tangent-linear, adjoint, and K-matrix models. The remainder of the CRTM framework (atmospheric profile layering, radiative transfer, etc) remained the same so the RTTOV integration provided the first opportunity to compare *only* the impact of the different gas absorption algorithms.

For the forward model comparison, brightness temperatures for the NOAA-16 HIRS/3 and selected channels of Aqua AIRS were computed using both the CompactOPTRAN and RTTOV AtmAbsorption algorithms in the CRTM. The diverse 52-profile dataset sampled from ECMWF 60-level model fields[1] and interpolated to the AIRS 100-layers was used as input to the calculations. The RTTOV coefficients used were also at the same layering to avoid wrapping in any interpolation errors into the results. Comparisons for some of the NOAA-16 HIRS/3 and Aqua AIRS channels are shown in Figures 9.4.1 and 9.4.2 respectively. It is clear which channels produce significantly different results between the two algorithms. The profile dependence of the brightness temperature differences is generally small, with larger differences seen in channels that have significant water vapor and ozone absorption.

A comparison of K-matrix model results for a selected NOAA-16 HIRS/3 and Aqua AIRS channel and a selected ECMWF profile are shown in Figure 9.4.3a and 9.4.3b respectively. Quantitative comparisons of the Jacobians have not yet been done, but the initial results are very encouraging. In general, the comparison of the temperature Jacobians is very good. Water vapour and ozone Jacobians compare well for strongly absorbing channels, and poorer for weakly absorbing channels. These results evince the algorithmic sensitivities where absorption is weak and the details of the computation tend to be important. For the stronger absorption channels, the shapes of the Jacobians tend to be well matched even if the magnitudes may not be. One interesting thing that was noticed is that there seems to be a strong correlation between the shapes of the water vapour and ozone Jacobians. The CompactOPTRAN- based CRTM exhibits this feature more prominently, but the RTTOV-based CRTM results also indicate a similar behavior. Also, while the CompactOPTRAN algorithm will always produce smoother Jacobians than RTTOV, it should be explicitly noted that the Jacobian comparisons shown here are relative – that is, we have not yet compared them to line-by-line model Jacobians so no determination should be made as to the correctness of the Jacobians based on how well behaved they may be in the vertical.

The full report detailing this work is available as NWP-SAF Visiting Report from EUMETSAT titled “Incorporation of RTTOV-8 in the JCSDA CRTM.”

[1] See Chevallier,F., Dec.2001, “Sampled databases of 60-level atmospheric profiles from the ECMWF analyses”, EUMETSAT/ECMWF SAF programme, Research Report No. 4.

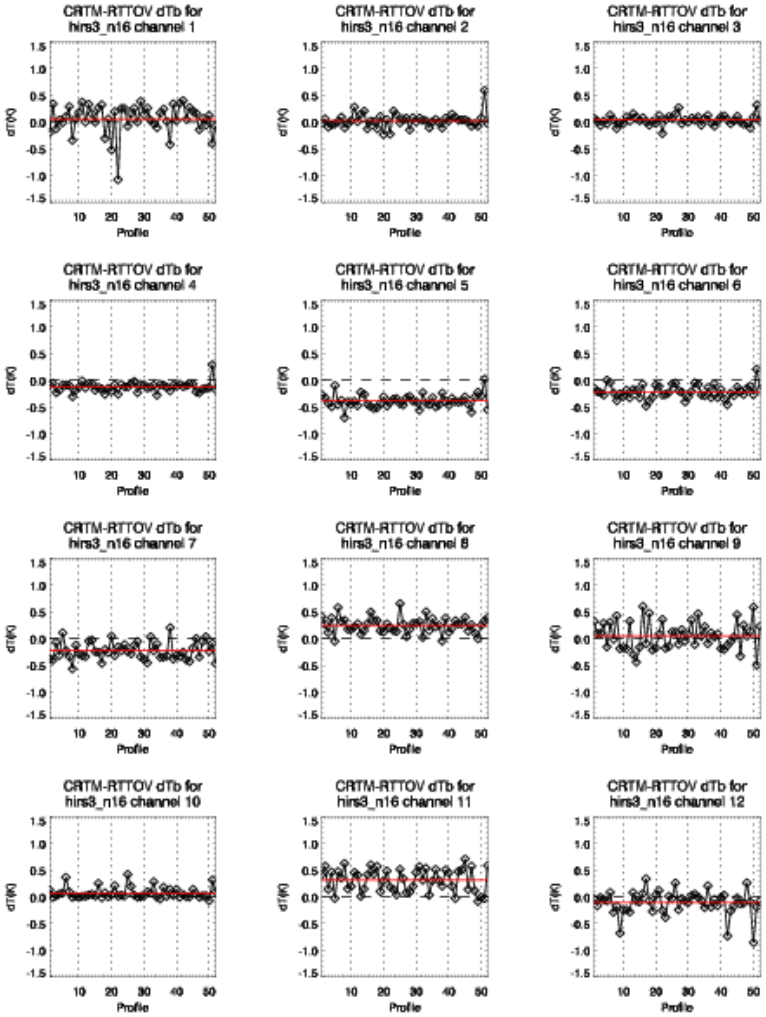

Figure 9.4.1: Forward model brightness temperature differences between using CompactOPTRAN and RTTOV as the AtmAbsorption algorithm in the CRTM for the first 12 channels of NOAA-16 HIRS/3.

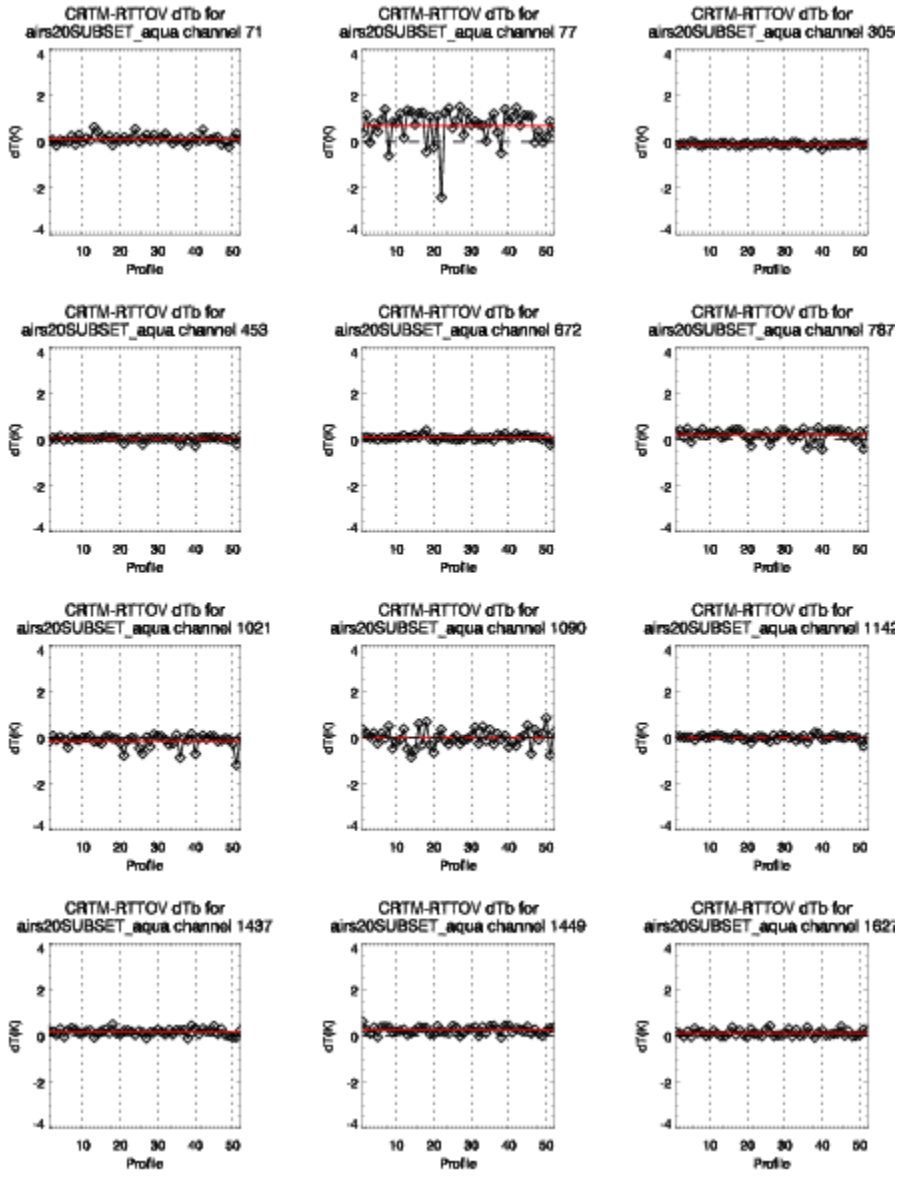

Figure 9.4.2: Forward model brightness temperature differences between using CompactOPTRAN and RTTOV as the AtmAbsorption algorithm in the CRTM for 12 selected channels of Aqua AIRS.

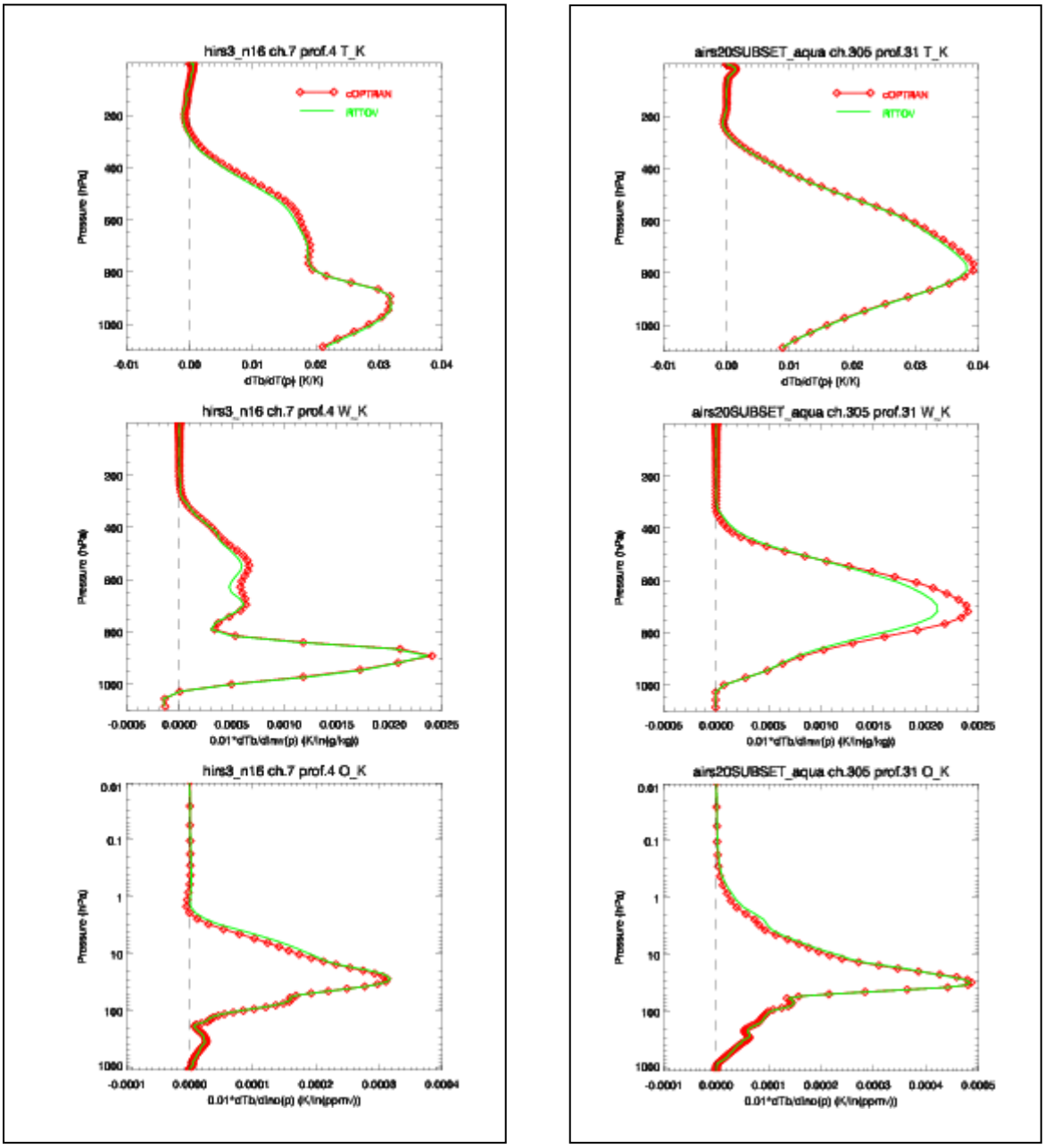

Figure 9.4.3: Temperature (top), water vapour (middle) and ozone (bottom) Jacobian profile comparisons between using CompactOPTRAN and RTTOV as the AtmAbsorption algorithm in the CRTM. *Panel (a)* - channel 7 of NOAA-16 HIRS3 for ECMWF profile #4. *Panel (b)* - channel 305 of Aqua AIRS for ECMWF profile #31

Updated line-by-line computations and preparations for new sensors

The procedure for generating sensor transmittance coefficient (TauCoeff) datafiles used in the CRTM CompactOPTRAN gas absorption model is a two-step process. The first step involves a line-by-line model (LBLRTM) to compute sensor resolution transmittances for a dependent profile set. The second step feeds these transmittances into the regression scheme to produce the fast model TauCoeffs (currently, Yong Han of NESDIS handles this part of the CRTM TauCoeff generation). Improvements in the line-by-line model (and, less frequently, in the sensor response functions) require that the transmittance database be recomputed periodically. During 2006, the LBLRTM software was upgraded to v9.4 and the entire infrared transmittance database used in the CRTM TauCoeff generation process was recomputed. These computations are relatively intensive: over two weeks about 200GB of monochromatic transmittances are generated and convolved down to about 20GB of sensor resolution transmittances.

In addition to the database regeneration, the transmittances and CRTM TauCoeff files for GOES-13 and Metop-A (HIRS/4, AVHRR/3, AMSU-A, and MHS) sensors were also produced. With the addition of these new sensors the CRTM can currently produce radiances for 74 sensors, both current and historic. For the GOES-13 Sounder, and the other operational GOES Sounders, channel/detector specific TauCoeffs were also produced along with the "regular" channel TauCoeffs (where the detector responses are averaged). This was done at the request of the global data assimilation group at NCEP/EMC to allow for the assimilation of 1x1 FOV GOES sounder radiances (previously only the 5x5 FOV averages were assimilated).

Source code is currently under development to produce the transmittances for interferometer instruments such as IASI and CrIS. As of December 2006, the support functions to transform spectra and interferograms back and forth have been tested with the focus on minimization of Gibbs phenomena (i.e. ringing) in the final result by application of spectrum edge filters.

CRTM Test Suites

Development of additional test codes for the CRTM in 2006 did not progress as far as was anticipated due to the emphasis placed upon updating the CRTM for multi-sensor use. Nevertheless, the codes that were developed did reveal several issues for the tested components that impact their final implementation in the CRTM.

Radiance Bias Correction Impact on GDAS

The bias correction of satellite radiances is important for enhancing the impact on forecast skill. During 2006, working with John Derber of NCEP/EMC the method of satellite data bias correction in the NCEP Global Data Assimilation System (GDAS) was modified in tests with the goal of improving the use of satellite radiances. The current operational bias correction scheme applies a slowly varying scan angle correction and an air mass correction to the computed radiances. The initial change made to the GDAS bias correction was to apply the air mass correction prior to the scan angle bias update, which should, on average, trend the biases to zero. In addition, the average of the scan angle bias correction was removed and effectively added to the constant term of the air mass bias correction. The impact these two changes had on the across-scan bias corrected brightness temperatures is shown in Figures 9.4.4a and 9.4.4b for NOAA-16 AMSU-A channel 3 and NOAA-17 HIRS/3 channel 8. The impact of the updated bias correction scheme is quite evident for AMSU-A (other AMSU-A channels show similar improvements). The improvement in the HIRS/3 case is not as evident but there is a relatively clear reduction in the amount of across-scan variability.

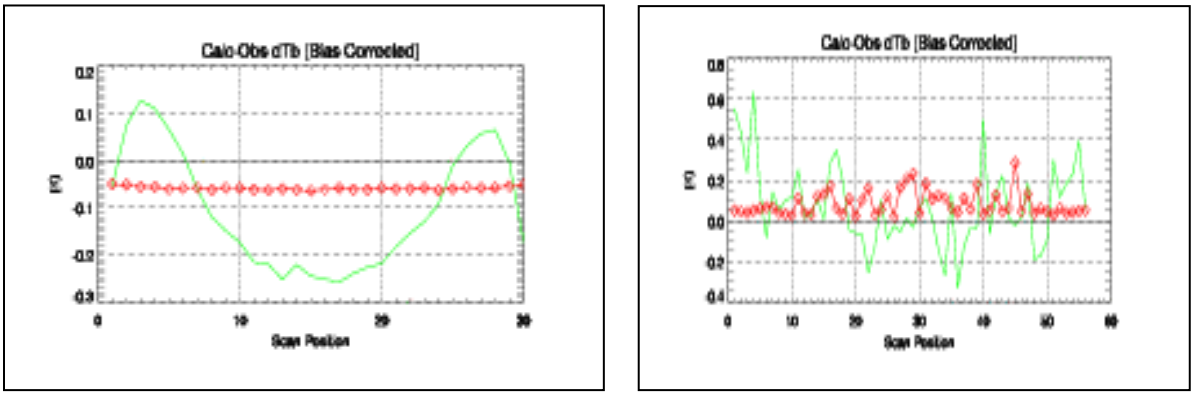

(a) (b)

Figure 9.4.4: Impact of changes to GSI radiance bias correction on *Panel (a)* NOAA-16 AMSU-A channel 3 and *Panel (b)* NOAA-17 HIRS/3 channel 8. The green curve is the GSI control run and the red curve is the GSI test run with the updated bias correction scheme. Both control and test runs were done with the Oct2006 GSI release and covered the time period 07-Oct to 06-Nov 2006.

To determine if the updated bias correction scheme was an improvement, the amount of data making it past quality control in the GSI was the first quantity inspected. These values for the same sensors and channels as Figure 9.4.4a and 9.4.4b are shown as a time series in Figure 9.4.5a and 9.4.5b respectively. The change for the AMSU-A is relatively small with the number of observations decreasing slightly with the updated bias correction. However, the change in the number of HIRS/3 observations is very large. This large change explains the change shown in Figure 9.4.4b – the across-scan variation is reduced because many more observations are contributing to the average. The ultimate determination of whether or not the updated bias correction scheme is an improvement is whether or not forecast skill is improved. The results of those runs are still preliminary but the initial results show mixed but generally neutral impact due to the large increase of HIRS/3 observations. The reasons for this are still under investigation.

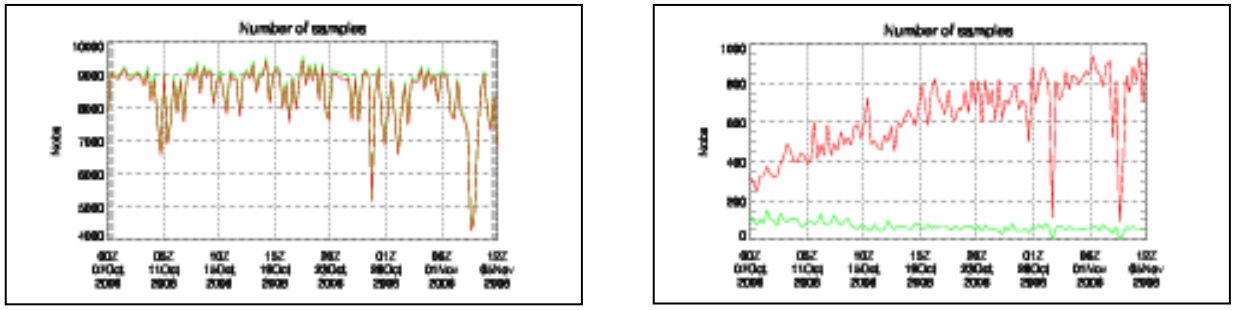

(a) (b)

Figure 9.4.5: Impact of the updated bias correction scheme in the amount of data making it past quality control in the GSI for *Panel (a)* NOAA-16 AMSU-A channel 3 and *Panel (b)* NOAA-17 HIRS/3 channel 8. The green curve is the GSI control run and the red curve is the GSI test run with the updated bias correction scheme. Both control and test runs were done with the Oct2006 GSI release and covered the time period 07-Oct to 06-Nov 2006.

9.5 NCEP Collaboration – Ralph Petersen

Proposed Work
This effort supports initial distribution of models and supporting data to specific candidate developing countries. Specific activities in 2006 focused on continued planning and development of a forecaster training program on the use of NWP output to be conducted in parallel with model implementation. These efforts are being fully coordinated with NWS/IA.

Summary of Accomplishments and Findings
In November 2005, Dr. Ralph Petersen represented NWS/NCEP/EMC at the meeting of the WMO Working Group on Numerical Experimentation in St. Petersburg Russia. He presented a number of papers describing current and planned numerical modeling and data assimilation activities in the US. A detailed set of annotated minutes of the meeting has been provided directly to NCEP, including action items and areas of concern. Final discussion of this activity occurred in early 2006.

In September 2006, Dr. Petersen gave an invited talk to the WMO AMDAR Panel. In November, Dr. Petersen was an invited lecturer at a WMO Workshop on Severe Weather Forecasting conducted at Pretoria, South Africa for forecasters from developing countries in southern African. In December, Dr. Petersen gave an invited lecture at the bi-annual meeting of the WMO Commission on Aeronautical Meteorology, reviewing international aviation forecasting improvements over the past 20 years and providing guidance concerning the direction of future forecast improvement priorities. Preparation for these events was supported in part by these funds. In 2007, additional funds are expected to come directly from NWS/IA instead of NWS/NCEP/EMC.

Publications and Conference reports
Petersen, R. A., 2006: Travels with Charlie: An invited paper on the future direction of international aviation meteorology presented at the WMO Commission on Aeronautical Meteorology, Geneva, Switzerland.

Petersen, R. A., S. Bedka, W. Feltz, and E. Olson, 2006: Evaluation of the WVSS-II Sensor Using Co-located In-situ and Remotely Sensed Observations. An invited paper for the WMO AMDAR Panel Science Workshop, Silver Spring, MD.

9.6 WVSS Field Program – Wayne Feltz, Ralph Petersen

Proposed Work
Efforts for 2006 were conducted in four areas: 1) finalizing the evaluation of the co-located WVSS-II/radiosonde data taken in 2005, 2) development of an alternative reporting algorithm to increase WVSS-II data precision for values greater than 10 g/kg, 3) support of a second WVSS-II field assessment in Louisville using sensors modified to improve data taken on descent, and 4) continuation of efforts to determine the time/space variability of low-level atmospheric moisture. Based upon consultation with NOAA program management, it was determined that the duration of the second field assessment needed to be extended from one to two weeks. As a result, resources for portions of the time/space variability study were diverted to cover a portion of the cost of the field efforts.

Summary of Accomplishments and Findings

Finalize evaluation of the co-located WVSS-II/radiosonde data taken in 2005

Analysis of the results from the 2005 field program were completed and provided to NOAA. The assessment was constrained by: 1) A design problem occasionally produced erroneous reports in areas of high humidity and clouds on descent. In order to determine differences in good quality reports made by both the aircraft and rawinsonde, only aircraft ascents were evaluated, 2) Some of the early WVSS-II units allowed small amounts of moisture to be trapped in the laser sensing unit. To minimize the effects of this bias, the assessment was limited to regions where the observed mixing ratio was greater than 2 g/kg., and 3) It was discovered that WVSS-II observations were being truncated before transmission to the ground. Reports of less than 10 g/kg had precision of at least 0.1 g/kg, while reports greater than 10 g/kg had precisions of only 1 g/kg, producing RH reporting errors of 5%. As a result, analyses were performed separately for the full data set and for observations above and below 10 g/kg. Both of the engineering problems referenced in 1) and 2) have subsequently been addressed, and an alternative reporting procedure was implemented to avoid data truncation.

Statistical evaluations were made of the performance of a variety of factors important for the optimal objective use of the aircraft data in combination with other data sources by assessing: 1) similarity of reports from the different observing systems and different aircraft, 2) biases between ascent and descent reports from individual aircraft, 3) variability between different aircraft (to assess instrument calibration and effects of aging), and 4) capability to capture sharp moisture gradients accurately, including as aircraft emerge from clouds.

Overall statistical comparisons show very small biases between WVSS-II and Radiosonde data sets. Root Mean Square (RMS) and Standard Deviation (SD) fits are around 1 g/kg for specific humidity, especially in the more stable areas of the lower troposphere in these night-time comparisons. When the data are divided according to reporting precision, the results for observations below 10 g/kg improve significantly, while comparisons of data subjected to larger truncations show much more variability. For values below 10 g/kg (see Figure 9.6.1-left), the SD fit for these data approaches 0.5 g/kg in the boundary layer. Comparisons of Relative Humidity (RH) for these data (derived from a combination of aircraft moisture data and rawinsonde temperature observations to remove biases in the aircraft temperature reports) show accuracies near 5%. This meets WMO requirements.

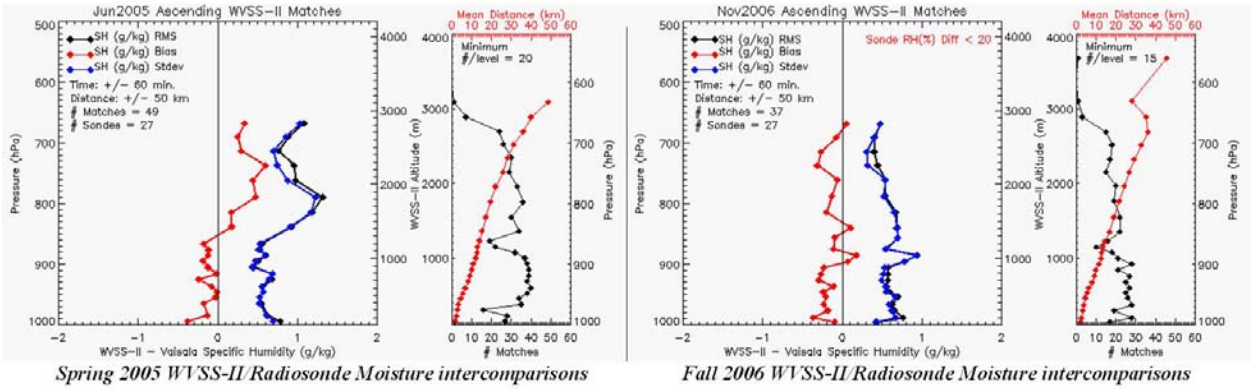

Spring 2005 WVSS-II/Radiosonde Moisture intercomparisons *Fall 2006 WVSS-II/Radiosonde Moisture intercomparisons*

Figure 9.6.1: Intercomparisons of WVSS-II and Radiosonde Moisture for Spring 2005 (left) and Fall 2006 (right)

Development of an alternative reporting algorithm to increase WVSS-II data precision for values greater than 10 g/kg

An alternative reporting scheme was developed in response to the field program finding regarding an order of magnitude reduction of reported mixing ratio precision for values greater than 10 g/kg. The alternative reporting scheme preserves the intended precision of better than 0.1 g/kg for all reports without increasing the number of digits required for report transmission. It should be noted that the previous reporting precision would have provided little value for NWP applications. The new scheme shown in Figure 9.6.2 was documented and reviewed by NOAA, UPS, WMO and ARINC. The scheme was being implemented on UPS aircraft for the November 2006 field program.

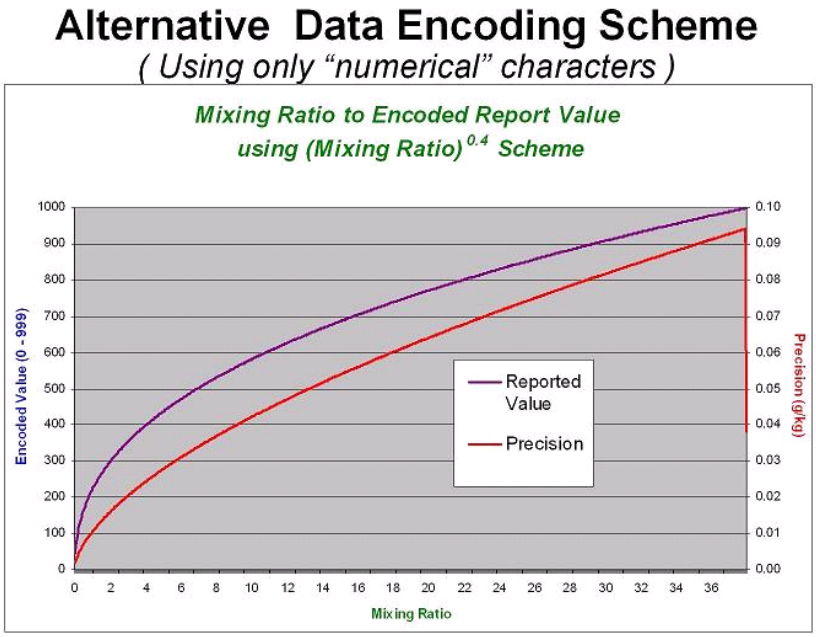

Figure 9.6.2: Alternative data encoding scheme precision. The reported data are constrained to a fixed number of digits used for transmission. The new scheme provides precision of approximately .1gm/Kg throughout the data range.

Support of a second WVSS-II field assessment in Louisville using sensors modified to improve data taken on descent

A second, two-week long field program was conducted in November 2006 with the objectives of: 1) revalidating the results of the 2005 test in a colder environment, and 2) assessing the performance of WVSS-II sensor modifications to address the problems of trapped moisture and retention of moisture during aircraft descent. A total of 28 rawinsondes were successfully launched immediately before and after the two periods of landings and takeoffs of UPS aircraft at Louisville, KY. Review of the data show that approximately six of the revised WVSS-II sensors are still not functioning properly. Of the remaining data, over 30 aircraft-to-radiosonde match-ups were obtained within one hour of the radiosonde launch times. Early assessment results in Figure 9.6.1-right show that the differences between the radiosonde and aircraft data during ascent are very similar to those obtained during 2005, with small biases and SDs on the order of 0.5 g/kg or less throughout the lower half of the troposphere. Data sets can be obtained from:

http://cimss.ssec.wisc.edu/wvssii/

Continuation of efforts to determine the time/space variability of low-level atmospheric moisture

Efforts continue to determine the time/space variability of low-level atmospheric moisture by assessing the temporal characteristics of the AERI data sets using time series analysis and then relating the results to important weather events in the area. Using the results of these optimal time frequency studies, time-to-space conversion techniques will be applied to combine the AERI and Wind Profiler data to determine critical spatial scales. The results will provide currently missing quantitative guidance concerning the optimal spacing and frequency of aircraft data. Due to the expansion of the 2006 WVSS-II field test, some of this work has been rescheduled to next year.

Before the time-to-space conversions can be done, assessments of the accuracy of the 6-minute Wind Profiler data used to transport the moisture away from the observation point are needed. As a first step, data from the ARM-CART site were used to develop a new Quality Control procedure for the data which eliminated 30-40% of the reports, but improved subsequent intercomparisons by about 1 m/s. Temporal variability was them assessed using successive reports from the single Wind Profiler site, while spatial variability was determined by inter-comparing Wind Profiler and contemporaneous radiosonde data. Using this combination of data sets, we were able to: 1) obtain estimates of the Wind Profiler instrument error (~1 m/s), 2) obtain information about the atmospheric variability associated with simultaneous, co-located data, and 3) approximate how that variability increases in both space and time. The study is being completed at multiple layers throughout the troposphere and for both night and day conditions. This information is essential for the next phase of these studies, and for use of the data within mesoscale data assimilation systems. A formal paper will be submitted for publication in 2007.

Publication and Conference Reports

Bedka, S., R. A. Petersen, W. Feltz, and E. Olson, 2006: Evaluation of the WVSS-II Sensor Using Co-located In-situ and Remotely Sensed Observations. ISTP Profiling Conference, Boulder, CO.

Petersen, R. A., 2006: A recommended scheme for reporting encoded mixing ratios from the WVSS-II observing systems. Submitted to NOAA/NWS/OST, Silver Spring, MD.

Petersen, R. A., 2006: Travels with Charlie: An invited paper on the future direction of international aviation meteorology presented at the WMO Commission on Aeronautical Meteorology, Geneva, Switzerland.

Petersen, R. A. and K. Bedka, 2006: Determining the representativeness and accuracy of 6-minute Wind Profiler data. ISTP Profiling Conference, Boulder, CO.

Petersen, R. A. and K. Bedka, 2006: Determining the representativeness and accuracy of six-minute Wind Profiler data. 2nd Thorpex Science Review, Landshut, Germany.

Petersen, R. A., S. Bedka, W. Feltz, and E. Olson, 2006: Evaluation of the WVSS-II Sensor Using Co-located In-situ and Remotely Sensed Observations. An invited paper for the WMO AMDAR Panel Science Workshop, Silver Spring, MD.

Petersen, R. A., W. Feltz, E. Olson and S. Bedka, 2006: Evaluation of the WVSS-II Moisture Sensor using co-located in-situ and remotely sensed observations, AMS Integrated Observing Systems Conference, Atlanta, GA.

Petersen, R. A. and W. Moninger, 2006: Assessing two different commercial aircraft-based sensing systems. AMS Integrated Observing Systems Conference, Atlanta, GA.

Petersen, R. A., W. Feltz, and S. Bedka, 2006: FINAL REPORT - Results of the June 2005 WVSS-II – Rawinsonde Intercomparison Study. Submitted to NOAA/NWS/OST, Silver Spring, MD.

9.7 Passive Microwave Radiance Assimilation of Clouds & Precipitation–Ralf Bennartz and Tom Greenwald

Proposed Work
This is a necessary first step to prepare for the assimilation of observed radiances of current and future passive microwave satellite sensors in the framework of the GFS/GDAS under cloudy and precipitating conditions. The initial task is development and test of appropriate fast forward, tangent linear and adjoint microwave radiative transfer models for clouds and precipitation. A follow-on task is to monitor biases between simulated and satellite observed microwave radiances and the associated adjoint sensitivities for GFS/GDAS.

Summary of Accomplishments
The Successive Order of Interaction (SOI) radiative transfer model for scattering atmospheres has been fully integrated into the Community Radiative Transfer Model (CRTM) and tested by JCSDA. The tangent linear and adjoint model are fully functional, tested, and integrated into the CRTM, as well.

A solar source term has been introduced into the SOI. Currently the SOI is fully functional in the solar spectral range in an azimuthally averaged mode. Azimuthal resolution as well as an adjoint version are planned.

Cloud overlap studies as well as the use of new microphysics parameterizations to represent scattering by ice particles at high microwave frequencies have been finished and resulting publications are in press.

Initial comparison of SOI with the fast 2-layer radiative transfer model used at CIMSS for GOES-R Risk Reduction activities has been performed.

This project ended in June 2006.

Publications and Conference reports
Kim, M.J., M. Kulie, C. O'Dell, and R. Bennartz, 2007: Scattering of ice particles at microwave frequencies: A physically based parameterization. In press Journal of Applied Meteorology and Climatology

O'Dell, C., P. Bauer, R. Bennartz, 2007: A fast cloud overlap parameterization for microwave radiance assimilation. In preparation. In press Journal of Atmospheric Sciences.

Heidinger, A., C. O'Dell, T. Greenwald, and R. Bennartz, 2006: The Successive Order of Interaction Radiative Transfer Model, Part I: Model Development. Journal of Applied Meteorology, 45, 1388-1402.

O'Dell, C., A. Heidinger, T. Greenwald, and R. Bennartz, 2006: The Successive Order of Interaction Radiative Transfer Model, Part II: Model Performance and Applications. Journal of Applied Meteorology, 45, 1403-1413.

Greenwald, T.; Bennartz, R.; O'Dell, C. and Heidinger, A., 2005. Fast computation of microwave radiances for data assimilation using the 'successive order of scattering' method. Journal of Applied Meteorology, Volume 44, Issue 6, 2005, pp.960-966. Call Number: Reprint # 4462.

Bennartz, R., C. O'Dell, T. J. Greenwald, and A. K. Heidinger, 2004: Fast passive microwave radiative transfer in precipitating clouds: Towards direct radiance assimilation. Proceedings of SPIE, Volume 5654, 33-37.

10 NPOESS Studies

10.1 VIIRS Radiance Calibration/Validation, VIIRS/CrIS Cloud Property Investigations, and CrIS/ATMS/GPS Soundings and Visualization: IGS Progress Report – Paul Menzel

Proposed Work
Data and products from MODIS, AIRS, AMSU, CHAMP are being used as proxy for VIIRS, CrIS, ATMS, and Radio Occultation sensor capabilities to test algorithms that will produce the required EDRs. This work reduces risk and assures successful transition from the current polar orbiting operational environmental satellites to the future NPOESS.

Significant Accomplishments and Findings

- Participated in analysis of VIIRS vacuum test data
- Explored AIRS/MODIS intercalibrations and CART site determination of calculated and observed differences in MODIS radiances in preparation for VIIRS post-launch radiance validation
- Demonstrated CrIS cloud profiles alleviating VIIRS night-time cloud problems (using AIRS and MODIS data)
- Drafted paper on combining radio occultation CHAMP data with infrared and microwave AIRS / AMSU data
- Studied sounding retrieval optimization by quantifying sensitivity of AIRS temperature and moisture profile retrievals to CO_2 and O_3 amounts
- Continued development of HYDRA visualization tools for interrogation of multispectral data by adding collocation of MODIS data with AIRS and CALIPSO

Estimating Cloud Amount Profiles with AIRS
The past year was spent refining an algorithm to estimate a cloud amount profile from AIRS spectral measurements. As reported last quarter, a cloud radiative transfer model is used wherein cloud amount and cloud top pressure are adjusted to match calculated with measured radiances for the AIRS spectral bands.

A case study was processed for an AIRS granule over the lidar located in Barrow, Alaska on 17 October 2004 at 22 UTC (see Figures 10.1.1 and 10.1.2). The AIRS found clouds from 5 to 10 km in amount of 10 to 20% at each level; the lidar found clouds from 4 to 10 km. This good

agreement between the AIRS and lidar determinations is encouraging. More case studies are being pursued and MODIS data is being incorporated so that the AIRS 15 km cloud amount profiles can be used as the initial condition where from the cloud top pressure at 1 km resolution is inferred with the MODIS IR channels (4, 11, 12 μm).

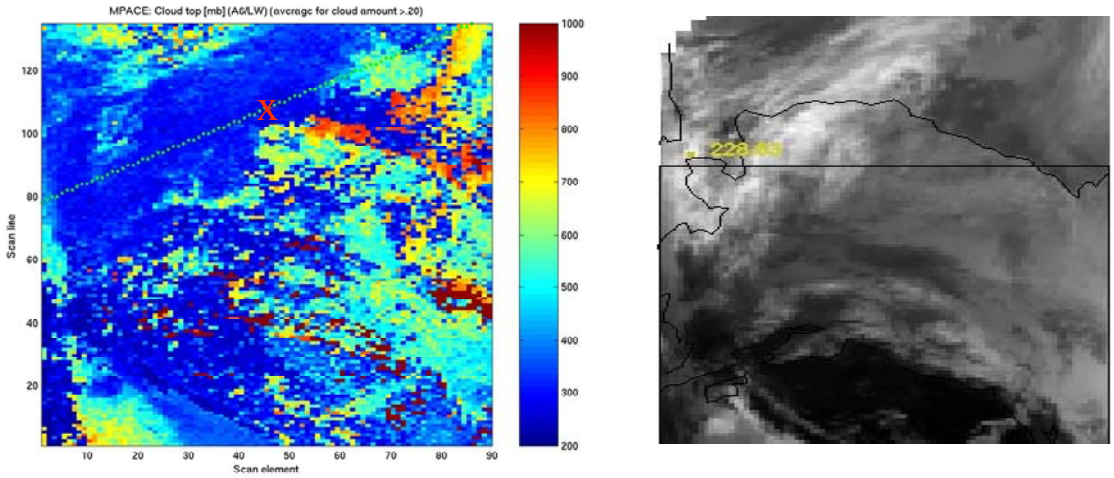

Figure 10.1.1: Average cloud pressure of levels with cloud amount greater than 20% along with direction of prevailing wind at lidar site (red x) indicated by dotted line (left). Image of the AIRS 919 cm-1 granule for 17 October 2004 at 22 UTC.

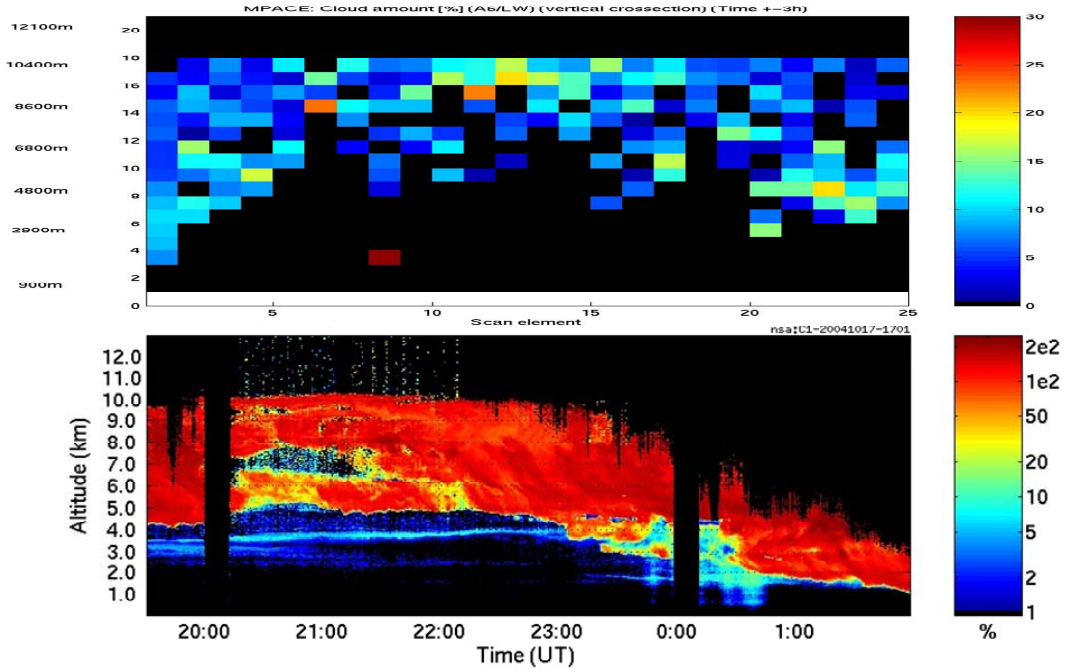

Figure 10.1.2: Transect of cloud amount profile along direction of prevailing wind at lidar site where the time of the cloud overpass at the lidar site is estimated from the wind speed (top). Coincident lidar particulate circular depolarization ratio (bottom).

GPS and Sounders

The set of collocated AIRS/AMSU/GPS/RAOB measurements was extended through December 2005; calculation of regression coefficients taking radiances and refractivities to profiles was accomplished with real rather than simulated data. Thereafter the impact of GPSRO data on AIRS/AMSU retrieval products including the AIRS Science Team level 2 (collection 4) temperature products was studied. A vertical optimal interpolation (OI) was used.

GPS data was found to improve the AIRS/AMSU retrievals by 0.5 K around 250 hPa pressure level. Using the real data regression coefficients produced better quality temperature retrievals around the 200 hPa pressure level and in the lower troposphere (Figure 10.1.3).

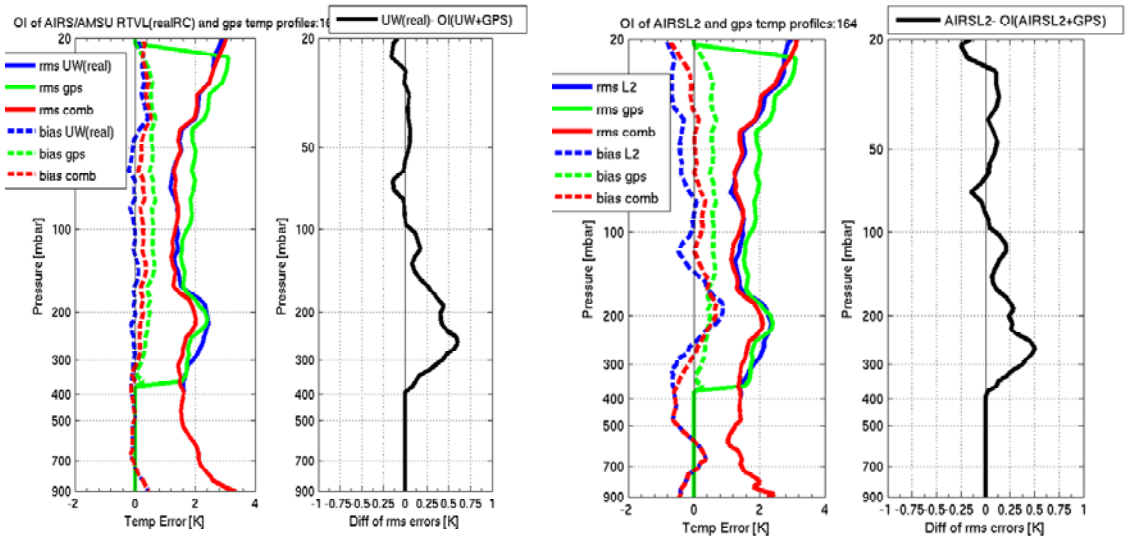

Figure 10.1.3: (left) AIRS/AMSU retrievals (real RC used) improved by GPS data (right) collection 4 AIRS level 2 products by GPS data.

CIMSS also started beta testing the Radio Occultation Processing Package (ROPP) v0.9 for EUMETSAT GRAS SAF. It has modules to handle input / output of the RO data, the associated Forward Model, and the 1DVAR variational assimilation.

Visualization Tools

HYDRA is now able to track the same latitude and longitude on simultaneous AIRS and MODIS data sets. This enables the sub-pixel information available in the MODIS 1 km resolution to influence selection of AIRS pixels for clear or cloudy sky investigations (Figure 10.1.4). HYDRA also added the capability to view CALIPSO backscatter measurements co-located with MODIS multispectral radiance measurements. Figure 10.1.5 shows an example for 24 September 2006 of data taken over Antarctica; the CALIPSO data over the green line in the MODIS granule is shown at high resolution in the lidar viewer (the blue line is co-located with the red dot).

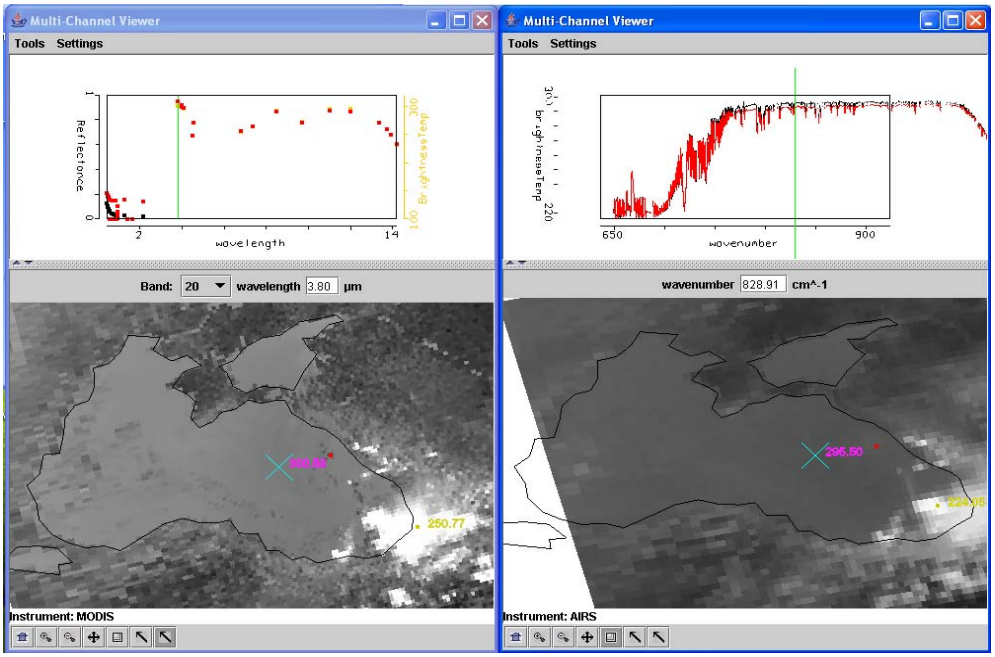

Figure 10.1.4: HYDRA with AIRS (left) and MODIS (right) co-located display of spectra. The MODIS 3.8 micron image is indicating some cloud contamination within the AIRS pixel in the location of the red dot; the red spectra (over the red dot) is cooler than the black clear sky spectra (over the cross).

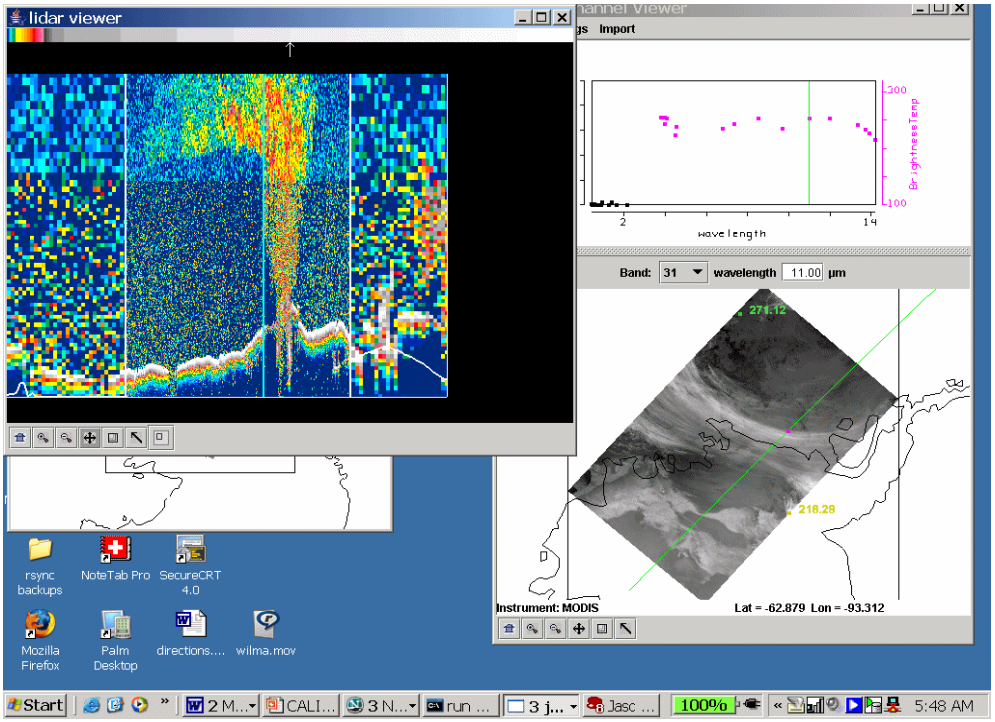

Figure 10.1.5: HYDRA display of CALIPSO attenuated backscatter (at 532 nm) and Aqua MODIS infrared window image for 24 September 2006.

Conferences and Papers
Rink et al paper on "HYDRA – a Multispectral Data Analysis Toolkit." was published in the February 2007 issue of the *Bull Amer Meteor Soc*. It introduces the multi-spectral data analysis toolkit, describes the various functions, and presents several examples with MODIS and AIRS data. HYDRA is now being used by several US and international scientists to analyze MODIS and AIRS data and to help prepare for IASI data analysis.

E. Borbas attended the GPS session at the annual European Geophysical Union (EGU) meeting in Vienna, Austria in late March 2006 and presented the GPS plus AIRS/AMSU results.

Paul Menzel and Paolo Antonelli taught week-long remote sensing courses in Krakow, Poland in May and Ostuni, Italy in June that included group projects that culminated in student presentations on their MODIS and AIRS investigations (accomplished with HYDRA). Twenty students attended each of the courses. The students demonstrated good comprehension of the material presented and started research projects that will continue.

Borbas, E.E., W. P. Menzel, and E. Weisz paper on "Deriving atmospheric temperature of the tropopause region/upper troposphere by combining information from GPS radio occultation refractivity and high spectral resolution infrared radiance measurements" was submitted to *Jour Appl Meteor and Clim* in January 2007.

10.2 Cloud Environmental Data Records – Andy Heidinger, Michael Pavolonis and Richard Frey

Proposed Effort
The main effort and outcome of this proposal is to work with the IPO, NGST, and NPP to improve the VIIRS Cloud Environmental Data Records (EDRs) using our experience with the heritage products from the current NOAA operational imagers. To date, we have been successful in collaborating with NGST on the VIIRS cloud mask and cloud type algorithms. In terms of the VIIRS cloud mask, we helped NGST correct errors and implement new tests aimed at improving the SST performance. For the VIIRS cloud type, we have suggested algorithm improvements that mitigate errors noted by NGST in the baseline algorithm. In addition, we plan to expand this direct collaboration into other cloud EDR algorithms.

The secondary goal of this study is to start processing global MODIS data through VIIRS algorithms. This capability would complement NGST's approach of using simulated data for testing and verification. By processing MODIS data through VIIRS algorithms globally, we can use our traditional validation approaches to expose weakness in VIIRS algorithms that might go unnoticed until after launch. In addition, we plan to run modified algorithms in parallel with the VIIRS baseline algorithms and demonstrate improvements for future algorithm updates.

Lastly, this study allows for the support of VOAT/IPO analyses that arise, as NGST or the IPO require assistance in defining new specifications or modifying EDR algorithms. The investigator of this project currently serves as the chair of the VIIRS operational algorithm team (VOAT).

Summary of Accomplishments and Findings
The University of Wisconsin VIIRS cloud group participated in several code comparisons between the operational MODIS cloud mask (Collection 5) and the VIIRS cloud mask (VCM). In particular, we identified one logic path in the VIIRS snow detection algorithm that does not

exist in the MODIS code, along with a logic error that led to spurious results when using ancillary snow cover inputs. Also identified were differences in threshold values that define boundaries separating the four clear-sky confidence categories (confident clear, probably clear, probably cloudy, confident cloudy) output by the two algorithms. The two sets of values remain to be rectified.

VIIRS cloud properties retrieved from measurements in the 8 – 12 micron infrared window will be sensitive to the parameterization of surface emissivity, especially over land surfaces where surface emissivity can be highly variable across small spatial scales. In addition, the surface emissivity can vary significantly from channel to channel in the 8 - 12 micron window. The infrared cloud property retrievals require that the clear sky radiance for each cloudy pixel be available. The current VIIRS methodology obtains the clear sky radiance via interpolation from surrounding pixels that were determined to be clear. This clear sky radiance estimation technique works best over the open ocean when clear sky measurements lie in close proximity to the cloudy pixels. Over land, surface properties (emissivity, skin temperature) can be highly variable, so interpolation across larger distances will be prone to larger errors. Even over the ocean, the clear sky radiance estimation may be very poor when the interpolation technique is applied in very cloudy regions. An alternative methodology to obtain clear sky radiances is to use numerical weather prediction (NWP) model temperature, moisture, and ozone profiles and a fast radiative transfer model to calculate clear sky radiances for each satellite pixel. While this methodology is computationally fast, one drawback has always been the lack of quality information on surface emissivity. However, a new global high spatial and spectral resolution surface emissivity database (Seemann et al., 2006) is now available, which makes this method for obtaining clear sky radiances much more attractive. We believe that the VIIRS infrared retrievals would benefit from an improved characterization of the clear sky radiances that is not dependent on the actual presence of clear sky measurements. Figure 10.2.1 illustrates the impact of using the Seemann et al. surface emissivity database. In this example, atmospherically corrected radiance parameters at 8.5, 11, and 12 microns (derived in part from calculated clear sky radiances) were used to detect and characterize different types of high clouds, indicated by the yellow, red, and orange colors. The scene encompasses the Sahara Desert, where surface emissivity is highly variable both spatially (see Figure 10.2.1) and spectrally. When the surface emissivity database is used, as opposed to using a constant surface emissivity, the sensitivity to optically thinner high clouds is greatly increased, indicative of a more accurate clear sky radiance calculation. The VIIRS infrared cloud property retrievals would be more robust if this sort of methodology for determining the clear sky radiance was adopted. In the future, we will show the direct impact of the NWP/fast model methodology on retrievals of cloud height, optical depth, and particle size.

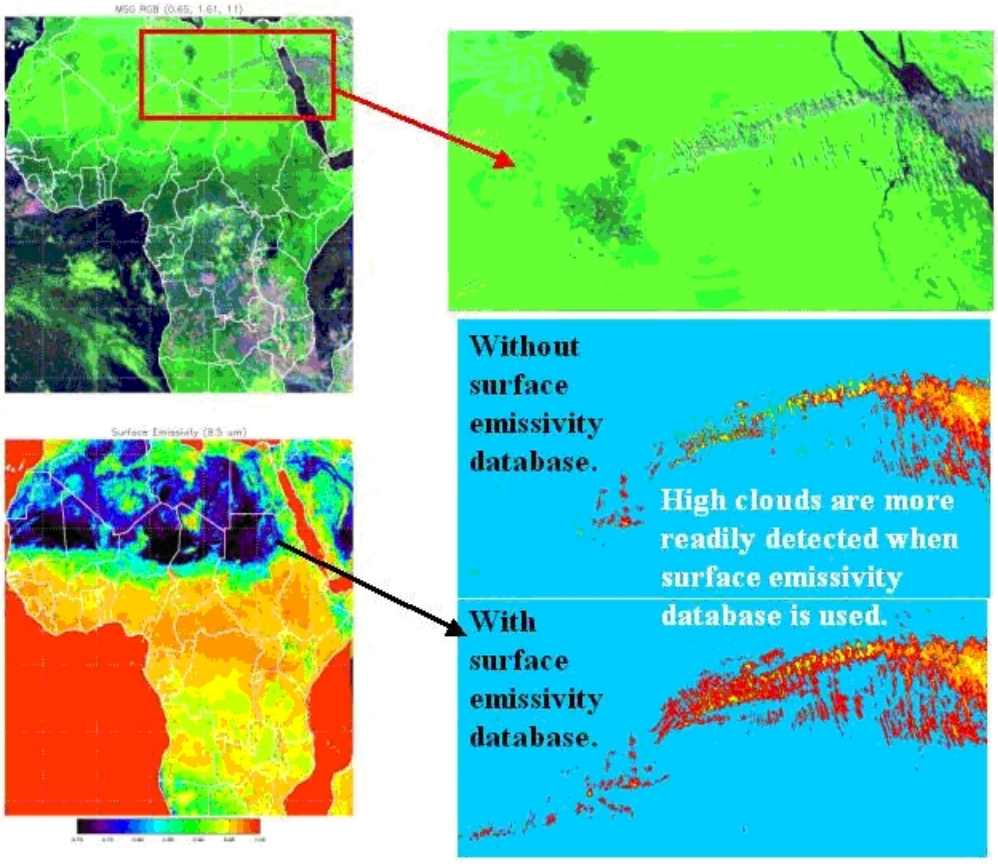

Figure 10.2.1: An illustration of the impact of using the Seemen et al. surface emissivity database on cloud property retrievals over the African continent. The yellow, red, and orange colors in the bottom/right panels indicate different classes of high cloud. The sensitivity to optically thinner high clouds is increased when the surface emissivity database is used in the clear sky radiance calculations. The VIIRS infrared cloud property retrievals would benefit from an improved determination of the clear sky radiance such as shown here.

Publications/Presentations

Heidinger, Andrew; Baum, B. A. and Yang, P.. Consistency of cloud ice properties estimated from MODIS, AVHRR and SEVIRI. Conference on Atmospheric Radiation, 12th, and Conference on Cloud Physics, 12th, Madison, WI, 9-14 July 2006.

Hutchison, Keith; Lisager, B.; Jackson, J. M.; Roskovensky, J. K.; Heidinger, A. K.; Pavolonis, M. J.; Kopp, T. J. and Frey, R. A.. The VIIRS cloud mask. Symposium on Future National Operational Environmental Satellites, 3rd, San Antonio, TX, 14-18 January 2007 (preprints)

10.3 Validating Snow and Ice Products in Polar Regions – Jeff Key and William Straka

Background

The goal of this project is to generate snow and ice products in an operational environment at direct broadcast (DB) sites in the Arctic and Antarctic, and to provide automatic validation of these products. Snow/ice and cloud products are being generated with contractor code (Northrop

Grumman Space Technology, NGST) and our own algorithms, then validated with surface measurements and other data sets, when and where available, in real-time. MODIS data is being used as a proxy for VIIRS data. Products of interest include ice/snow surface temperature, ice/snow albedo, sea ice age, sea ice motion, snow and ice cover, cloud mask, cloud pressure, and cloud particle phase. Additionally, other high-latitude products that may eventually become VIIRS Environmental Data Records (EDRs) will be generated and validated, most notably polar winds. The proposed system builds on a DB product generation system and product suite already in place and running at McMurdo, Antarctica and at Tromsø, Norway. The work includes the generation of VIIRS EDRs, using the contractor code, and compares it to an established algorithm. The benefits of using real-time direct broadcast data are that (1) it provides for an unlimited number of validation cases, as opposed to the more common situation where only a few ideal test cases are used, (2) it provides a truly operational environment, and (3) it prepares us for future DB implementations of NPP and NPOESS products.

Accomplishments

The core parts of each EDR operational code set are used in our direct broadcast processing system, which operates on MODIS Level 1b data. The ice surface temperature (IST) operational code is currently running at Tromsø, Norway (since May 2006) and McMurdo, Antarctica (IST only; since June 2006). Additionally, the snow cover code is running at Tromsø. The two VIIRS IST algorithms are being compared to each other as well as comparing them to the IST algorithm that was being generated at the sites previously (Key et al., 1997). Less than 0.5% of the pixels in the 1-channel VIIRS IST algorithm have a larger than 2 degree difference when compared the two 2-channel algorithms (VIIRS 2 channel and Key et al., 1997). The areas and magnitudes of the differences between the 2-channel and 1-channel algorithms are similar. Studies to determine the nature of the differences are underway.

In addition to inter-comparing the various algorithms, we are also comparing the satellite-derived ice surface temperatures to surface observations. We are looking at established WMO surface sites as well as other observational systems, particularly the Automatic Weather Stations (AWS) across Antarctica. The AWSs are maintained by the SSEC Antarctic Meteorological Research Center and their international partners. There are six sites in the Arctic (all WMO sites) and nine sites in Antarctica that are currently being used in the validation study. More sites may be added in the future as data becomes available. Daily analysis, statistics and histograms are being produced in real-time for evaluation of the various algorithms. In addition, a 10-day time series of the differences is generated. An example of a histogram showing the difference between the VIIRS 2-channel algorithm and the surface site at Eagle, Antarctica (since day 274 of 2006) as well as the 10-day time series using data collected from Terra are shown in Figure 10.3.1.

Options for validation of the snow mask are being explored. One of these includes the MODIS snow/ice processing flag. The snow/ice binary mask code will be implemented in McMurdo in the near future.

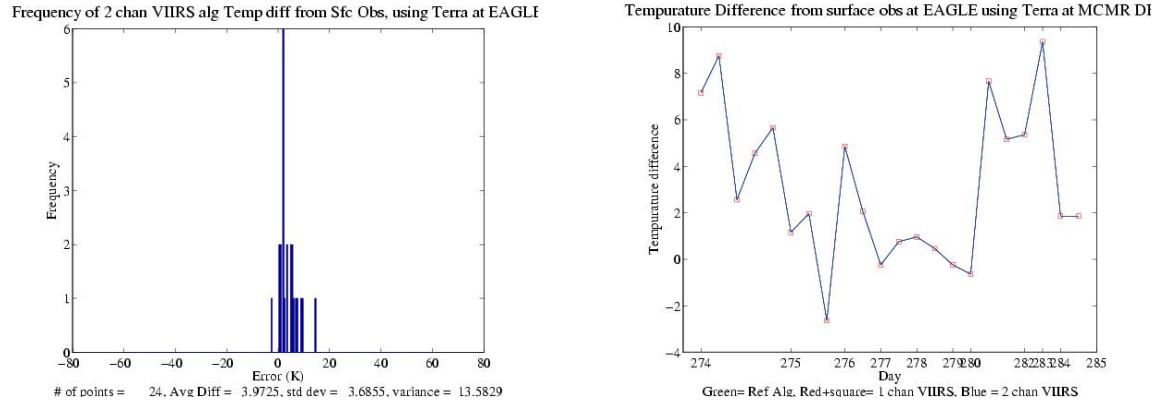

Figure 10.3.1: Histogram of the differences between the VIIRS 2-channel IST algorithm and the temperature measured at the surface at Eagle, Antarctica (left) and a 10-day time series of the differences (right).

Publications

Liu, Y., J. Key, R. Frey, S. Ackerman, and W.P. Menzel, 2004, Nighttime polar cloud detection with MODIS, *J. Appl. Meteorol*., 92, 181-194.

Hall, D.K., J. Key, K.A. Casey, G.A. Riggs, and D.J. Cavalieri, 2004, Sea ice surface temperature product from the Moderate Resolution Imaging Spectroradiometer (MODIS), *IEEE Trans. Geosci. Remote Sensing*, 42(5), 1076-1087.

11 VISIT Participation –Scott Bachmeier, Tom Whittaker, and Scott Lindstrom

Proposed Work

We proposed to continue exploring methods to improve techniques for effective distance learning activities that are part of the Virtual Institute for Satellite Integration Training (VISIT) program.

Summary of Accomplishments and Findings

During the January-December 2006 period, two updates to the VISITview software were made to enable the use of "animated GIF" images, and to provide the framework for eventually adding support for other "multimedia" file formats. Code was also added to broaden support for showing HyperText Markup Language (HTML) formatted text to supplement lessons. In addition, the version of the Java Runtime Environment distributed with VISITview was updated to a more recent release.

During October, we provided technical support for the World Meteorological Organization (WMO) two-week High Profile Training Event (HPTE). The HPTE used VISITview to provide "live" interactive collaboration and training sessions between a number of centers around the world, involving more than 100 WMO member countries and more than 4,000 participants.

In December, an invited presentation was made at Brazil's Congresso Brasileiro Meteorologia (CBMET) general assembly, and a two-hour workshop was given to more than 30 participants from mostly Brazil and Argentina to walk through the process of developing VISITview-based lessons.

The capability of utilizing operational real-time Advanced Weather Information Processing System (AWIPS) workstations at CIMSS was fully realized in 2006. This new resource greatly enhances the process of VISIT lesson content creation by allowing immediate access to a diverse array of meteorological data from current weather events, in an AWIPS format that is familiar to National Weather Service (NWS) forecasters. We also facilitated the transfer of MODerate-resolution Imaging Spectroradiometer (MODIS) imagery and CIMSS Regional Assimilation System (CRAS) model forecast products into the AWIPS Operational Build 7 which is running here at CIMSS.

Two new VISITview lessons were completed during the period: the "CRAS Forecast Imagery in AWIPS" (developed in collaboration with Bob Aune of NOAA/NESDIS/STAR) and the "MODIS Products in AWIPS" instructional modules describe (a) the CRAS model-derived IR window channel and water vapor channel forecast imagery, and (b) the polar-orbiting MODIS satellite imagery and products that are now being distributed to the National Weather Service Central and Southern Region AWIPS servers on an experimental "demonstration mode" basis. These two lessons provide a variety of AWIPS examples that highlight the unique operational utility of these new model and satellite products.

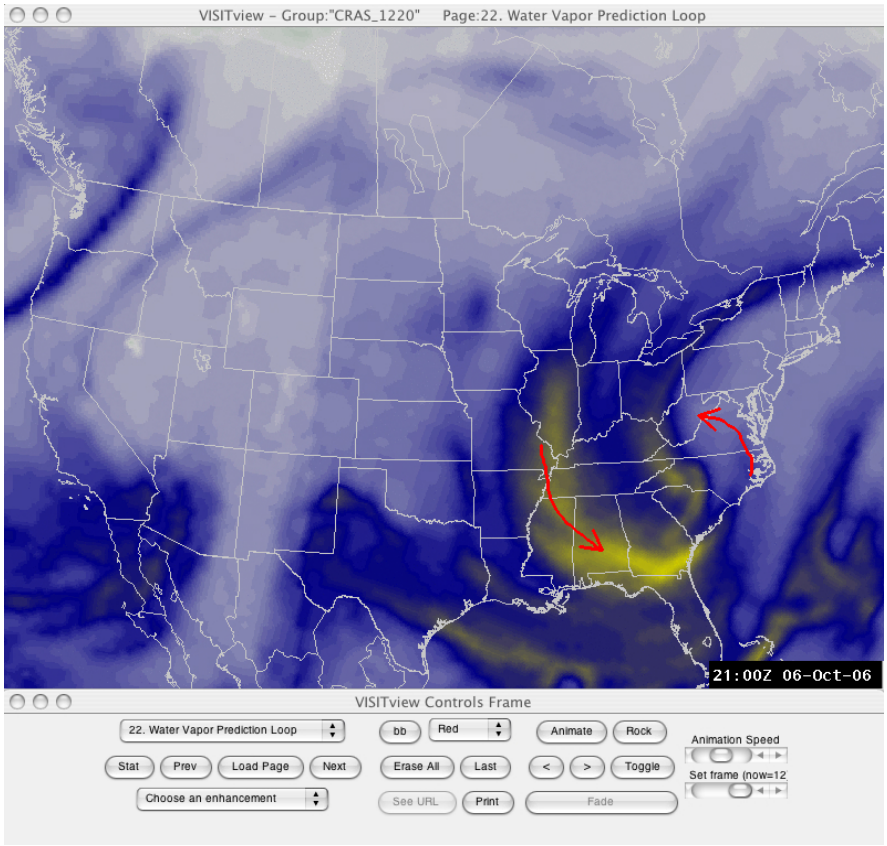

Figure 11.1: Screen capture from the "CRAS Forecast Imagery in AWIPS" VISITview lesson, showing an example of the model-generated water vapor channel synthetic satellite imagery.

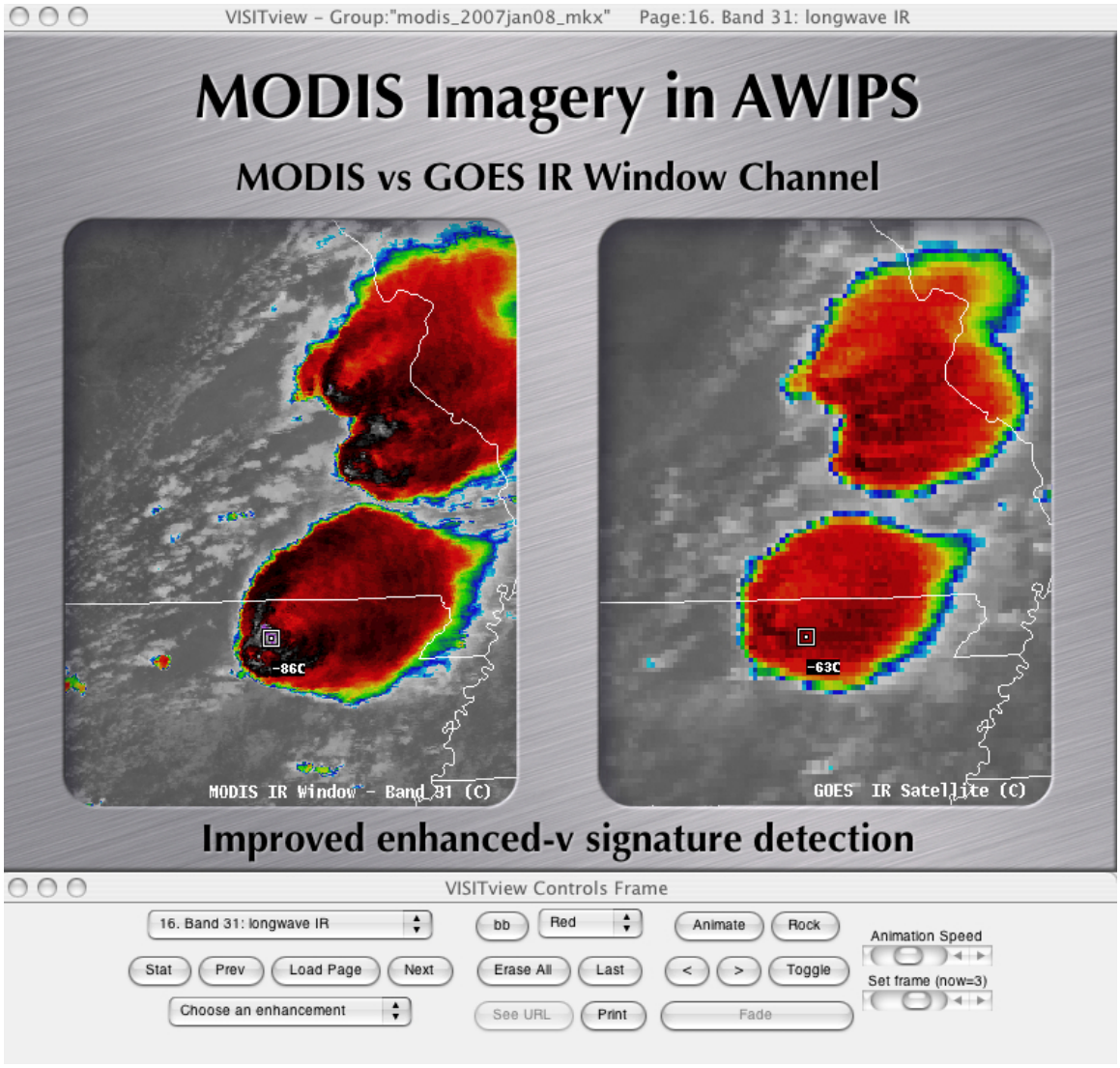

Figure 11.2: Screen capture from the "MODIS Products in AWIPS" VISITview lesson, showing improved enhanced-v signature detection using the 1-km resolution IR channel on MODIS (compared to the 4-km resolution IR channel on GOES).

Work also continued to update existing versions of the "TROWAL Identification", "Mesoscale Convective Vortices", "Water Vapor Channel Satellite Imagery", "GOES High Density Winds", "The Enhanced-V Signature: A Satellite Indicator of Severe Weather", and "GOES Sounder Data and Products" VISITview lessons, adding new examples gathered using the real-time AWIPS workstations at CIMSS. The ongoing process of periodically revising these existing instructional modules with new content helps to keep the material relevant and follow the pace of today's changing learning objectives. During calendar year 2006, CIMSS instructors presented 35 separate VISITview sessions (presenting both the existing and new VISITview lessons), reaching a total of 113 NWS forecast offices.

Finally, work continued on the development of follow-up water vapor channel satellite imagery lessons which cover more advanced applications to weather analysis and forecasting. The first in this particular series of instructional modules is "Water Vapor Imagery and Potential Vorticity

Analysis", which we plan to complete and add to the VISIT training calendar during the first quarter of 2007. This new VISITview lesson will discuss advanced water vapor imagery interpretation and the validation of numerical weather prediction output by utilizing the close relationship between water vapor channel radiances and model potential vorticity fields.

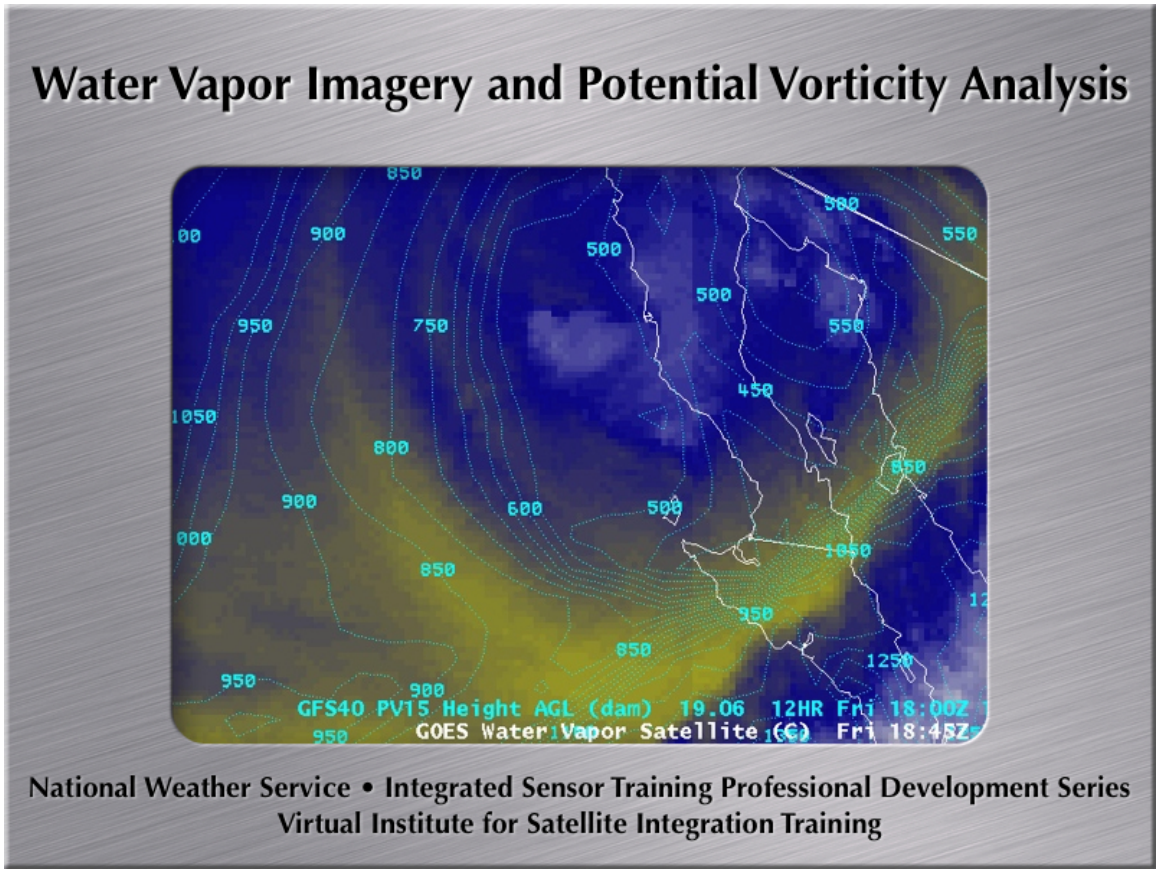

Figure 11.3: Screen capture of the title slide for the new "Water Vapor Imagery and Potential Vorticity Analysis" VISITview lesson, which was in the development phase and will soon be completed.

12 SHyMet – Steve Ackerman, Scott Bachmeier

Proposed Work

The role of CIMSS in SHyMet is to 1) provide advice on the educational design of the program, 2) assist in the development of the curriculum, 3) support distance education activities, 4) develop and test appropriate satellite education materials, and 5) assist in the teaching of the courses as appropriate.

Summary of Accomplishments and Findings

For the inaugural SHyMet Intern Course (April-June 2006), content was developed for the training topics "GOES Sounder Data and Products" and "GOES High Density Winds". The "GOES Sounder Data and Products" lesson provides an introduction to the data and products available from the latest generation of GOES Sounder instruments, along with examples of sounder Derived Product Imagery (DPI) and their applications to weather analysis and

forecasting. Special attention is given to the recent change to Single Field of View (SFOV) sounder DPI in AWIPS. The "GOES High Density Winds" lesson reviews techniques for measuring satellite winds (atmospheric motion vectors), and provides details on the display of GOES high density winds on AWIPS. These distance learning courses were developed and delivered using the VISITview software. Each of these two SHyMet lessons were offered a total of 8 times, with 38 NWS interns attending the Sounder lesson and 27 interns attending the Satellite Winds lesson during the 3 month period.

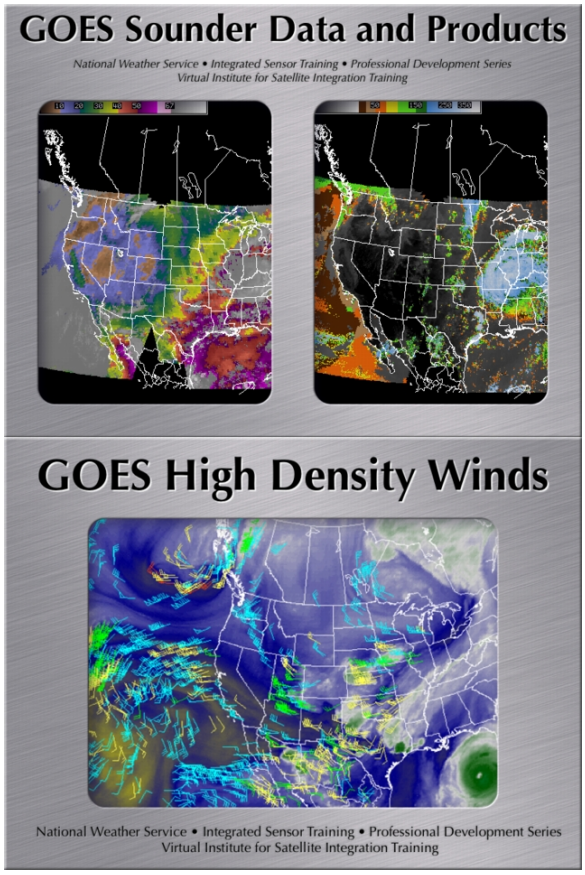

Figure 12.1: Title slides from the "GOES Sounder Data and Products" and "GOES High Density Winds" VISITview lessons delivered as part of SHyMet. Each of these two ShyMet lessons were offered a total of 8 times, with 38 NWS interns attending the Sounder lesson and 27 interns attending the Satellite Winds lesson during the 3 month period.

13 Advanced Dvorak Technique – Timothy Olander

Proposed Work

The latest McIDAS version of the ADT was to be released to the NOAA/NESDIS Satellite Analysis Branch (SAB) prior to the start of the 2006 North Atlantic tropical cyclone (TC) season. Once the ADT was successfully installed at SAB, the algorithm performance would be evaluated during the TC season by SAB forecasters. Comments and evaluations regarding the ADT performance would be provided as necessary, with certain ADT algorithm modifications being immediately integrated and evaluated to alleviate any major performance issues. Following the 2006 TC season, any remaining issues would be discussed with SAB forecasters and solutions

integrated into the ADT algorithm. Thorough testing would be performed to evaluate the impact of all algorithm modifications upon ADT performance.

Summary of Accomplishments and Findings

The ADT version 7.1 was released to SAB on 20 April 2006. This version contained several new advancements of the technique. Performance of the ADT was monitored by the SAB forecasters during the 2006 Atlantic TC season, with several issues brought to the attention of the CIMSS scientists. Many of these issues were minor and fixed/implemented immediately for the next ADT release. An intensity overestimate bias was also noted when compared with the estimates obtained by the SAB forecasters using the more subjective Dvorak Technique. Based on these findings and recommendations, a new statistical analysis was performed using the original CIMSS ADT training sample adding the 2006 data sample. The bias was eliminated from the 2006 cases with minor impact on the original training sample.

An official benchmark report on the 2006 ADT performance was not obtained by CIMSS from SAB. However, continuous discussions during the 2006 TC season between the two parties proved to be a sufficient proxy for an official document.

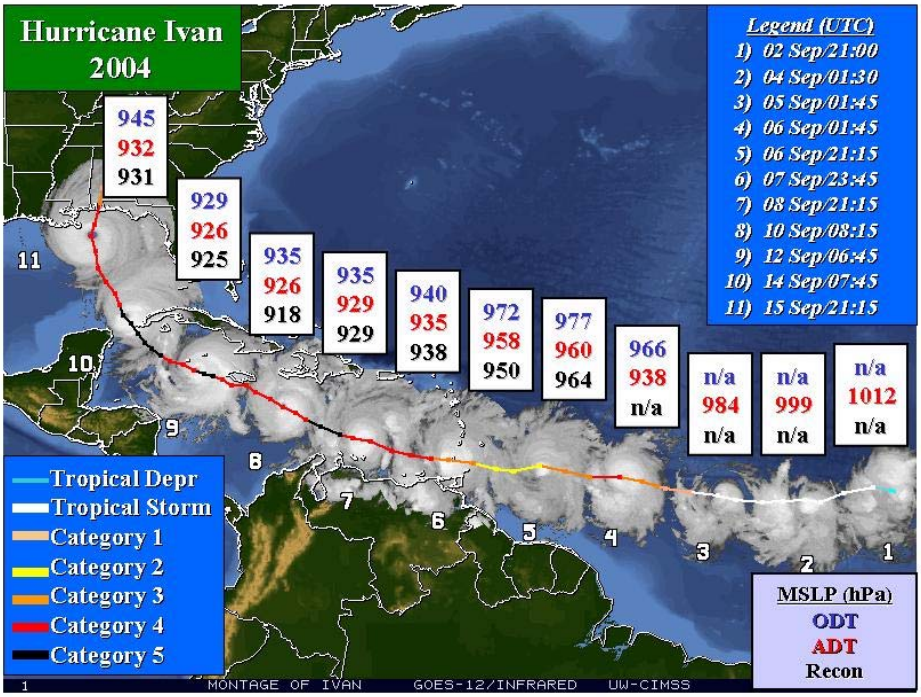

Figure 13.1: Satellite montage image of Atlantic Hurricane Ivan (2004) with ADT and ODT intensity estimates of MSLP versus aircraft reconnaissance measurements (in hPa).

Publications and Conference Reports

A poster presentation outlining the ADT version 7.1 was shown at the 27th AMS Conference on Hurricanes and Tropical Meteorology in Mobile, AL.

The journal article titled "The Advanced Dvorak Technique (ADT) – Continued Development of an Objective Scheme to Estimate Tropical Cyclone Intensity using Geostationary Infrared

Satellite Imagery" (Olander and Velden) was accepted for publication in the American Meteorological Society (AMS) journal "Weather and Forecasting".

14 Understanding Marine Bio-Physical Feedback in the Coupled Ocean-Atmosphere System using Ocean Color Remote Sensing Information – Zhengyu Liu

Proposal Goals and Accomplishments

This is a systematic study of the potential marine bio-physical feedback in a fully coupled ocean-atmosphere model. The solar penetration depth field derived from the ocean color remote sensing will be implemented into the ocean component of the Fast Ocean Atmosphere Model. The effect of the observed attenuation field on the sea surface temperature and thermocline temperature will be examined with various sensitivity experiments. We will examine the effect of the solar penetration depth on the annual mean, seasonal cycle, interannual ENSO variability, interdecadal Pacific Decadal Oscillation and the long term climatology. This work will be important for the assessment of the utility of ocean color remote sensing observation for the understanding of the biophysical feedback of the marine ecosystem on global ocean and climate.

Annual mean SST

As a first test and for future understanding of the mechanism, we performed a 100-year simulation with a uniform solar penetration depth of 17-m over the world ocean. The result shows a substantial impact on global SST (Figure 14.1). The most dramatic result is a substantial improvement of the equatorial cold tongue/warm pool in both the Pacific and Atlantic. Coupled models so far all suffer from a common serious problem in its equatorial climate, the cold tongue penetrates westward too far, substantially suppressing the warm pool. As a result, the warm pool in our model is about 2oC colder than in the observation. The inclusion of solar penetration improves precisely the warm pool the most, offering a promise for the improvement of coupled climate model. To our knowledge, this result has not been reported in fully coupled model so far. In addition, the equatorial annual cycle is also improved substantially, as reported by Schneider and Zhu. Finally, there is a substantial change of the SST in the extratropics, cooling in the subtropical gyre and warming in the subpolar gyre, a result that has not been reported so far.

To understand the mechanism of the SST change, we further added two members to form a three member ensemble experiment. The study of the ensemble experiment suggest that the SST change is robust. Physically, the loss of solar penetration to the subsurface induces a cooling on the surface and a warming in the subsurface, initially. In several months, the SST, however, is overwhelmed by the upwelling of subsurface warming anomaly in the regions of the equator and subpolar gyre. In the subtropics, however, the downward subduction does not affect the SST change, leaving it as cold as in its initial development. According to this mechanism, we speculate that a further deepening of the solar penetration depth should induce a similar SST change. This speculation is confirmed by an additional simulation with a double solar penetration depth (2*17m=34-m), which produces a SST change from the 17-m penetration depth run almost the same as the difference between the 17-m run and the base run.

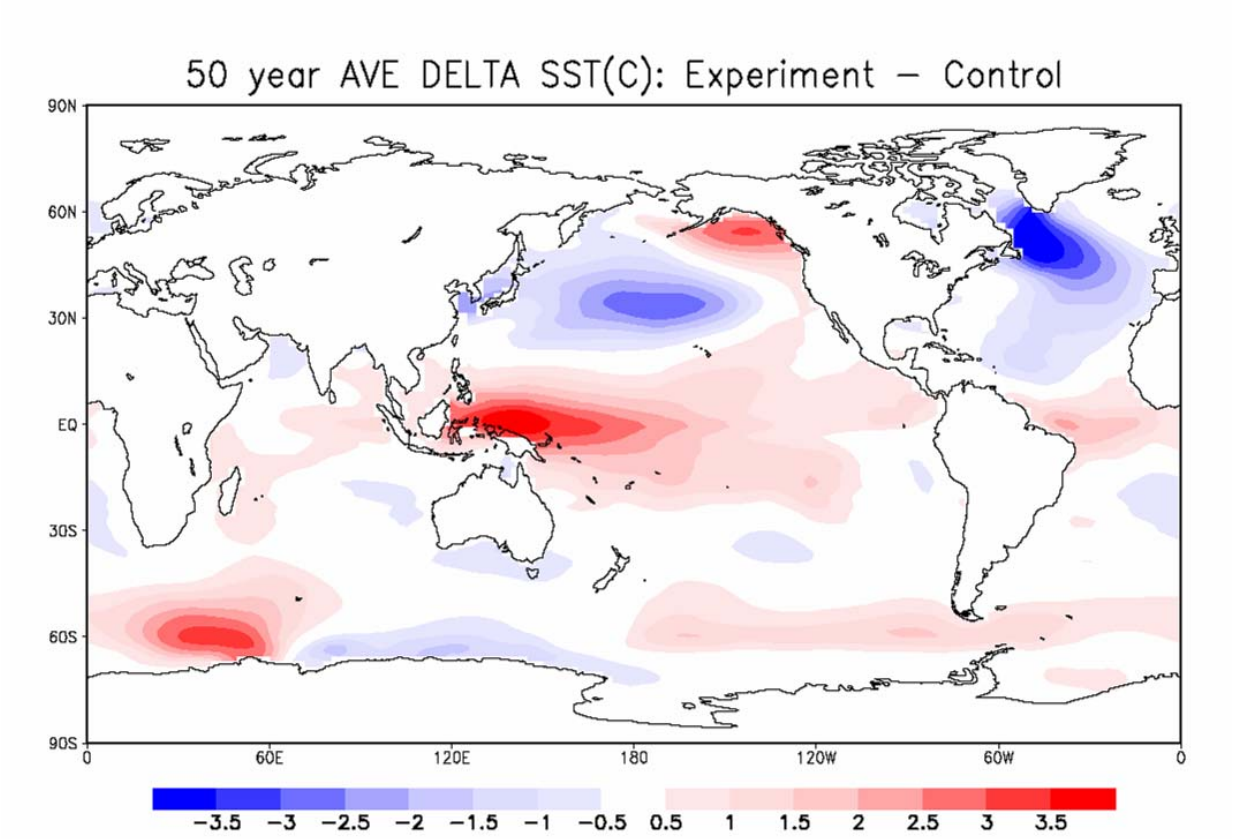

Figure 14.1: SST difference between the simulation with a uniform 17-m solar penetration depth and the simulation without solar penetration.

We have completed a series of experiments with different solar penetration depth, idealized and observed, to study the sensitivity of the coupled model response to solar penetration. The experiments completed and in progress are:

a) penetration 17-m (400 years)
b) penetration 34-m (400 years)
c) SeaWifs observed penetration depth (annual mean): 150 years
d) SeaWifs observed penetration depth (annual cycle): 150 years.

All the simulation suggest that the solar penetration improves the equatorial annual mean SST, with the westward penetration of the equatorial cold tongue reduced dramatically. In this phase, we further examined the annual cycle of the SST and found that the inclusion of solar penetration improves the equatorial annual cycle dramatically. (see discussion on Figure 14.2 below). We also started examining the impact of the penetration depth on interannual variability, especially ENSO (see discussion on Figure 14.3 below).

Annual Cycle

The improvement of the equatorial annual cycle can be seen clearly in Figure 14.2, which shows the time-longitude plot of the equatorial SST along the equator. In the case without solar penetration (middle panel), the SST exhibits a strong semi-annual cycle, as in most other coupled models. There are two strong cooling in February and October, in contrast to the observation

which has the warming in March and cooling in October. With the SeaWifs annual cycle of solar penetration, the equatorial annual cycle shows precisely a warming in March and cooling in October (left panel), virtually the same as the observed annual cycle. Further analysis of other runs suggest that this improvement of the annual cycle also appears in other runs with fixed annual mean solar penetration depth. One example is seen in the lower-left panel of Figure 14.3, which is the case of a fixed 17-m penetration. Therefore, the phase of the correct annual cycle is not caused by that of the penetration. Instead, it is the change of the annual mean solar penetration that produces this change of the annual cycle. The process that improves the annual cycle will be a major task to be studied in the future. One hypothesis is that the improved annual mean state improves the equatorial asymmetry of the mean state, which then will favor southern hemisphere annual cycle signal to penetrate into the equator, providing the correct phasing. We need to further examine this hypothesis.

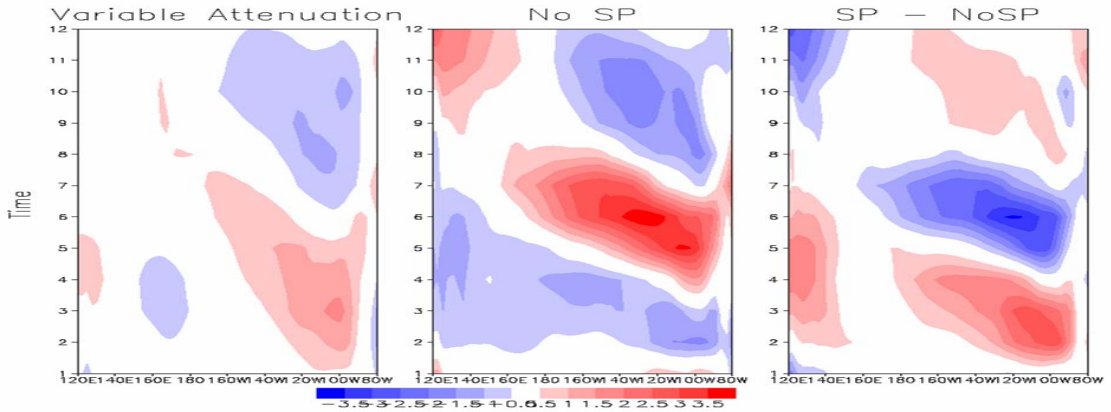

Figure 14.2: Time-longitude plot of equatorial SST annual cycle in the case of the observed annual cycle of SeaWifs solar penetration depth (left), no solar penetration (middle) and the difference.

ENSO variability

We further explored the impact of solar penetration on ENSO. Figure 14.3 shows the interannual time series of monthly SST anomaly in the eastern equatorial Pacific (upper panel). A visual comparison of the case with 17-m penetration depth (solid) and the case without solar penetration (dash) shows a stronger ENSO in the case with solar penetration. Furthermore, the ENSO variability seems to be more regular. This can be seen more clearly in the power spectrum of the penetration case (lower-middle) and no-penetration case (lower-right). The quasi-3-year peak stands out much more clearly in the case with penetration. It remains to be seen if the change of ENSO is systematic in these sensitivity experiments. Furthermore, it remains to be studied if the change of ENSO is due to the change of the annual mean state or the annual cycle of the state. It also remains to be studied if the phase-locking of ENSO is also improved with solar penetration.

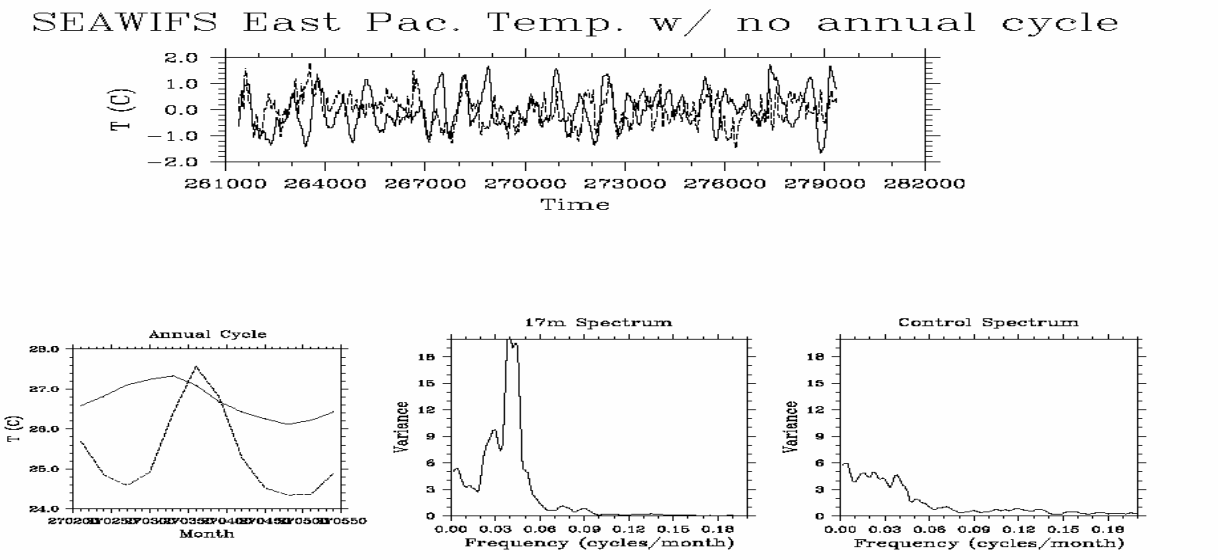

Figure 14.3: (Top) Time series of interannual SST anomaly in the eastern equatorial Pacific for the case without solar penetration (dash) and with a 17-m solar penetration (solid). The power spectrum for the case with solar penetration and without solar penetration are shown in the lower middle and lower right panel, respectively. The annual cycle of the penetration run (solid) and no penetration run (dash) are also shown in the lower left panel.

Publications

Liu, Z., E. Hokanson, L. Wu and P. Behling, 2006: The effect of oceanic solar penetration on the simulation of coupled climatology and seasonal cycle. In preparation.

Hokanson, E., 2005: Solar penetration and coupled ocean-atmosphere system. M.S. thesis, Dept. Atmos. Oceanic Sci.

Hokanson, E., 2005: Solar penetration and coupled climate system. June, 2005, Presentation at the DOE climate workshop at Argonne National Lab.

15 Polar Winds from Satellite Imagers and Sounders – Jeff Key

Project Goals

The primary objective of this project is to develop a satellite-based, tropospheric wind product covering both polar regions using a combination of instruments. At CIMSS we are continuing the development of the MODIS cloud-drift and water vapor winds product, working with our co-investigators at Rutgers University, NESDS/ORA, and Colorado State University on variational thermal wind estimation methods for use with ATOVS and AMSU, combining the imager and sounder winds for a vertically and horizontally complete, satellite-based polar wind observation system, extending the polar winds record back in time approximately 20 years using the AVHRR and TOVS instruments, and working closely with the NASA Global Modeling and Assimilation Office, as well as the Joint Center for Satellite Data Assimilation (JCSDA) to improve the use of the satellite-derived polar winds in numerical weather prediction (NWP) models. We are quantifying the impact of including the polar winds in numerical weather forecast systems, and seeking to understand why the polar winds have the impact that they do. The combined polar winds product will be a very important tool for investigating the robustness of the assimilation

system through an examination of differences in satellite-derived and modeled temperature and wind fields.

The project is funded by the NASA Earth Observing System (EOS) program through NESDIS (J. Key, PI).

Accomplishments
During the past year the following was accomplished:

- MODIS polar winds continue to be produced in real-time with a 3-5 hour delay. They are used operationally by 10 numerical weather prediction (NWP) centers in six countries. MeteoFrance and the National Center for Atmospheric Research (NCAR) began assimilating the MODIS winds in their operational forecast systems during the past year.
- Model output from several different experiments were investigated to determine possible mechanisms that propagate the polar wind information into mid- and low-latitudes. This is the focus of D. Santek's dissertation research.
- A system to generate MODIS winds with direct broadcast (DB) data was developed and implemented at Tromsø, Norway, to complement the existing system implemented last year at McMurdo, Antarctica. The U.S. Navy and the UK Met Office have begun operational use of the DB winds.
- Comparisons were performed between TOVS, AVHRR, and ERA-40 winds. Results are very encouraging and indicate that a combined TOVS/AVHRR product will provide an accurate, detailed wind product for the Arctic region.
- Two of the investigators (Velden and Key) took part in the 8th International Winds Workshop held in Beijing, April 2006.
- Historical AVHRR winds have been generated for a 21-year period (with additional funding from STAR).

The direct broadcast (DB) winds are becoming increasingly important. Generally, the final MODIS polar wind product lags the observing time (the time MODIS views an area) by about 3-5 hours. The lag is largely due to the delay in the availability of the level 1B MODIS data from the NASA Goddard Space Flight Center via a NOAA computer system (the NOAA "bent pipe"). The 3-5 hour delay in the availability of wind information is too long for many regional or limited area data assimilation systems. (This includes a somewhat artificial delay of 100 minutes because a triplet of three consecutive orbits is used, and the final wind vector time is assigned that of the middle orbit.) In 2005, a system was developed to generate the MODIS winds with direct broadcast MODIS data in order to reduce the overall processing time. The system has been implemented the system at McMurdo, Antarctica, and Tromsø, Norway. All processing is done on site. In mid-March, 2006, the Fleet Numerical Meteorology and Oceanography Center (FNMOC, U.S. Navy) began operational use of the MODIS winds that are generated on-site in McMurdo. In mid-April, FNMOC began operational use of MODIS winds generated on-site in Tromsø, Norway. Recently, the UK MetOffice began using the DB winds, and EUMETSAT now distribute the winds via EUMETCast. Other weather prediction centers are expected to use the DB winds operationally in the near future. Additional DB sites in the Arctic and Antarctic are being considered. Real-time results are available at http://stratus.ssec.wisc.edu/db/.

Publications (since project inception)
Santek, David, J. Jung, T. Zapotocny, J. Key, and C. Velden, 2006. Mechanisms that propagate polar satellite-derived atmospheric motion vector information into lower latitudes. *Proceedings of the 14th Conference on Satellite Meteorology and Oceanography*, American Meteorological

Society, Atlanta, GA, 29 January-2 February 2006.

Velden, C., and many co-authors, 2005: Recent innovations in deriving tropospheric winds from satellites. *Bull. Amer. Meteor. Soc*., **86**, 205-223.

Francis, J.A., E. Hunter, J. Key, and X. Wang, 2005: Clues to variability in Arctic minimum sea ice extent. *Geophys. Res. Lett.*, 32, L21501, doi:10.1029/2005GL024376.

Francis, J., E. Hunter, C. Zou, and J. Key, 2004, Arctic tropospheric winds from satellite sounders, *7th International Winds Workshop*, Helsinki, Finland.

Key, J., D. Santek, C.S. Velden, J.M. Daniels, W. Bresky, and W.P. Menzel, 2005, Polar winds from satellite imagers for numerical weather prediction and climate applications, *Proceedings of the 8th Conference on Polar Meteorology and Oceanography*, American Meteorological Society, San Diego, California, 10-13 January 2005.

Zou, C.-Z., and W. Zheng, 2005, An improved algorithm for atmospheric wind retrievals from satellite soundings over the polar region, *8th Conference on Polar Meteorology and Oceanography*, *American Meteorological Society*, San Diego, California.

Zou, C.-Z., 2005, An improved algorithm for atmospheric wind retrievals from satellite soundings over the polar region, *8th Conference on Polar Meteorology and Oceanography*, *American Meteorological Society*, San Diego, California.

16 Retrospective Analysis of Arctic Clouds and Radiation (SEARCH) – Jeff Key

Project Goals

The objective of this project is to understand Arctic climate change using satellite data. The research not only examines overall changes in the Arctic during the past 20 years, but also explores feedback mechanisms, regional variability in climate change, and the relationship between Arctic change and the global climate system. Our focus is on clouds and radiation but attention is also given to surface properties, especially pertaining to recent trends in Arctic snow cover and sea ice that can induce a temperature-cloud-albedo feedback. The investigators are J. Key, X. Wang, and Y. Liu. This project ended in May 2006.

Accomplishments

Our accomplishments and findings include:

1. Satellite retrieval techniques for use with the AVHRR Polar Pathfinder (APP) dataset were refined and validated with data from SHEBA and from Barrow, Alaska.

2. Surface, cloud, and radiation characteristics for 23 years of APP data, covering the period 1982-2004, have been estimated, and a data product has been made available to the public. The new product is called the extended AVHRR Polar Pathfinder, or APP-x.

    - An analysis of trends shows that the Arctic has been cooling at the surface during the winter, particularly over the ocean, but warming at other times of the year,

particularly over land. The surface albedo has decreased, especially during the autumn months. Cloud amount has been decreasing during the winter but increasing in spring and summer. During summer, fall, and winter, cloud forcing has tended toward increased cooling (or decreased warming). This implies that if Arctic cloud cover had not been changing the way it has over the past two decades, surface temperatures would probably have risen at an even greater rate than what has been observed.

- Decreases in sea ice extent and albedo that result from surface warming modulate the increasing cloud cooling effect, resulting in little or no change in the radiation budget.

- Changes in summer albedo over Alaska correlate with a lengthening of the snow-free season that has increased atmospheric heating locally by 3 W/m-2/decade. Current trends in shrub and tree expansion could further amplify this by 2-7 times. (Done in collaboration with T. Chapin, University of Alaska)

3. The APP-x product was used in combination with horizontal heat and moisture advection derived from the TIROS Operational Vertical Sounder (TOVS) Path-P product, and with clear sky temperature inversion data derived from the High Resolution Infrared Radiation Sounder (HIRS, part of TOVS). The goal was to examine the relationship between trends in cloud properties, temperature inversion characteristics, advection, and surface radiation. This work was done with J. Francis, Rutgers University, and Y. Liu, CIMSS (both funded separately).

    - The decreasing trend in winter surface temperature over the central Arctic cannot be explained solely by large-scale atmospheric circulation changes. There is a strong coupling between changes in surface temperature and changes in inversion strength, but that trends in some areas may be a result of advection aloft rather than warming/cooling at the surface.

    - Other researchers have reported that the loss of Arctic perennial ice cover is almost 10% per decade. We found that the relative roles of advection and radiation in this process vary by region.

Publications (since project inception)

Journal

Chapin, F.S., M. Sturm, M.C. Serreze, J.P. McFadden, J.R. Key, A.H. Lloyd, A.D. McGuire, T.S. Rupp, A.H. Lynch, J.P. Schimel, J. Beringer, H.E. Epstein, L.D. Hinzman, G. Jia, C.-L. Ping, K. Tape, W.L. Chapman, E. Euskirchen, C.D.C. Thompson, J.M. Welker, and D.A. Walker, 2005, Role of land surface changes in Arctic summer warming, Science, vol. 310, doi: 10.1126/science.1117368, October 28.

Francis, J.A., E. Hunter, J. Key, and X. Wang, 2005, Clues to variability in Arctic minimum sea ice extent, Geophys. Res. Letters, vol. 32, L21501, doi: 10.1029/2005GL024376, November 15.

Liu, Y., J. Key, R. Frey, S. Ackerman, and W.P. Menzel, 2004, Nighttime polar cloud detection with MODIS, J. Appl. Meteorol., submitted (January 2004).

Liu, Y., J. Key, A. Schweiger, and J. Francis, 2006, Characteristics of satellite-derived clear-sky

atmospheric temperature inversion strength in the Arctic, 1980-1996, J. Climate, 19(19), 4902-4913.

Liu, Y., J. Key, and X. Wang, 2006, The Influence of Changes in Cloud Cover on Recent Surface Temperature Trends in the Arctic, J. Climate, submitted (September 2006).

Overpeck, J.T., M. Sturm, J.A. Francis, D.K. Perovich, M.C. Serreze, R. Benner, E.C. Carmack, F.S. Chapin III, S.C. Gerlach, L.C. Hamilton, L.D. Hinzman, M. Holland, H.P. Huntington, J.R. Key, A.H. Lloyd, G.M. MacDonald, J. McFadden, D. Noone, T.D. Prowse, P. Schlosser, and C. Vörösmarty, 2005, Arctic system on trajectory to new, Seasonally ice-free state, EOS, 86(34), 309-314.

Wang, X. and J. Key, 2003, Recent trends in Arctic surface, cloud, and radiation properties from space, Science, 299(5613), 1725-1728.

Wang, X. and J. Key, 2005, Arctic surface, cloud, and radiation properties based on the AVHRR Polar Pathfinder data set. Part I: Spatial and temporal characteristics, J. Climate, 18(14), 2558-2574.

Wang, X. and J. Key, 2005, Arctic surface, cloud, and radiation properties based on the AVHRR Polar Pathfinder data set. Part II: Recent trends, J. Climate, 18(14), 2575-2593.

Zuidema, P., B. Baker, Y. Han, J. Intrieri, J. Key, P. Lawson, S. Matrosov, M. Shupe, R. Stone, T. Uttal, 2005, An Arctic springtime mixed-phase cloudy boundary layer observed during SHEBA, J. Atmos. Sci., 62, 160-176.

Theses

Wang, X. 2003, "Arctic Climate Characteristics and Recent Trends from Space", Ph.D Dissertation, University of Wisconsin-Madison, December 2003.

Conference Papers

Uttal, T., S. Frisch, X. Wang, J. Key, A. Schweiger, S. Sun-Mack, and P. Minnis, 2005, Comparison of monthly mean cloud fraction and cloud optical depth determined from surface cloud radar, TOVS, AVHRR, and MODIS over Barrow, Alaska, *Proceedings of the 8th Conference on Polar Meteorology and Oceanography*, January 9-13, San Diego.

Uttal, T., S. Frisch, X. Wang, and J. Key, 2004, Long-term observations of cloudiness, radiation, and aerosols with permanent atmospheric observatories, Proceedings of the ACIA International Scientific Symposium "Climate Change in the Arctic", Reykjavik, Iceland, November 9-12.

Wang, X. and J. Key, 2004, Arctic climate characteristics and recent trends from space, Proceedings of the SPIE International Asia-Pacific Symposium, Honolulu, Hawaii, November 8-12.

Wang, X. and J. Key, 2004, Satellite-derived Arctic climate characteristics and recent trends, Proceedings of *the 13th Conference on Satellite Meteorology and Oceanography*, Norfolk, Virginia, September 20-24.

Uttal, T. Sun-Mack S., P. Minnis and J. Key, 2003: Comparison of Surface AND Satellite Measurements of Arctic Cloud Properties, 7th Conf on Polar Meteorology and Oceanography.

Wang, X. and J. Key, 2003, Recent Arctic climate trends observed from space and the cloud-radiation feedback, *Proceedings of the Seventh Conference on Polar Meteorology and Oceanography*, American Meteorological Society, Hyannis, MA, May 12-16.

17 Development and Application of a 20-Year Satellite-Derived Wind Data Set for the Polar Regions – Jeff Key

Background

An accurate depiction of the wind field in numerical climate prediction models is essential for studying surface-atmosphere interactions, feedback mechanisms, and climate change. For example, a recent study of Arctic climate trends over the last 20 years showed that changes in cloud and surface properties are a function of large-scale circulation rather than local processes. Unfortunately, it appears that two of the most useful tools for studying recent climate change, the NCEP/NCAR and European Center for Medium-range Weather Forecasts (ECMWF) Reanalysis products, have large errors in the wind field for areas with little or no wind observations like the polar regions.

The objective of this project is to generate a 20-year tropospheric wind data set covering both polar regions, poleward of approximately 65 degrees latitude, using historical Advanced Very High Resolution (AVHRR) Global Area Coverage (GAC) data from NOAA satellites. The winds data set will extend the record back 20 years, providing an invaluable product for the verification of, and assimilation in, climate prediction models. This project falls under the NOAA Mission Goal of understanding climate variability and change to enhance society's ability to plan and respond.

The project Principal Investigator at CIMSS is Christopher Velden. A graduate student, Richard Dworak, is performing the data acquisition and analysis. Dave Santek assists as necessary. Jeff Key, NOAA/NESDIS, works in collaboration with CIMSS scientists, and is the NESDIS point of contact for the project.

Accomplishments

All GAC data for the project have been acquired, navigated, and calibrated. The period of coverage is 1982-2002 (21 years). Although multiple NOAA satellites are typically in orbit, only one satellite is employed at any given time. The data were acquired from the Center for Satellite Applications and Research (STAR) AVHRR archive. The European Centre for Medium-Range Weather Forecasts (ECMWF) ERA-40 Reanalysis data serves as the model background for the wind processing. The ERA-40 data are 2.5 by 2.5 degree GRIB files that contain temperature, humidity, geopotential height, mean sea-level pressure and uv wind profiles. They are converted into 1 degree resolution for wind retrievals.

The MODIS polar winds procedure has been adapted for use with the AVHRR data. Winds have been generated for both polar regions. AVHRR wind vectors from January 1982 to August 2002 have been calculated for both the Arctic and Antarctic with minimal gaps. Figure 17.1 gives an example of AVHRR GAC winds over the Arctic.

Validation and intercomparison studies have been performed. For over 300,000 cases over the Arctic and Antarctic, the root-mean-square (rms) wind speed difference between AVHRR and ERA-40 is 3 m/s and the average direction difference is less than 1 degree. The speed rms and average direction difference are slightly greater over the Antarctic. In addition, the AVHRR winds are, on average, slower than ERA-40 at lower levels (below 700 hPa) and faster than ERA-40 at upper levels (above 400 hPa).

Comparisons were also made with radiosonde winds (rawinsondes). The average absolute and root-mean-square (rms) speed differences increase with height. However, over both the Arctic

and Antarctic there is a noticeable decrease in the normalized rms values with height. Additionally, the average absolute and rms direction differences decrease with height. Overall, the quality of the AVHRR winds improves with increasing atmospheric height, and the quality of the AVHRR winds are better over the Arctic than the Antarctic, especially at low levels where the AVHRR winds are of poor quality over the Antarctic.

A comparison of AVHRR and ERA-40 winds with rawinsonde data not assimilated into the reanalysis shows that, overall, AVHRR has much lower speed bias and rms values than ERA-40. However, ERA-40 did have slightly better direction bias and rms values.

These validation studies indicate that the inclusion of AVHRR winds into future reanalysis products should have positive impacts in reducing the positive speed biases seen in reanalyses.

A three month sample of the AVHRR winds (January through March 1989) was sent to ECMWF to be tested in their new reanalysis. Furthermore, dynamical reasons for differences between ERA40 and AVHRR winds over the Arctic are currently being investigated.

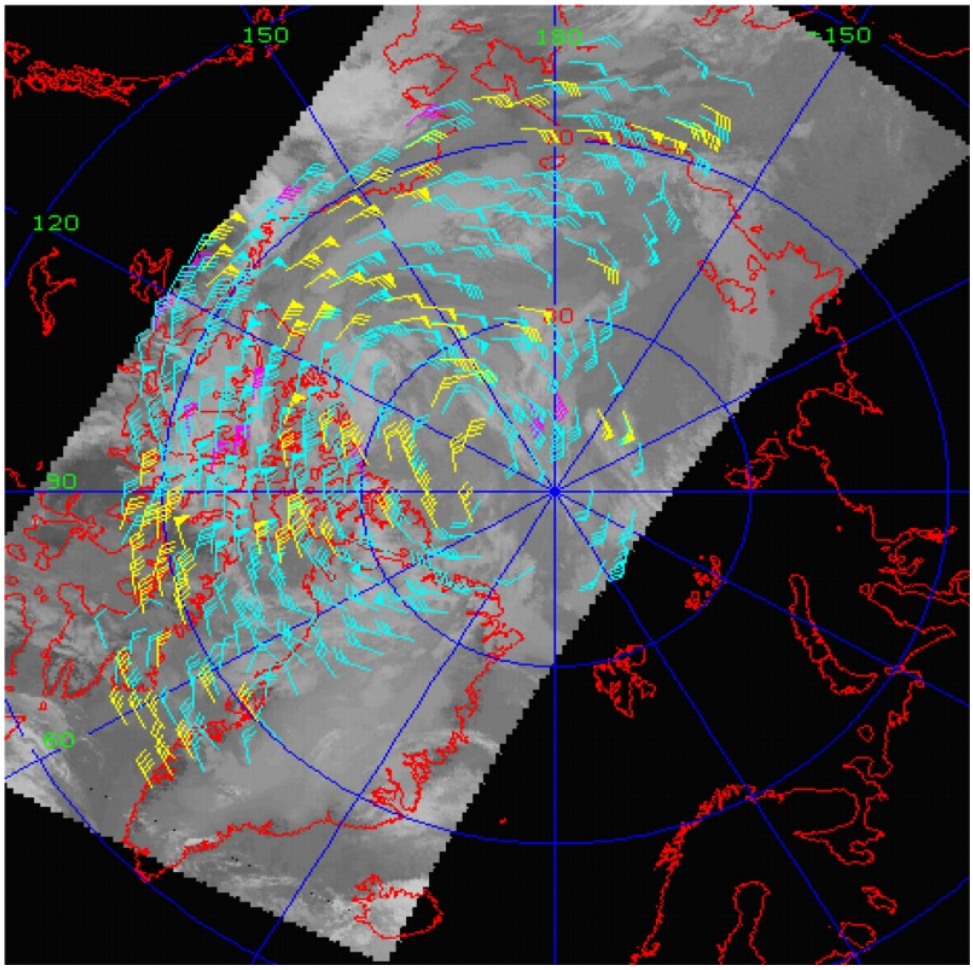

Figure 17.1: An example of winds produced from NOAA-11 AVHRR on August 5, 1993 at 1800 UTC. The background is the AVHRR 11 micron brightness temperature image. Wind vectors are grouped into three height categories (for illustration only): below 700 hPa (yellow), from 400 to 700 hPa (cyan), and above 400 hPa (magenta).

18 International Polar Orbiting Processing Package – Allen Huang

Proposed Work
The Cooperative Institute for Meteorological Satellite Studies (CIMSS) of the Space Science and Engineering Center (SSEC) at the University of Wisconsin-Madison proposes to become a partner, along with the NPOESS Integrated Program Office (IPO) and the NASA GSFC Direct Readout Laboratory (DRL), in the development of the International Polar Orbiter Processing Package (IPOPP). The package will enable the worldwide X-band DB community to process, visualize, and evaluate NPP Sensor Data Records and Environmental Data Records (SDRs and EDRs). The package will be a key enabling technology for the X-band DB user community in its transition from the NASA Earth Observing System (EOS) to NPP and NPOESS and other future generation of polar orbiting systems. The guiding principles of the IPOPP project are to:

(1) Meet the high expectations of the DB community for mission continuity from EOS to NPP and NPOESS with user friendly processing packages for global as well as regional optimized value added applications;'
(2) Enable global feedback loop for NPP/NPOESS Cal/Val campaigns, allowing DB users to contribute their regional validated processing approaches/products to assist and improve global calibration/validation efforts;
(3) Establish a continuity to support other polar orbiting systems.

Summary of Accomplishments and Findings
Created IPOPP requirements Document

- Define functional requirement
- Define software requirement
- Define enterprise requirement

Created work breakdown structure among partners

- **Define project management responsibility**
- **Define Products and algorithms (RDR/SDR/EDR to SPA) and assign responsibility**
- **Define Processing infrastructure**
  - Signal processing
  - Protocol processing
  - Data management
  - Process management
  - Utilities and tools
- **Define Information Services**
- **Define System integration, packaging and beta testing**
  - SPA verification
  - Infrastructure verification
  - Packaging for distribution
  - Local testing

  - Beta testing

- **Define Enterprise Services**
  - Documentation
  - Web portals
  - User forum
  - Mailing list
  - Training/Workshops

Define work plan for the coming year

- Assisted in the evaluation the existing approaches for transforming IDPS algorithms into a form where they can be run on Linux. And to recommend a strategy for adoption by IPOPP.
- Conduct algorithm evaluation for:
  - Ancillary data requirements
  - Algorithm interdependencies
  - Suitability for real-time direct broadcast processing
- NISGS installation on SSEC cluster for testing and evaluation.
- Assemble initial test data sets.
- Collect and provide important documents to the IPOPP team.
- Establish IPOPP team website and/or mailing list.
- Establish software development environment on draca.
- Create draft of IPOPP user website (e.g., FAQ, relevant documents, schedules)
- Preparing for Polar Max 2007 for the demonstration of a real-time processing system which runs a subset of VIIRS and equivalent MODIS algorithms in parallel driven by Aqua MODIS direct broadcast proxy data.

Conducted IPOPP design and coordination meeting to

- Create Baseline Requirements Document.
- Decompose architecture into modular components.
- Allocate components to teams.
- Agreement of IPOPP Development Plan.

19 NOAA EOPA Remote Sensing and CIMSS IMAPP Training and Education Workshop - Allen Huang

Proposed Work
The Cooperative Institute for Meteorological Satellite Studies (CIMSS) at the University of Wisconsin-Madison (UW-Madison) proposes to collaborate with the NOAA National Weather Service (NWS), International Activities (IA) office, and other NOAA and NASA participants, to present a workshop in Buenos Aires, Argentina on acquiring and using NASA EOS MODIS and AIRS measurements.

The program includes participation by CIMSS and NOAA scientists, as well as guest lecturers from NASA and from participating countries in South America. The overall objective of this workshop is to facilitate understanding of general remote sensing principals and applications of

the NASA EOS MODIS and AIRS instruments and the data processing and science applications available through the International MODIS/AIRS Processing Package software developed at CIMSS.

Summary of Accomplishments and Findings

Fund received on December of 2006 and work will begin on 2007 to

1. To attend Capacity Building GEOSS Americas Working Group meeting in AMS 2007 Annual meeting
2. Plan for conducting IMAPP training workshop in the later half of 2007 in South America (host site to be identified after Capability Building Meeting) to support GEOSS America partners' effort.
3. The EOPA Training workshop project is to include participation of CIMSS and NOAA scientists, as well as guest lecturers from NASA and from participating countries in South America. The overall objective of this workshop is to facilitate understanding of general remote sensing principals and applications of the NASA EOS MODIS and AIRS instruments and the data processing and science applications available through the International MODIS/AIRS Processing Package software developed at CIMSS. This workshop will be presented in support of the NOAA Earth Observation Partnership of the Americas (EOPA).

The proposed research project addresses the following NOAA mission goals :

- Serve society's needs for weather and water information
- Provide critical support for the NOAA mission

Furthermore, it supports NOAA's Cross-Cutting Priorities in the areas of:

- Integrating global environmental observations and data management
- Promoting environmental literacy

Exercising international leadership

20 Geo-location of VHRR Data from Kalpana Satellite – Sanjay Limaye

Summary

Visible, Thermal Infrared and Water vapor channel imagery acquired by the Kalpana satellite operated by the Indian Space Research Organization (ISRO) is routinely being received at NOAA/NESDIS through a dedicated link with India Meteorological Department (IMD) in New Delhi, India. These data are then acquired by the Space Science and Engineering Center, University of Wisconsin, Madison. An automated process to determine the image center coordinates (from limb location in thermal infrared images) for geolocation has been developed and applied routinely. The quality of the geolocation is monitored by comparing the image determined locations of a few selected coast-line containing regions of the image with the expected, known coordinates, providing a continuing record of the quality of the geo-location. By applying a general conic fit to the limb points, the overall characteristics of the Earth image (size, orientation and eccentricity) are also determined.

The automated process of geolocation has been working without any failure since July 27, 2005 at SSEC, and the results to date indicate that the geolocation in the central part of the disk is generally accurate to within 1 to 1.5 IR pixels with the "static" map projection model that ignores the spacecraft movement and any pointing deviations over the period during which the image is acquired. Systematic trends in the offsets are seen both in longitude (northern hemisphere, towards the Eastern and Western parts of the image) and in latitude (southern hemisphere), which

suggest instrument related origins. Better geo-location is therefore possible, if additional information were made available by IMD and ISRO.

The progress made on this effort has been periodically communicated to Dr. Al Powell and Dr. Ramesh Sinha as well as the International Affairs Office at NOAA via e-mail. Discussions with ISRO and IMD whenever opportunities arose have also been useful in maintaining a productive dialog on the geo-location issue. Although the VHRR data re now rendered useful for some applications, further improvement is possible and desired. However, this can occur only with the cooperation and collaboration of IMD and ISRO. A geo-location workshop involving ISRO, NOAA, IMD and SSEC is desired and is proposed during the next year's efforts.

VHRR data are now being utilized to implement the rainfall determination project by Dr. Robert Kuligowsky (NOAA) and are being accessed from SSEC's real-time data servers.

Accomplishments
Accomplishments to date are as follows:

(1) Routine retrieval of Kalpana VHRR data in HDF 4.0 format form NOAA/NESDIS computers established.
(2) Kalpana Data converted into McIDAS multi-banded area format (three channels)
(3) Limb points retrieved from Band 2 (thermal infrared data)
(4) General conic fit applied to the retrieved limb points to determine the properties of the Earth image. The process is repeated iteratively to reject any spurious points due to noise or other anomalies as determined by the deviation from the ellipse fit exceeding a certain threshold. The ellipse properties include the position of the image center (line, sample), the size of the image (semi-major and semi-minor axes), the orientation of the image (angle between the scan line and the semi-major axis) and the eccentricity of the ellipse.
(5) A geolocation transform for a perspective view of the Earth is applied using the Kalpana spacecraft location provided in the HDF header (altitude, latitude and longitude).
(6) Selected coast line regions are sampled to determine the navigation offset between the expected (known) location of landmark features and the locations computed from the image by applying the navigation transform. Cross correlation of a 32 x 32 pixel template is used to determine the offset in the navigated image.
(7) The image properties and the geolocation offsets are logged for long term trends analysis.
(8) Navigation transform is incorporated into the data staged on the Kalpana data server at SSEC so that external users can have access to the geolocated data.
(9) Navigation tiles are posted on a web server for internal use between personnel at NOAA/NESDIS, IMD and ISRO so that each agency has access to the geolocation information and problems can be identified and corrected.
(10) Kalpana geolocation code and the HDF to area conversion code has been incorporated into the current release of McIDAS (Version 7.03) that has been distributed through the McIDAS Users Group.
(11) Kalpana geolocation code has been provided to Dr. Ramesh Sinha at NOAA along with the code for generation of McIDAS areas from the HDF format.
(12) Dr. Kuligowsky has been accessing data from the SSEC Kalpana Data server since ~ January 2006 for rainfall studies, a joint Indo US Project.

(13) Dialog with IMD and ISRO persons cognizant with Kalpana geolocation issues has been maintained through periodic e-mail, telephone and visits (as opportunities arise) to see how improvements can be made to the geolocation of the data.

Introduction

Routine visible and thermal IR imagery is being received at NOAA/NESDIS from India Meteorological Department routinely since ~ 1999. Water vapor imagery was added to These transmitted data were largely unusable due to an inability to use the accompanying geo-location information. An alternate approach to render these data useful by generating the geo-location information was been demonstrated by NOAA through the use of manually located landmarks in visible images to arrive at a geo-location transform with the knowledge of the spacecraft position with respect to the earth at the time of data acquisition. The manual process worked for the day time imagery but had a moderate failure rate for routine operations and failed at night and when clouds prevented detection of the landmarks during the day.

An alternate process to arrive at the geo-location information was proposed and demonstrated by determining the image center information and then utilizing the sub-spacecraft location and altitude provided by IMD/ISRO. The approach and the results being obtained are described below.

Background: The Problem of Geo-location of the Kalpana VHRR Data

Far fetched as it may seem, the VHRR data have not been geo-located with an accuracy comparable to the resolution of the instrument. The exact reasons for these are not known and can only be surmised. It is apparent from many interactions with IMD staff that a lack of capable software and expertise in addressing the issues and their impacts contributed to it. Once the bilateral data exchange began, University of Wisconsin was interested in acquiring the data, however the request to NOAA was not fulfilled pending resolution of the geo-location (1998 – 2003). With the announcement of a conference for Next Steps in Strategic Partnership between India and the US, which was held in Bangalore during June 2004, a renewed effort was made to resolve the geolocation of VHRR data by approaching both IMD and ISRO (Limaye, 2004). This was the first time ISRO apparently became aware of the geo-location issue which led to an independent effort within ISRO to tackle it and to date that effort is continuing.

As a result of informal dialog with IMD and some developments within IMD, the data volume, data type and the number of bands transmitted to NOAA/NESDIS changed in February 2005. Instead of sending only six to eight thermal infrared images and day-time images with some line documentation over the dedicated line, IMD now transmits three channel images in HDF 4.0 format eight times a day with two 30 minute apart images twice a day. Except for occasional interruptions due to power failures or hardware failure at IMD, the data transmission has been generally without gaps. The changeover from the "raw" data format with line documentation (no format was ever provided by IMD to decode these data) to the HDF format also meant that no attitude information was no longer available for geo-location efforts since in the HDF format that information was stripped. This was not a major loss due to the fact that neither IMD nor ISRO had provided the data format and so the attitude information could not be decoded, and the switch to the HDF format at least provided another channel of the data with some navigation information attached. A key piece for geo-location, is not provided in the HDF format – the image center corresponding to the sub-spacecraft latitude and longitude. So the geo-location issue is primarily to determine the image center. This is described below.

Image Center Determination

The algorithm for finding the image was based on the experience of navigation of planetary images acquired from spacecraft missions and ground based telescopes. For thermal infrared images it is possible to discern the entire limb which makes the center determination much easiest using a general conic fit using the least squares. For visible images the limb determination is possible only over approximately half of the disk and the visible limb location changes with time of day and with seasons. While the resolution of the visible VHRR images is four times that of the infrared images, the quality of the image center determined is not significantly better due to the fact that only about ~ 160º of the limb is sampled.

Limb Point Determination

The edge of the Earth disk or the limb is determined from the thermal infrared images by using the maximum local derivative along a radial scan across the edge.

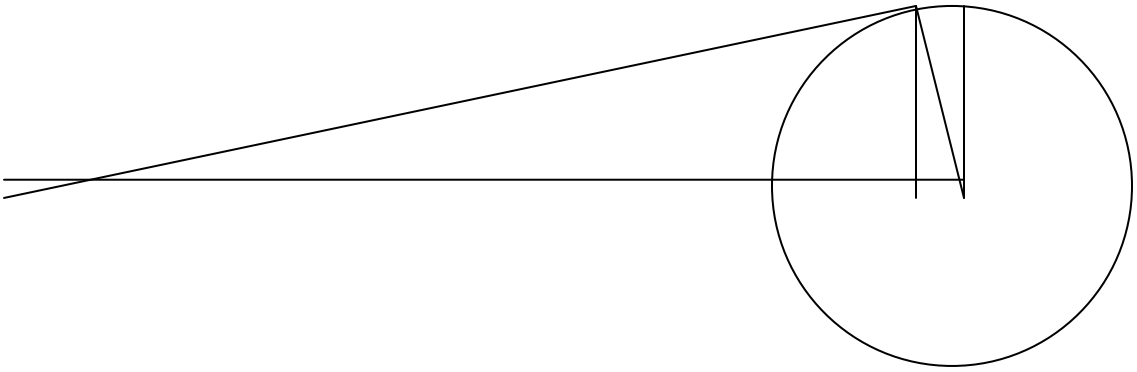

Figure 20.1: The geometry of Kalpana images.

General Ellipse Fit to the limb

From the altitude of the Kalpana satellite in geosynchronous orbit, the shape of the earth in the infrared images is expected to appear as a conic section, with an eccentricity close to the oblateness of the solid Earth. In the infrared, atmospheric envelope is detectable at the edge, approximately 10 km altitude, or about 2 infrared pixels of VHRR data.

All the limb points determined from the Earth images are expected to satisfy the general equation for a conic:

$$Ax^2 + Bxy + Cy^2 + Dx + Ey + F = 0$$

Since each point on the limb must satisfy the same equation, one may expect a small error ε in each point to account for the limb location errors, so that:

$$Ax_i^2 + Bx_iy_i + Cy_i^2 + Dx_i + Ey_i + F = \varepsilon_i$$

A least squares solution for the coefficients A,B,C,D,E and F is then obtained by minimizing $\Sigma\, \varepsilon_i^2$ where Σ represents summation over all the limb points.

The best fit coefficients determine the ellipse properties, semi major and minor axes, the origin of the ellipse or the center of the image and the orientation of the ellipse and the eccentricity.

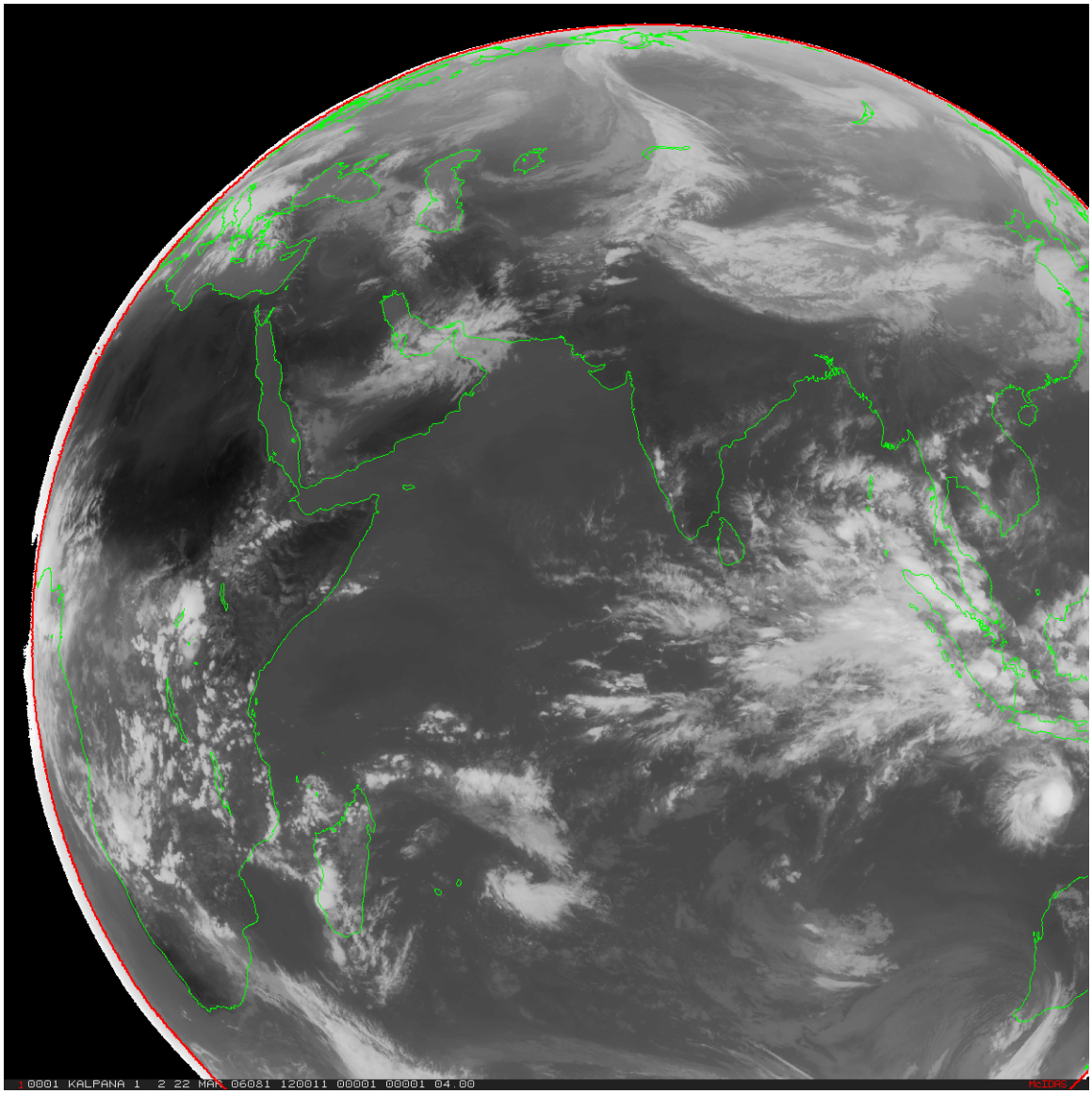

Figure 20.2: This figure shows the location of the limb points determined along with a map overlay after the navigation transform is applied.

The limb finding, center determination process has been demonstrated to be running smoothly without any failures since July 2005. This is a vast improvement over the approach of determining landmarks in the visible images and then applying the transform since this can be done only during the day and fails when clouds mask the landmarks – a problem not faced by the lib determination technique.

Summary of the Kalpana Geolocation Results

The times when Kalpana images were acquired during the day that were received at SSEC from the NOAA/NESDIS servers and geolocated are shown in Figure 20.3. Table 20.1 provides the

average size of the semi-major and minor axes determined from these data (277 7 images), with the respective standard deviation.

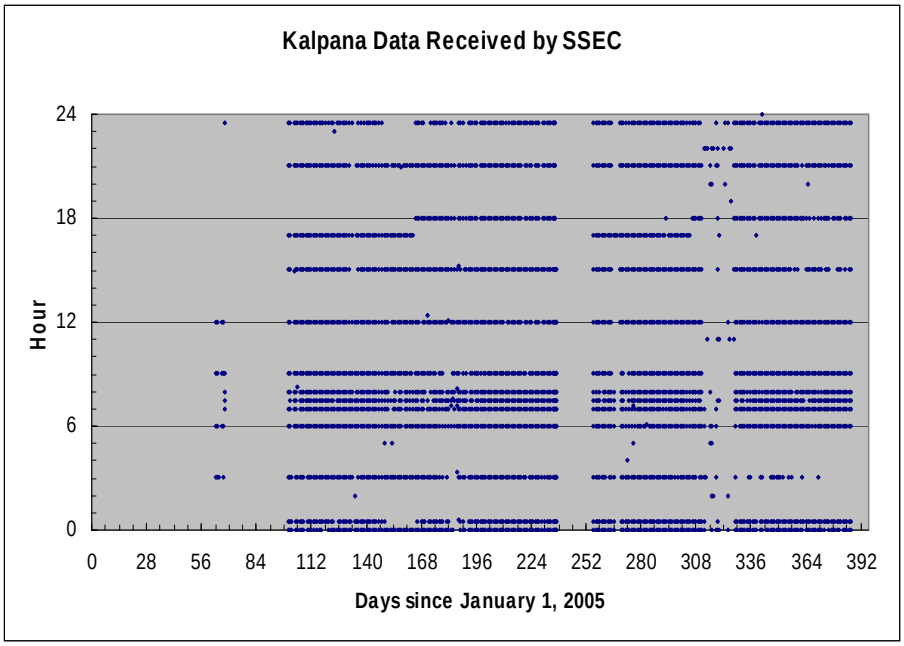

Figure 20.3: Kalpana data received and geolocated at SSEC.

Figures 20.4 and 20.5 show the lengths of the semi-major and semi-minor axes for each image as determined from fits to the thermal infrared channel data as expressed in terms of equivalent pixels. Abrupt changes in the size are seen on Day 251, but no cause has been determined.

Table 20.1. **Average image properties from data navigated through January 2006**

Property	A	B	Ecc
	Visible pixels	Visible pixels	
Average Value	2732.0 ± 3.1	2725.3± 2.6	0.0690 ± 0.0103
Since Day 251	2729.6 ± 1.7	2723.5 ± 2.1	0.0662 ± 0.0088

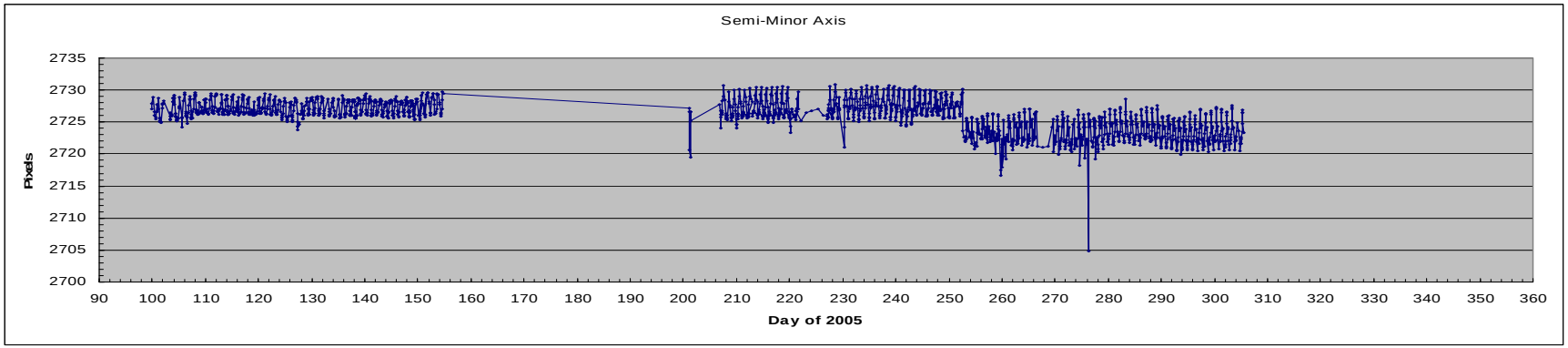

Figure 20.4: Length of the semi-major axis for each Kalpana image as determined from fits to the limb in the infrared data (equivalent visible pixels).

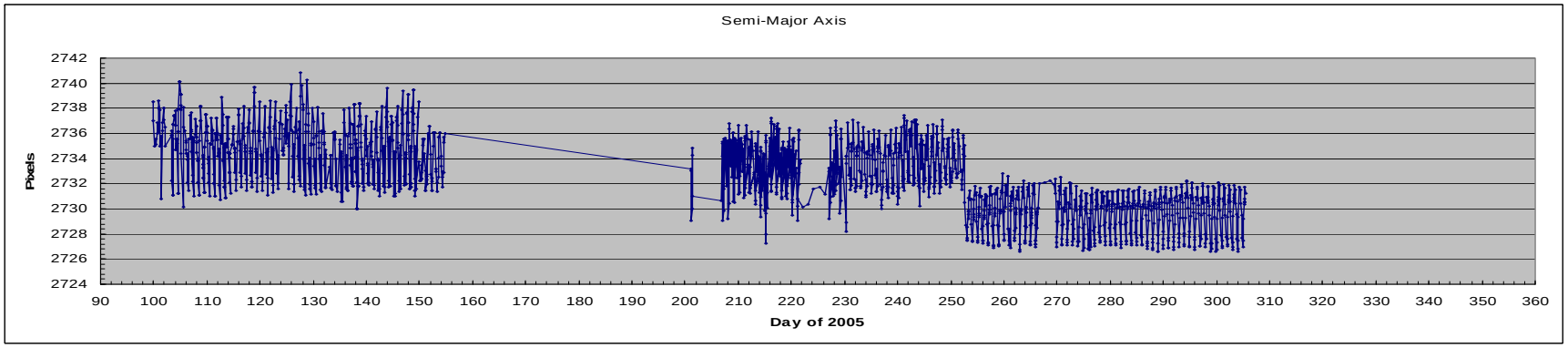

Figure 20.5: Length of the semi-minor axis for each Kalpana image as determined from fits to the limb in the infrared data (equivalent visible pixels).

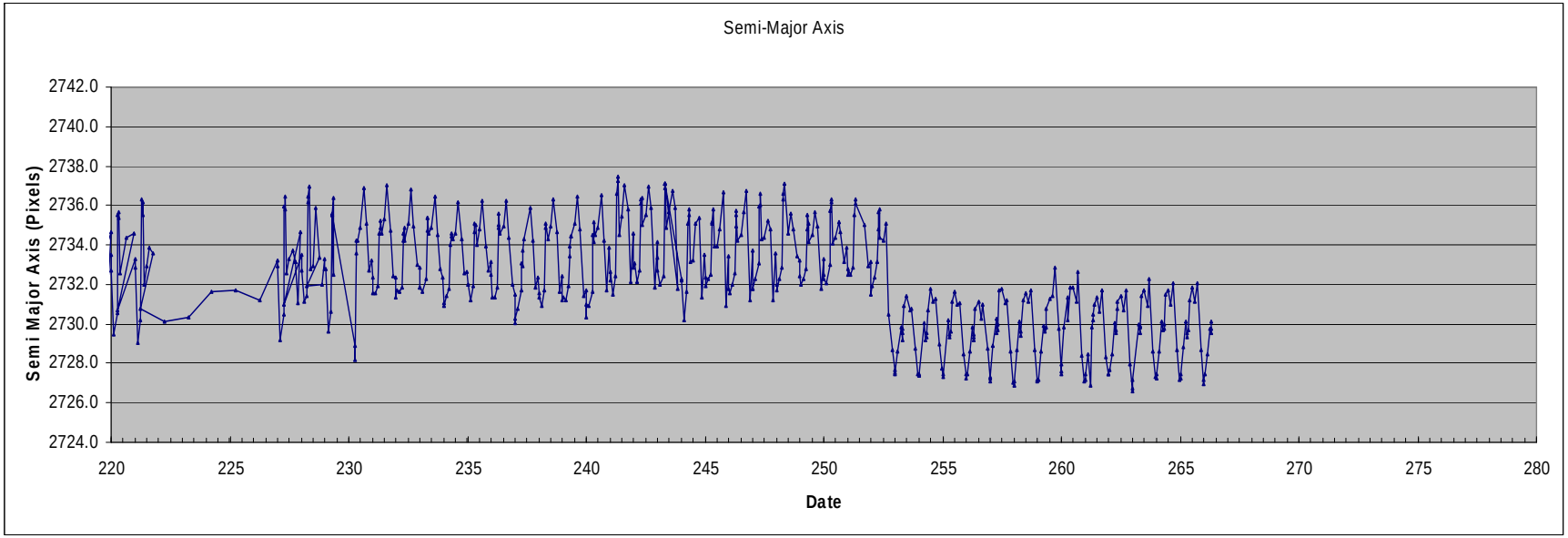

Figure 20.6: A Diurnal signature in the size of the Earth image in the VHRR data is evident.

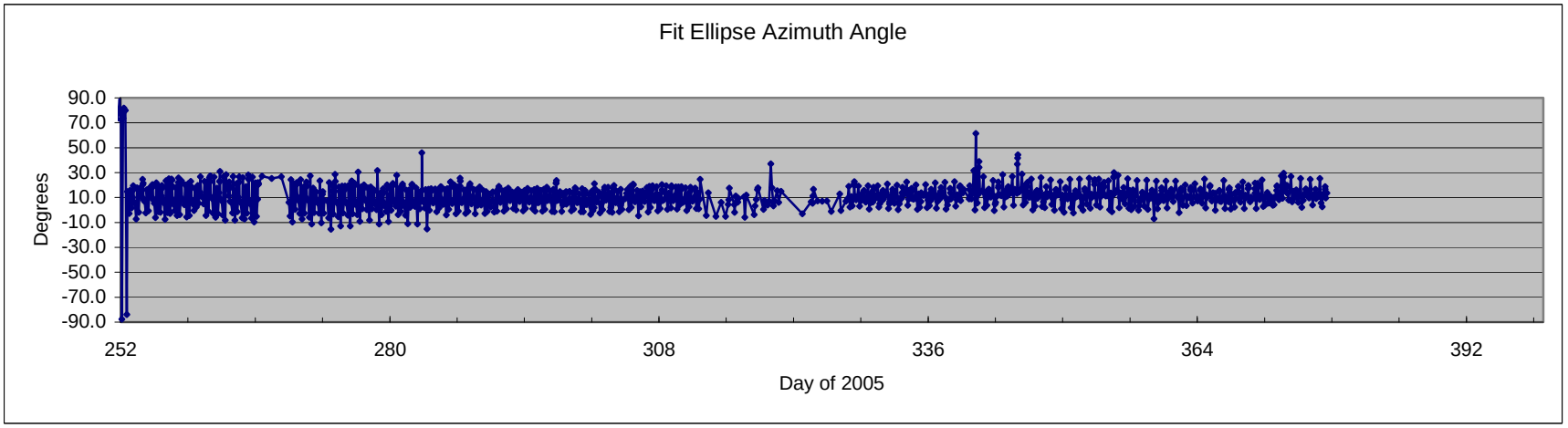

Figure 20.7: Azimuth angle of the ellipse fit to the Earth image also shows a diurnal pattern.

A diurnal signature is clearly evident in the Earth image ellipse fit in the VHRR infrared data as shown in Figure 20.6 (Semi-major axis) and the azimuth angle of the ellipse or the angle between the equatorial plane and the VHRR scan direction (Figure 20.7). Such diurnal signature suggests an instrumental source and this may explain some of the aspects of the VHRR data.

Table 20.2 provides a summary of the offsets determined by locating a well defined coast-line in four quadrants of the image, including the central region. For Srilanka, the offsets in terms of IR lines and samples is ~ 1.3 lines and 0.2 samples, close to the requirement of one IR pixel accuracy. In other parts of the image however the offsets are slightly larger for in the cross-scan direction, indicating that there is some systematic bias, perhaps due to instrumental performance. This finding as been communicated to Dr. Kiran Kumar (Space Applications Center, ISRO, Ahmedabad), who has confirmed it from an independent analysis. This is being further investigated and will be continued in Year 2 of this effort.

Table 20.2.

Kalpana VHRR Geolocation offsets
University of Wisconsin Algorithm (Limb Fit+ Center Finding)
January 1, 2006

Region		Visible Lines	Visible Elements	IR Lines	IR Elements
Qatar	Average	-2.1	7.1	-0.5	1.8
	RMS	4.2	4.6	1.0	1.1
Srilanka	Average	5.2	-0.9	1.3	-0.2
Poor stats due to ITCZ, actual quality is quite good	RMS	9.1	11.0	2.3	2.7
S. Madagascar	Average	22.6	1.9	5.6	0.5
	RMS	7.3	7.7	1.8	1.9
W. Australia	Average	18.9	4.5	4.7	1.1
	RMS	4.7	3.8	1.2	0.9

Summary

An acceptable scheme for geolocation of the VHRR data from Kalpana satellite has been developed and implemented, rendering these data useful for many quantitative studies. Further improvements appear possible, pending a productive dialog with ISRO. It is important to determine whether the geolocation results are indicative of the VHRR on Kalpana satellite only or are generic to the VHRR design/performance on other spacecraft such as INSAT 3A. It is desired to obtain INSAT-3A VHRR data from IMD to examine this further.

21 Extended GOES Operations at High Inclination Orbit – Tim Schmit

Proposed Work

The proposed work is to study the impact on image and data product quality resulting from the predicted high inclination orbit of GOES 10. This proposal consists of two tasks related to the GOES-10 XGOHI project: GVAR testing and select product testing.

Summary of Accomplishments and Findings

Limited work was done on this project in 2006 because the XGOHI schedule for sample data sets was pushed back to early 2007, and GOES-10 only arrived on station at 60 West in early December. The GOES-10 GVAR signal has been acquired and the routine data are being archive by the SSEC Data Center (see sample in Figure 21.1). Several telecoms with the XGOHI team in the Washington DC area were held.

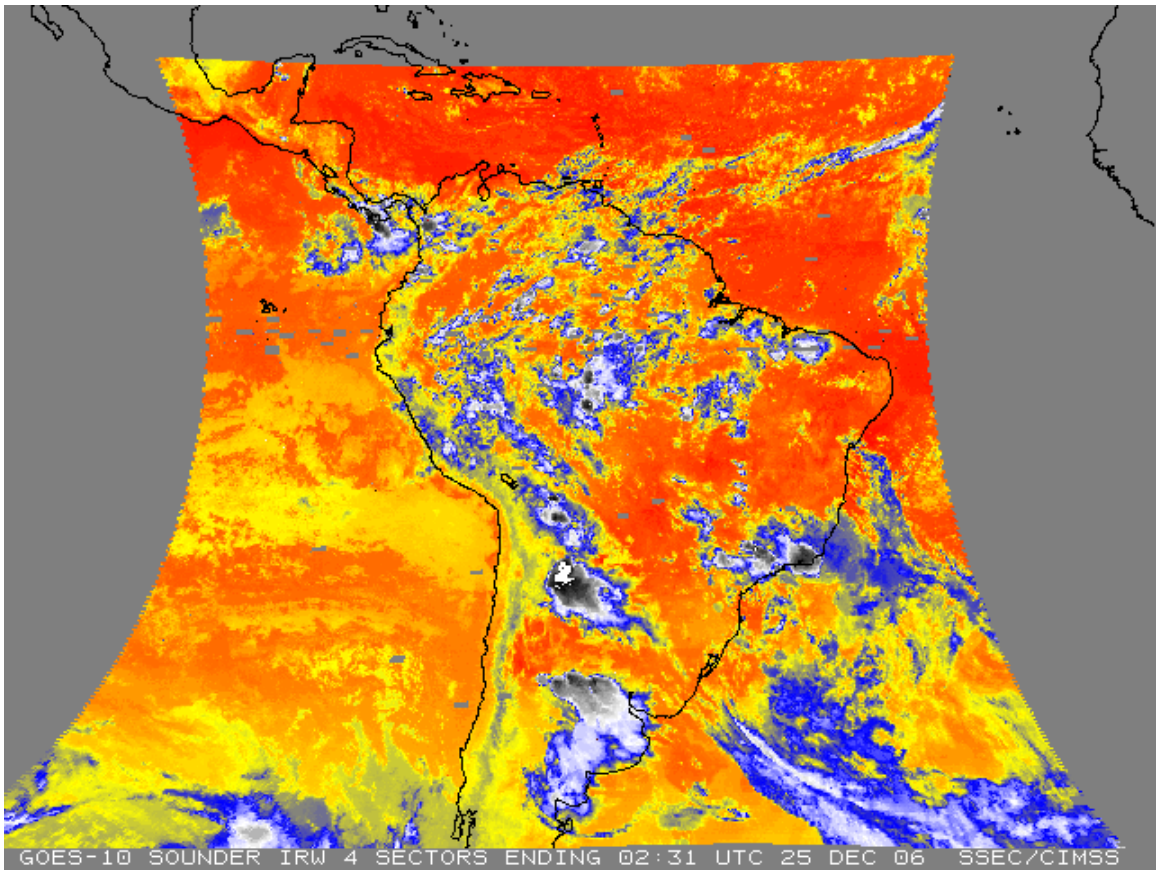

Figure 21.1: Sample GOES-10 Sounder infrared window composite of the four sectors.